Molecular Analysis of Genes Involved in the Biosynthesis and Regulation of Hormaomycin, an Exceptionally Complex Bacterial Signaling Metabolite

Dissertation

zur

Erlangung des Doktorgrades (Dr. rer. nat.)

der

Mathematisch-Naturwissenschaftlichen Fakultät

der

Rheinischen Friedrich-Wilhelms-Universität Bonn

vorgelegt von

Xiaofeng Cai

aus Shanxi, China

Universität Bonn

2013

Angefertigt mit Genehmigung der Mathematisch-Naturwissenschaftlichen Fakultät der Rheinischen Friedrich-Wilhelms-Universität Bonn.

Gutachter:

1. Prof. Dr. Jörn Piel

2. Prof. Dr. Uwe Deppenmeier

3. Prof. Dr. Peter Dörmann

4. Prof. Dr. Hans-Georg Sahl

Tag der Promotion: 11.10.2013

Erscheinungsjahr: 2013

This dissertation is dedicated to my family with love and gratitude……

Abstract

Hormaomycin (HRM) is a nonribosomal peptide antibiotic isolated from *Streptomyces griseoflavus* W-384. It contains several unprecedented nonproteinogenic building blocks bearing chlorine, nitro or cyclopropyl moieties (Andres et al., 1989). HRM acts as a bacterial hormone by inducing cellular morphogenesis and increasing production titers of antibiotics in other *Streptomyces* spp.. Additionally, HRM is an antibiotic with high potency against coryneform actinomycetes (Andres et al., 1990) and also exhibits *in vitro* activity against a range of malarial parasites, such as *Plasmodium falciparum* (Otoguro et al., 2003).

Studies of HRM biosynthesis have been hampered by genetically inefficient manipulation of its producing strain *S. griseoflavus* W-384. In addition, the inconsistent and low production of HRM in wild type strain has prevented us from investigation of its antibacterial and hormonal mechanism of action.

In order to address these problems, *S. griseosflavus* W-384 was firstly optimized for genetic engineering. The protoplast transformation system was established, allowing us to introduce two types of foreign plasmids (integrative and free-replicating) into this strain. Additionally, a conjugation system to mediate plasmid transfer between *Escherichia coli* and *S. griseosflavus* W-384 was optimized. The results provided the practical procedures to perform further molecular analysis of HRM biosynthetic genes.

To enhance the fermentation titres of HRM, the role of its cluster-encoded regulatory genes was investigated. A copy of *hrmA* or *hrmB* was placed under control of the constitutive *ermE** promoter on the pWHM4*-based vector and was individually expressed in *S. griseosflavus* W-384, resulting in an increase of HRM production and its analogues as much as 135-fold. For the HrmB overproducer, six novel bioactive HRM analogues were isolated and characterized. This study demonstrates that HrmA and HrmB are positive regulators in HRM biosynthesis. A third regulatory gene, *hrmH*, was identified as a protein capable of shifting the

metabolic profile of HRM and its derivatives. Its manipulation resulted in the generation of an additional HRM analogue.

To elucidate the HRM biosynthetic pathway, functional analysis of genes involved in the biosynthesis of unusual amino acids was carried out by gene knock-outs as well as genetic and chemical complementations. The results suggested that *hrmI* and *hrmJ* are essential for the biosynthesis of 3-(*trans*-2'-nitrocyclopropyl)alanine [(3-Ncp)Ala]. Manipulation of *hrmD* revealed its indispensable role in the biosynthesis of 4-propenylproline [(4-Pe)Pro]. Additionally, an eighth HRM analogue (HRM A_8) was generated by feeding 4-ethinylproline [(4-Et)Pro] into *hrmD* mutant. HRM A_8 will be further employed to determine molecular target of antibacterial and hormonal activities by "Click chemistry". The gene knock-out and genetic complementation of *hrmQ* further proved that HrmQ is a halogenase catalyzing the chlorination of 5-chloro-1-hydroxypyrrole-2-carboxylic acid [Chpca].

HRM, as a signaling metabolite, can induce the aerial mycelia formation and sporulation in other *Streptomyces* spp.. To investigate its hormonal mode of action, HRM was tested against seven *bld* mutants derived from well-known *Streptomyces coelicolor* A3(2) and three bald mutants generated from *Streptomyces griseus*.

By overexpression of pathway-specific activators and mutasynthesis, eight HRM analogues were discovered and generated. Antibiotic assays with the eighth new congeners provided insights into structure-activity relationship and identified structural positions that could permit the generation of active analogs suitable for pull-down studies and target identification. Molecular analysis of the biosynthetic genes gave deeper insights into the HRM biosynthesis.

Contents

List of Figures

List of Tables

Chapter 1 Introduction

1.1 Streptomycetes as antibiotic producers

Streptomycetes are Gram-positive soil-dwelling filamentous and sporulating bacteria that belong to the phylum of Actinobacteria. Over 500 *Streptomyces* species were discovered, they act as a "cleaner" in nature which can break down dead plant or animal matter and make organic nutrients available to the ecosystem. Compared to other bacteria, streptomycetes exhibit more sophisticated and characterized colonial morphologies. *Streptomyces* colonies growing on the agar plates are usually dry and often excrete colorful pigments, allowing us to visually observe the production of secondary metabolites (**Figure 1.1**).

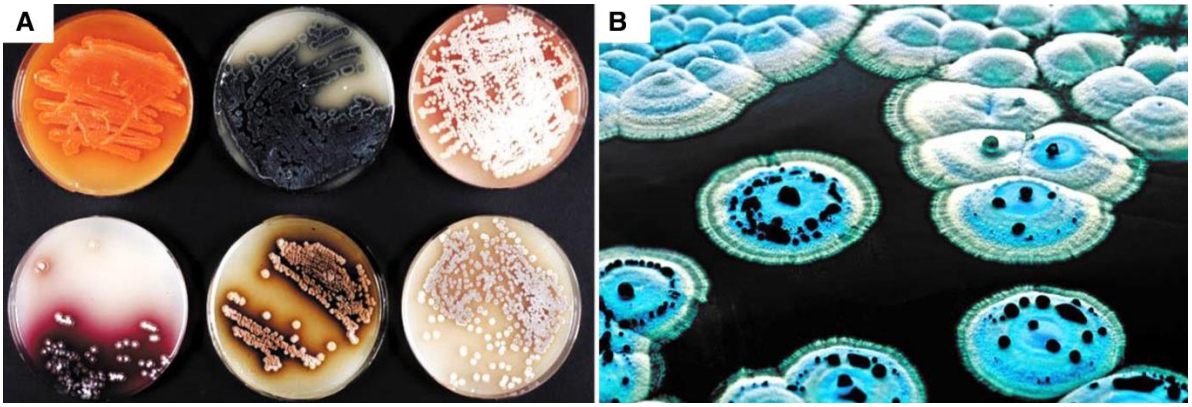

Figure 1.1: The typical morphologies of *Streptomyces* colonies grown on the agar plates (Photo by Tobias Kieser, Celia Bruton and Jennifer Tenor). **A,** The typical morphologies of *Streptomyces* colonies producing colorful pigments. **B,** A close view of the colonies of the model strain, *Streptomyces coelicolor* A3(2) producing antibiotic actinorhodin, a blue pigment.

Streptomycetes also possess a very complex developmental life cycle (**Figure 1.2**) that resembles that of filamentous fungi. They reproduce and disperse through the formation of spores. The morphological differentiation of *Streptomyces* spp. is coordinated with environmental changes throughout entire developmental program, allowing them to adapt to diverse conditions (Hopwood 2007; Flärdh and Buttner 2009). When a *Streptomyces* spore is triggered and germinates in its suitable physiological condition and nutrients, it will grow to form filamentous substrate mycelium by extension and branching during taking up the nutrient

from the surrounding substrate. In response to the depletion of nutrients and to unidentified signals, the substrate mycelium densely interlaces together to generate aerial mycelium. In general, the production of antibiotics is initiated at the transition between these two phases (Flärdh and Buttner 2009). Aerial hyphae break the surface tension from the substrate and grow into the air. Next, the aerial hyphae undergo massive septation and differentiate into a long chain of uninucleated compartments. Finally, these compartments develop into mature spores containing a single copy of the genome per each and continue with next generation when encountering favorable conditions (Hopwood 2007).

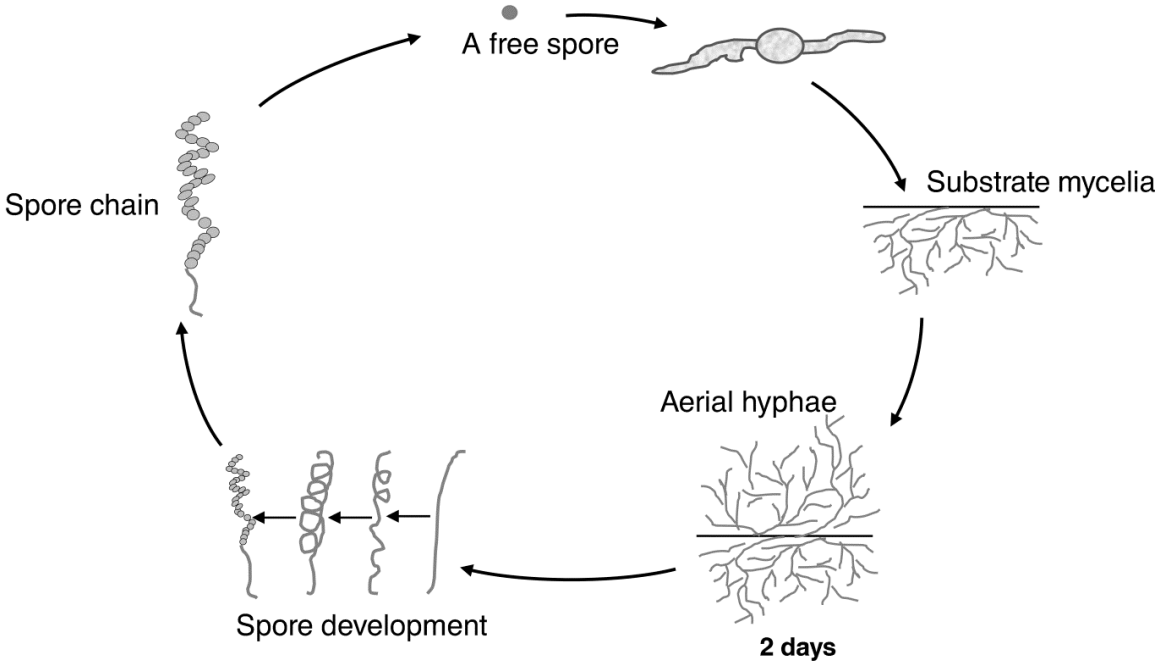

Figure 1.2: The life cycle of streptomycetes. Modified from (Angert 2005). A free spore germinates under favorable conditions, and then grows to form substrate mycelium by extension and branching. After ~2 days, substrate mycelium grows away into the air to form aerial mycelium. Finally, the distal parts of aerial mycelium undergo septation to develop a chain of spores. The spores get mature and released to continue with the next generation.

Streptomyces genomes carry a much higher G + C content (more than 70%) than those of most other Gram-positive bacteria, such as *Staphylococcus* spp., *Streptococcus* spp., and *Bacillus* spp. (less than 50%) (Hopwood 2006). It is known that streptomycetes possess linear chromosomal DNA and plasmids, as compared to the common circular chromosomes and plasmids in other prokaryotes. Terminal inverted repeats (TIRs) are situated at both ends of the

linear DNA, ranging from 24 to 500 kb with terminal proteins covalently attached to their free 5' ends (Sakaguchi 1990; Hopwood 2006). TIRs often exhibit high frequency of genetic instability including deletions, amplifications and even circulations during the developmental progress of streptomycetes, which has no influence on vitality but may play an important role in evolution (Volff and Altenbuchner 1998). The chromosomal DNA is 8-11 Mb in size which is twice as large as that of *Escherichia coli* or *Bacillus subtilis* (Kieser et al., 1992). The first complete genome sequence of *Streptomyces coelicolor* A3(2) was published in 2002 (Bentley et al., 2002). Subsequently, genomic analysis of other species became available in the following years, such as *Streptomyces avermitilis*, an industrial producer of antiparasitic compounds avermectins (Ikeda et al., 2003), *Streptomyces scabies*, the plant scab parasite (Loria et al., 2006), and *Streptomyces griseus*, a producer of the first antituberculosis agent streptomycin (Ohnishi et al., 2008). *Streptomyces* genomes harbor many genes for secondary metabolites which group into clusters including biosynthetic, regulatory and resistant genes. For instance, the *S. coelicolor* A3(2) chromosome contains more than 20 gene clusters encoding known or predicted secondary metabolites and accounting for 5% of entire genome (Bentley et al., 2002). *S. avermitilis* carries over 30 gene clusters for secondary metabolites, which is 6% of the whole genome (Ikeda et al., 2003).

The most attractive property of streptomycetes is the ability to produce numerous secondary metabolites with a range of biological activities. Many of these compounds can be used as antibacterial, antiparasitic, antifungal, antitumor and immunosuppressive agents in human medicine, agriculture, and food industries. Over two-thirds of clinically useful antibiotics are produced by *Streptomyces* spp. (**Figure 1.3**) (Kieser 2000).

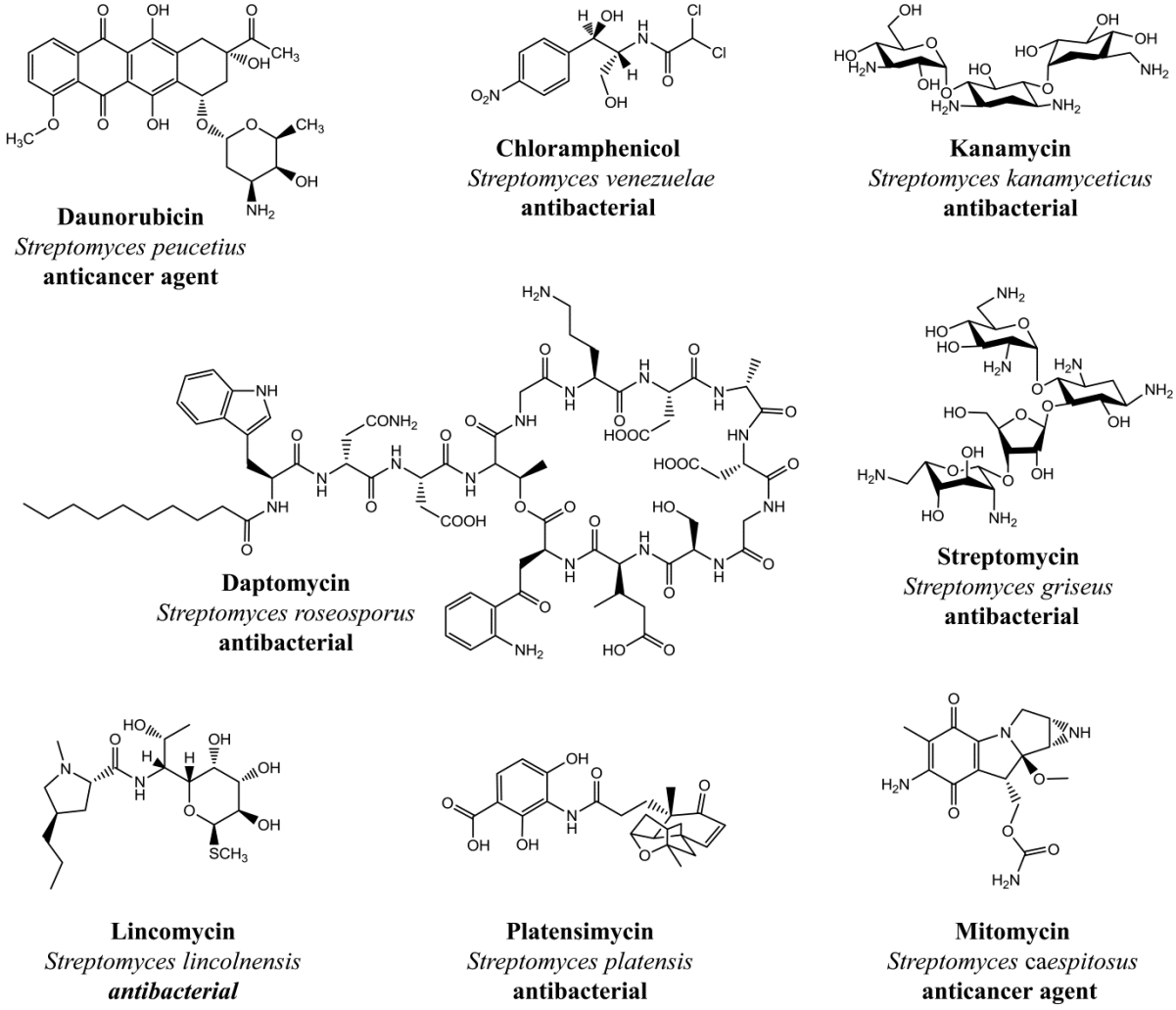

Figure 1.3: Clinically useful antibiotics produced by *Streptomyces* spp..

For decades, natural products have been the most important source of new drugs. But since early 1990s, inappropriate antibacterial treatment and overuse or misuse of antibiotics have contributed to the emergence of antibacterial resistance. Thus, antibacterial resistance is a major challenge in the discovery of new drugs. Routine screening methods are very difficult to discover novel effective antibiotics. To meet this demand, semisynthesis has been utilized to modify the present drugs for increasing the stability and potency, but failed to generate novel bioactive compounds with structural diversity (Newman 2008). Therefore, recently, lots of biologists and chemists have turned attention to marine and unusual environments for discovery of new drugs (Fenical and Jensen 2006; Wilson and Brimble 2009). However, this does not mean that streptomycetes, as excellent ubiquitous drug producers are exhausted to provide new compounds. It was estimated that only 3% of antibiotics from streptomycetes

have been characterized so far (Watve et al., 2001).The past decade of research on genetic basis of secondary metabolism has provided us some promising strategies to obtain novel natural products: (I) Engineering of biosynthetic pathways from different organisms has been proven to be an efficient approach to generate natural product-like compounds (Wilkinson and Micklefield 2007; Luzhetskyy et al., 2007). (II) Genome sequencing projects have opened up exciting new avenues for discovery of new compounds. It is demonstrated that a microorganism has the potential to produce far more secondary metabolites than the number of verified natural products by bioinformatic analysis of its full genome sequence. However, the production of these orphan secondary metabolites is too low to be detected or not active under standard fermentation conditions (Challis 2008a). Therefore, activation of such cryptic gene clusters or their expression in suitable heterologous hosts may lead to isolation of novel interesting natural products.

Polyketides (PKs) and nonribosomal polyketides (NRPs) are two large classes of natural products that possess a wide range of functional and structural diversity with a variety of bioactivities. To understand the biosynthesis and regulation of these molecules will allow us to genetically manipulate the biosynthetic pathway and eventually generate novel natural products. In the following sections, a brief introduction to the biosynthesis of these two types of compounds will be reviewed, and followed with the three different approaches to obtaining new natural compounds by utilizing PKs and NRPs assembly mechanism. In addition, the regulation of antibiotic biosynthesis in *Streptomyces* spp. will be briefly introduced. The final part of introduction will be the summary of previous research on the biosynthesis of hormaomycin (HRM), a signaling nonribosomal peptide, which provides the foundation for this doctoral work.

1.2 Biosynthesis of PKs and NRPs

Many PKs and NRPs compounds have been applied in clinic. The famous examples of PKs include the antibacterial erythromycin (Staunton and Wilkinson 1997; Staunton 1998), antifungal nystatin (Brautaset et al., 2000), antitumor agent epothilone (Walsh et al., 2003) and antiparasitic avermectin (Ikeda and Omura 1995) (**Figure 1.4**).

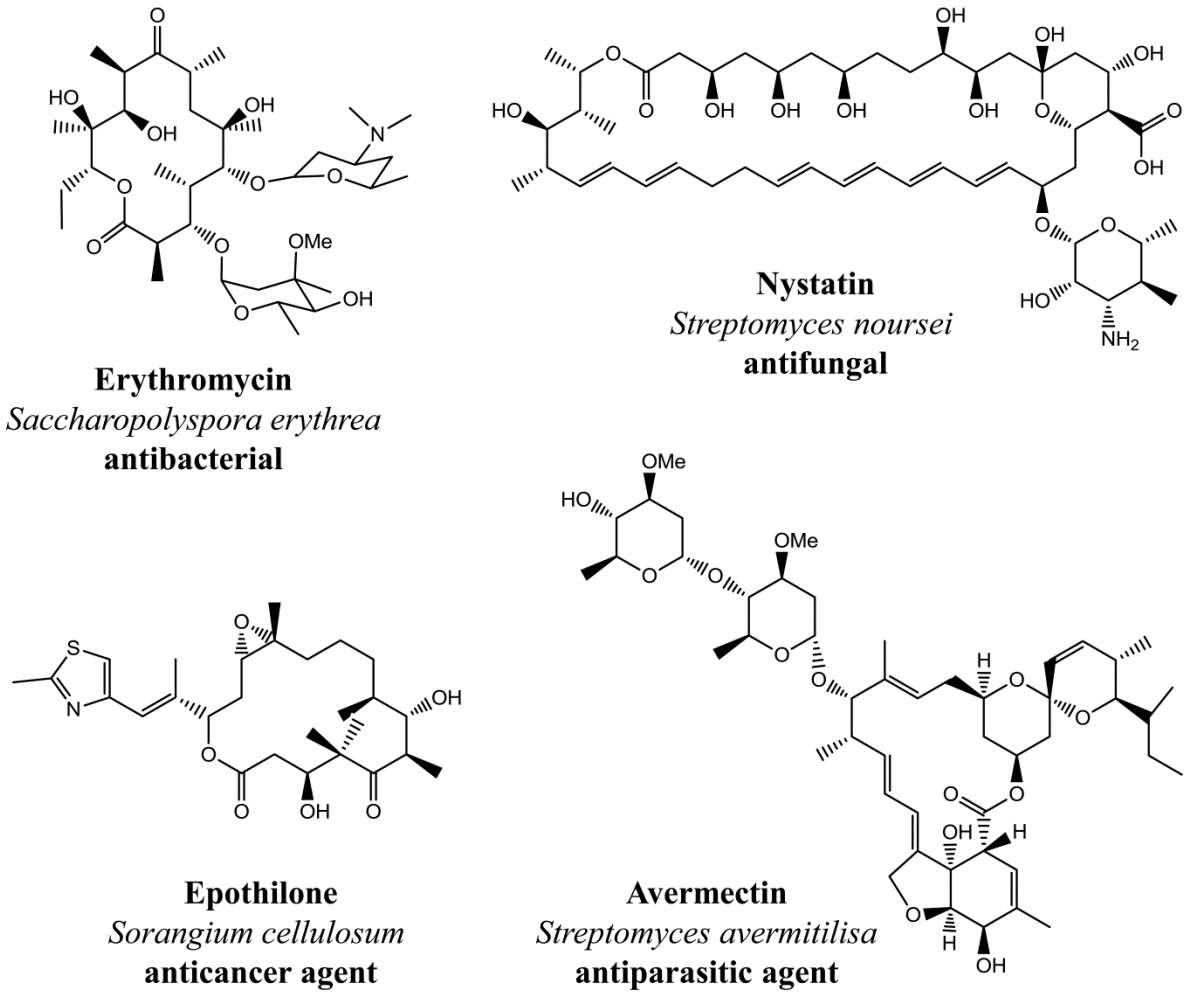

Figure 1.4: Examples of biologically active PKs.

Some well-known NRPs include antibacterial vancomycin (Samel et al., 2008) and the PKs/NRPs anticancer agent bleomycin (Shen et al., 2002) and immunosuppressant cyclosporin A (Weber et al., 1994) (**Figure 1.5**).

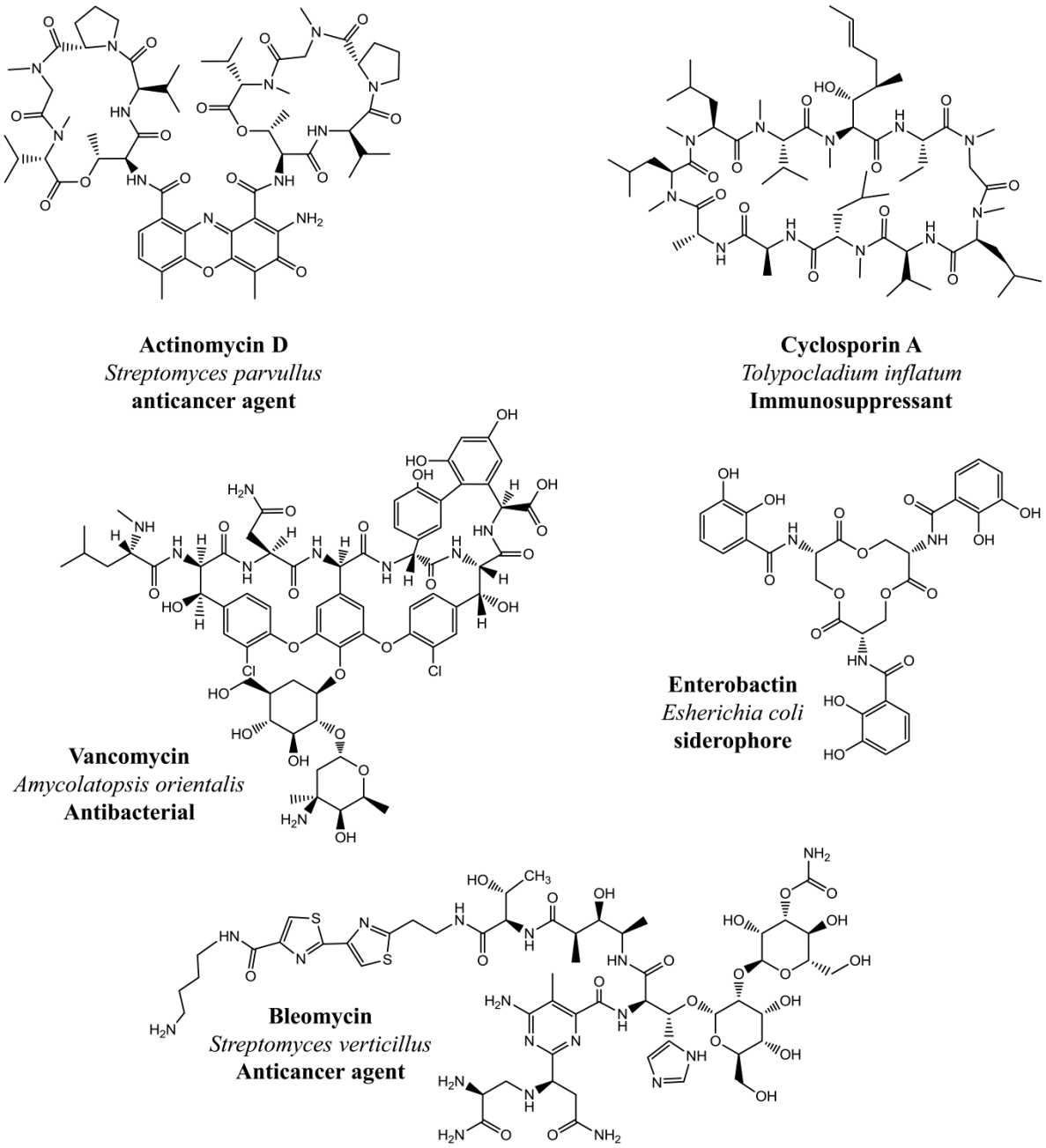

Figure 1.5: Examples of biologically active NRPs and PKs/NRPs.

1.2.1 Polyketide biosynthesis

PKs are assembled by multifunctional enzyme complexes called polyketide synthases (PKSs) through repetitive decarboxylative Claisen condensations of specific building blocks. PKSs typically composed of repeated modules with distinct functions. Each module minimally consists of three domains: a ketosynthase (KS), an acyl carrier protein (ACP) and an acyltransferase (AT). The starter and extender units are present in the host as coenzyme A (CoA)

thioesters. PKSs mostly utilize acetyl-CoA or propionyl-CoA as starter units and malonyl-CoA and methylmalonyl-CoA as the common extender units. However, malonyl-CoA and methylmalonyl-CoA can also be utilized as starter units (Leadlay et al., 2001; Waldron et al., 2001) and CoA derivatives of other carboxylic acids can also serve as extender units, such as ethylmalonyl-CoA and methoxymalonyl-CoA (Reeves et al., 2001; Haydock et al., 1995). The simplest starter unit acetyl-CoA is attached to a cysteine thiol of KS domain catalyzing condensation. The chain extender unit malonyl-CoA is bound to a thiol residue of ACP. During the condensation between acetyl and malonyl units, one unit of CO_2 is released to yield an extended chain in the form of a β-keto ester bound to the ACP (**Figure 1.6**).

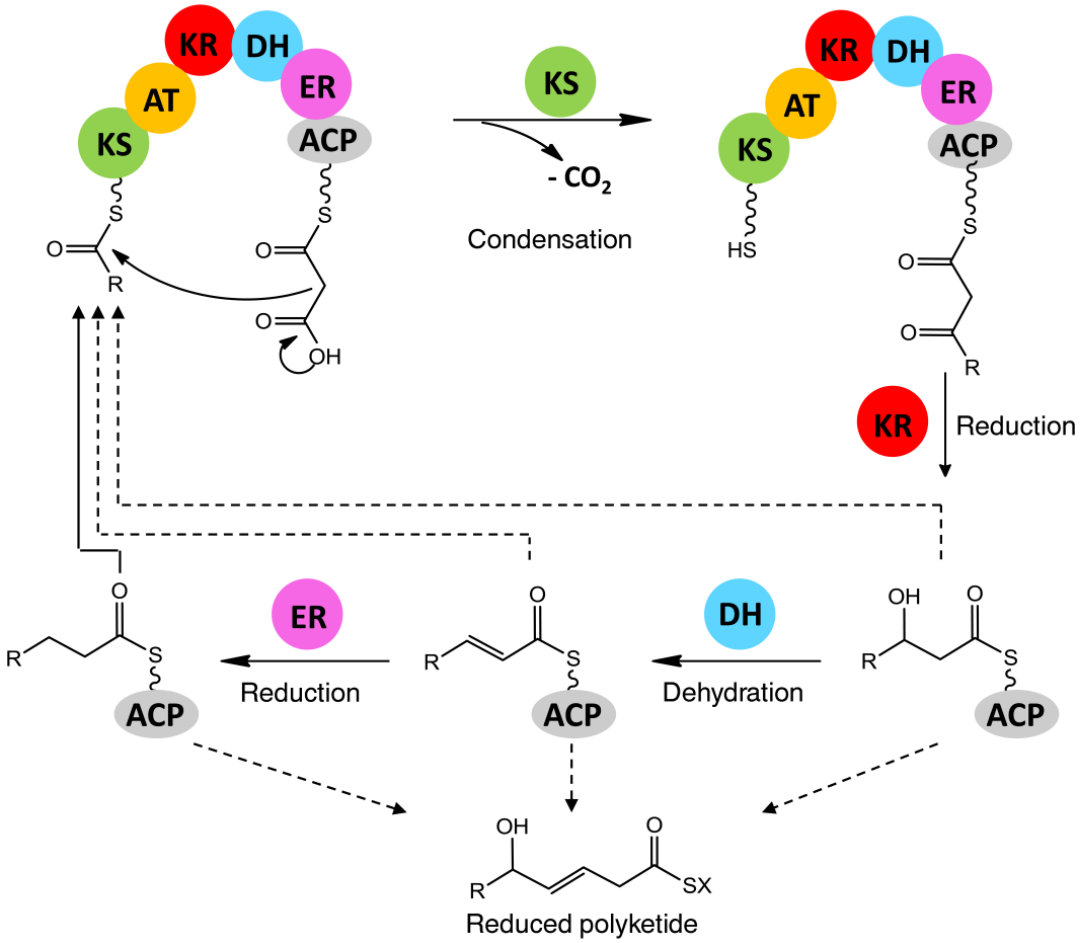

Figure 1.6: Basic steps during polyketide biosynthesis.

The 4'-phosphopantetheine (4'-PP) residue attached to ACP, which functions as a long flexible arm that carries the growing chain and delivers it to the KS domain in the following module for

the next cycle of chain elongation (Staunton and Weissman 2001). PKS modules often contain some additional domains for various functional modifications on the polyketide chain. For example, the hydroxyl group is catalyzed by ketoreductase (KR) domain, the removal of H_2O is caused by dehydratase (DH) domain and the formation of a fully saturated bond is from enoyl reductase (ER) domain (Peirú et al., 2010). In general, the initiation and termination modules are slightly different from PKS extension modules. An initiation module often lacks a KS domain and the starter unit is selected by AT domain and transferred to the ACP domain, generating the activated thioester bond (Fischbach and Walsh 2006). The termination module takes place at the last stage of polyketide synthesis to release the final polyketide catalyzed by the thioesterase (TE) domain (Fischbach and Walsh 2006).

Based on the modular features of the PKSs, PKSs are generally categorized into three types: type I, type II and type III PKSs. The PKSs are also can be divided into two classes, iterative and noniterative PKSs. Type I PKSs are multimodular megasynthases composed of linearly arranged domains. In noniterative type I PKSs, each extension module only catalyzes one elongation cycle, which is collinear with the sequence of biosynthetic reactions of PKs. Consequently, the chemical structures of the PKs can be predicted according to the order of PKSs genes and *vice versa* (Hertweck 2009). A well-known example is the erythromycin A PKS, 6-deoxyerythronolide B (6-dEB) synthase (DEBS) from *Saccharopolyspora erythraea* (Donadio and Katz 1992). One propionate starter unit and six units of methylmalonyl-CoA extender are assembled by this PKS to give 6-dEB, as a moiety of erythromycin A. The entire PKS (DEBS) consists of three polypeptides, DEBS1, DEBS2 and DEBS3. Each DEBS contains two modules that participate in the chain elongation and modification to build up a linear polyketide chain that is finally released into 6-dEB catalyzed by TE (Cortes et al., 1990) (**Figure 1.7**).

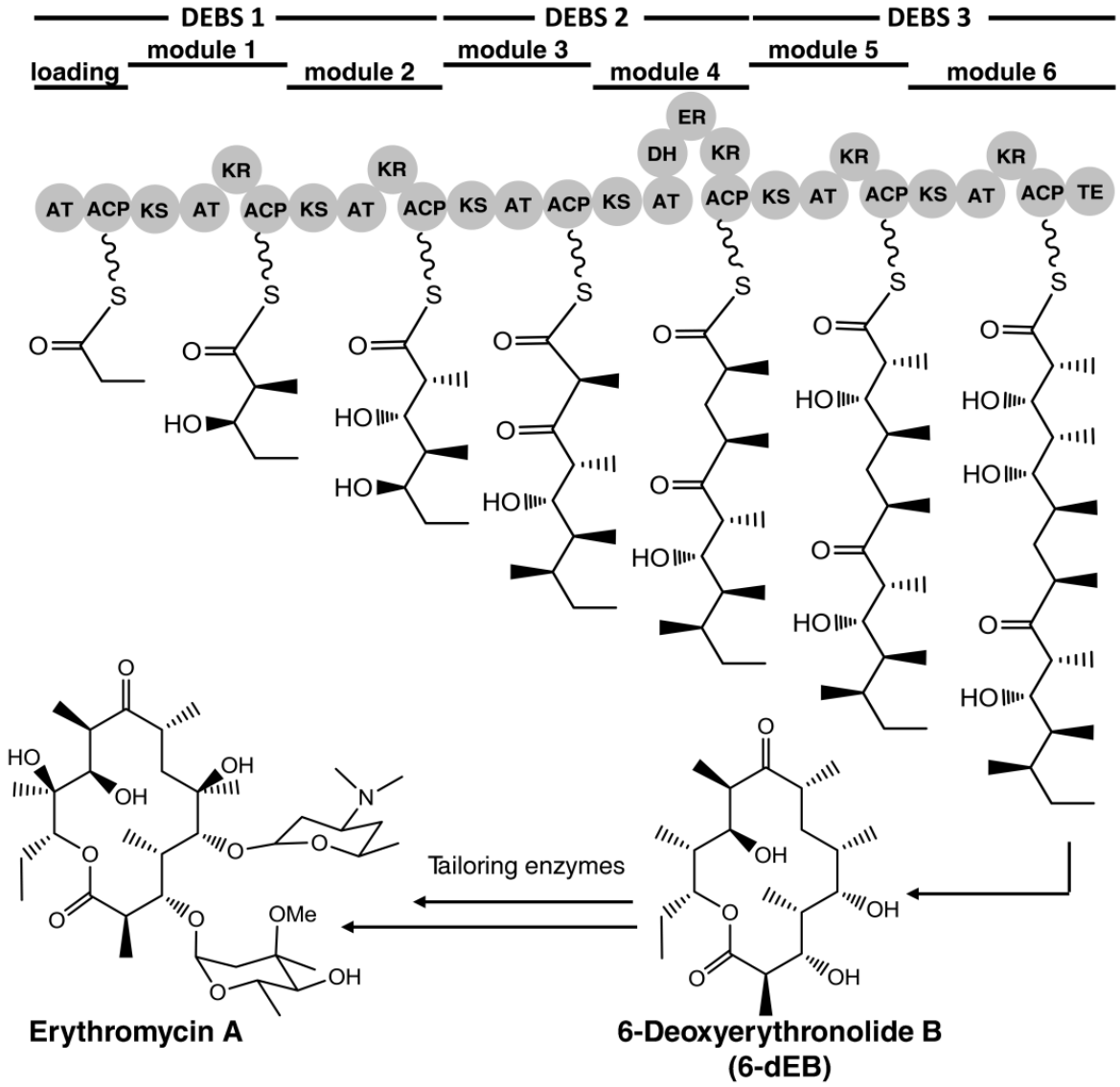

Figure 1.7: The biosynthetic pathway of erythromycin A that is a well-known polyketide assembled by type I PKS. Adapted from (Cortes et al., 1990). The entire PKS contain six modules. Each module consists of three domains, KS, AT and ACP. Some modules possess optional domains for modifications such as, KR, DH, and ER.

However, some recently discovered type I PKSs do not follow the one-to-one correspondence relationship between the PKS architectures and the chemical structures of PKs. In these enzymes, each module lacks an integral AT domain. As opposed to the *cis*-AT PKSs, the essential AT activities are carried out in *trans* by free-standing ATs encoded by genes that are physically separated from the PKS genes (Piel 2002; Cheng et al., 2003). Therefore, this type of PKSs is referred to as *trans*-AT PKSs. In comparison with *cis*-AT PKS-derived PKs, the metabolite structures assembled by *trans*-AT PKSs are usually difficult to be predicted following the co-linearity rule owing to the presence of several unusual sets of domains.

Phylogenetic studies also suggest that multimodularity in *cis*- and *trans*-AT PKSs evolved independently (Jenke-Kodama et al., 2006). *Trans*-AT PKS-derived PKs have been isolated from many bacteria, insects and marine sponges (**Figure 1.8**) (Piel 2010), most of which possess bioactivities and some may be used as antibiotics or potential anticancer agents. Deep investigation of the biosynthetic enzymology of these remarkable natural products will lead to the discoveries of novel natural products by combinatorial biosynthesis.

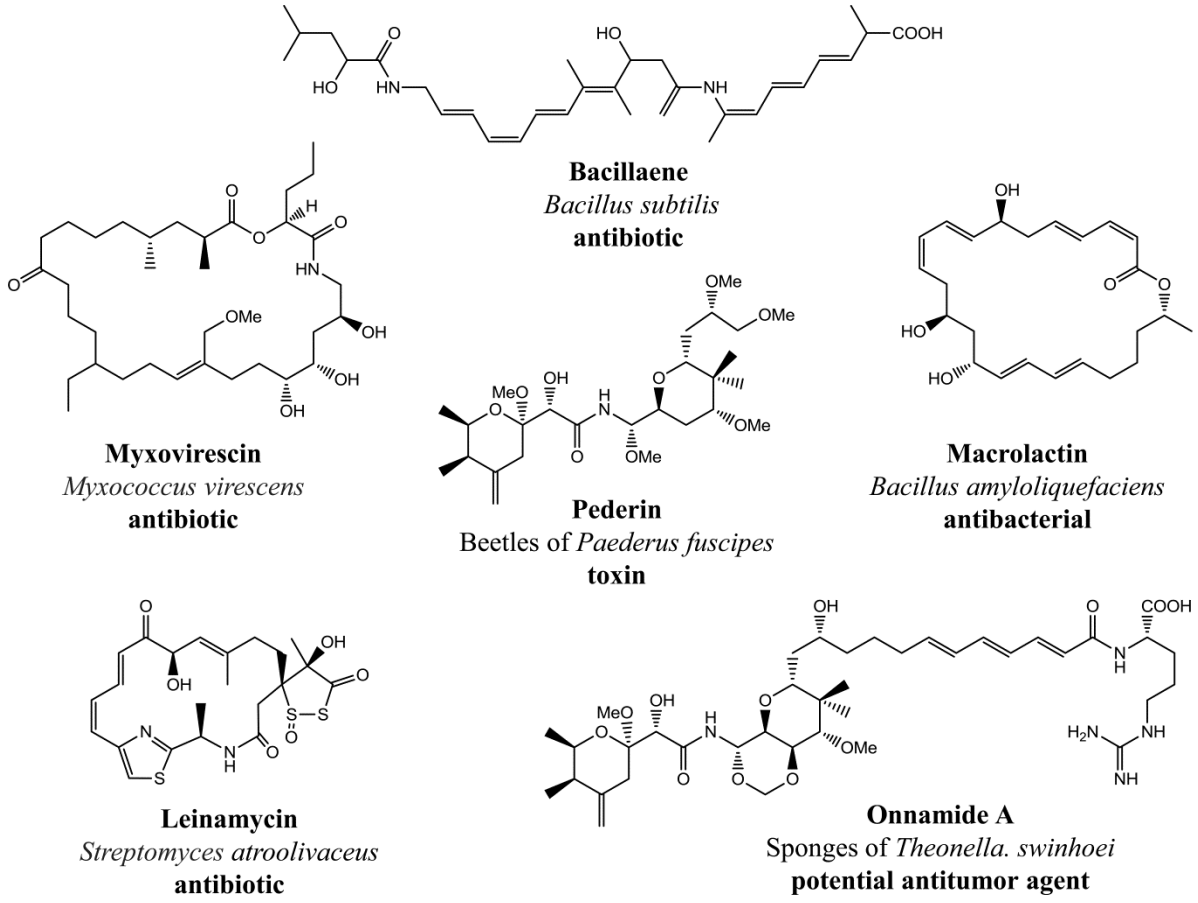

Figure 1.8: Examples of bioactive *trans*-AT PKS-derived PKs.

In contrast to the multimodular enzymes mentioned above, iterative type I PKSs possess one large multidomain module carrying all the active sites required for polyketide biosynthesis, The single multifunctional protein is used iteratively to catalyze multiple cycles of chain extension and subsequent β-keto processing. These PKSs are typically involved in the biosynthesis of fungal polyketides, such as 6-methylsalicylic acid (Staunton and Weissman 2001) (**Figure 1.9**) and lovastatin (Kennedy et al., 1999).

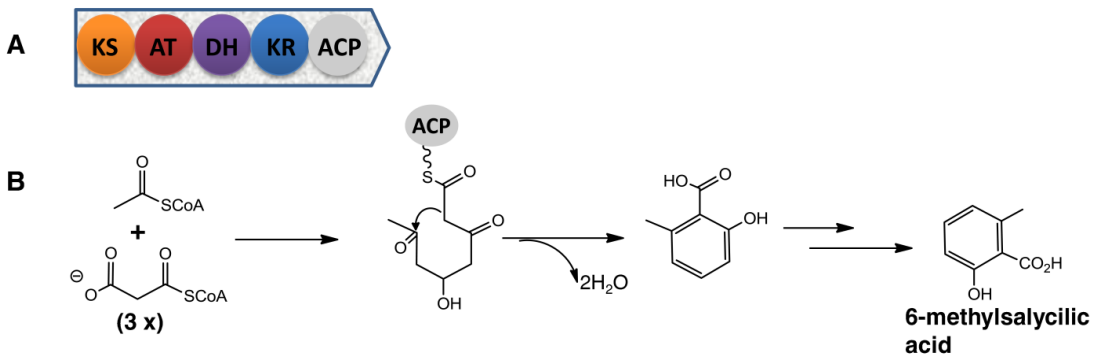

Figure 1.9: The organization of domains in iterative type I PKSs and biosynthetic pathway of 6-methylsalycilic acid. **A,** An iterative type I PKS, is one large multidomain protein assembled by following domains, KS, MAT, DH, KR and ACP, which is iteratively used during the polyketide biosynthesis. **B,** Biosynthesis of 6-methylsalycilic acid

Type II PKSs consist of multiple proteins, each of which is mono-functional. An example is the aromatic polyketide actinorhodin that is produced by *S. coelicolor* A3(2), the biosynthesis of which is assembled by type II PKSs (**Figure 1.10**).

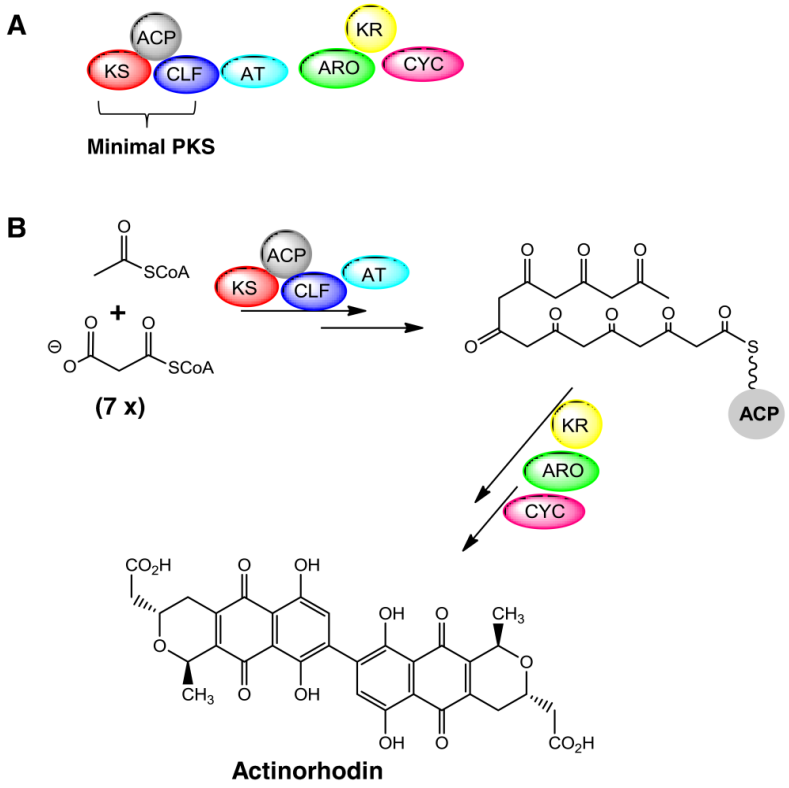

Figure 1.10: The organization of proteins in type II PKSs and biosynthetic pathway of actinorhodin. **A,** Type II PKSs consist of multiple mono-functional subunits, KS, CLF, ACP, AT, KR, ARO and CYC. **B,** Biosynthetic pathway of actinorhodin.

These proteins are used iteratively for the assembly of the polyketide chain. Within type II PKSs, the polyketide chain is built up by iterative cycles of elongation while remaining covalently tethered to an ACP scaffold and is finally modified through the action of tailoring enzymes to yield a structurally complex polycyclic aromatic compound.

Type III PKSs are homodimeric iterative PKSs and contain two independent active sites each of which catalyzes single or multiple condensation reactions to generate polyketides with different lengths. In contrast to type I and II PKSs, type III PKSs lack ACPs and KSs, but acyl-CoA substrates are incorporated directly (Shen 2003). The well-known examples of this family are plant-specific naringenin-chalcone synthases (CHSs) and stilbene synthases (STSs), providing the starting substances for the biosynthesis of a large number of biologically important substances such as phenylpropanoid metabolites (Austin and Noel 2003). CHSs and STSs are ubiquitous in plants, but type III PKSs are also present in bacteria such as *S. griseus* (Funa et al., 1999) and fungi such as *Neurospora crassa* (Funa et al., 2007; Rubin-Pitel et al., 2008);.

1.2.2 Nonribosomal peptide biosynthesis

NRPs are a big family of natural products that are synthesized by nonribosomal peptide synthetases (NRPSs), which are found in many bacteria, fungi, sponge and other higher organisms. These metabolites exhibit functional biological activities including antibiotics (e.g. penicillin, actinomycin, vancomycin, and daptomycin), siderophores (e.g. enterobactin and mycobactin), toxins (e.g. microcystins**,** nodularins, and cyanotoxins), immunosuppressive agents (e.g. rapamycin and cyclosporin), and so on (**Figure 1.5**). The assembly of nonribosomal peptide by NRPSs provides an alternative approach for the production of polypeptides via a biosynthetic pathway different from the well-known translation mechanism. NRPSs are organized in modules, each of which is usually responsible for the incorporation of an amino acid into the growing peptide chain (**Figure 1.11**) (Condurso and Bruner 2012). The structural diversity of nonribosomal peptides depends on the number and order of modules within NRPSs. Each module minimally consists of an adenylation (A), a thiolation (T) or a

peptidyl carrier protein (PCP), and a condensation (C) domain (Fischbach and Walsh 2006; Felnagle et al., 2008; Condurso and Bruner 2012).

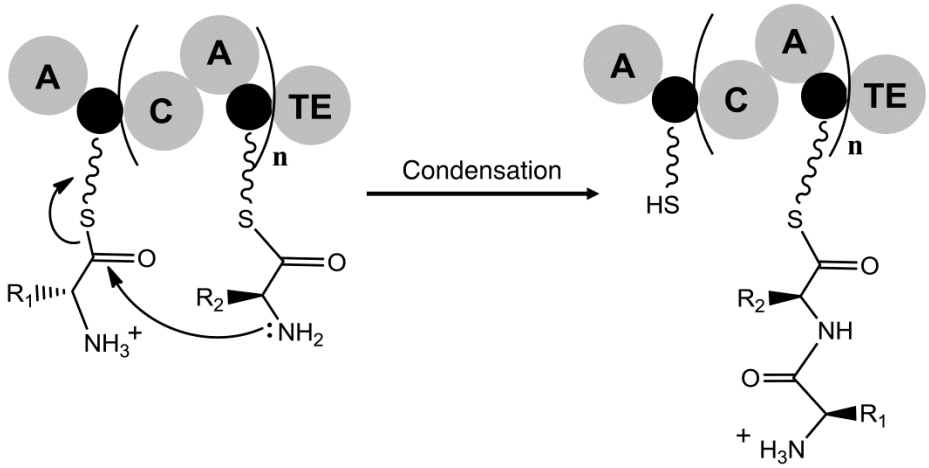

Figure 1.11: The reaction mechanism involved in nonribosomal peptides biosynthesis. Black ball, PCP or T domain.

The amino acid residue is selectively activated by A domain as amino acyl adenylate at the expense of ATP and Mg^{2+}. The thiol moiety 4'PP attached to PCP attacks to the activated amino acid to form an aminoacylthioester intermediate via thiolation (Finking and Marahiel 2004). The C domain is responsible for catalyzing the peptide bond formation between two activated amino acids on adjacent modules to yield the growing peptide chain through condensation. Additional tailoring domains optionally present in each individual module such as formylation (F), cyclization (CYC), oxidation (Ox), reduction (Red), N-methylation (NMT) and epimerization (E) for modifications of amino acids. After a series of repeating steps of adenylation and condensation, the growing peptide chain reaches the final module containing a TE domain. This TE domain catalyzes the release of final product. Very often, the final peptide undergoes multiple modifications, such as glycosylation, acylation, halogenation or hydroxylation, to yield structurally diverse natural products that exhibit various biological activities. Such modification genes are unusually associated with NRPS genes and organized in the same gene clusters (Fischbach and Walsh 2006; Felnagle et al., 2008; Condurso and Bruner 2012).

The assembly mechanisms involved in the biosynthesis of NRPs and PKs as well as the modular architectures of NRPS and PKS system have provided the basis to generate the natural product-like compounds via genetically engineering the known biosynthetic pathways, such as combinatorial biosynthesis and precursor-directed biosynthesis. With these foundations, novel structurally and functionally diverse natural products can be discovered through genome mining.

1.3 Combinatorial biosynthesis

Since the first hybrid "unnatural" natural product, mederrhodin A, was generated via the genetic manipulation of PKS biosynthetic pathway between *S. coelicolor* A3(2) and *Streptomyces sp.* AM-7161 (Hopwood et al., 1985), combinatorial biosynthesis has become a promising and efficient tool for (Floss 2006; Menzella and Reeves 2007) developing novel structurally diverse natural products via genetically engineering the biosynthetic pathway of natural products. To develop new compounds with potential pharmaceutical use, this strategy depends on enzymes with broad substrate tolerance for improving the properties of drugs, such as absorption, toxicity and excretion.

Manipulation of modular PKSs and NRPSs has been the major focus of combinatorial biosynthesis, contributing to the production of more structurally diverse natural compounds libraries (Menzella and Reeves 2007). The modification of compounds by combinatorial biosynthesis generally relies on whether this compound is made through linear or branched biosynthetic pathway. For example, in the linear biosynthetic pathway, the modifications of single or multiple domains in one module of multifunctional PKS involved in erythromycin biosynthesis led to 61 different 6-DEB analogs (McDaniel 1999). The novel compounds can also be generated by introduction of modification domains involving in glycosylations, methylations, oxidations, halogenations, and epimerizations. For instance, the *Streptomyces peucetius dnmV* mutant defective in the biosynthesis of daunosamine, a sugar moiety in daunorubicin, was replaced by the *eryBIV* gene from the erythromycin producer

Saccharopolyspora, resulted in a strain producing the antitumor drug of 4'-epidoxorubicin (Madduri et al., 1998). Combinatorial expression of *hrmQ* encoding a halogenase in HRM biosynthesis with genes of the clorobiocin gene cluster led to the production of hybrid aminocoumarins with an additional chlorine (Heide et al., 2008). However, in a branched biosynthetic pathway, the compound is usually assembled from several components biosynthesized separately. Each biosynthetic building block can be switched into similar components derived from other organisms, leading to the generation of hybrid compounds. For instance, novclobiocin 102 or novclobiocin 114 was created by exchange of biosynthetic genes involved in novobiocin and chlorobiocin biosynthesis from two different *Streptomyces* spp. (Eustaquio et al., 2004).

In addition to engineering biosynthesis of polyketides, there is current interest in engineering NRPSs to generate peptide with potential bioactivities. According to the assembly mechanism of NRPSs, the structural diversity of peptides mostly depends on the precursors that can be incorporated into nonribosomal peptides, including different amino acids, aromatic acids or hydroxyl acids. It is known that the A domain is responsible for recognition, activation, and incorporation of different precursors into peptides. Therefore, the substrate selectivity of A domain can be changed via mutation of several amino residues in substrate-binding pocket (Stachelhaus et al., 1999; Challis et al., 2000; Eppelmann et al., 2002).

1.4 Precursor-directed biosynthesis

Precursor-directed biosynthesis (PDB) represents a means to generate the analogues of known clinically important natural products by feeding unnatural precursors into producing organisms (**Figure 1.12**). These precursors can be recognized and incorporated into the enzymatic cascades to give new compounds PDB is often applied in providing a series of structurally diverse analogues of PKs and NRPs. Many clinically important natural product analogues have been generated successfully via this approach.

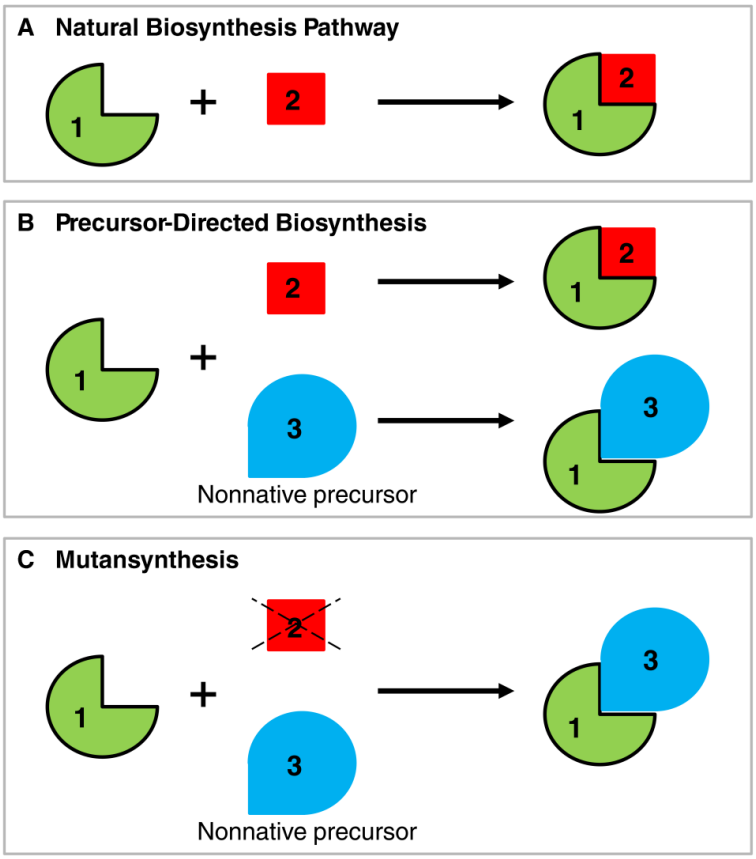

Figure 1.12: The general principle of precursor-directed biosynthesis and mutasynthesis. **1**, a substance (in green); **2**, a native precursor (in red); **3**, a nonnative precursor (in blue); **1+2**, a natural product; **1+3**, a precursor-directed product. **A,** Natural biosynthesis. **2** is incorporated into **1** to form **1**+**2**. **B,** Precursor-directed biosynthesis. **3**, as a competitor of **2**, is fed into the fermentation culture, leading to the production of **1+2** and **1+3**. **C**, Mutasynthesis. The fermentation broth of a mutant strain, which is unable to provide **2**, is fed with **3**, only resulting in the production of a single product **1+3**.

There are many successful examples of PDB. The β-lactam antibiotic penicillin V (phenoxymethylpenicillin) is generated by adding the phenoxyacetic acid to the fermentation broth of *Penicillium chrysogenum* (Demain and Elander 1999). 15-propargyl erythromycin A, a novel antibiotic, as equipotent as the widely used macrolide erythromycin A was generated by feeding a set of diketides into an engineered *E. coli* strain evolved for improved polyketide production (Harvey et al., 2012). A library of ammosamides G-P was created through adding a variety of aryl and alkyl amines into the fermentation media of *Streptomyces variabilis* (Pan et al., 2013).

However, PBD often leads to a mixture of natural and unnatural products with similar physical properties, thus the difficulties in separation of this mixture will be a basic problem for PDB

(Kennedy 2008). Thereby, mutasynthesis, as an alternative approach of PDB, is derived from PDB. The only difference between these two methods is that the desired novel compound can be generated efficiently through mutasynthesis by feeding a particular precursor into a mutant strain that is deficient in the natural product biosynthetic pathway.

The principle of mutasynthesis was first proven by the generation of four new analogues of neomycin via feeding a mutant of *Streptomyces fradiae* 3535 unable to synthesize the antibiotic neomycin with aminocyclitols streptamine and 2-epistreptamine (Shier et al., 1969). The term "Mutasynthesis" was firstly coined by Rinehart *et al.* (Kenneth 1977) and originally proposed to be an alternative approach to classical PDB, leading to increased titres of the target natural product analogues with structural diversity (Birch 1963). Many of applications of mutasynthesis have been successful since the first demonstration in 1969. Some examples are summarized in **Table 1.1**.

Table 1.1: Some important compounds generated via mutasynthesis.

Mutants	Nonnative precursors	Product	Activity	Reference
Streptomyces avermitilis	Cyclohexanecarboxylic acid	Doramectin	Antiparasitic	(McArthur 1998)
Streptomyces fradiae	Streptamines; Epistreptamine	Hybrimycins; Neomycins	Antibiotic	(Shier et al., 1969); (Rinehart 1977)
Streptomyces tendae Tü901	Pyrimidines; Benzoic acid derivatives	Nikkomycin X and Z; Nikkomycin Bx/Bz	Insecticidal and acaricidal; Antibiotic	(Delzer et al., 1984); (Bormann et al., 1999)
Pseudomonas aeruginosa	Salicylic acid analogues	Pyochelins	Iron transporter	(Ankenbauer et al., 1991)
Streptomyces roseochromogenes	3-dimethylallyl-4-hydroxybenzoic acid analogues	Clorobiocin analogues	Antibiotic	(Galm et al., 2004)
Streptomyces hygroscopicus	4,5-dihydroxycyclohex-1-enecarboxylic acid analogues	Rapamycin analogues	Anticancer agent	(Ritacco et al., 2005)
Streptomyces parvulus Tü4055	different dicarboxylic acid	Borrelidin analogues	Antibiotic; antimalarial	(Moss et al., 2006)

In addition to the examples listed above, there still remain further important applications of mutasynthesis. For instance, reblastatin analogues were generated via adding 3-amino-5-hydroxybenzoic acid (AHBA) analogues into the mutant of geldanamycin producer *Streptomyces hygroscopicus* K390-61-1, which provide the potential candidates of antitumor agents (Rascher et al., 2005). The new ansamitocin derivatives belonging to maytansinoids, as "warheads" in tumor-targeted immunoconjugates (Yu 2005), were prepared by feeding aminobenzoic acid analogues into fermentation cultures of *Actinosynnema pretiosum* HGF073 that is unable to synthesize the required starter unit AHBA, which offer the basis for structure-activity relationship (SAR) studies (Knobloch et al., 2011).

PDB has been demonstrated as a powerful tool to yield a series of analogues of known important drugs, some of which possesses novel activities. However, it still has limitation that the resulting compounds often lack structural diversities. Therefore, recently developed genome mining is becoming a promising strategy to discover structurally and functionally diverse novel natural products.

1.5 Genome mining for natural product discovery

Genome mining is a technique to seek and identify genes responsible for the biosynthesis of natural products based on the full genome sequence data of a variety of organisms (**Figure 1.13**) (Challis 2008b).

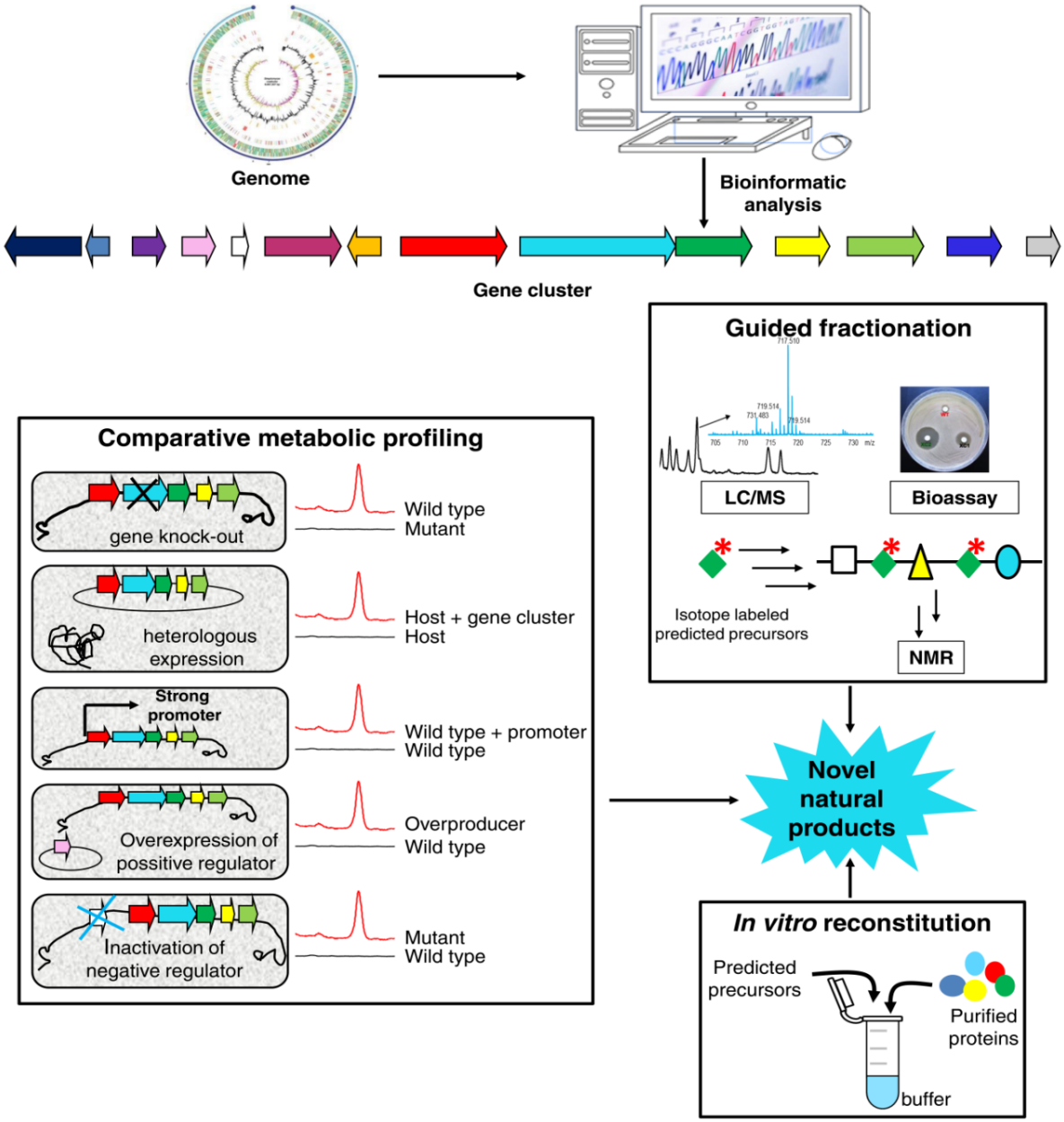

Figure 1.13: Genome mining for natural product discovery.

Comparative analysis of whole genome sequences can reveal biosynthetic gene clusters for potential new secondary metabolites that are not structurally related to previously uncovered compounds and often are overlooked under standard cultivation conditions. The likely reason is that the gene clusters encoding these new secondary metabolites are usually silent or barely expressed (Winter et al., 2011). The whole genome sequencing of a wide range of organisms, including actinomycetes, myxobacteria, cyanobacteria, fungi, and plants revealed the metabolic capacities of these organisms to produce a wide range of structurally complex natural products with diverse bioactivities. Many novel natural products have been successfully discovered by

genome mining, including polyketides, nonribosomal peptides, as well as terpenes (**Figure 1.14**).

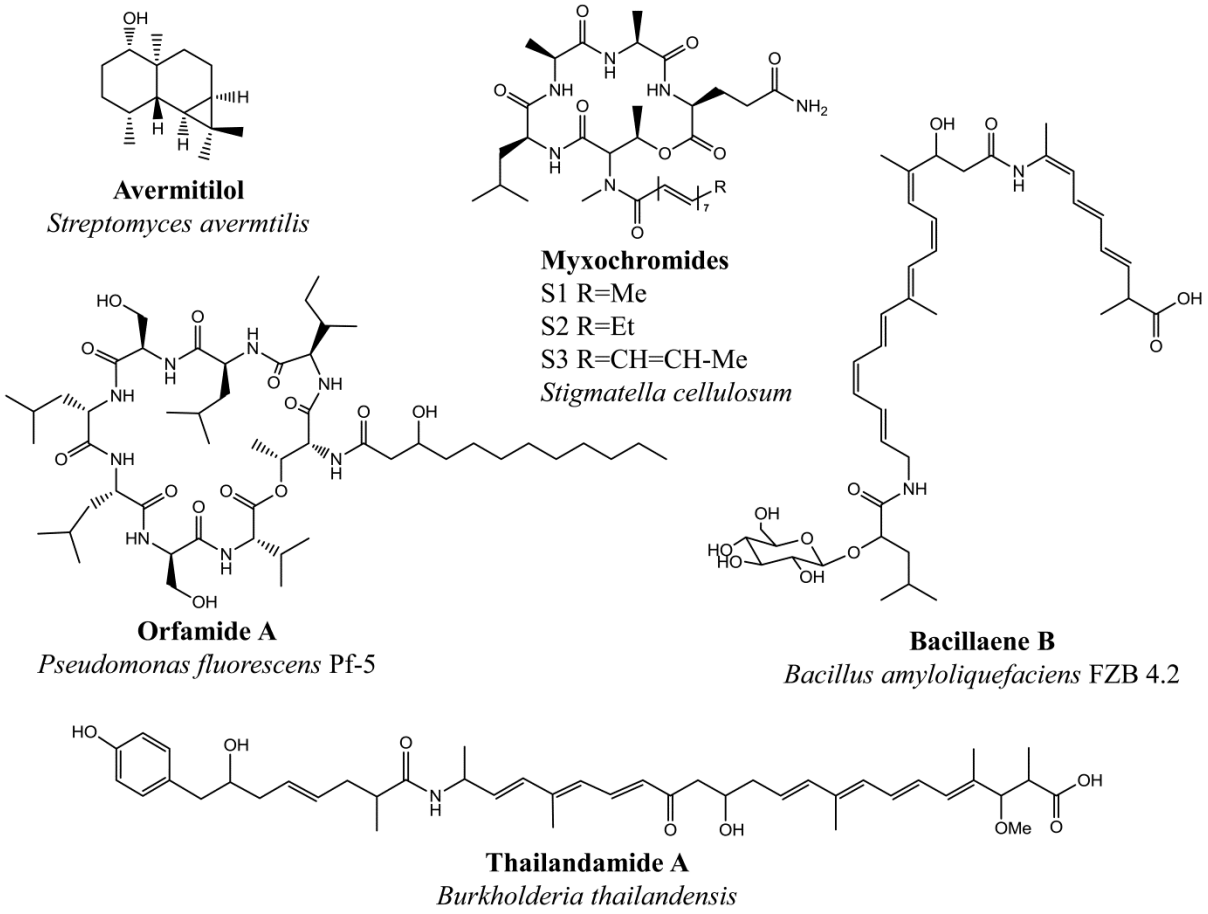

Figure 1.14: Some natural products discovered by genome mining.

The co-linearity rule of modular PKSs and NRPSs has facilitated the logical prediction of the structural features of new natural products assembled by these two systems that are unveiled by genome sequencing (Fischbach and Walsh 2006). Typically, more than one PKSs or NRPSs modules are responsible for the biosynthesis of polyketides or nonribosomal peptides. AT domains in PKS modules or A domains in NRPS modules generally share conserved sequence motif, which suggests their substrate specificity (Haydock et al., 1995; Stachelhaus et al., 1999; Challis et al., 2000). The presence of tailoring domains in individual modules often allows us to predict that the metabolic building blocks get modified initially before its incorporation into the final products (Fischbach and Walsh 2006). The structural features of cryptic metabolites can often be derived via application of the above bioinformatic analysis

and their assembly line modular systems (Challis and Ravel 2000; McAlpine et al., 2005; Banskota et al., 2006; Nguyen et al., 2008; Chen et al., 2007; Freeman et al., 2012).The putative physico-chemical properties of cryptic metabolites also can be predicted based on the above derived structural features. Thus, the cryptic products with predicted physico-chemical properties can be easily screened and analyzed in their fermentation broths. This approach has been successfully employed for discovery of several natural products from cryptic pathways (Lautru et al., 2005; McAlpine et al., 2005; Banskota et al., 2006)

The genomisotopic approach is another approach to uncover the cryptic metabolites by feeding isotope-labelled predicted precursors of the natural products into the fermentation broths of organisms. The target compound can be subsequently identified by radio-liquid chromatography-mass spectrometry (radio-LC-MS) or nuclear magnetic resonance (NMR). For example, the culture of *Pseudomonas fluorescens* Pf-5 was fed with L-[^{15}N]Leu, enabling the targeted purification of the novel cyclic lipopeptide orfamide A guided by ^{1}H-^{15}N heteronuclear multiple-bond correlation spectroscopy (HMBC) NMR (Gross et al., 2007). This approach is of value to be applied in the discovery of peptides, particularly peptides containing non-proteinogenic building blocks, but less useful in polyketide targeting.

Another very important approach to unveil unknown metabolites is comparative metabolic profiling of wild type and mutants. For this purpose, the essential genes involved in PKSs and NRPSs governing the biosynthesis of secondary metabolites have to be inactivated. Subsequent comparative metabolic profiling between wild type and its mutants by high performance liquid chromatography (HPLC) shows the corresponding natural compounds in the wild type strain. For instance, myxochromides S1-3 (**Figure 1.14**) isolated from *Stigmatella cellulosum* are identified by this approach (Wenzel et al., 2005), and bacillaene B from *Bacillus amyloliquefaciens* FZB 42 (**Figure 1.14**) assembled by *trans*-AT PKS/NRPS (Chen et al., 2006; Moldenhauer et al., 2010).

Heterologous expression of entire cryptic gene clusters has become a promising alternative way to detect the corresponding natural products. The *sav76* gene encoding the terpene synthase of *S. avermitilis* was heterologously expressed in *E. coli* (Chou et al., 2010). Incubation of resulting protein with farnesyl diphosphate led to the isolation and characterization of avermitilol (**Figure 1.14**) which was not detected in the wild type strain, *S. avermitilis* (Chou et al., 2010). Extra copies of *sav76* were introduced into the genome-minimized *S. avermitilis* mutant (Komatsu et al., 2008) under control of the native promoter, which led to the production of avermitilol, along with small amounts of avermitilone, germacrene A, B and viridiflorol. The corresponding terpene synthases have been determined in the *S. avermitilis* genome (Chou et al., 2010). It also has been demonstrated that cryptic microviridin gene clusters from cynobacteria can be heterologously expressed in *E. coli* (Ziemert et al., 2010).

In addition to the approaches described above, some other strategies also have been applied in activation of silent gene clusters to obtain the novel natural products. For instance, comparative metabolic profiling (Bok et al., 2006; Bergmann et al., 2007), *in vitro* reconstitution (Lin et al., 2006) and cocultivation of different organisms to trigger the expression of silent gene cluster (Bertrand et al., 2013; König et al., 2013).

Natural product biosynthesis is often governed by complex regulation systems in their organisms. It has been demonstrated that manipulation of regulatory genes located in silent gene clusters can lead to the discovery of novel natural products (Gottelt et al., 2010; Bergmann et al., 2007). The genus *Streptomyces* is a very important source for natural products, the genome of which contains dozens of secondary metabolites gene clusters besides those for characterized compounds (Bentley et al., 2002). The regulation system in *Streptomyces* spp. is particularly complex and controls not only gene expression during development but also at the onset of antibiotic production (Bibb 2005). Thereby, investigation of regulatory genes in *Streptomyces* spp. can provide important insights into drug discovery.

1.6 Regulation of antibiotic biosynthesis in *Streptomyces* spp.

Previous studies suggested that the expression of physically distinct gene clusters in the chromosome are usually subjected to multiple levels of regulation (Bibb 2005; Huang et al., 2005). The regulators encoded by genes located within gene clusters are referred to as pathway-specific regulators. Such regulators often play a key role in triggering the expression of their own biosynthetic gene clusters, which belong to "low level" regulators. Some of these regulators are the only key factors in triggering the onset of antibiotic biosynthesis. Overexpression of such regulatory genes may lead to the significant increase of antibiotic production (Gramajo et al., 1993). The onset of the antibiotic biosynthesis is often coordinately controlled by both pathway-specific regulators and pleiotropic regulators. In contrast to pathway-specific regulatory genes, pleiotropic regulatory genes are usually situated outside of the biosynthetic gene clusters and involved in the regulation of multiple antibiotics biosynthesis and morphological differentiation in a " higher level" way (Huang et al., 2005).

Pathway-specific regulators can be broadly classified into two families, SARP (*Streptomyces* antibiotic regulatory protein) family, and LAL (Large ATP-binding regulators of the LuxR) family (Bibb 2005). SARPs, are also known as OmpR family containing an OmpR-like DNA-binding domain, which have been found involved in the regulation of production of a wide variety of secondary metabolites. For example, ActII-ORF4 and RedD governing the production of actinorhodin (ACT) and undecylprodigiosin (RED), respectively in *S. coelicolor* A(3)2 (Arias et al., 1999; Takano et al., 1992); Takano et al., 1992), and SfmR2 and SfmR3 controlling saframycin production in *Streptomyces lavendulae* (Li et al., 2008). Among above examples, it has been shown that *actII-ORF4* and *redD* are positive regulatory genes that contain TTA codon as a special feature. However, some exception still exists. For instance, AfsR, as one of well-understood SARP family proteins, belonging to pleiotropic regulators, is encoded by *afsR* gene which is located outside of any gene cluster in *S. coelicolor* A3(2) and it has direct or indirect effect on at least two secondary metabolites biosynthesis. Relative to the SARP family, the LAL family is little understood of their overall role in the regulation of

antibiotics production. These proteins possess an ATP/ADP-binding domain at the N terminal end and a DNA-binding domain at the C terminal end (Henikoff et al., 1990). For example, PikD involved in pikromycin production and three LAL homologues encoded in nystatin gene cluster (Wilson et al., 2001). Studies about the mutation or deletion of these proteins suggest the presence of a more complex regulatory cascade governing the production of these natural products (Bibb 2005).

The pleiotropic regulators characterized so far mostly respond to environmental changes such as nutrition conditions, pH or temperature, and function as global regulators to control both morphological differentiation and secondary metabolites in *Streptomyces* spp.. Stress caused by nutritional limitations can contribute to the generation of intracellular signaling messengers. For instance, when *S. colicolor* A3(2) is grown on media under conditions of amino acid starvation, the pleiotropic regulatory gene, *relA* is triggered and translated into a stringent factor ppGpp (Chakraburtty and Bibb 1997). This signaling molecule subsequently governs the antibiotic biosynthesis in *S. coelicolor*. Growing the *relA* mutant under the condition of nitrogen limitation leads to the defective biosynthesis of ppGpp, which fails to produce ACT and RED (Hesketh et al., 2001; 2007). These results indicate that ppGpp directly activates the pathway-specific regulators of ActII-ORF4 and RedD for the production of ACT and RED (Hesketh et al., 2007). Except for the failure in the biosynthesis of ACT and RED, the *relA* mutant shows a remarkable effect on morphological differentiation. The mutant exhibits a large white colony that is conspicuously different from the small grey colony from wild type strain (Chakraburtty and Bibb 1997). However, the phenotype of *relA* mutant can be restored by growing under conditions of phosphate limitation (Hesketh et al., 2001). DasR, a pleiotropic transcriptional repressor, inhibits the production of antibiotics. The inactivation of *das*R represses the chitin degradation and triggers the accumulation of N-acetylglucosamine (GlcNAc), a signaling molecule, and switches on the morphological development and antibiotic production (Rigali et al., 2008). Cyclic AMP receptor protein (Crp), as a master transcription regulator governs various cellular processes in many bacteria (Korner et al., 2003). In *S. coelicolor* A3(2), Crp binds to eight of 22 gene clusters and plays a key role of

controlling morphological development and antibiotics production (Derouaux et al., 2004a; 2004b). Overexpression of Crp leads to the upregulation of ACT, calcium-dependent antibiotic (CDA) and RED in *S. coelicolor* A3(2) (Gao et al., 2012). Introduction of Crp into different *Streptomyces* species activates the cryptic gene clusters to generate new secondary metabolites (Gao et al., 2012). These findings suggest that Crp, as a global regulator, provides a powerful tool for tapping the novel natural products with potential bioactivities.

The pleiotropic regulatory genes mentioned above mainly affect the antibiotics production. There are bifunctional regulators with indirect pleiotropic effect on secondary metabolites and direct influence on morphological differentiation, exemplified by the well-known *bld* genes in *S. coelicolor* A3(2). Mutants of *bld* genes fail to form aerial mycelia and subsequent sporulation, called "bald" mutants (Merrick 1976). These bald mutants are defective in secondary metabolism and colony appearance. For example, *bldA* encodes the only tRNA in *Streptomyces* recognizing leucine codon UUA. Its mutant loses the capacity to form aerial hyphae and produce antibiotics. The deficient antibiotics production in *bldA* mutant is partially due to the presence of TTA codons in pathway-specific regulatory genes controlling the biosynthesis of secondary metabolites (Chater and Chandra 2008).

In addition to pathway-specific and pleiotropic regulators, the antibiotic biosynthesis is also controlled by extracellular signaling hormones, such as, γ-butyrolactones produced by many streptomycetes. Initially, γ-butyrolactone was discovered in *S. coelicolor* A3(2); however, since the regulation system in *S. coelicolor* A3(2) is very complex and involves many regulatory cascades, the mechanism is still not clear. The characterized γ-butyrolactone is 2-isocapryloyl-3*R*-hydroxymethyl-γ-butyrolactone (A-factor) isolated from *S. griseus* (Horinouchi and Beppu 1992). In general, A-factor is required for development and secondary metabolism. AsfA is essential for the biosynthesis of A-factor. When the concentration of A-factor reaches a critical point, A-factor binds to the A-factor-specific receptor (Arp) attached to the promoter of *adpA*. Then, Arp is released from the promoter, leading to the transcription of *adpA*. AdpA belongs to AraC/XylS transcriptional regulator family, and activates the

transcription of *strR*, the pathway-specific regulatory gene for streptomycin biosynthesis, and induces the expression of other regulators involved in the morphological differentiation (Ohnishi et al., 1999; 2005) (**Figure 1.15**). Among these are AmfR that induces the subsequent expression of the SapB ortholog to initiate aerial-hypha formation, SsgA required for the regulation of sporulation septation, and σ^{AdsA}, an extracytoplasmic function (ECF) sigma factor of AdsA that is only involved in aerial mycelium formation (Horinouchi 2007).

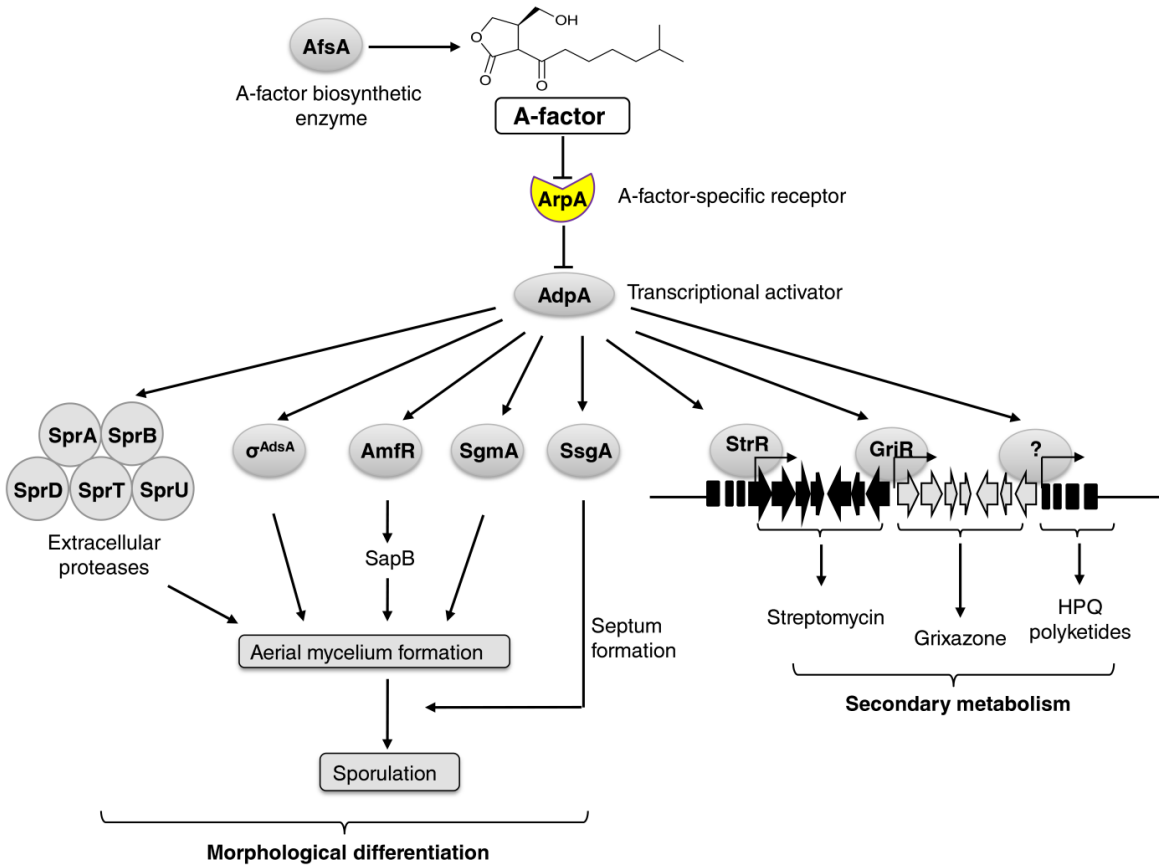

Figure 1.15: The A-factor signaling cascade in *S. griseus* (Adapted from Flärdh and Buttner, 2009). AfsA is required for the biosynthesis of A-factor. When A-factor accumulates, it will bind to its own receptor ArpA, which subsequently activate the expression of Adp regulon. AdpA, as a global regulator governs the expression of downstream genes involved in aerial mycelium formation, sporulation and secondary metabolism.

1.7 Aerial mycelium formation in *Streptomyces* spp.

The striking features of morphological differentiation in streptomycetes are the formation of aerial hyphae and subsequent sporulation presenting a fluffy grey lawn on the colony surface. *S.*

coelicolor A3(2) serves as a model for studies of both morphological development and secondary metabolism. The *bld* genes are involved in the onset of aerial mycelium formation (Horinouchi 1996). Many *bld* mutants have been generated that are defective in forming aerial hyphae (Lawlor et al., 1987; Nodwell et al., 1996; Elliot 1998; Pope et al., 1998; Bibb 2000; Bignell 2000; Molle and Buttner 2000). All the *bld* genes in *S. coelicolor* are part of a complex extracellular signaling cascade to regulate the aerial mycelium formation. The effect of *bldA* on morphological differentiation occurs through the UUA codon in the mRNA of *bldH* (Lawlor et al., 1987). BldH is analogous to AdpA in *S. griseus* controlling the development and secondary metabolism (McCormick and Flardh 2012). Most of *bld* mutants can be restored to form aerial hyphae and produce antibiotics completely or partially when they are grown on the medium with poor carbon sources, except for the *bldB* mutant (Willey et al., 1993). The *bldB* gene encodes a DNA-binding protein, involved in catabolic repression in *Streptomyces*. Mutation of *bldB* results in complete loss of antibiotics production and defective morphological differentiation (Pope et al., 1998). BldC is a putative transcriptional activator which belongs to the MerR family. The *bldC* mutants are defective in differentiation and antibiotic production on minimal medium and show severe delay on the aerial mycelium formation on rich medium (Hunt et al., 2005). BldD, as a small DNA-binding protein can bind to the promoters of *whiG*, *bldN* and *sigH* (Elliot 1998; 2001).The *bldG* gene encodes a developmental anti-anti-sigma factor, as a regulator of stress response involved in antibiotic production and sporulation (Bignell 2000). BldK is an oligopeptide importer that is responsible for the import of an extracellular signal molecule that can induce the production of secondary extracellular signal molecule acting on the products of *bldA* and *bldH* to initiate the development and secondary metabolism (Nodwell et al., 1996). σ^{BldN} encoded by *bldN* is a ECF family sigma factor that is analogous to that of σ^{BldN} in *S. griseus* , which is required for aerial mycelium formation in *S. coelicolor* (Bibb 2000). BldM, as the only known target of σ^{BldN}, is an atypical response regulator for following biological action in morphological development and secondary metabolism (Molle and Buttner 2000).

Small surface-active peptide (SapB) is required for coating the surface of *S. coelicolor* hyphae

in a hydrophobic sheath, allowing the hyphae to escape from the aqueous colony and to form aerial mycelium in the air (Willey et al., 1991). Extracellular complementation studies have demonstrated that the aerial hyphae formation of all the characterized *bld* mutants can be restored by the growth of *bld* mutants near wild-type *S. coelicolor* strain or addition of purified SapB protein (Willey et al., 1993). These findings suggest the important role of SapB in morphogenesis. SapB has been structurally characterized as a lantibiotic-like peptide, derived from *ramS* gene in *ram* gene cluster (Kodani et al., 2004). It shows no antibiotic activity but acts as an extracellular signal for the initiation of development (Kodani et al., 2004). In addition to SapB, there are at least two classes of other proteins, the chaplins and the rodlins, involved in the synthesis of the hydrophobic sheath (Flärdh and Buttner 2009; Chater 2001). The deletions of all chaplin genes in *Streptomyces* result in the failure of aerial mycelium formation on either poor or rich medium. The expression of SapB depends on the presence of chaplins (Capstick et al., 2007).

It has been demonstrated that the *bld* genes are required for the production of SapB and chaplins on rich medium (Capstick et al., 2007; Nodwell and Losick 1998; Willey et al., 1991; Willey et al., 1993). A hierarchical extracellular signaling cascade has been proposed based on the studies of extracellular complementations among all characterized *bld* mutants (Willey et al., 1991; Willey et al., 1993; Nodwell et al., 1996; Nodwell and Losick 1998). Based on this scheme (**Figure 1.16**), the *bldJ* mutant is defective at the earliest step in sending signal 1 proposed to be an extracellular oligopeptide which is uptaken by the BldK oligopeptide permease. The *bldK* and *bldL* mutants can secret signal 1, but fail to produce signal 2. Mutations of *bldA* and *bldH* in *S. colicolor* are capable of producing both signal 1 and signal 2, but unable to make signal 3, the subsequent steps in the signaling of *bldG*, *bldC*, *bldD* and *bldK* mutants perform in the same way. Therefore, the *bldJ* mutant can accept and respond to the signals sent by any of other mutants defined in the cascade to develop aerial mycelium, but *bldJ* mutant itself is unable to provide the signals facilitating the aerial growth of any of other mutants. But the *bld* gene effect is not as simple as this cascade. For instance, *bldB* and *bldN* mutants can not be stimulated by any other mutant (Nodwell and Losick 1998). The reason for this is still unknown.

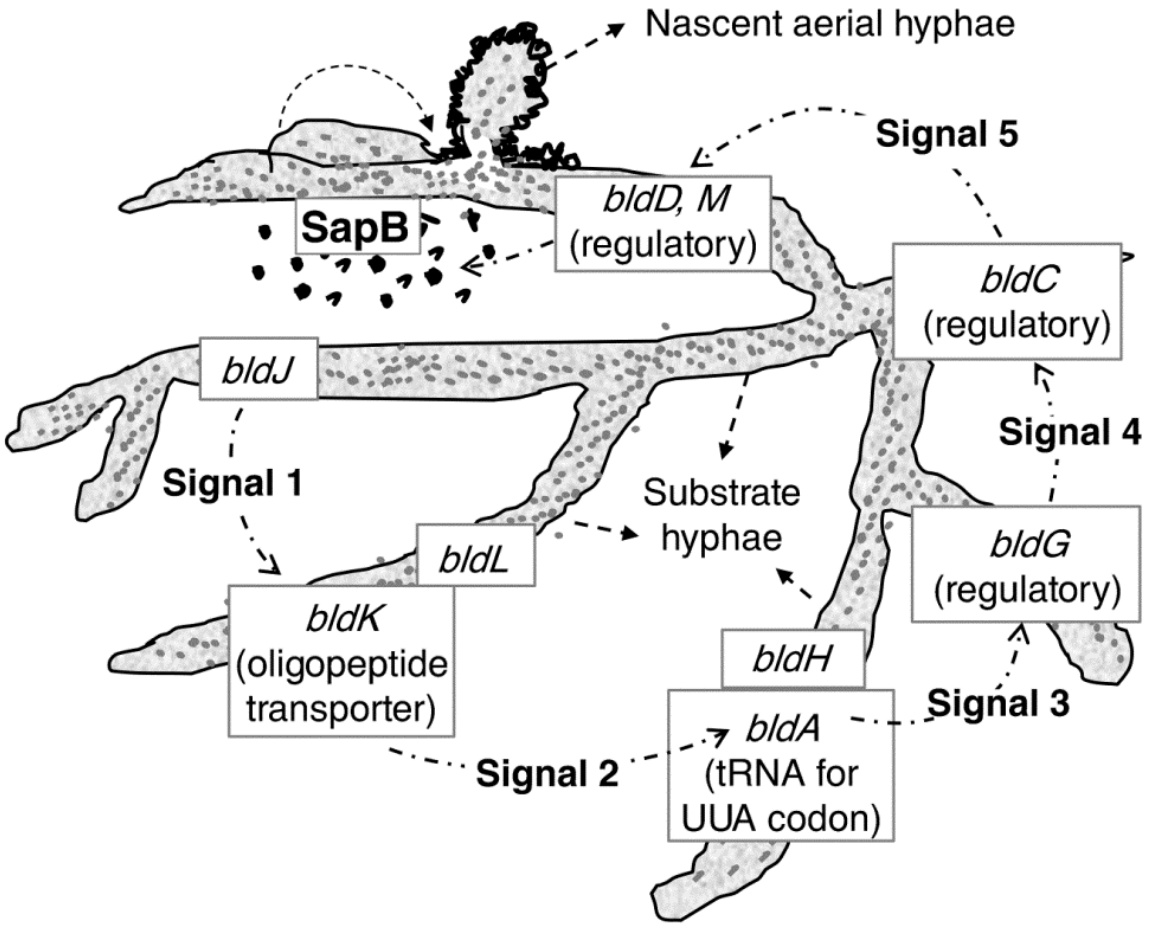

Figure 1.16: Extracellular signaling cascade involved in aerial mycelia formation in *S. coelicolor* (Adapted from Chater 1998).

1.8 Hormaomycin and its biosynthesis

Hormaomycin (HRM) was first isolated from a fermentation broth of *Streptomyces* sp. AC-1978 (Omura et al., 1984). The compound has been partially characterized by Omura *et al.*, named as takaokamycin (Omura et al., 1984). HRM was isolated again from *Streptomyces griseoflavus* W-384 in the Zähner group (Andres et al., 1990; Andres et al., 1989). Subsequent structural elucidation was carried out, revealing an unusual depsipeptide with an extraordinary structure (**Figure 1.17**). It consists of eight building blocks, L-isoleucine [L-Ile] as the only proteinogenic amino acid, along with six non-proteinogenic amino acids, two units of (2*S*,3*R*)-3-methylphenylalanine [(β-Me)Phe], one of D-*allo*-threonine [D-*allo*-Thr], two units of 3-(*trans*-2'-nitrocyclopropyl)alanine [(3-Ncp)Ala], one unit of 4-(*Z*)-propenylproline

[(4-Pe)Pro] as well as one residue of 5-chloro-1-hydroxypyrrole-2-carboxylic acid [Chpca] (**Figure 1.17**). The latter three components are to date unique (Andres et al., 1989; Rössner et al., 1990).

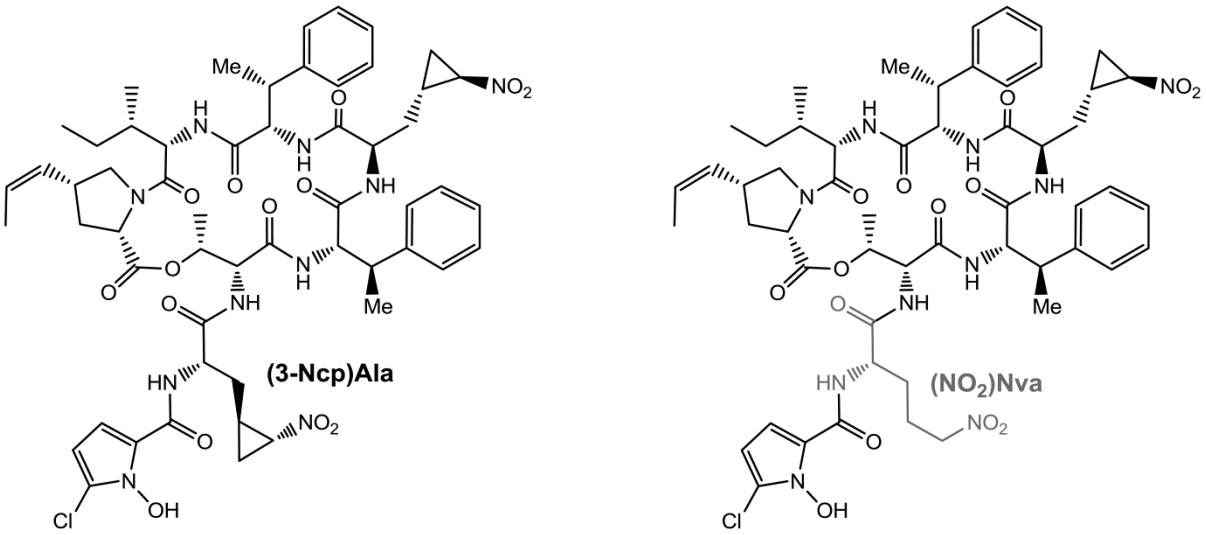

Figure 1.17: The bacterial hormone hormaomycin (HRM) (left) and the antifungal nonnatural analogue hormaomycin D_2 (right) obtained from feeding 5-nitronorvaline [(NO_2)Nva] into the fermentation culture of *S. griseoflavus* W-384.

HRM belongs to the few known signaling metabolites (**Figure 1.18**) (Recio et al., 2004; Kondo et al., 1988; Kitani et al., 2011; Horinouchi 2002; Igarashi et al., 2001) acting as autoregulators that are effective in morphological differentiation such as aerial mycelia formation and stimulation of antibiotic production in other *Streptomyces* species (Andres et al., 1990). Additionally, HRM itself is an antibiotic with extremely potent activity against coryneform actinomycetes at picomolar concentrations (Andres et al., 1990). The HRM antibacterial and hormonal mechanism of action is so far unknown. HRM also exhibits high *in vitro* activity against the causative agent of malaria tropica, *Plasmodium falciparum* (Otoguro et al., 2003).

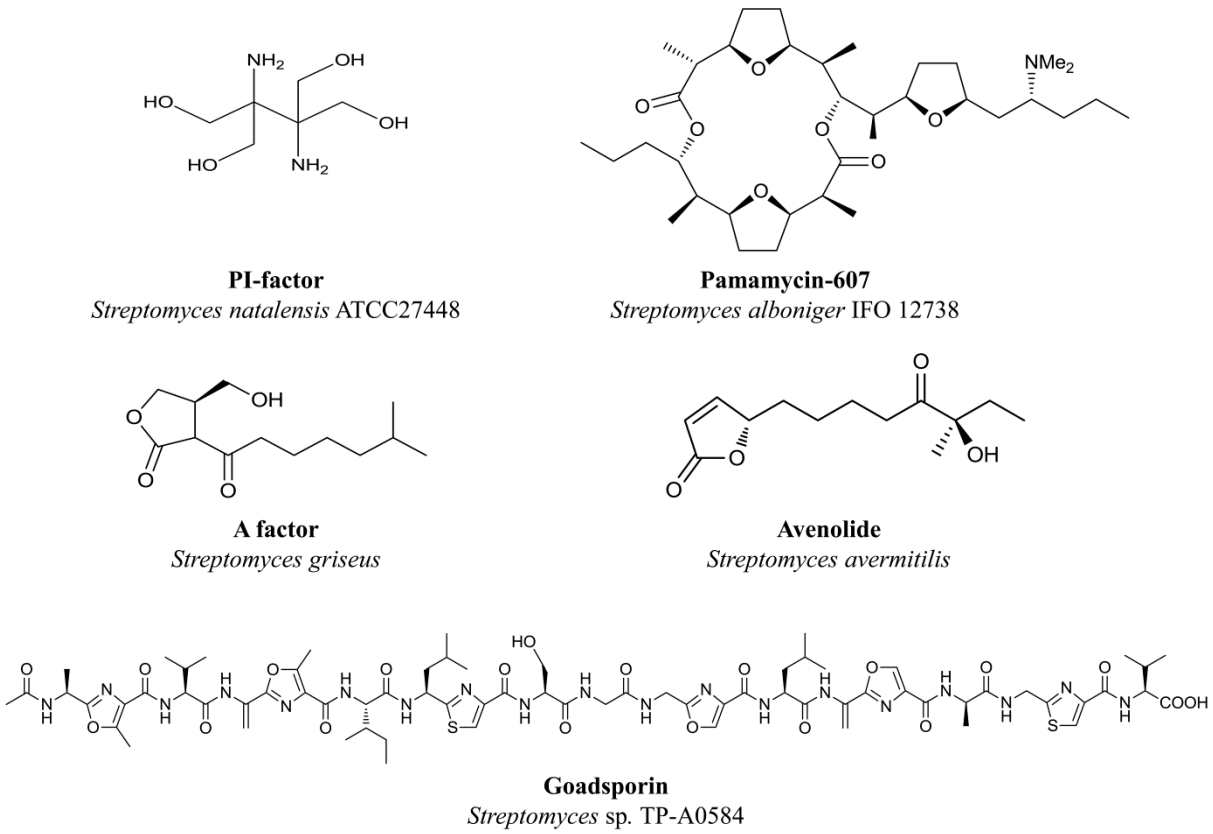

Figure 1.18: Some examples of low-molecular signals from streptomycetes.

Previous feeding studies (Brandl et al., 2005; Höfer et al., 2011) to investigate the precursors of the unusual building blocks established the precursors of the moieties in HRM. These are L-Pro for Chpca, L-Phe for (β-Me)Phe, L-Tyr for (4-Pe)Pro and L-Lys and 4-hydroxy- L-Lys for (3-Ncp)Ala. However, the precise steps during these transformations are so far unknown. Some genes involved in the biosynthesis of these building blocks have been identified. For example, the *hrmQ* gene, predicted to encode a halogenase, has been integrated into the clorobiocin pathway, resulting in the generation of a novel clorobiocin with a 5-chloro-pyrrole moiety analogous to the starter unit of HRM by combinatorial biosynthesis (Heide et al., 2008). These results established that HrmQ acts as a chlorinase catalyzing the chlorination involved in Chpca formation. Another well-studied gene is *hrmF*, encoding an iron-dependent oxidoreductase which performs the cleavage of L-3,4-dihydroxyphenylalanine (L-DOPA). The enzyme was kinetically characterized and exhibits a K_m of 3.35 μM and a k_{cat} of 57.8 min^{-1} (Höfer et al., 2011) . Interestingly, HrmF was incubated with L-DOPA analogues and able to cleave a wide range of catechol derivatives, including unsubstituted catechol, revealed its

flexible substrate specificity (Höfer et al., 2011).

In addition, novel HRM analogues were generated by feeding several modified amino acids into the fermentation broth of *S. griseoflavus* W-384 via precursor-directed biosynthesis. The resulting analogues possess variations at the positions of (3-Ncp)Ala and (β-Me)Phe (Kozhushkov et al., 2005; Zlatopolskiy and de Meijere 2004; Zlatopolskiy et al., 2006). Comparison of the bioactivities of these analogues to those of HRM has revealed a HRM analogue hormaomycin D_2 (**Figure 1.17**) incorporated (NO_2)Nva unit with new antifungal activity against *Candida albicans* with a similar potency as the clinically used fungicide nystatin (Radzom 2006). These results have demonstrated that chemical structural variations can lead to the generation of novel bioactive peptides and also indicate that the A domains in NRPS involved in assembling HRM exhibit considerable substrate flexibility, which is very appealing to generate novel bioactive HRM derivatives by metabolic engineering and mutasynthesis.

Due to the intriguing structure and diverse bioactivities of HRM, the HRM biosynthetic gene cluster was isolated to characterize its biosynthesis (Höfer et al., 2011). A 48,409 bp region of 23 ORFs (*hrmA* to *hrmW*) was identified that could be convincingly attributed to HRM biosynthesis. The overall architecture of the gene cluster resembles other nonribosomal systems and consists of two giant NRPS genes surrounded by other biosynthetic gene candidates involved in amino acid biosynthesis, regulation and transport (**Figure 1.19**).

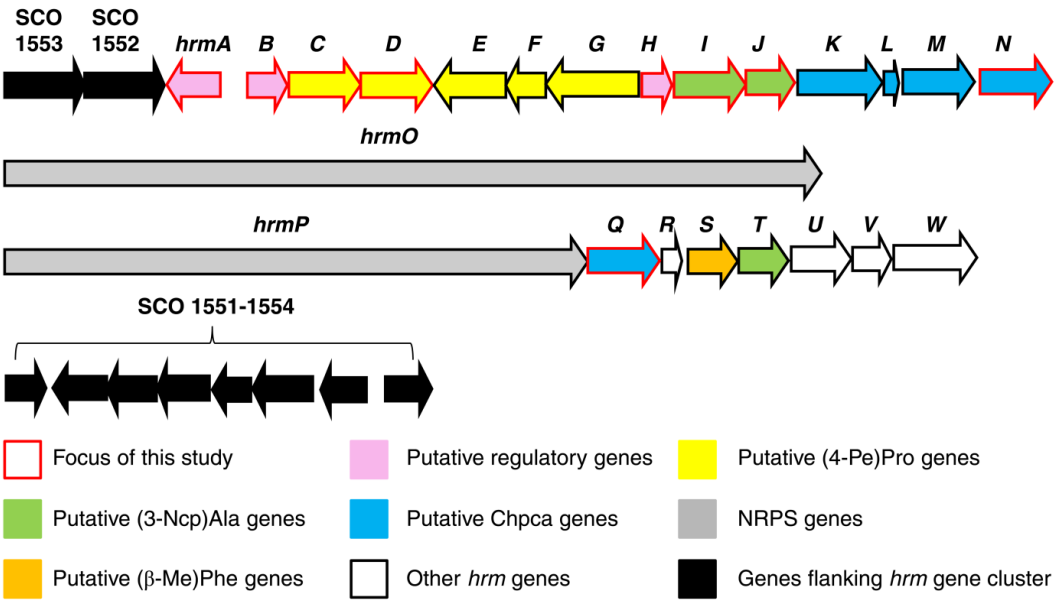

Figure 1.19: Organization of the hormaomycin (HRM) biosynthetic gene cluster from *S. griseoflavus W-384*. Genes proposed to be involved in precursor biosynthesis are labeled in yellow, green, blue and orange. The SCO labels above genes shown in black refer to close homologs present in the *S. coelicolor* genome.

The functions of proteins encoded by *hrm* genes were deduced, as shown in **Table 1.2** (Höfer et al., 2011).

Table 1.2: Proposed functions of proteins involved in hormaomycin (HRM) biosynthesis (Höfer et al., 2011).

Protein	Amino Acids	Proposed Function	Sequence Similarity (protein, origin)	Similarity/ Identity	Accession Number
HrmA	321	AraC-type transcriptional regulator	SCO0287, *Streptomyces coelicolor*	84/75	CAB54172
HrmB	197	Positive regulator	NovE, *Streptomyces caeruleus*	73/60	AAF67498
HrmC	358	Methyltransferase	LmbW, *Streptomyces lincolnensis*	72/57	CAA55769
HrmD	298	F420-dependent oxidoreductase	SCO3591, *S. coelicolor*	63/52	CAA22223
HrmE	326	Tyrosine hydroxylase	LmbB2, *S. lincolnensis*	55/47	CAA55748
HrmF	185	DOPA-cleaving oxidoreductase	TomH, *Streptomyces achromogenes*	69/61	ACN39014
HrmG	599	γ-Glutamyl transpeptidase Endoribonuclease	LmbA, *S. lincolnensis*	73/64	CAA55746
HrmH	132	Putative regulator	YjgH, *Kinetococcus radiotolerans*	80/60	YP_001362405

Protein	Amino Acids	Proposed Function	Sequence Similarity (protein, origin)	Similarity/ Identity	Accession Number
HrmI	350	unknown	PSPTOT1_5436, *Pseudomonas syringae* pv. Tomato	72/57	ZP_03398361
HrmJ	227	unknown	PSPTOT1_5541, *P. syringae* pv. Tomato	70/51	ZP_03398362
HrmK	527	Acyl-CoA-Synthetase	CaiC, *Oscillatoria sp.* PCC 6506	50/34	ZP_07113995
HrmL	91	Type II peptidyl carrier protein	VinL, *Streptomyces halstedtii*	59/40	BAD08369
HrmM	388	Acyl-CoA dehydrogenase	MoeH5, *Streptomyces clavuligerus*	51/33	YP_002190358
HrmN	389	Acyl-CoA dehydrogenase	Strop_4265, *Salinispora tropica*	49/36	YP_001161071
HrmO	5252	NRPS (C-A-PCP-C-A-PCP-E-C-A-PCP-C-A-PCP-E)	RHA1_ro00141, *Rhodococcus* sp. RHA	40-60% domain identity	YP_700135
HrmP	3471	NRPS (C-A-PCP-C-A-PCP-C-A-PCP-TE)	PstC, *Streptomyces ghanaensis*	40-60% domain identity	ZP_06575792
HrmQ	448	Halogenase	ChlB4 *Streptomyces antibioticus*	79/64	AAZ77674
HrmR	72	MbtH Homolog	SCO3218, *S. coelicolor*	81/58	CAB38589
HrmS	329	Methyltransferase	MppJ, *Streptomyces hygroscopicus*	67/52	AAU34201
HrmT	301	Diaminopimelate epimerase	DAPF2 (SAV3161), *S. avermitilis*	63/47	BAB69347
HrmU	427	Integral membrane antitransporter	CZA382.28, *Amycolatopsis orientalis*	68/56	CAB45049
HrmV	156	ABC transporter ATP binding protein	ABC-transporter, *Streptomyces cattleya*	78/66	AEW99195
HrmW	563	Intergral membrane protein	JNB_10189, *Janibacter* sp. HTCC2649	38/26	ZP_00994281

Eight homologs of PCP have been identified, which are proposed to covalently bind the eight building blocks during HRM biosynthesis. One of them is a free-standing PCP encoded by *hrmL* gene, the others are integrated into each module of NRPSs HrmO and HrmP (**Figure 1.20**).

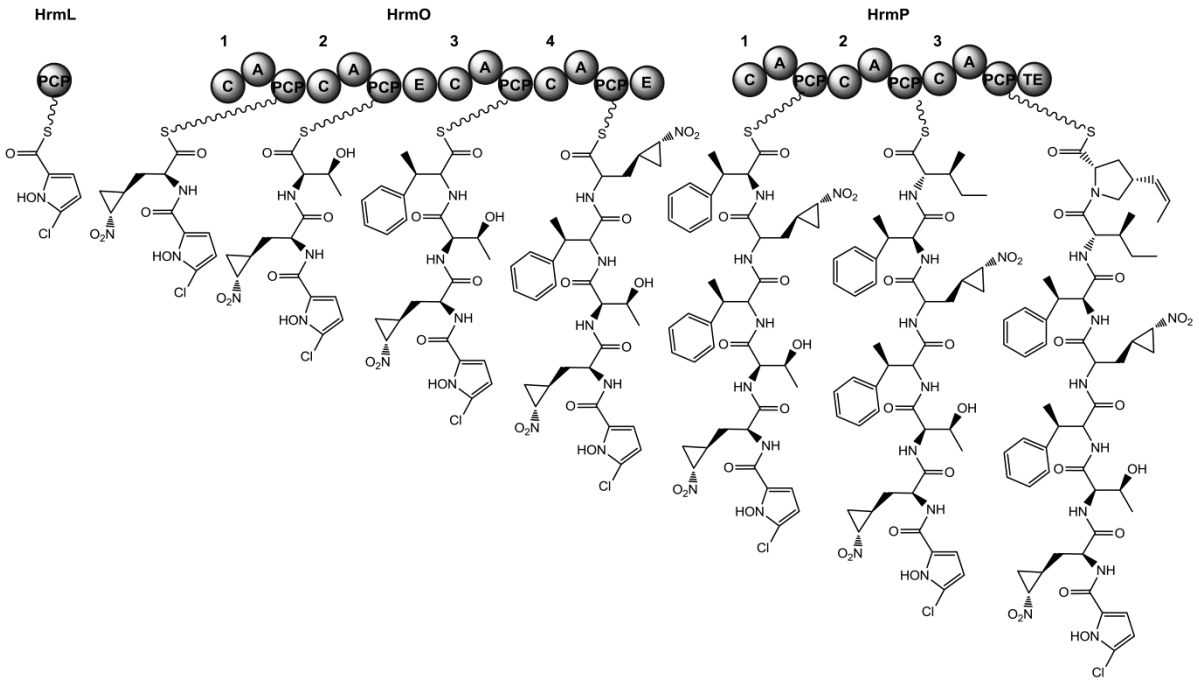

Figure 1.20: The assembly of HRM biosynthesis. Numbers represent the start of each individual NRPS module (Höfer et al., 2011).

Comparative bioinformatic analysis of NRPSs genes (Crüsemann et al., 2013) have revealed that many of the modules exhibit high DNA similarity to each other. Particularly, the regions encoding A domains responsible for the activation of amino acids showed more than 90% nucleotide identity. For example, in HrmO, the first A domain ($HrmO1_A$) and the fourth A domain ($HrmO4_A$) both can activate (3-Ncp)Ala, and the third A domain in HrmO ($HrmO3_A$) and the first A domain in HrmP ($HrmP1_A$) are both able to activate (β-Me)Phe (Crüsemann et al., 2013). Remarkably, even some A domains activating different amino acids also share high DNA identity, with the exception of a core region around 400 bp encoding the binding-pocket residues to determine the substrate specificity (Stachelhaus et al., 1999). Such phenomenon suggested that A domains underwent recombination during evolution, leading to a switch of substrate specificity.

All native A domains involved in HRM biosynthesis have been heterologously expressed in *E. coli*, but initially did not exhibit significant activities *in vitro*. Subsequently, it has been demonstrated that many A domains show activities *in vitro* only when coexpressed with a small MbtH-like protein. MbtH-like proteins therefore act as integral components of many NRPSs

(Felnagle et al., 2010). Since HrmR is a homolog of MbtH encoded in the *hrm* gene cluster, subsequent coexpression of each A domain with HrmR was carried out. The resulting domains were subjected to a γ[$^{18}O_4$]-ATP mass exchange assay to determine and characterize their amino acid selectivities (Phelan et al., 2009). Some domains showed substrate flexibility, especially HrmP2$_A$, which prefers to activate valine *in vitro* over the native isoleucine (Crüsemann et al., 2013; Crüsemann 2012).

Evolution-guided A domain engineering studies were performed by fusion of the outer regions of one A domain with the core of other A domains. This yielded three engineered A domains, O2f$_A$, O4f$_A$ and P2f$_A$ (Crüsemann 2012; Crüsemann et al., 2013). These fused A domains were coexpressed with HrmR, and characterized by A domain exchange assay, showing that a swap of the core can change the substrate specificity. The results provide insights into the HRM biosynthetic pathway, facilitating the generation of novel HRM analogues by mutagenesis. The high substrate selectivity of (3-Ncp)Ala and (4-Pe)Pro activating A domains *in vitro* also support that these two unique amino acids are biosynthesized before being loaded onto the PCP and assembled by the NRPS.

The studies described above have provided insights into HRM building block selection and assembly of this unique peptide. To elucidate the precise HRM biosynthetic pathway, the *hrm* genes had to be studied by gene knock-out, for which no protocol was available, and complementation *in vivo*, as well as by expression of genes for further enzymatic assays *in vitro*. Establishment of a gene knock-out system can also facilitate the generation of HRM analogues through mutasynthesis. Furthermore, the HRM antibacterial and hormonal mode of action was not known at this stage.

Chapter 2 Research Goals

Hormaomycin (HRM) possesses a remarkable structure with a variety of bioactivities, which contains several unique building blocks. The special characteristics of HRM promoted us to investigate its unusual biosynthesis and antibacterial and hormonal mechanism of action. The HRM biosynthetic gene cluster has been isolated and sequenced recently, which gave us the opportunity to study and to genetically modify the biosynthetic pathway.

However, the lack of a genetic manipulation system of the HRM producer has hampered the investigation of HRM biosynthetic pathway at the molecular level. The first goal of this work was to optimize the genetic manipulation system of HRM wild-type producer *S. griseoflavus* W-384 by establishing efficient conditions for the introduction of foreign DNA via PEG-mediated protoplast transformation and conjugation.

HRM production by *S. griseoflavus* W-384 is very erratic and only provides small amounts of compound. Therefore, the second goal of this study was to increase the production of HRM as a basis for further investigation of the antibacterial and hormonal mechanism of action. For this purpose, two putative pathway-specific positive regulatory genes, *hrmA* and *hrmB* were individually introduced into *S. griseoflavus* W-384 or inactivation of the putative negative regulatory gene *hrmH* to test whether this yields HRM overproducers.

The structural variation of a compound often facilitates slight to dramatic shifts in the pharmacological profiles of the compound. The analysis of HRM biosynthetic genes was supposed to allows us to better understand HRM biosynthesis, which served as the basis for the generation of HRM analogues. In this work, several genes involved in biosynthesis of the unusual building blocks, *hrmQ* for Chpca, *hrmI*, *hrmJ* for (3-Ncp)Ala, and *hrmC*, *hrmD*, *hrmN* for (4-Pe)Pro were analyzed via gene knock-outs as well as genetic and chemical complementations. The resulting knock-out mutants were employed to generate HRM analogues through mutasynthesis for SAR studies.

HRM acts as a bacterial hormone that can induce aerial mycelium formation in other *Streptomyces*. It is well-known that the formation of aerial mycelium in the model strain *S. coelicolor* A3(2) is governed by a regulatory cascade involving products of the *bld* genes (*bldJKLAHGCDM*). HRM was exposed to the regulatory bald mutants that are defective in the formation of aerial mycelium and derived from *S. coelicolor* A3(2) to test whether this peptide could restore aerial mycelium formation. This possibly provided us insights into determination of the molecular target in the signaling cascade for HRM to initiate the aerial mycelium formation.

Chapter 3 Results and Discussion

3.1 Establishment of genetic manipulation system in *S. griseoflavus* W-384

The genetic manipulation of *Streptomyces* spp. began in the Hopwood`s lab in the early 1970s (Chater 1999; Hopwood 1999). Most of work was dealing with the establishment of efficient methods for DNA transformation (Bibb et al., 1978; Matsushima and Baltz 1985), conjugation (Mazodier et al., 1989; Flett et al., 1997)and transduction as well as construction of DNA cloning system and discovery and applications of transposons (Hahn et al., 1991). All the previous studies paved the way for modern genetic manipulation in *Streptomyces* spp.. The continuous studies on the genetic features of *Streptomyces* and the gradual improvement of gene cloning techniques have contributed significantly to the rapid development of genetic manipulation in *Streptomyces* spp., such as Red/ET recombination systems. This has allowed researchers to modify *Streptomyces* spp. genetically and to generate its mutants efficiently (Datsenko and Wanner 2000; Gust et al., 2003), to establish heterologous expression systems making the expression of genes of interest much easier as well as to perform combinatorial biosynthesis as a powerful tool in attempts of generating novel “unnatural natural products” (Pfeifer et al., 2002; Hopwood et al., 1985). However, *Streptomyces* is a highly divergent genus. Within this genus, there is a major genetic difference between different species. Therefore, development of the best genetic manipulation systems is a crucial step towards further studies for each individual strain.

In general, the optimization of genetic manipulation system in *Streptomyces* spp. is accomplished by PEG-assisted protoplast fusion and conjugation based on the model strain *S. coelicolor* A3(2). The PEG-assisted protoplast fusion for *Streptomyces* spp. was firstly developed in 1977 and readily applied for foreign DNA transformation, thereby facilitating genetic engineering of this commercially important genus (Hopwood et al., 1977; Baltz and Matsushima 1981). This includes harvesting of mycelia, removal of cell wall, filtration of protoplast and PEG-induced fusion between DNA and protoplasts (Nybo et al., 2010; Zhou et

al., 2008). Conjugation is the intergeneric transfer of plasmids from *E. coli* to *Streptomyces* strains, which was initially reported by Mazodier *et al* (1989) (Flett et al., 1997). The vectors containing the appropriate origin of transfer (*oriT*) require transfer functions to be supplied by *E. coli* donor strain carrying the plasmid that provides *tra* gene (**Figure 3.1**).

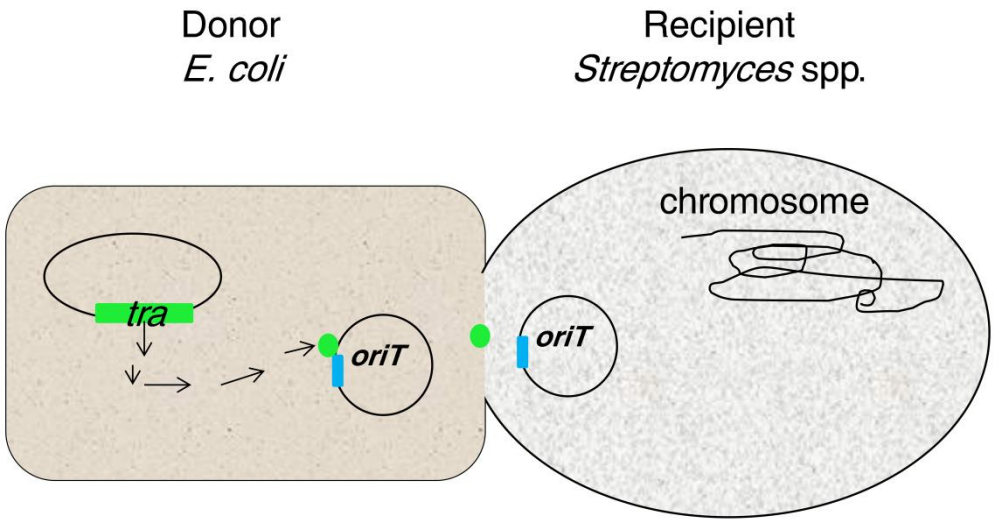

Figure 3.1: Conjugation system from *Escherichia coli* to *Streptomyces* spp.. The plasmid carrying *tra* gene can express a transfer protein for helping the plasmid with *oriT* get through the tunnel between two cells to the side of *Streptomyces* spp..

Previous studies indicated that genetic manipulations in *S. griseoflavus* W-384 was very difficult (unpublished data), which hampered functional studies on HRM biosynthetic genes. Hence, it was necessary to establish and optimize the genetic manipulation system of this strain in order to transform foreign DNA easily for further gene knock-out, expression and modification. Furthermore, the efficient transformation system would also provide us with the possibility to screen for high-yielding strains. Sequencing the whole genome of *S. griseoflavus* W-384 has enabled the identification of more than fourteen gene clusters involved in the biosynthesis of secondary metabolites. Establishment of a genetic manipulation system would open up the possibility to investigate the biosynthetic pathways of HRM and other interesting metabolites and to generate novel compounds by genetic engineering.

3.1.1 Optimization of growth conditions of *S. griseoflavus* W-384

3.1.1.1 Antibiotics susceptibility test of *S. griseoflavus* W-384

Herein, the sensitivity of *S. griseoflavus* W-384 was tested to several common antibiotics in order to further screen the transformants. *S. griseoflavus* W-384 was cultivated at 30 ℃ for 5 days on MM medium supplemented with antibiotics at the different concentrations ranging from 0 μg/mL to 100 μg/mL (**Table 3.1**). It was shown that *S. griseoflavus* W-384 was extremely sensitive to apramycin, kanamycin, thiostrepton and streptomycin with the minimal inhibitory concentration (MIC) of 10 μg/mL while spectinomycin can be used as an alternative for screening with higher concentration.

Table 3.1: Antibiotics susceptibility of *S. griseoflavus* W-384. +++: growing very well, ++：growing well, +/-: growing not so good, -: no growth, NA: not analyzed.

Antibiotics	**Concentration (μg/mL)**				
	0	10	25	50	100
Apramycin	+++	-	-	-	NA
Kanamycin	+++	-	-	-	NA
Thiostrepton	+++	-	-	-	NA
Streptomycin	+++	-	-	-	NA
Spectinomycin	+++	++	+/-	-	-

3.1.1.2 Optimization of sporulation media

Since a *Streptomyces* spore suspension at high concentration is required in this work for further preparation of protoplasts, screening of transformants as well as fermentation, using ideal media for sporulation are very important and necessary. To obtain the best media for sporulation, 10 μL of *S. griseoflavus* W-384 spore suspension (1×10^8 spores/μL) was spread on six different kinds of common agar media (GYM, M2+, GYS, LB, 2CM and MM), respectively. The agar plates were incubated at 30 ℃ for six days.

After cultivation, among six tested media shown in **Figure 3.2**, GYM was the best sporulation medium due to the even distribution of spores to form a gray lawn and the fastest growth starting from the third day. *S. griseoflavus* W-384 also had a good sporulation on M2+ agar

plate but slower growth. No sporulation was observed on the other media (2CM, LB and MM). In addition, the same plates were incubated at 37 ℃ to check if this temperature gave better sporulation. It was observed that this strain could grow at 37 ℃ but no sporulation was observed. Therefore, the optimal condition for sporulation of *S. griseoflavus* W-384 was on GYM medium at 30 ℃ for five days.

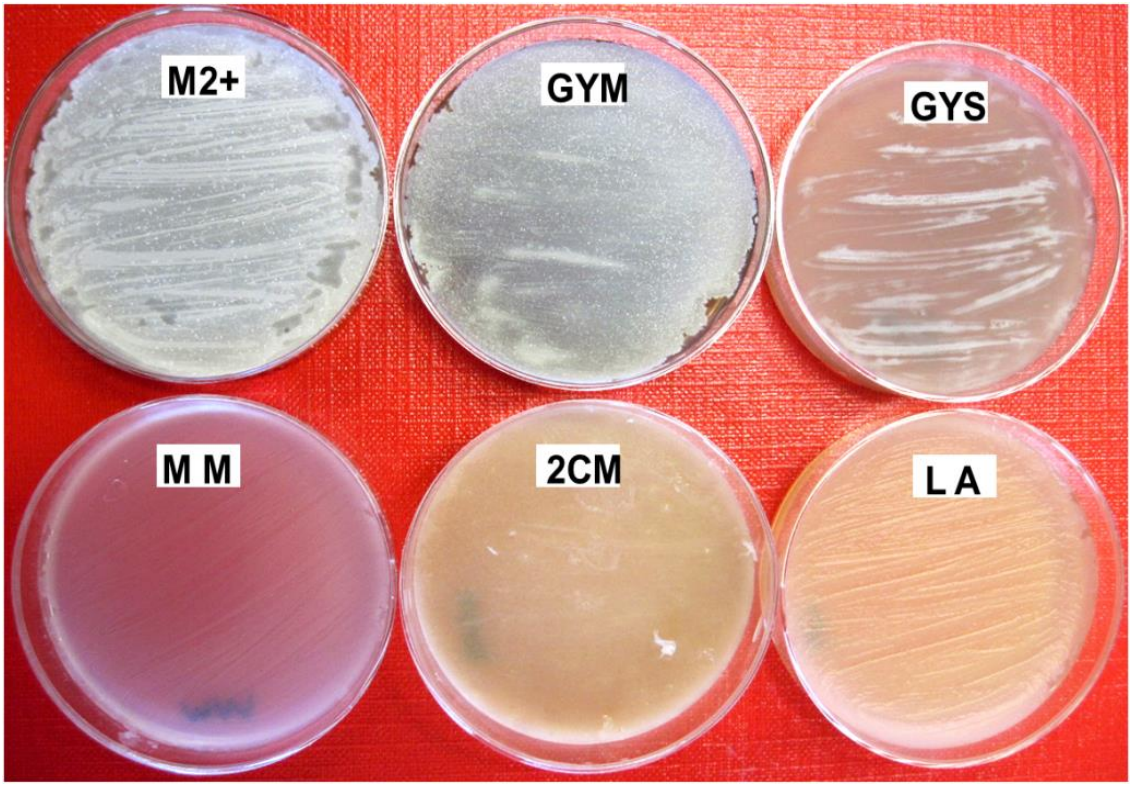

Figure 3.2: Sporulation of *S. griseoflavus* W-384 on different agar media.

3.1.1.3 Optimization of submerged media for mycelial growth of *S. griseoflavus* W-384

Mycelial growth of *Streptomyces* in liquid media is very important for many purposes, for example, the production of secondary metabolites and the general genetic manipulation including preparation of protoplasts, conjugation, isolation of genomic DNA or plasmid. Here, six frequently-used submerged *Streptomyces* media were tested for the growth of *S. griseoflavus* W-384. 10 μL of *S. griseoflavus* W-384 spore suspension (1×10^8 spores/μL) were added to 20 mL liquid media (YEME, superYEME, SGGP, MS, TSB and MMS) and grown at 30 ℃, 250 rpm, for two days. Afterwards, the mycelia were harvested and the

supernatants were discarded. To compare the mycelial growth in different media, the wet cell weights from different media were measured.

Table 3.2: Mycelial growth of *S. griseoflavus* W-384 in different submerged media. The wet cell weight in table is the average value of triplet cultivation.

Media	**YEME**	**superYEME**	**MS**	**SGGP**	**TSB**	**MMS**
Sucrose content	34%	34%	-	-	-	-
Wet cell weight (g)	no growth	no growth	2.58	0.52	3.74	0.81

As shown in **Table 3.2**, *S. griseoflavus* W-384 could not grow in the liquid media containing sucrose. The wet weight of the cells growing in TSB was higher than those in other media. However, the mycelia grown in TSB sticked together and formed lots of big pellets, which made protoplast preparation inefficient. The mycelia in MS not only grew well, but also seemed fine morphologically. Therefore, MS medium was considered as the optimal medium for mycelial growth of *S. griseoflavus* W-384.

3.1.2 Efficient conditions for protoplast preparation and regeneration of *S. griseoflavus* W-384

S. griseoflavus W-384 strain was grown in MS media at 30 ℃, 250 rpm, for two days. Then the mycelia were harvested, washed with 10.3% sucrose twice and resuspended in P buffer. Afterwards, the mycelia were divided into four portions; in which was supplemented with lysozyme (50 mg/mL) at the final concentration range of 1 to 3 mg/mL. The incubation time was set up at the range from 0 to 2 hours. According to the routine procedure of model strain *S. coelicolor* A3(2), the incubation temperature was set up at 30 ℃. After incubation, the protoplasts were filtered through sterilized absorbent cotton. The protoplasts were observed by microscope (**Figure 3.3**).

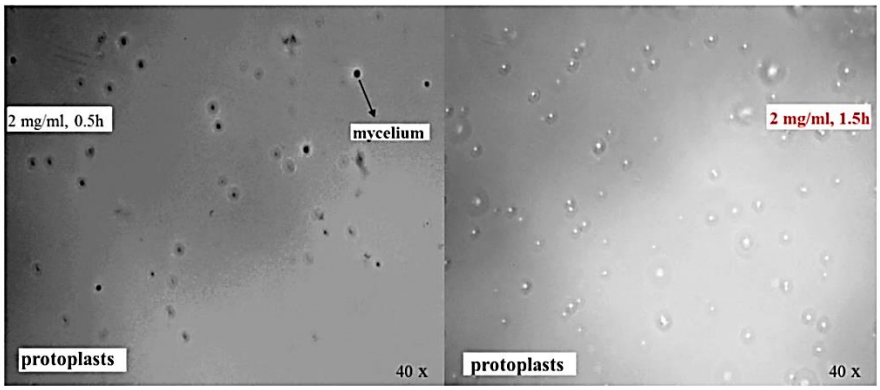

Figure 3.3: The protoplast viability micrograph of *S. griseoflavus* W-384 with 2 mg/mL final concentration of lysozyme at 0.5 h and 1.5 h (×40).

For protoplast regeneration, protoplasts were diluted serially in 0.1% SDS instead of P buffer to eliminate the influence from mycelia. As the control, they were plated on R5 regeneration medium with the same sets of dilution in P buffer. Then, the protoplasts were spread on R5 plates. After incubation of 24 hours at 30 ℃, the optimal condition of protoplast formation was determined according to the numbers of exact regeneration colonies. The protoplasts treated with 0.1% SDS eventually were killed off due to lack of cell wall protection while the mycelia were grown as usual on R5 plates. The exact regeneration numbers equal to the numbers of regeneration colonies from protoplasts diluted with P buffer minus the numbers of regeneration colonies from protoplasts diluted with 0.1% SDS. The result is shown in **Figure 3.4**. It was shown that lysozyme at the final concentration of 2 mg/mL and incubation for 1.5 h was the optimal condition for the formation of *S. griseoflavus* W-384 protoplasts.

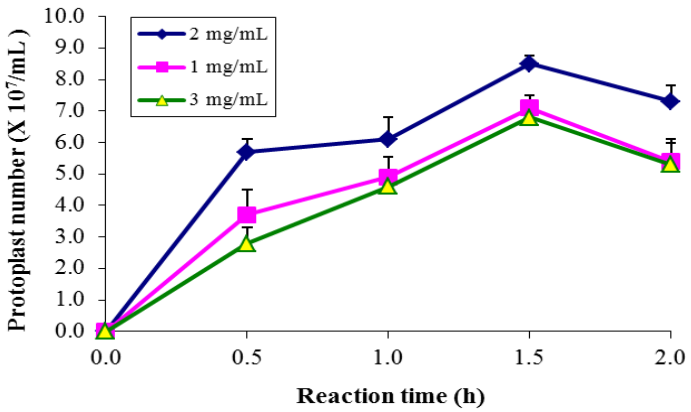

Figure 3.4: The effect of concentration of lysozyme (mg/mL) and incubation time (h) on the protoplast regeneration of *S. griseoflavus* W-384.

3.1.3 Protoplast transformation in *S. griseoflavus* W-384

Integrative and free-replicating plasmids are commonly used in *Streptomyces* spp.. However, the transformation efficiency between these two types of plasmids is different. Generally, the transformation of integrative ones was much easier than that of free-replicating ones because the integrative ones can be integrated into the *Streptomyces* genome. In this study, two plasmids were chosen from the two different types above for protoplast transformation.

3.1.3.1 Protoplast transformation of integrative plasmid

pSET152 is a well-known integrative plasmid widely used in *Streptomyces* spp.(Bierman 1992). It carries the gene *attP* encoding an integrase, which enables it bind to *attB* site in the chromosomes of *Streptomyces* spp. (**Figure 3.5**). Therefore, the presence of an *attB* site in the chromosome would allow it to replicate together with the genome of *S. griseoflavus* W-384.

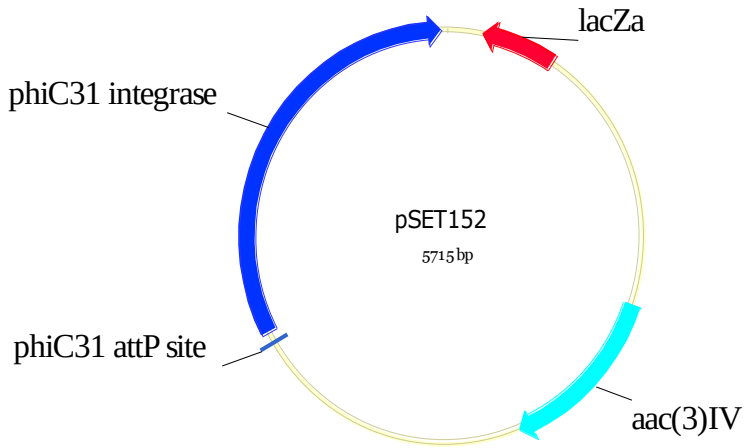

Figure 3.5: Physical map of pSET152.

In general, *Streptomyces* spp. possess strong restriction systems to inhibit the invasion of foreign DNA. Thus, pSET152 was transformed into *E. coli* ET12567 to obtain non-methylated pSET152 before being introduced into *S. griseoflavus* W-384 through PEG-mediated protoplast transformation based on the routine procedure of *S. coelicolor* A3(2) as described by Kieser *et al*. (2000).

After overlaying apramycin (25 μg/mL) on R5 plate and incubation for five days, plenty of

colonies were grown on R5 plates, suggesting that *S. griseoflavus* W-384 could accept foreign demethylated DNA and the efficiency of protoplasts prepared with optimal condition was very well (**Figure 3.6**).

Figure 3.6: The transformants of pSET152 in *S. griseoflavus* W-384.

To test if the resulting transformants were integrated with apramycin resistance gene from pSET152, five colonies were picked and plated on GYM agar media supplemented with apramycin (25 μg/mL) for sporulation. After incubation for five days, the spores were collected from GYM plates and subsequently inoculated into MS liquid media for further isolation of genomic DNA. The genomic DNA from the five colonies was used as templates for PCR amplification of apramycin resistance gene using the primer pair XF1A and XF1B. The results, as shown in **Figure 3.7**, indicated that all the colonies were resistant to apramycin.

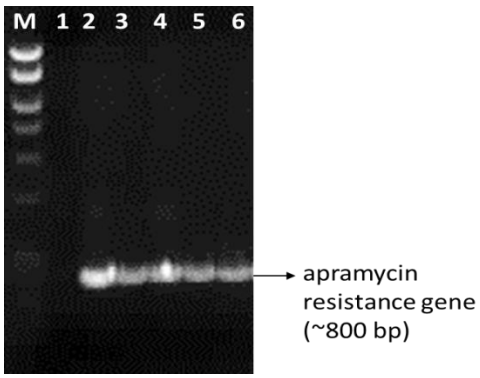

Figure 3.7: Agarose gel analysis of transformants of pSET152 in *S. griseoflavus* W-384. Lane M**,** l00 bp DNA ladder; lane 1, PCR products of genomic DNA from the WT strain; lanes 2-6, PCR products of genomic DNA from the pSET152 transformants.

3.1.3.2 Protoplast transformation of pWHM4*, a free-replicating plasmid

pWHM4* (**Figure 3.8**) is a free-replicating plasmid that contains a *Streptomyces* origin of replication and a thiostrepton resistance gene allowing screening transformants.

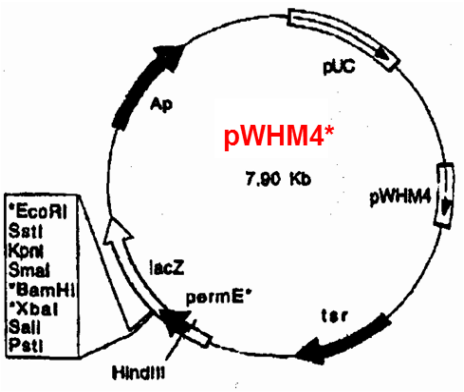

Figure 3.8: Physical map of pWHM4* (Matseliukh 2001).

Before being introduced into *S. griseoflavus* W-384, pWHM4* from *E. coli* DH5α was transformed into *E. coli* ET12567 in order to obtain demethylated DNA. After adding thiostrepton (12.5 μg/mL) on R5 plate followed by incubating at 30 ℃ for five days, less transformants were grown on the plate relative to that of pSET152 as shown in **Figure 3.9**.

Figure 3.9: The transformants of pWHM4* in *S. griseoflavus* W-384.

Several transformants were picked, inoculated into GYM supplemented with thiostrepton (12.5 μg/mL), and then incubated at 30 ℃ for seven days. The resulting spores derived from the transformants mentioned above were harvested and inoculated into MS liquid medium containing thiostrepton (12.5 μg/mL), respectively. After incubation with shaking at 30 ℃ for

two days, genomic DNA was isolated from the mycelia, and then introduced into *E. coli* DH5α. After incubation overnight at 37 ℃, a lot of *E. coli* DH5α colonies with ampicillin resistance were grown on LB agar plate supplemented with ampicillin. To confirm if these colonies harbor pWHM4* plasmid, they were inoculated into LB liquid media supplemented with ampicillin and grown at 37 ℃ overnight with agitation. The plasmids were extracted from the overnight culture and digested with *Bam*HI. As shown in **Figure 3.10**, all of the tested colonies contained the correct plasmid, demonstrating that protoplast transformation of *S. griseoflavus* W-384 with free-replicating plasmids was successful.

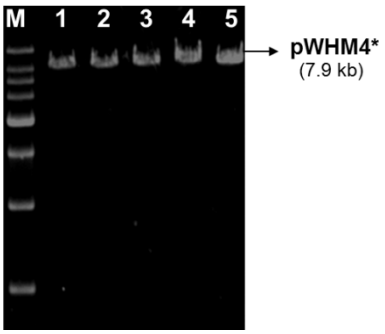

Figure 3.10: Agarose gel analysis of pWHM4* transformants. Lane M, 1 kb DNA ladder; lanes 1-5, digestion of plasmids isolated from the pWHM4* transformants.

3.1.4 Intergeneric conjugation into *S. griseoflavus* W-384

Conjugation as an approach of the intergeneric transfer offers some advantages. The procedure is not only relatively simple to perform, but also prevents foreign plasmid DNA from extracellular nuclease activity. Therefore, it has been considered as a powerful tool for gene transfer, which was successfully used in most *Streptomyces* strains. In this work, the donor bacterium was *E. coli* ET12567/pUZ8002. The pUZ8002 was integrated into the chromosome of *E. coli* ET12567, thereby providing a *tra* gene encoding an integrase. The foreign plasmid DNA used here was pSET152 carrying an origin of transfer, which was proved to be integrated into the chromosome of *S. griseoflavus* W-384 based on the previous study on protoplast transformation as described above.

3.1.4.1 Transformation of pSET152 into *S. griseoflavus* W-384 by conjugation

Transformants of *E. coli* ET12567 containing pSET152 were firstly obtained and cultivated in LB liquid media containing chloramphenicol, apramycin and kanamycin at 37 ℃ until the OD600 reached 0.4. Then, the cells were harvested, washed with fresh LB twice to remove the residue of antibiotics and finally resuspended in 500 μL fresh LB. Meanwhile, *S. griseoflavus* W-384 spores were heat-shocked in 500 μL of 2 × YT media at 50 ℃ for 10 min, and cooled down at room temperature. Afterwards, these two types of bacteria were mixed up, spread on MS agar plates containing 10 mM $MgCl_2$ and incubated at 30 ℃ for 16-20 hours, then flooded with 1.5 mL of sterilized water mixed with 25 μL of apramycin (50 μg/mL) and 20 μL of nalidixic acid (25 μg/mL). After incubation for several days, the conjugants grew on the plates. A few conjugants were picked and grown on GYM agar plates containing apramycin and nalidixic acid for further screening of apramycin resistance (**Figure 3.11**).

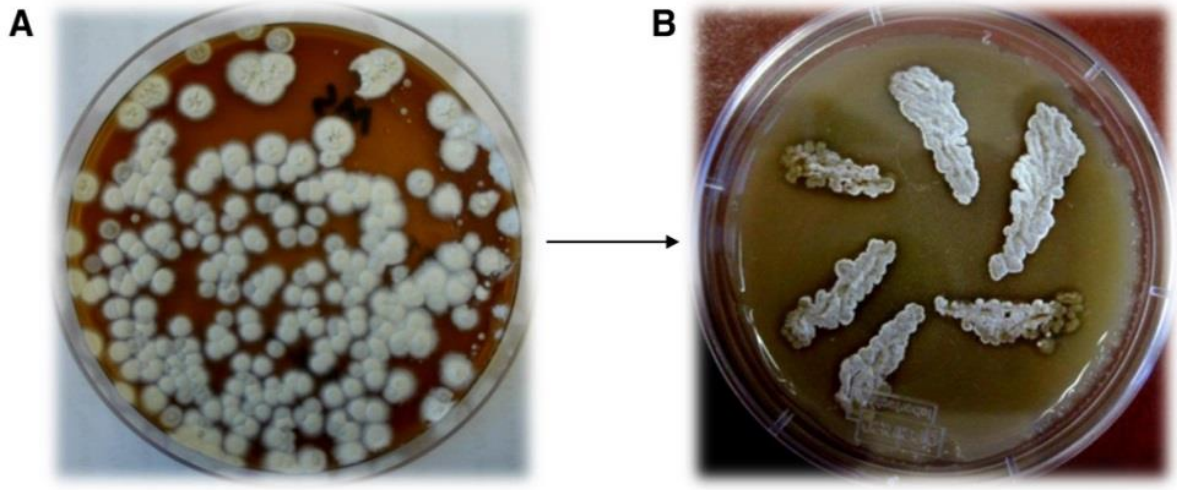

Figure 3.11: Conjugants of pSET152 into *S. griseoflavus* W-384 on MS agar plate. A, Conjugants grown on MS plate containing apramycin and nalidixic acid. **B,** Screening of a few conjugants on GYM agar plate supplemented with apramycin and nalidixic acid.

Since these conjugants possess an apramycin resistance, it was deduced that the resistance of conjugants came from the plasmid of pSET152, but it also might be caused by spontaneous mutation. It is therefore necessary to characterize these exconjugants on a genetic level.

3.1.4.2 Confirmation of conjugants on a genetic level

The spores of above conjugants were harvested from GYM plates. Three of above conjugants were inoculated into MS liquid medium containing apramycin while *S. griseoflavus* W-384 was considered as a negative control. All the strains were cultivated at 30 ℃ with shaking for two days. The genomic DNA was isolated after incubation, and then taken as a template to amplify the apramycin resistance gene by PCR using the primer pair XF1A/1B (**Figure 3.12**). Agarose gel analysis of all the PCR products (**Figure 3.12**) indicated that the apramycin resistance of all the exconjugants was from pSET152 and the conjugation was successful.

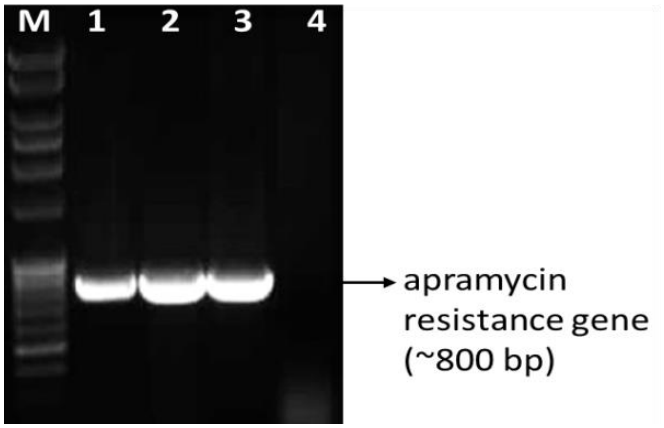

Figure 3.12: Agarose gel analysis of conjugants of pSET152 in *S. griseoflavus* W-384. Lane M, l00 bp DNA ladder; lanes 1-3, PCR products of three conjugants; lane 4, PCR products from the WT strain.

3.1.5 Discussion

In this chapter, a genetic manipulation system of *S. griseoflavus* W-384 was established via optimization of cultivation conditions, protoplast formation and regeneration. Then, two types of plasmids were successfully introduced into *S. griseoflavus* W-384 by either protoplast transformation or conjugation.

The integrative plasmid pSET152 used in this study, which contains an *attP* site derived from phage ΦC31 that can be integrated into the chromosome of *S. griseoflavus* W-384. The results

suggested the presence of at least one *aatB* sites in the *S. griseoflavus* W-384 genome. Thus, the plasmids derived from phage ΦC31 also can be introduced into *S. griseoflavus* W-384.

Streptomyces spp. often possess strong restriction systems. In many cases, methylated foreign DNA is not accepted. Therefore, the foreign DNA is supposed to be demethylated via transformation into *E. coli* ET12567. In the initial study of protoplast transformation, both methylated pSET152 and demethylated pSET152 could be individually introduced into *S. griseoflavus* W-384. The results implied that *S. griseoflavus* W-384 did not have a strong restriction system, because it can accept both types of DNA. However, demethylated pSET152 showed much higher efficiency of transformation into *S. griseoflavus* W-384 than that of DNA without demethylation.

3.2 Examination of regulatory genes in hormaomycin biosynthesis

Previous work has provided some insights into the biosynthesis of the unusual building blocks and has established that the peptide is assembled by NRPSs (Höfer et al., 2011; Crüsemann et al., 2013; Crüsemann 2012). However, a significant challenge during studies on the pathway and the as-yet unknown mode of action are the low production titers of *S. griseoflavus* W-384 and its propensity to irreversibly lose its biosynthetic capability. The regulation of *Streptomyces* natural products is often complex and commonly involves several layers of pathway-specific and/or global regulators. Genetic engineering of these regulatory systems is taken as an approach to increase production titers (Bibb 2005). Since HRM itself also acts as a metabolic and developmental regulator in *Streptomyces* spp., an understanding of the factors governing its production would also be an important basis to unravel the intricate regulatory network in intra- and interspecies HRM signaling. Therefore, in this study, the regulatory genes in HRM biosynthesis was investigated to create improved HRM producers and understand the regulation during the HRM biosynthesis.

3.2.1 Bioinformatic analysis of three candidates for regulatory genes in *hrm* gene cluster

Previous bioinformatic analysis (Höfer et al., 2011) revealed the existence of three regulatory genes, *hrmA*, *hrmB* and *hrmH*, encoded within hormaomycin biosynthetic gene cluster, where HrmA and HrmB were predicted as positive regulators. HrmA is homologous to transcriptional regulators belonging to the AraC family (Martin and Rosner 2001), showing 35% protein sequence identity to TxtR, an AraC/XylS cellobiose-binding protein that induces thaxtomin production in *S. scabies* (Joshi et al., 2007). HrmB is homologous to a small family of regulators with poorly understood mechanisms that includes NovE, a transcriptional activator of novobiocin biosynthesis (Dangel et al., 2008), and LmbU, a positive regulator of lincomycin biosynthesis (Chen et al., 2011). All three homologues contain a TTA codon for leucine that is rare in streptomycetes and indicates regulation by the $tRNA^{UUA}$-encoding gene *bldA* (Leskiw et al., 1991). In addition to *hrmA* and *hrmB*, *hrmH* was also tentatively included in the list of regulatory gene candidates. Homologues of HrmH belong to the poorly characterized YjgF/Yer057p/UK114 family. Members with known function exhibit diverse, often regulatory functions. For example, mammalian UK114 (=endoribonuclease L-PSP) is a potent inhibitor of cell-free protein synthesis by disintegrating polysomes through fragmentation of polysomal mRNA (Oka et al., 1995; Morishita et al., 1999), and *Salmonella enterica* YjgF (RidA) and the human homolog UK114 inhibit threonine dehydratase-dependent phosphoribosylamine formation *in vitro*, apparently by deaminating a biosynthetic intermediate (Lambrecht et al., 2010). Since these homologues can interact with nucleic acids as well as small molecules, it was not clear at this stage whether HrmH might be a regulator or a biosynthetic enzyme.

3.2.2 Overexpression of pathway-specific activators HrmA and HrmB to improve hormaomycin production

Since *hrmA* and *hrmB* were candidates for activator genes, it was investigated whether their overexpression results in a specific increase of HRM production. To construct the desired overproducers, the experiments were carried out according to the strategy depicted in **Figure**

3.13.

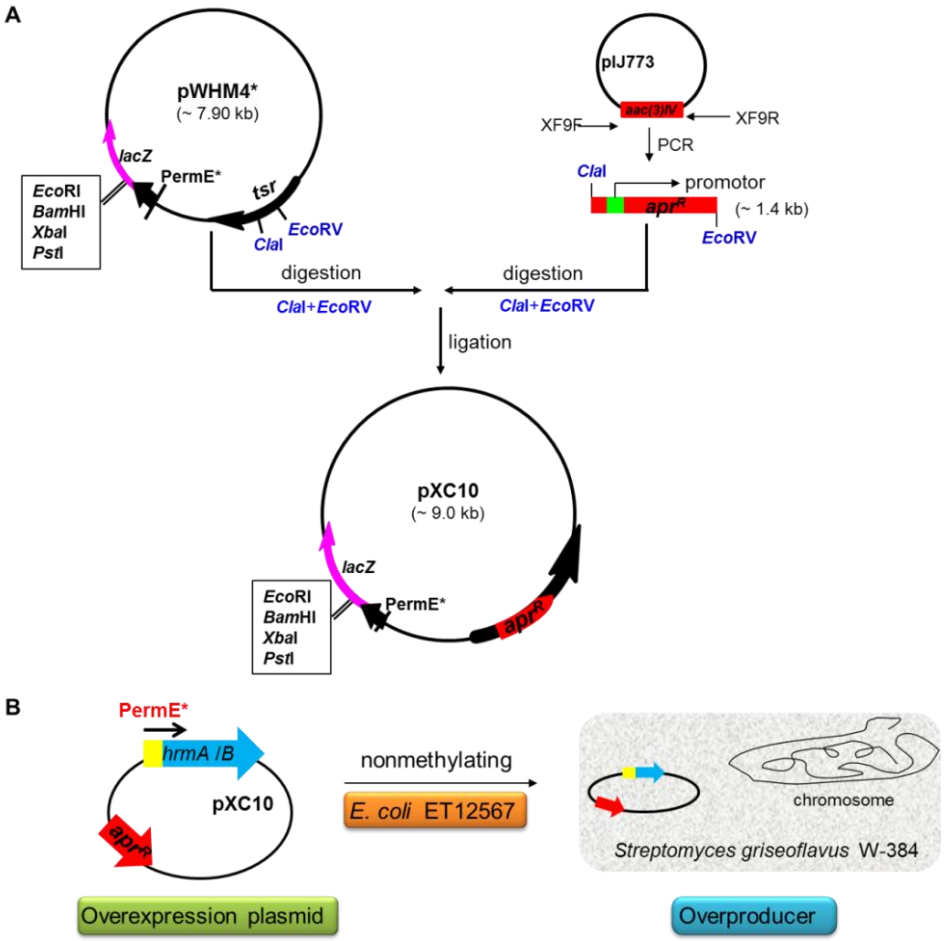

Figure 3.13: The strategy for construction of HRM overproducers. **A,** Modification of *Streptomyces* expression plasmid pWHM4*; **B,** Construction of HrmA and HrmB overexpression strains.

In this study, pWHM4* was modified for further convenience of screening. Firstly, the apramycin resistance gene (*apr*^{R}) was amplified from pIJ773 using the primer pair XF9F/9R by PCR. The PCR products were purified from an agarose gel and cut with *Cla*I and *Eco*RV, meanwhile pWHM4* was similarly digested and purified (**Figure 3.14A**). Subsequently, the ligation was performed by mixing the PCR products of *apr*^{R} with pWHM4* and was subsequently transformed into *E. coli* DH5α. Since the thiostrepton resistance gene (*tsr*) in pWHM4* was disrupted and replaced with *apr*^{R}, the transformants harbored apramycin resistance. The transformants were randomly selected and further confirmed by digestion with *Cla*I and *Eco*RV. The plasmids with the correct bands after digestion were referred to as pXC10, a new *Streptomyces* auto-replicating expression vector. The genes *hrm*A and *hrm*B were

amplified from *S. griseoflavus* W-384 genomic DNA using primer pairs XF10F/10R and XF11F/11R, then cloned into pBluescript SK-II(+) using *Eco*RI and *Xba*I and verified by sequencing. The plasmids extracted from the resulting transformants were screened by double digestion (**Figure 3.14B**).

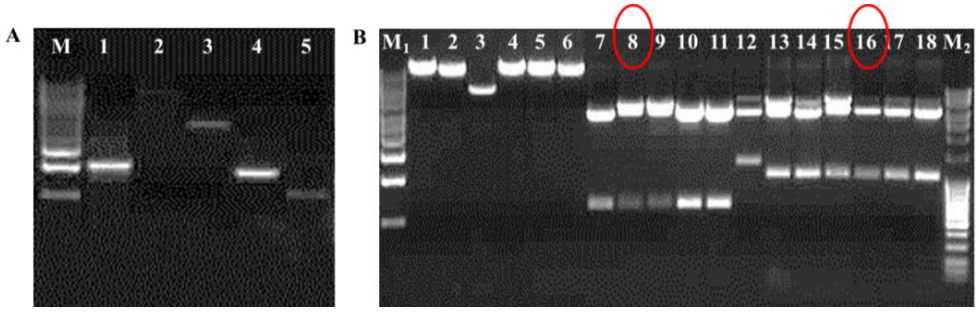

Figure 3.14: Agarose gel analysis of pXC11 and pXC12. **A,** Lane M, 1 kb DNA ladder, lane 1, *apr*^{R} with promoter (~1.1 kb), lane 2, pWHM* digested with *Cla*I+*Eco*RV (~7.9 kb), lane 3, pBluescript SK-II(+) digested with *Xba*I+*Eco*RI (~3.0 kb), lane 4, *hrmA* PCR products (~1.0 kb), lane 5, *hrmB* PCR products (~0.6 kb); **B,** Lane M_1, 1 kb DNA ladder, lanes 7-11, digestion of pXC11 with *Xba*I+*Eco*RI, lanes 13-18, digestion of pXC12 with *Xba*I+*Eco*RI, M_2, 100 bp DNA ladder. pXC11, *hrmA* ligated to pBluescript SK-II(+), pXC12, *hrm*B ligated to pBluescript SK-II(+). Lanes 8 and 16 contain plasmids pXC11 and pXC12 used for further study with the correct sequences of *hrmA* and *hrmB*, respectively.

The candidate DNA with the correct bands was sequenced. Then, the plasmids with *hrmA* and *hrmB* based on pBluescript SK-II(+) vector were named as pXC11 and pXC12, respectively. The DNA fragments of *hrmA* and *hrmB* cut from pXC11 and pXC12 were individually ligated into pXC10 under the control of the constitutive promoter *ermE** from the erythromycin resistance gene (Bibb et al., 1985) to give pXC14 and pXC13 (**Figure 3.15**).

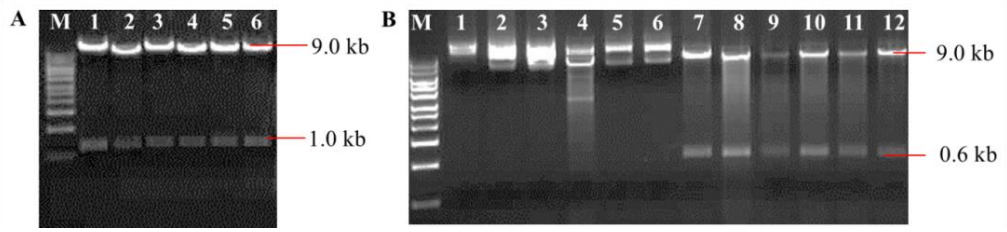

Figure 3.15: Agarose gel analysis of pXC14 and pXC13. **A,** Lane M, 1 kb DNA ladder, lanes 1-6, digestion of pXC13 with *Xba*I+*Eco*RI. pXC14, *hrmA* ligated to pXC10; **B,** Lane M, 1 kb DNA ladder, lanes 1-12, digestion of pXC13 with *Xba*I+*Eco*RI (lanes 1-6 are false positives). pXC13, *hrmB* ligated to pXC10. pXC10 is a modified pWHM4* with apramycin resistance.

The resulting plasmids were individually introduced into *E. coli* ET12567 to get non-methylated DNA and were then transformed into *S. griseoflavus* W-384 by PEG-mediated protoplast transformation according to the procedures optimized above to give potential transformants with apramycin resistance. The genomic DNA was isolated from the potential transformants containing pXC14 or pXC13 and independently transformed them into *E. coli* DH5α. The plasmid DNA from the resulting transformants was identified by enzymatic digestion with *Eco*RI and *Xba*I (**Figure 3.15**). Finally, the HrmA overexpression strain and HrmB overexpression strain were generated and considered as two overproducer candidates. To obtain ideal fermentation conditions for HRM production, triplet experiments were performed by cultivation of the wild type strain in 50 mL of MMS media in 250 mL flasks either baffled with springs or shaken with glass beads. The cell weights, PH value of fermentation cultures from flasks either baffled with spring or glass beads were compared (**Figure 3.16**). The results suggested that the optimal condition for HRM production is cultivation of the wild type strain in 250 mL flask baffled with spring at pH value of 9 at 27 ℃.

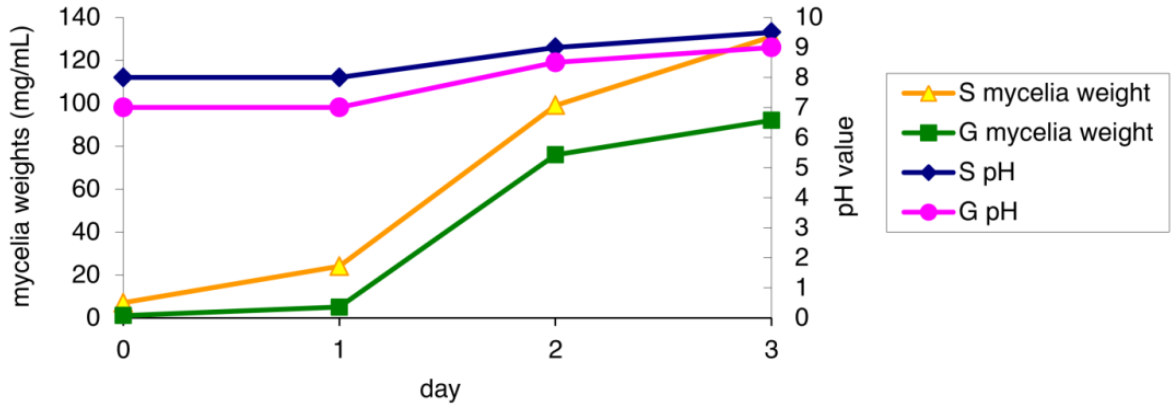

Figure 3.16: Comparison of mycelia growth of *S. griseoflavus* W-384 in different conditions. (**S**, spring-baffled flask; **G**, flask shaken with glass beads.).

Subsequently, triplet fermentation of the two overproducer candidates and wild-type (WT) was carried out in MMS media in the flasks baffled with spring to confirm their constant production of HRM. The supernatants from the above cultures were harvested and extracted with ethylacetate (EtOAc) three times. The analysis of the culture extracts by HPLC at UV of 273 nm revealed that HRM production from the HrmA overexpression strain was increased 40-fold

relative to the WT while HRM production from the HrmB overexpression strain was increased 135-fold relative to the WT (**Figure 3.17**). Therefore, the HrmA overexpression strain and HrmB overexpression strain were referred as to the HRM overproducers, which were named as XC1 and XC2, respectively. These results are consistent with a role as pathway activators for both genes.

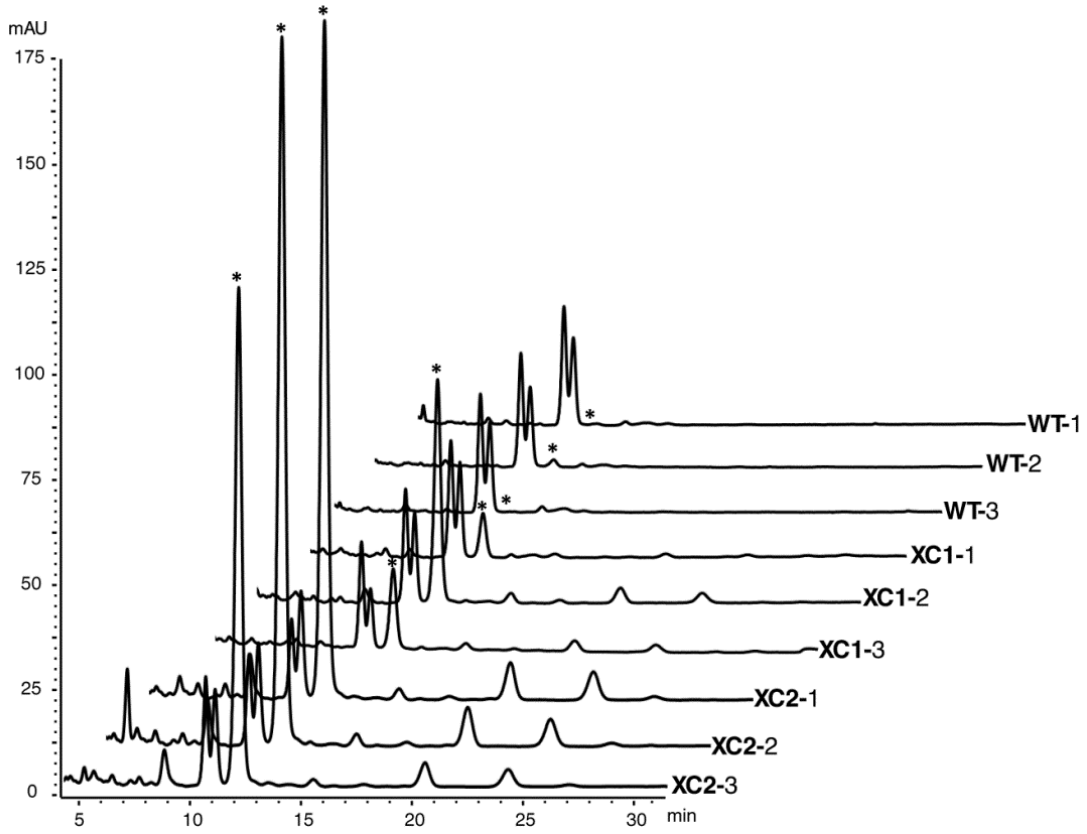

Figure 3.17: Comparison of HPLC traces of extracts from triplet fermentation of WT (WT-1, WT-2, WT-3), XC1 (XC1-1, XC1-2, XC1-3) and XC2 (XC2-1, XC2-2, XC2-3). * stands for HRM at retention time of 12.8 min at UV of 273 nm.

To test whether these two activators function in an additive way that would allow us to further increase HRM titers, a *hrmA*/*hrmB* double-expression strain XC3 was created via introducing another *hrmB*-overexpression plasmid pXC31 (*hrmB* ligated into pWHM4* under control of the *ermE** promoter with thiostrepton resistance) into XC1. However, analysis of its metabolic profile did not indicate up-regulation beyond the level of the previous best producer XC2 (**Figure 3.18**).

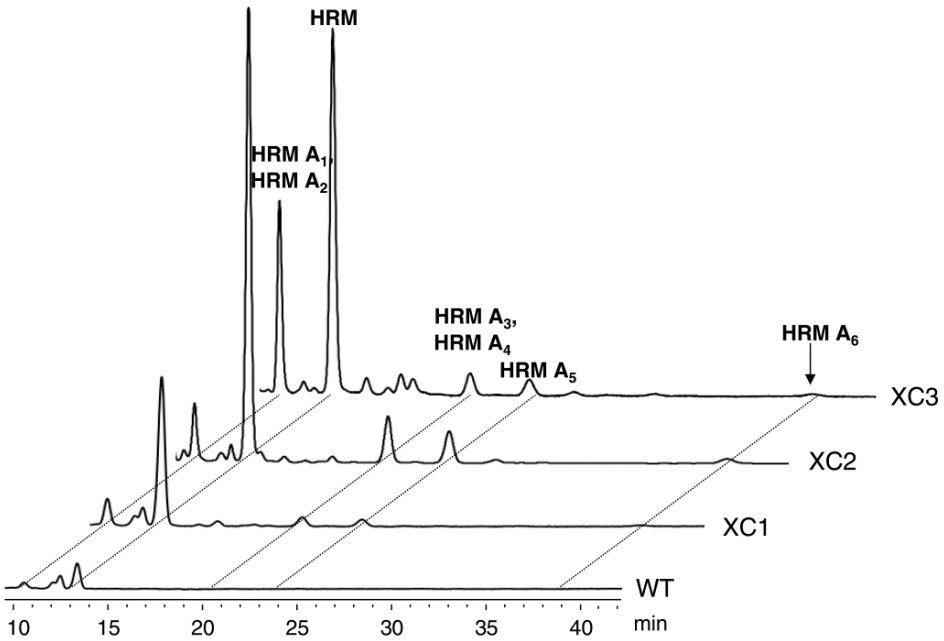

Figure 3.18: HPLC profiles of WT, XC1, XC2 and XC3. HRM A_1-A_6 are HRM analogues isolated from XC2. The detection wavelength was 273 nm. The retention times of HRM and HRM derivatives (HRM A_1-A_6) are: 10.2 min (HRM A_1, HRM A_2), 13.4 min (HRM), 20.3 min (HRM A_3, HRM A_4), 23.4 min (HRM A_5) and 38.5 min (HRM A_6).

The same amount (20 μL) of supernatants from the two overproducers XC1 and XC2, as well as the WT strain were tested against *Arthrobacter crystallopoietes* ATCC1548. The results showed that XC1 and XC2 exhibit much higher bioactivity than the WT strain, with XC2 as the apparently best overproducer (**Figure 3.19**).

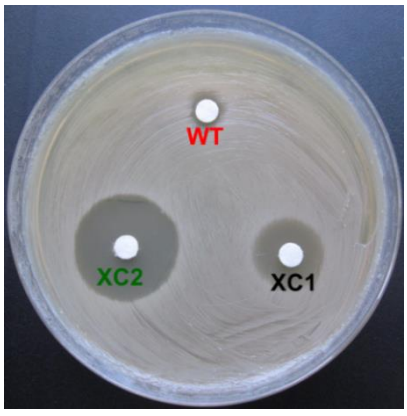

Figure 3.19: Bioassay of the supernatants from WT, XC1 and XC2 against *A. crystallopoietes* ATCC1548.

Upon closer examination of the HPLC profiles obtained from the regulatory mutants, a series of

new compounds were observed in all three strains. Subsequently, these new compounds were isolated. The initial analyses of electrospray ionization-liquid chromatography-mass spectrometry (ESI-LC-MS) and tandem mass spectrometry (MS/MS) were carried out by Dr. Roberta Teta in the Mangoni group in University of Napoli and Dr. Max Crüsemann in the Piel group. The results indicated that these new compounds were structurally related to HRM. Specific search for their ions in LC-MS runs showed that they are also produced by WT, but at extremely low amounts. To determine their structures, peptides produced by XC2 were purified. The resulting six compounds were subsequently subjected to the MS/MS and NMR analyses and characterized by Dr. Roberta Teta and Dr. Max Crüsemann. All tandem mass spectra were interpreted by Dr. Roberta Teta using an adapted version of the peptide nomenclature proposed by Roepstorff and Fohlman (Roepstorff and Fohlman 1984) as modified by Johnson (Johnson et al., 1987). If the charge is retained on the N-terminal fragment, the ion is classified as either *a* or *b*, if the charge is retained on the C-terminus, the ion type is either *x* or *y*. A subscript indicates the number of residues in the fragment; *d* indicates an ion type due to the side chain cleavage. The most significant fragments produced by tandem mass analysis for HRM (*m/z* 1151.4546 for $C_{55}H_{69}N_{10}O_{14}ClNa$) are depicted in (**Figure 3.20**).

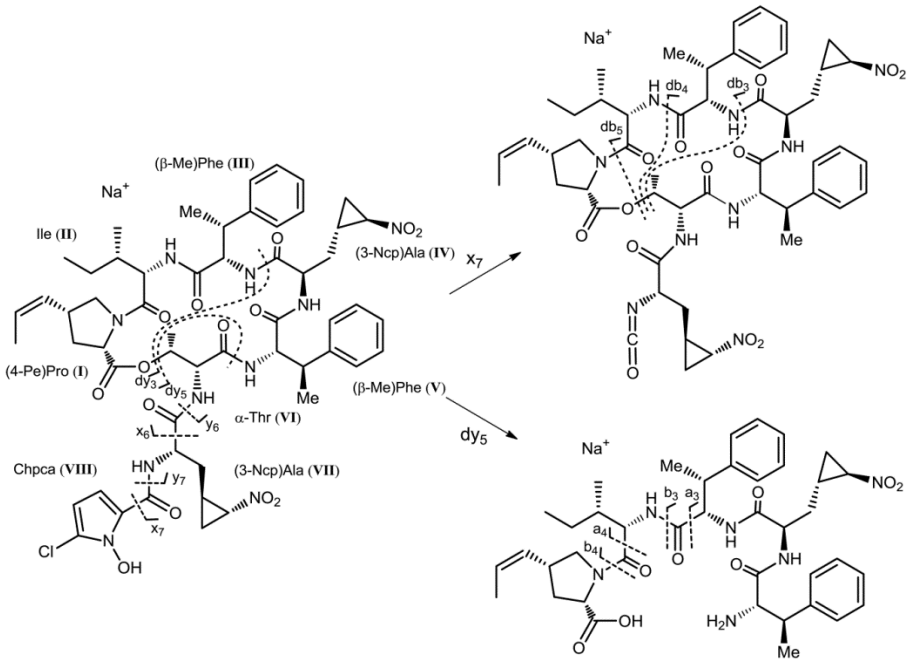

Figure 3.20: Tandem MS fragmentation of HRM.

The most abundant ion in the MS/MS spectrum of HRM is found at *m/z* 1034.4586 and is due to the loss of the chlorinated pyrrole ring; it is a C-terminal fragment composed of seven amino acids, and is thus called x_7. Further fragmentation of this ion in an MS^3 experiment involves ring opening by cleavage of the ester bond between the α-Thr (VI) side chain and (4-Pe)Pro (I) carboxyl, yielding the linear peptide *d*, followed by amide bond cleavages to give the N-terminal ions db_3, db_4, and db_5. The pseudomolecular ion undergoes a similar double cleavage of the α-Thr ester bond and of an amide bond, but with retention of the charge on the C-terminal fragments, giving the linear fragments dy_3 (*m/z* 452.2520) and dy_5 (*m/z* 769.3888). Further C-terminal fragmentation of the latter ion (Mangoni 2012) produces ions b_4, a_4, b_3, and a_3. All the analytical data of HRM A_1-HRM A_6 including MS/MS and NMR analyses was reported in Max Crüsemann's thesis in 2012. The chemical structures of these six new HRM analogues were shown in **Figure 3.21**.

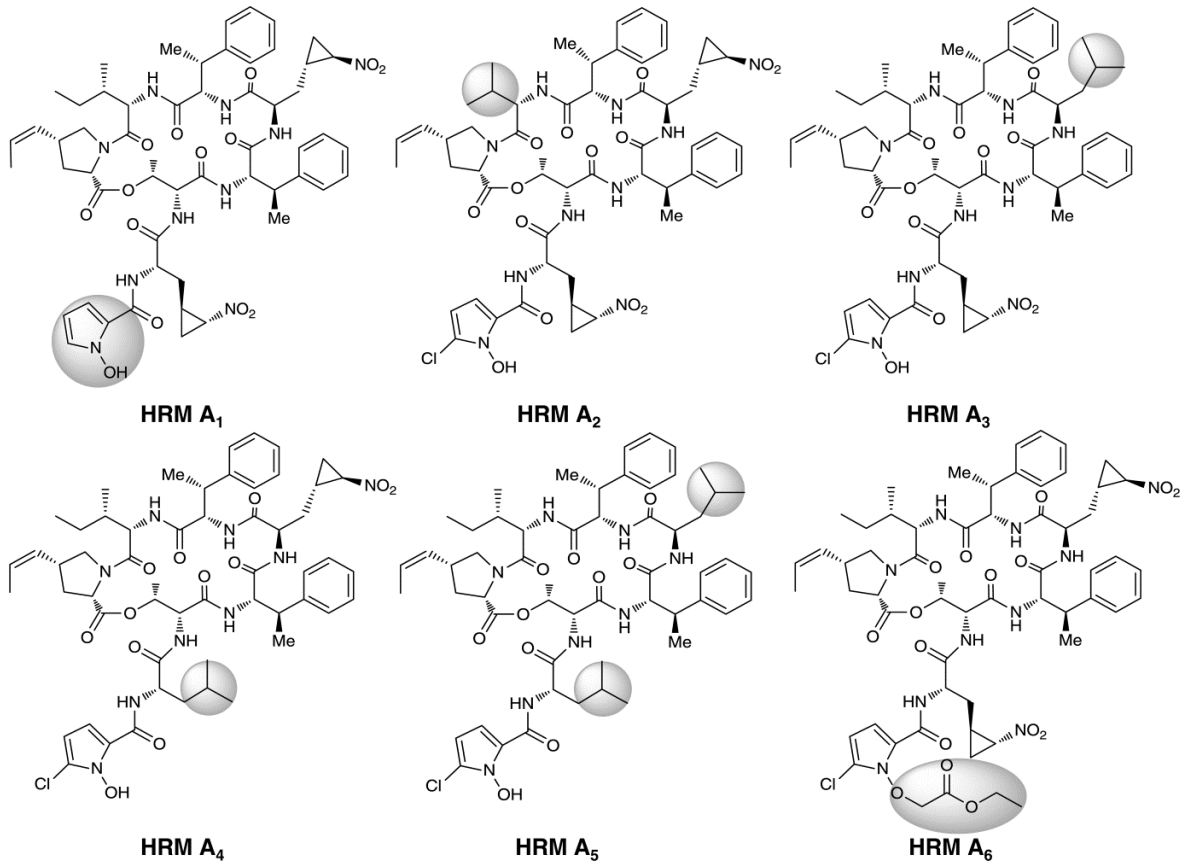

Figure 3.21: The structures of hormaomycin derivatives HRM A_1-HRM A_6.

In comparison to HRM, HRM A_1 lacks the chlorine moiety in the Chpca starter unit, and in HRM A_2, a valine residue is incorporated instead of isoleucine. HRM A_{3-5} all possess leucine substitutions for various (3-Ncp)Ala units. In an effort to further enhance production of HRM A_{3-5}, L-leucine was supplemented into the *hrmB*-overproducing strain, resulting in a modest increase in their titers with a concomitant decrease in HRM production (**Figure 3.22**).

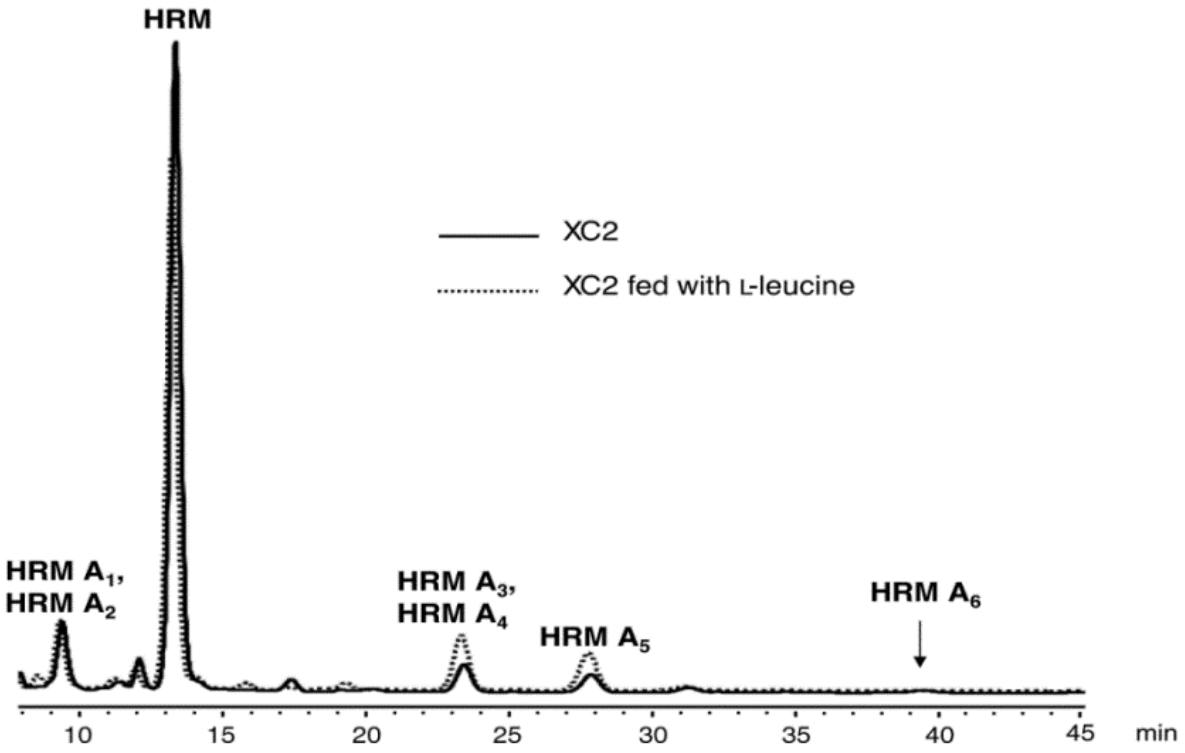

Figure 3.22: Chemical feeding of XC2 with L-leucine.

3.2.3 Analysis the role of *hrmH*, another putative regulatory gene

HrmH was initially predicted to be a putative negative regulator. To check if HrmH negatively regulates the HRM biosynthesis, the *hrmH* gene was subjected to the inactivation to increase HRM production. The *hrmH* mutant (ΔH) was generated by replacement with an apramycin resistance gene cassette according to the strategy of PCR-targeting for mutagenesis in *S. coelicolor* A3(2) (Gust et al., 2003) (**Figure 3.23**).

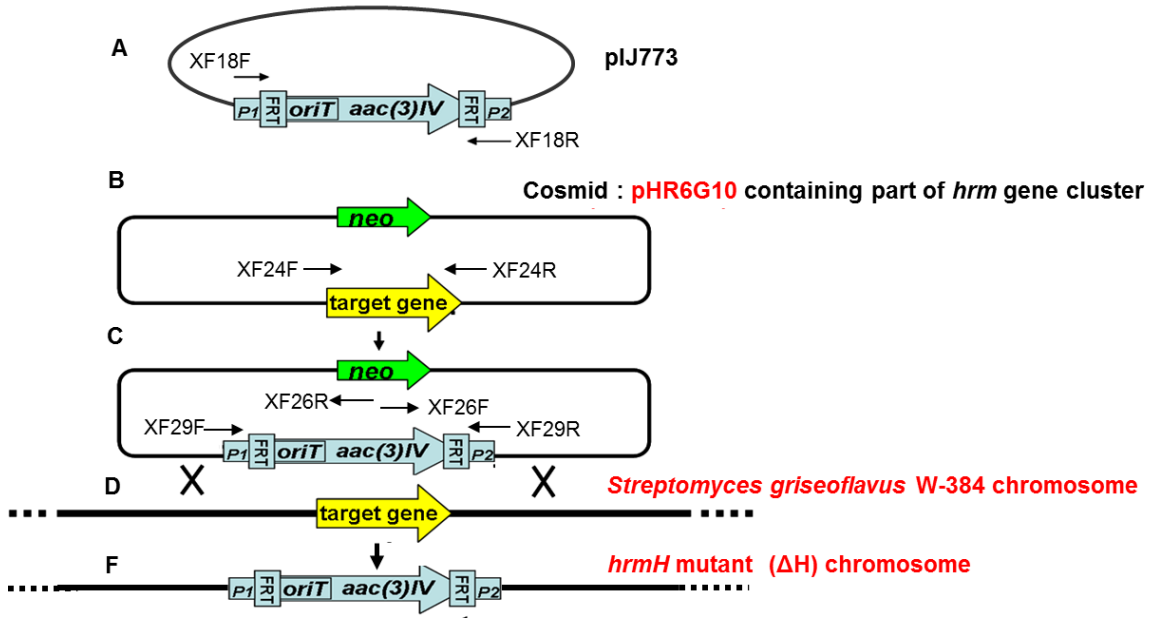

Figure 3.23: The strategy for construction of the ΔH via a PCR-targeted replacement. Adapted from Gust et al., 2003.

A 1.4 kb fragment containing the apramycin resistance cassette amplified from pIJ773 (Gust et al., 2003) using the primer pair XF18F/18R was used to disrupt *hrmH* in pHR6G10. The resulting mutants were further confirmed by PCR (**Figure 3.24**) using the primer pairs XF24F/24R, XF26F/29R, XF29F/26R and XF29F/29R (**Table 4.6**).

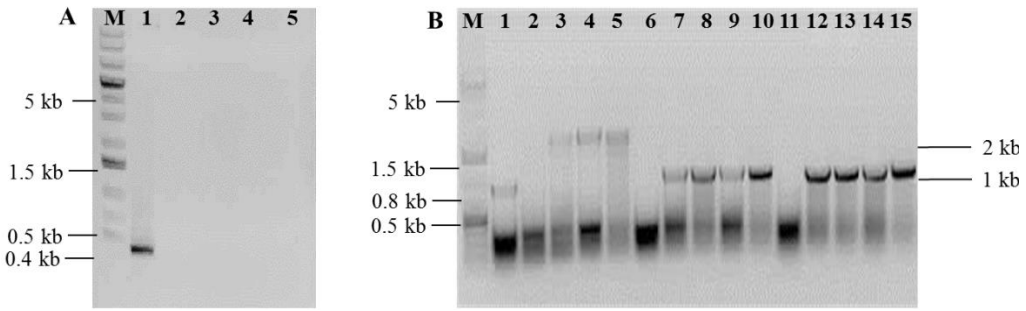

Figure 3.24: Agarose gel analysis of PCR products amplified from the genomic DNA of *S. griseoflavus* W-384 and ΔH mutant. A, Identification of genomic DNA from S. griseoflavus W-384 (lane 1) and four different transformants of ΔH (lanes 2-5) by PCR using the primer pair XF24F/24R to amplify the hrmH gene. B, Identification of genomic DNA from S. griseoflavus W-384 (lanes 1, 6, 11) and four different transformants of ΔH (lanes 2-5, 7-10, 12-15) by PCR using the primer pairs XF29F/29R, XF29F/26R, and XF26F/26R, respectively.

Triplet cultivation of the ΔH strain was performed. Unexpectedly, HPLC analysis of the corresponding culture extracts showed the same profiles that deletion of *hrmH* had no obvious

effect on HRM production but resulted in the observation of an additional metabolite as compared to the WT strain (**Figure 3.25**).

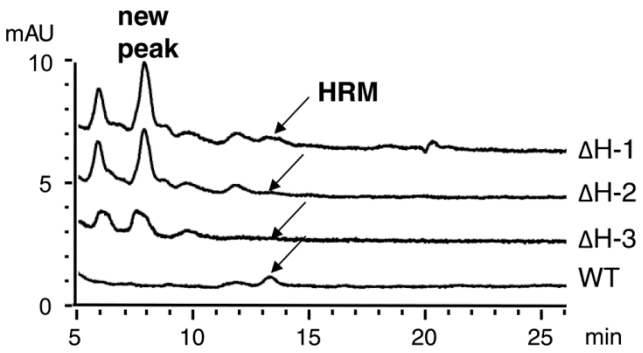

Figure 3.25: Comparison of HPLC traces of the ΔH extracts from triplet cultivation of ΔH (ΔH-1, ΔH-2, ΔH-3) with that of the WT strain. HRM is at 13.4 min, an additional metabolite (new peak) appeared in ΔH is at 7.2 min. HPLC was carried out at UV of 273 nm.

For genetic complementation of ΔH, the *hrmH* gene fragment was amplified from *S. griseoflavus* W-384 genomic DNA using primers XF24F/24R and was first inserted into pBluescript SK-II(+) to give pXC19. After sequence verification, the correct *hrmH* gene fragment was digested from pXC19 and ligated into pWHM4* to obtain pXC26. Finally, non-methylated pXC26 was introduced into the ΔH strain to generate the ΔH complement ΔH/HrmH. The required complements (ΔH/HrmH) were further identified by enzymatic digestion of plasmid DNA from transformants of *E. coli* DH5α (**Figure 3.26**).

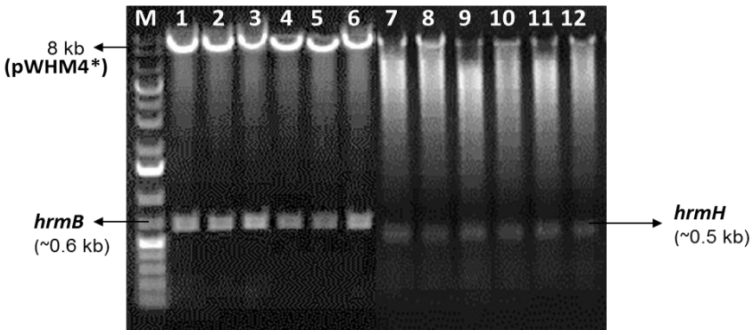

Figure 3.26: Agarose gel analysis of ΔH/HrmB and ΔH/HrmH. Lane **M**, 1 kb DNA ladder; lanes **1-6**, digestions of plasmids with *Xba*I and *Eco*RI isolated from transformants after introducing plasmid DNA from ΔH/HrmB into *E. coli* DH5α; lanes **7-8**, digestions of plasmids with *Xba*I and *Eco*RI isolated from transformants after introducing plasmid DNA from ΔH/HrmH into *E. coli* DH5α.

HPLC analysis of ΔH/HrmH showed the additional metabolite in ΔH decreased (**Figure 3.27A**). MS analysis of the HPLC-purified peak revealed a mass of 1103.464 Da for the $[M+H]^+$ ion (**Figure 3.27B**), which corresponds to a compound with 26 mass units less than HRM. This additional metabolite observed in ΔH was designated as HRM A_7.

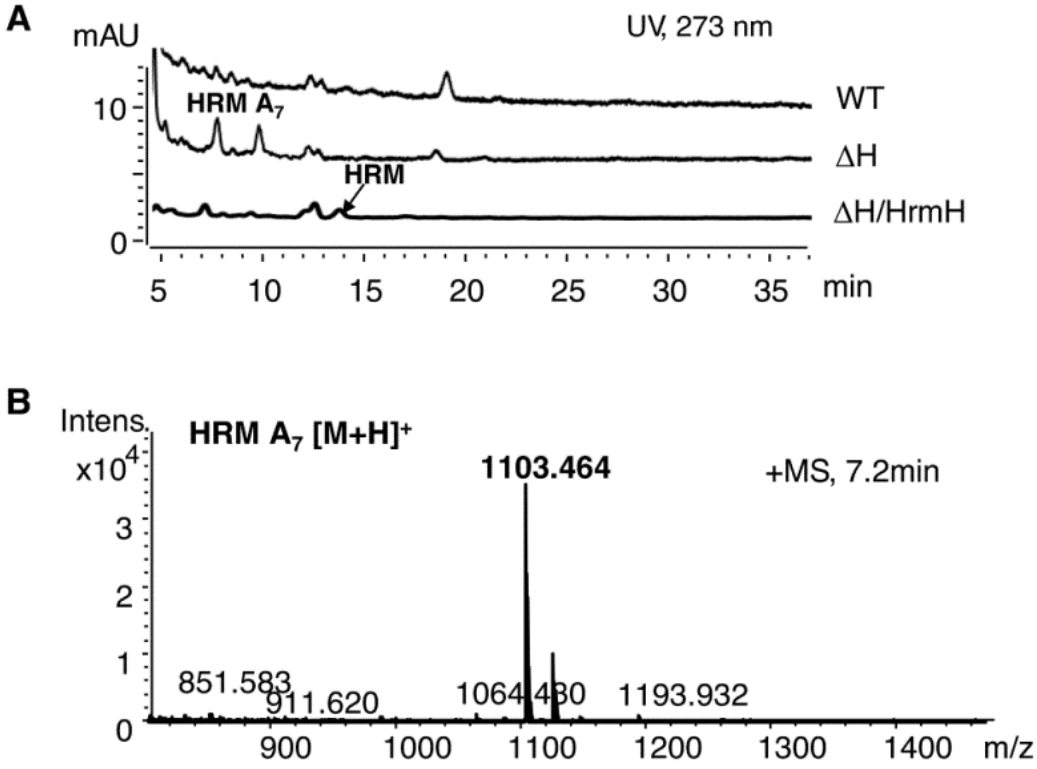

Figure 3.27: LC-MS analysis of extracts from the WT and the ΔH and ΔH/HrmH mutants. **A,** Comparison of HPLC traces from the WT, the ΔH and ΔH/HrmH. The retention time of HRM A_7 (a seventh HRM analogue) and HRM are at 7.2 min and 13.4 min, respectively. UV, 273 nm. **B,** Observed exact mass of HRM A_7.

Based on the molecular formula of $C_{55}H_{69}O_{14}N_{10}Cl$ for HRM with an exact mass of 1129.476 Da for $[M+H]^+$, the molecular formula of this new compound, HRM A_7, was estimated as $C_{53}H_{67}N_{10}O_{14}Cl$ with loss of C_2H_2 (calcd. Mass 1103.460 Da for $[M+H]^+$). Since the titers were too low for NMR analysis, the compound was initially analyzed by MS/MS analysis after isolation by HPLC. According to the tandem MS fragmentation of HRM (**Figure 3.20**), all the fragmentations of HRM A_7 showed the consistance with those of HRM except for 426.225 $[M+Na]^+$ (**Table 3.3**), corresponding to a modified tripeptide normally including (4-Me)Phe, L-isoleucine, and (4-Pe)Pro. Methanolysis to open the depsipeptide ring followed by MS/MS

analysis of the isolated peak narrowed down the modified fragment to L-isoleucine and (4-Pe)Pro, suggesting the non-natural amino acid (4-Pe)Pro was modified in HRM A_7.

Table 3.3: ESI tandem MS fragmentation pattern of hormaomycin (HRM) and HRM A_7.

Ion	HRM (Theoretical)	HRM A_7	HRM A_7 (Methanolysis)
$[M+Na]^+$	1151.458	1125.433	1157.454
	$C_{55}H_{69}N_{10}O_{14}ClNa^+$	$C_{53}H_{67}N_{10}O_{14}ClNa^+$	$C_{54}H_{71}N_{10}O_{15}ClNa^+$
Cl	1117.489	1090.438	1121.481
	$C_{55}H_{70}N_{10}O_{14}Na^+$	$C_{53}H_{68}N_{10}O_{14}Na^+$	$C_{54}H_{70}N_{10}O_{15}Na^+$
x_7	1034.468	1008.443	1040.453
	$C_{51}H_{65}N_9O_{13}Na^+$	$C_{49}H_{63}N_9O_{13}Na^+$	$C_{50}H_{67}N_9O_{14}Na^+$
y_7	1008.473	982.441	1014.477
	$C_{50}H_{67}N_9O_{12}Na^+$	$C_{48}H_{65}N_9O_{12}Na^+$	$C_{49}H_{69}N_9O_{13}Na^+$
x_6	878.414	852.382	884.402
	$C_{45}H_{57}N_7O_{10}Na^+$	$C_{43}H_{55}N_7O_{10}Na^+$	$C_{44}H_{59}N_7O_{11}Na^+$
y_6	852.427	826.392	858.431
	$C_{44}H_{59}N_7O_9Na^+$	$C_{42}H_{57}N_7O_9Na^+$	$C_{43}H_{61}N_7O_{10}Na^+$
dy_5	769.390	743.381	757.375
	$C_{40}H_{54}N_6O_8Na^+$	$C_{38}H_{52}N_6O_8Na^+$	$C_{39}H_{54}N_6O_8Na^+$
dy_4	608.306	582.242	596.294
	$C_{30}H_{43}N_5O_7Na^+$	$C_{28}H_{41}N_5O_7Na^+$	$C_{29}H_{43}N_5O_7Na^+$
dy_3	452.253	426.225	440.249
	$C_{24}H_{35}N_3O_4Na^+$	$C_{22}H_{33}N_3O_5Na^+$	$C_{23}H_{35}N_3O_4Na^+$
$dy_3 \rightarrow b_3$	291.168	-	279.170
	$C_{14}H_{24}N_2O_3Na^+$		$C_{13}H_{24}N_2O_3Na^+$

Based on this hypothesis, a series of feeding studies were carried out to determine the structure of the newly incorporated residue. In addition to supplementing fermentations of the WT, ΔH, and ΔH/HrmH strains with (4-Pe)Pro in control experiments, cultures were fed the commercially available L-pipecolic acid and (*2S,4R*)-4-methylpyrrolidine-2-carboxylic acid [*trans*-(4-Me)Pro] as precursor amino acid candidates with a matching mass and known occurrence in nonribosomal peptides (He 2006; Katz et al., 1977). As a control, (3-Ncp)Ala was also independently fed into the strains. As shown in **Figure 3.28A**, feeding with *trans*-(4-Me)Pro resulted in the appearance of a 10-fold enhanced peak in the HPLC trace as compared to the unsupplemented ΔH strain, and the retention time was identical to that of HRM A_7. In contrast, feeding of pipecolic acid did not change the metabolic profile, suggesting that

this compound is not incorporated. These results show that the presence or absence of HrmH has an effect on the fidelity of HRM biosynthesis. To further characterize the new peptide, it was isolated from the *trans*-(4-Me)Pro enrichment culture. The subsequent NMR analysis of this new peptide was carried out by Dr. Roberta Teta in the Mangoni group.

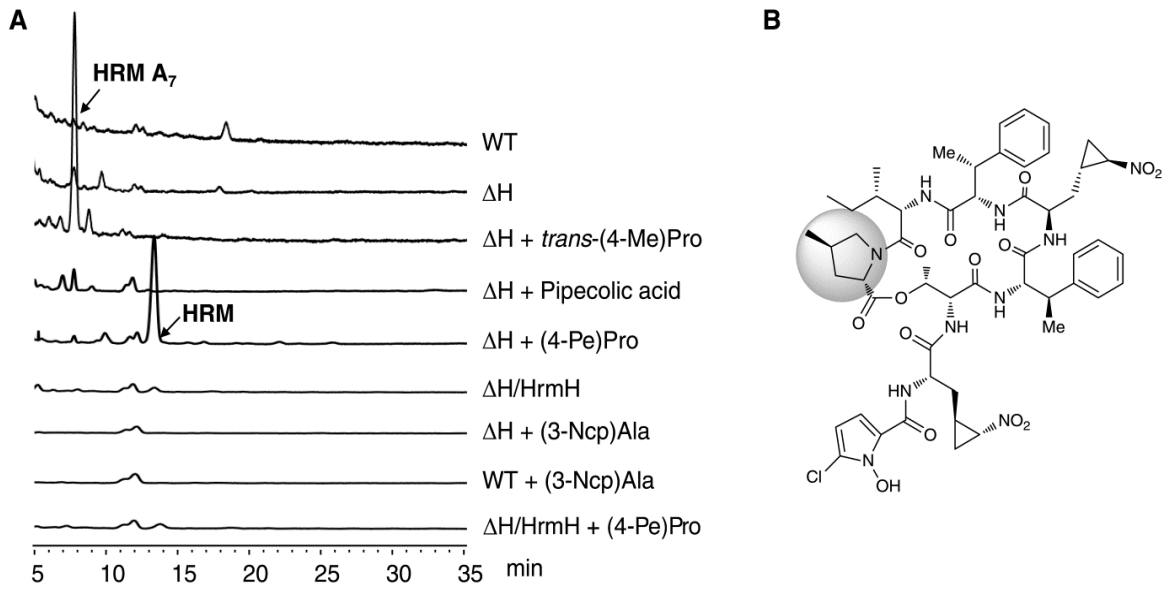

Figure 3.28: Chemical and genetic complementation of the ΔH. **A,** HPLC traces of the WT, ΔH, ΔH fed with *trans*-(4-Me)Pro [ΔH + *trans*-(4-Me)Pro], ΔH fed with L-pipecolic acid (ΔH+ Pipecolic acid), ΔH fed with (4-Pe)Pro [ΔH + (4-Pe)Pro], ΔH/HrmH, ΔH fed with (3-Ncp)Ala [ΔH + (3-Ncp)Ala], WT fed with (3-Ncp)Ala [WT + (3-Ncp)Ala], ΔH/HrmH fed with (4-Pe)Pro [ΔH/HrmH + (4-Pe)Pro]. The retention time of HRM A_7 and HRM are at 7.2 min and 13.4 min, respectively. UV, 273 nm. **B,** The structure of HRM A_7.

The following NMR analytical data were interpreted by Dr. Roberta Teta. The absence in the ^{1}H NMR spectrum (**Figure 3.29**) of HRM A_7 of the olefinic protons signals at δ 5.63 and 5.33, and the correlation in the correlation spectroscopy (COSY) spectrum (**Figure 3.30**) between H-4 at δ 2.57 with the methyl group at δ 1.07 (H_3-1') suggested that in HRM A_7, a methyl group at position 4 replaces the moiety present in HRM.

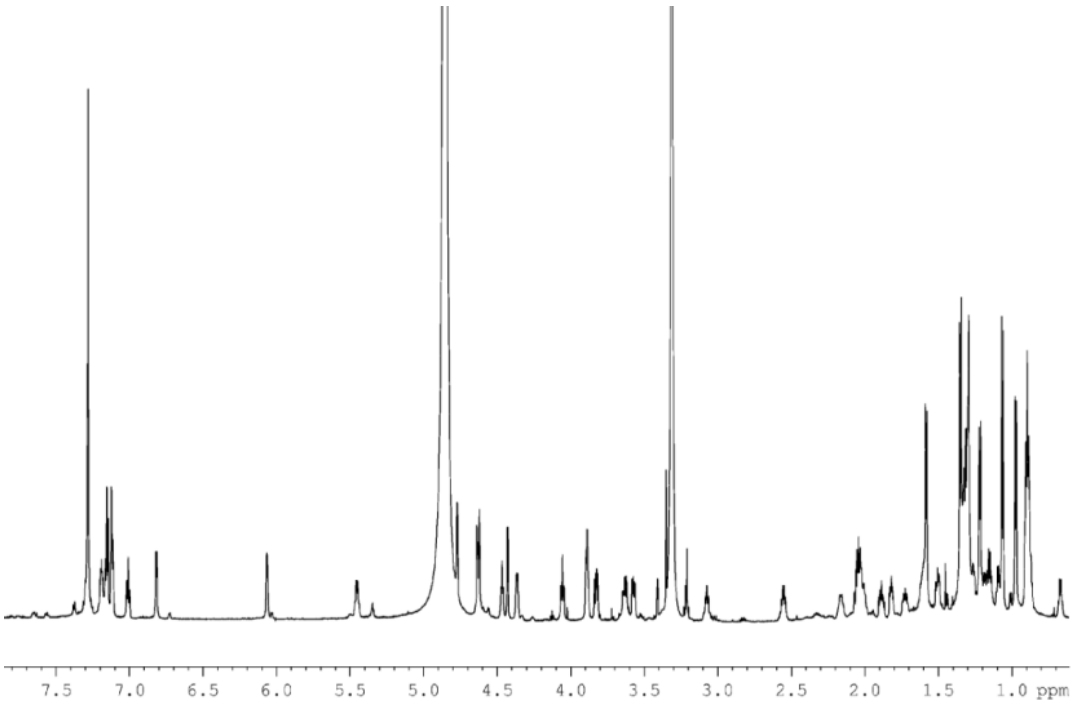

Figure 3.29: ^{1}H NMR spectrum (700MHz, CD_3OD) of HRM A_7.

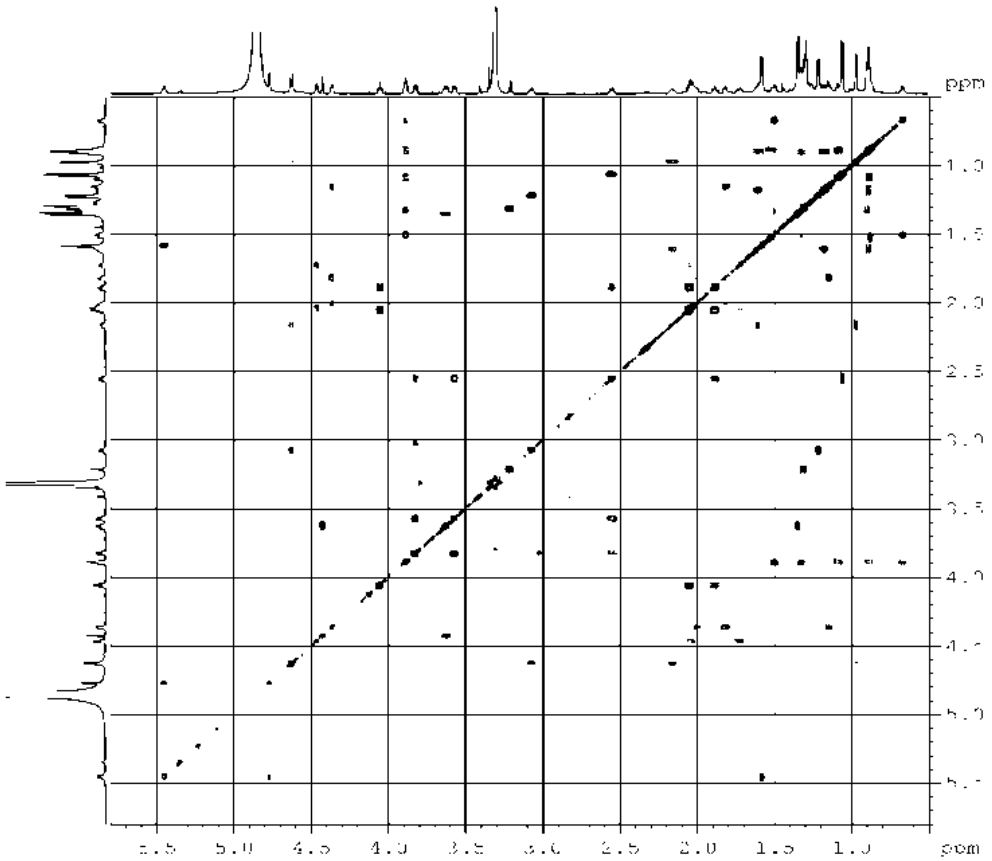

Figure 3.30: COSY spectrum (700MHz, CD_3OD) of HRM A_7 high field expansion.

This was confirmed by analysis of the total correlation spectroscopy (TOCSY) and heteronuclear single-quantum correlation spectroscopy (HSQC) spectra, which allowed assignment of all the protons and carbon atoms of 4-methylproline (**Table 3.4**).

Table 3.4: NMR signals of HRM A_7.

Aa	Position		δ_H [mult., *J* (Hz)]	δ_C [mult.]
(4-Me)Pro (I)	1		-	174.4 I
(4-Me)Pro (I)	2		4.07 (t, 7.5)	61.1 (CH)
(4-Me)Pro (I)	3	a	2.06 (ddd, 12.8, 7.5, 7.5)	36.9 (CH_2)
(4-Me)Pro (I)	3	b	1.90 (ddd, 12.8, 7.5, 6.2)	
(4-Me)Pro (I)	4		2.57 (octet, 6.2)	34.3 (CH)
(4-Me)Pro (I)	5	a	3.84 (dd, 10.4, 6.2)	55.6 (CH_2)
(4-Me)Pro (I)	5	b	3.58 (dd, 10.4, 5.0)	
(4-Me)Pro (I)	1’		1.07 (d, 7.0)	18.1 (CH_3)
Ile (II)	1		-	172.2 I
Ile (II)	2		4.64 (d, 10.6)	56.2 (CH)
Ile (II)	3		2.17 (m)	36.1 (CH)
Ile (II)	4	a	1.61 (m)	25.6 (CH_2)
Ile (II)	4	b	1.18 (dq, 8.3, 7.6)	
Ile (II)	5		0.89 (br. T, 7.0)	10.7 (CH_3)
Ile (II)	1’		0.98 (d, 6.7)	16.5 (CH_3)
(β-Me)Phe (III)	1		-	172.5 I
(β-Me)Phe (III)	2		4.44 (d, 5.4)	61.5 (CH)
(β-Me)Phe (III)	3		3.63 (dddd, 7.3, 7.3, 7.3, 5.4)	40.6 (CH)
(β-Me)Phe (III)	4		1.35 (d, 7.3)	14.3 (CH_3)
(β-Me)Phe (III)	1’		-	143.4 I
(β-Me)Phe (III)	2’		7.29 (ovl)	128.6 (CH)
(β-Me)Phe (III)	3’		7.19 (m)	128.0 (CH)
(β-Me)Phe (III)	4’		7.28 (ovl)	129.4 (CH)
(3-Ncp)Ala (IV)	1		-	174.2 I
(3-Ncp)Ala (IV)	2		3.89 (ovl)	54.5 (CH)
(3-Ncp)Ala (IV)	3	a	1.10 (ddd, 14.4, 6.8, 6.8)	33.3 (CH_2)
(3-Ncp)Ala (IV)	3	b	0.90 (ddd,14.4, 7.6, 7.6)	
(3-Ncp)Ala (IV)	1’		1.34 (ovl)	22.8 (CH)
(3-Ncp)Ala (IV)	2’		3.90 (br. D , 4.8)	60.2 (CH)
(3-Ncp)Ala (IV)	3’	a	1.51 (ddd, 10.3, 6.8, 4.8)	18.4 (CH_2)
(3-Ncp)Ala (IV)	3’	b	0.67 (q, 6.8)	
(β-Me)Phe (V)	1		-	171.5 I
(β-Me)Phe (V)	2		4.62 (d, 8.7)	59.7 (CH)
(β-Me)Phe (V)	3		3.08 (dq, 8.7, 7.2)	45.2 (CH)
(β-Me)Phe (V)	4		1.21 (d, 7.2)	18.4 (CH_3)

Aa	Position		δ_H [mult., *J* (Hz)]	δ_C [mult.]
(β-Me)Phe (V)	1’		-	143.3 I
(β-Me)Phe (V)	2’		7.10 (d, 7.5)	129.2 (CH)
(β-Me)Phe (V)	3’		7.14 (t, 7.5)	129.0 (CH)
(β-Me)Phe (V)	4’		7.00 (t, 7.5)	127.7 (CH)
α-Thr (VI)	1		-	169.5 I
α-Thr (VI)	2		4.77 (br. S)	59.1 (CH)
α-Thr (VI)	3		5.44 (dq, 7.0, 2.5)	73.1 (CH)
α-Thr (VI)	4		1.58 (d, 7.0)	18.5 (CH_3)
(3-Ncp)Ala (VII)	1		-	171.9 I
(3-Ncp)Ala (VII)	2		4.47 (br. D, 5.6)	54.5 (CH)
(3-Ncp)Ala (VII)	3	a	2.04 (ddd,, 13.2, 5.6, 5.6)	34.2 (CH_2)
(3-Ncp)Ala (VII)	3	b	1.72 (ddd, 13.2, 7.6, 7.6)	
(3-Ncp)Ala (VII)	1’		2.01 (ovl)	22.9 (CH)
(3-Ncp)Ala (VII)	2’		4.36 (ddd, 7.2, 3.6, 3.6)	60.4 (CH)
(3-Ncp)Ala (VII)	3’	a	1.82 (ddd, 10.2, 5.8, 3.6)	17.8 (CH_2)
(3-Ncp)Ala (VII)	3’	b	1.14 (ovl)	
Chpca (VIII)	1		-	161.6 I
Chpca (VIII)	2		-	118.6 I
Chpca (VIII)	3		6.80 (d, 4.8)	110.4 (CH)
Chpca (VIII)	4		6.06 (d, 4.8)	104.1 (CH)
Chpca (VIII)	5		-	120.5 I

A rotating frame nuclear overhauser effect spectroscopy (ROESY) spectrum allowed us to establish the relative configuration of (4-Me)Pro (I) as *trans* (in contrast, HRM contains a *cis*-4-*Z*-propenylproline) (**Figure 3.31**). The spectrum showed diagnostic dipolar couplings between H-2 and H_3-1’, which are in the 1,3-relationship in a five-membered ring, and therefore must be *cis* oriented. This stereochemical assignment was corroborated by several other NOEs (**Figure 3.32**). *Trans*-(4-Me)Pro is much less common than *cis*-(4-Me)Pro, and has been found only in two closely related depsipeptides from the plant *Pterula* sp. (Chen et al., 2006) and in monamycin D1 from *Streptomyces jamaicensis* (Hassall et al., 1971), compared to the ~19 known natural products containing *cis*-(4-Me)Pro. All the other configurations were assumed to be the same as in HRM because the NMR data were very similar.

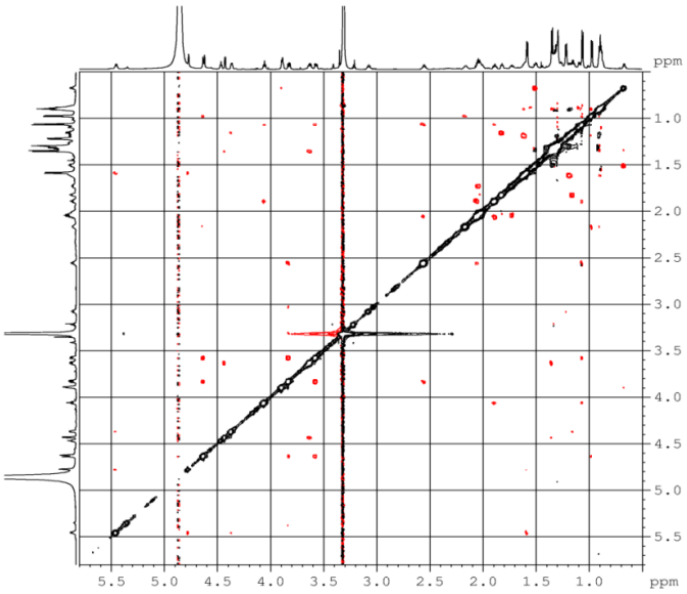

Figure 3.31: ROESY spectrum (700MHz, CD_3OD) of HRM A_7 high field expansion.

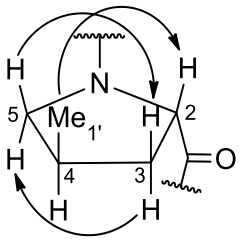

Figure 3.32: ROESY correlations in the (4-Me)Pro residue (I) of HRM A_7. Only 1,3 NOEs are reported. NOEs between *cis* vicinal protons are consistently much stronger than those between *trans* vicinal protons.

3.2.4 Inactivation of *hrmD* involved in the biosynthesis of (4-Pe)Pro

The unexpected metabolic phenotype observed for the ΔH mutant raised new questions about the role of HrmH. Since *trans*-(4-Me)Pro replaced (4-Pe)Pro in HRM A_7, the biosynthesis of (4-Pe)Pro was further investigated. Current knowledge about this complex sub-pathway comes from functional analysis of the HRM pathway and other routes that involve 4-alkyl-substituted Pro building blocks and homologous genes, i.e., lincomycin and pyrrolo[1,4]benzodiazepine antibiotics (Hu et al., 2007; Li et al., 2009a; Li et al., 2009b; Peschke et al., 1995). All these subpathways are initiated by extradiol cleavage of L-DOPA, which is generated by hydroxylation of L-tyrosine, and subsequent recyclization to form an unstable pyrroline intermediate. In contrast to HrmH, which is unique to the (4-Pe)Pro pathway, HrmD has close

homologs in the related pathways. The proteins are predicted to be F_{420}-dependent oxidoreductases likely involved in reducing and/or rearranging olefinic double bonds at a later stage of biosynthesis (Höfer et al., 2011). To investigate which influence the inactivation of a (4-Pe)Pro biosynthetic enzyme has on HRM production, an insertional *hrmD* mutant (ΔD) was created in a similar manner to ΔH (**Figure 3.23**).

Fermentation of the ΔD and ΔD/HrmD revealed a biosynthetic role of HrmD in HRM biosynthesis through complete abolishment of HRM, while genetic complementation with *hrmD* restored HRM production. Chemical complementation with (4-Pe)Pro also restored production and thus confirmed the direct role of HrmD in (4-Pe)Pro biosynthesis (**Figure 3.33**). Instead of HRM, the *trans*-(4-Me)Pro variant HRM A_7 was detected in extracts of ΔD fermentations. Upon addition of *trans*-(4-Me)Pro, the production of HRM A_7 increased in ΔD, paralleling the phenotype of the ΔH strain. These observations show that, similar to HrmD, HrmH influences the (4-Pe)Pro subroute of hormaomycin biosynthesis, but in contrast to HrmD is not absolutely required for the production of this residue.

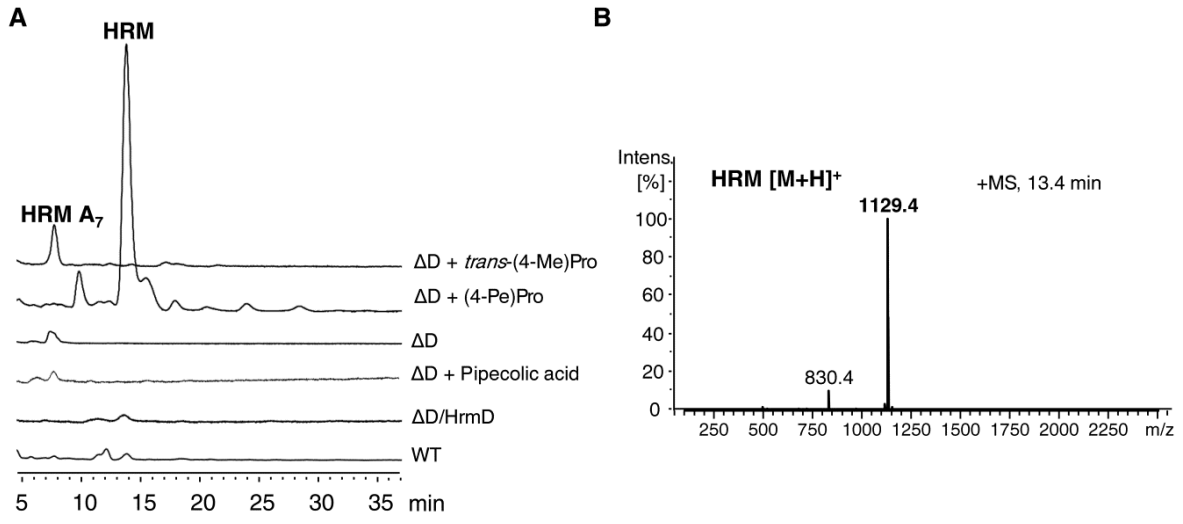

Figure 3.33: Genetic complementation and chemical feeding studies of the ΔD. **A,** HPLC traces of the ΔD, ΔD fed with (4-Me)Pro [ΔD + (4-Me)Pro], ΔD fed with L-pipecolic acid (ΔD + Pipecolic acid), and ΔD fed with (4-Pe)Pro [ΔD + (4-Pe)Pro], ΔD/HrmD, as well as the WT. **B,** MS analysis of HRM in ΔD fed with (4-Pe)Pro and ΔD/HrmD. The retention time of HRM A_7 and HRM are at 7.2 min and 13.4 min, respectively. UV, 273 nm.

3.2.5 Analysis of the origin of (4-Me)Pro

The function of HrmH was further interrogated by studying the biosynthetic origin of (4-Me)Pro. To test whether it is an intermediate or shunt product of the (4-Pe)Pro route or comes from a different source, a trideuterated form of the (4-Pe)Pro precursor L-DOPA [L-DOPA-(*ring*-d_3)] was fed into the WT and ΔH strains. In the WT and ΔH strains, the label was successfully incorporated into HRM (**Figure 3.34**).

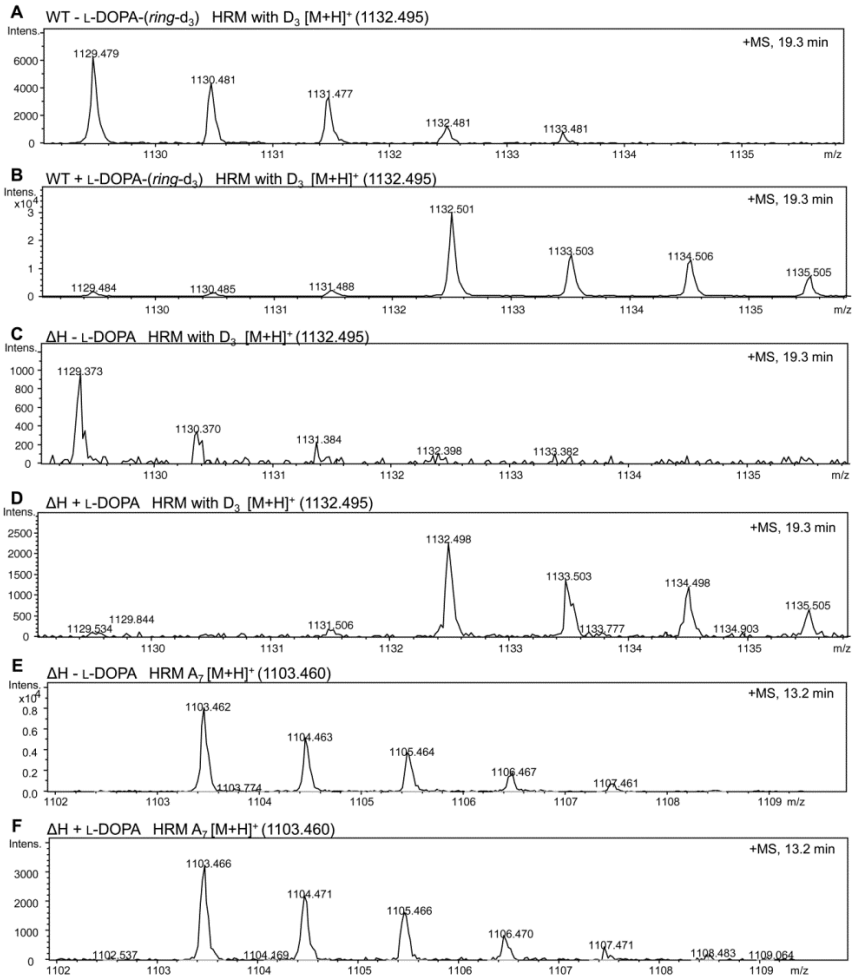

Figure 3.34: Comparison of the extracted ion chromatogram (EIC) from LC-MS analysis of the extracts from the WT and ΔH fed with L-DOPA-(*ring*-d_3). **A,** EIC of 1132.495 Da $[M+H]^+$ from the WT without feeding. **B,** EIC of 1132.495 Da $[M+H]^+$ from the WT fed with L-DOPA-(*ring*-d_3). **C,** EIC of 1132.495 Da $[M+H]^+$ from the ΔH without feeding. **D,** EIC of 1132.495 Da $[M+H]^+$ from the ΔH fed with L-DOPA-(*ring*-d_3). **E,** EIC of 1103.460 Da $[M+H]^+$ from the ΔH strain without feeding. **F,** EIC of 1103.460 Da $[M+H]^+$ from the ΔH fed with L-DOPA-(*ring*-d_3). HRM with D_3 $[M+H]^+$ (1132.495) is the exact mass of deuterate-labeled HRM; HRM A_7 $[M+H]^+$ (1103.460) is the exact mass that HRM A_7 was not be deuterate-labeled.

In contrast, MS analysis revealed no detectable labeling of HRM A_7 in both the WT and ΔH strains, and further supported that L-DOPA, as a precursor of HRM, is involved in HRM biosynthesis. This result suggested that (4-Me)Pro is not an intermediate in (4-Pe)Pro biosynthesis but rather originates from a source other than the HRM pathway. To identify a possible (4-Me)Pro pathway, the available genome sequence (GenBank: NZ_GG657758.1) of the HRM producer was searched for genes that might be involved in (4-Me)Pro biosynthesis or incorporation. However, no convincing gene candidate was identified.

3.2.6 Antibacterial assays for HRM A_1-A_7

HRM and its analogues were tested at five different concentrations (1, 0.1, 0.01, 0.001, and 0.0001 μg/mL) against *Arthrobacter crystallopoietes* ATCC15481 in liquid-based antimicrobial activity assays. The MIC values of these compounds are listed in **Table 3.5**.

Table 3.5: Bioassay test of HRM and HRM analogues against *A. crystallopoietes* ATCC15481.

HRM & HRM Analogues	MIC [μg/mL]
HRM	0.001
HRM A_1	0.01
HRM A_2	0.01
HRM A_3	0.001
HRM A_4	0.1
HRM A_5	1
HRM A_6	1
HRM A_7	0.001

All of the HRM analogues exhibited antibiotic activity against the test strain. HRM A_3 and HRM A_7 have similar activity to HRM, suggesting that there is the structural variability in the (4-Pe)Pro and the endocyclic (3-Ncp)Ala residues. In contrast, the exocyclic (3-Ncp)Ala moiety has a stronger influence on activity, since HRM A_4 and A_5 lacking this unit exhibit decreased activity. Similarly important but not absolutely required seem to be the chlorine atom and the leucine residue replaced in HRM A_1 and A_2.

3.2.7 Discussion

To study the many unusual biosynthetic and biological features of HRM, the limitations of inconsistent and low production had to be overcome. One aim of this study was therefore to exploit regulatory components in the HRM pathway to modify titers through metabolic engineering. Among the identified genes *hrmA*, *hrmB* and *hrmH*, individual overexpression of *hrmA* and *hrmB* resulted in significant increases in HRM production, with a maximal increase of 135-fold in the *hrmB* overexpression strain relative to WT. In numerous growth experiments, strains exhibited excellent stability. These results established HrmA and HrmB as pathway-specific positive regulators for HRM biosynthesis. The ability to significantly increase HRM production with *trans*-acting plasmids provides an effective and reproducible platform to study HRM biosynthesis in both WT and mutant strains.

A third gene, *hrmH*, was initially proposed to be a negative regulator in HRM biosynthesis (Höfer et al., 2011), yet disruption of *hrmH* had no detectable effect on HRM production. The peculiar phenotype observed with the ΔH strain, i.e., formation of the additional congener HRM A_7, allows for several possibilities of HrmH's role in HRM biosynthesis. Scenarios including a catalytic role in (4-Pe)Pro biosynthesis, down-regulation of *trans*-(4-Me)Pro biosynthesis or an alternative protection against its interference with the HRM pathway, up-regulation of (4-Pe)Pro biosynthesis, and down-regulation of other sub-pathways in HRM biosynthesis are all consistent with these data. However, some of these possibilities are incompatible when taken into context with our results for the (4-Pe)Pro-biosynthetic knockout strain ΔD. For instance, since HRM production was eliminated in ΔD while retained in ΔH, it is unlikely that HrmH is involved in the supplementation of (4-Pe)Pro in HRM biosynthesis. However, it should be taken into account that (4-Pe)Pro biosynthesis in *S. griseoflavus* W-384 has not been fully elucidated and that the HRM producer lacks a key enzyme present in homologous pathways (Höfer et al., 2011). All in all, our results reveal HrmH influences (4-Pe)Pro production and/or fidelity in HRM biosynthesis. Defining the precise mechanism for HrmH as transcriptional, translational, or small-molecule-mediated regulation in HRM biosynthesis will be the focus of future studies.

The complexities of regulatory mechanisms involved in antibiotic biosynthesis, hallmarked by *Streptomyces* secondary metabolism, are still poorly understood. Combined with our current excess of genetic information encoding proteins that are largely unverified and uncharacterized, manipulation of regulatory genes within secondary metabolic clusters often have unforeseen consequences. Unexpected changes in the timing, production, and metabolic profiles of secondary metabolites are often reported (Wang et al., 2011; Stratigopoulos et al., 2002; Matsuno et al., 2004; Gottelt et al., 2010; D'Alia et al., 2011; de la Fuente et al., 2002). Even genes initially labeled to have biosynthetic or unknown activities have been shown to harbor regulatory functions (Volokhan et al., 2005; Hwang et al., 2003). Manipulation of the previously proposed negative regulator *hrmH* revealed the unanticipated discovery of HRM A_7, which was shown to have (4-Pe)Pro replaced with *trans*-(4-Me)Pro (**Figure 3.28**). Interestingly, the source of *trans*-(4-Me)Pro remains undefined. The proposed biosynthetic routes for (4-Pe)Pro biosynthesis do not include *trans*-(4-Me)Pro as an intermediate (Höfer et al., 2011). Previous biochemical validation of the L-DOPA-cleaving activity of HrmF and its homolog in lincomycin biosynthesis did, however, highly suggest L-DOPA as an early intermediate in (4-Pe)Pro biosynthesis (Höfer et al., 2011; Colabroy et al., 2008). Feedings of deuterated L-DOPA in WT and ΔH cultures clearly showed *trans*-(4-Me)Pro production was independent from (4-Pe)Pro biosynthesis in *S. griseoflavus* W-384 (**Figure 3.34**).

Variants of (4-Me)Pro are known for a small number of other natural products, including nostopeptolide (Luesch et al., 2003) and echinocandins (Cacho et al., 2012), for which the biosynthetic genes are reported. To identify a candidate for a (4-Me)Pro pathway in the HRM producer, its genome (GeneBank: NZ_GG657758.1) was searched for homologues of genes present in the gene clusters. In addition, the genome was scanned for NRPS A domains with similar predicted substrate specificities as the 4-methylproline-accepting domain of the nostopeptolide NRPS, as well as for methyltransferases of the radical *S*-adenosylmethionine superfamily (Frey et al., 2008; Atta et al., 2010; Crone et al., 2012; Huo et al., 2012; Freeman et al., 2012) that might methylate proline. However, all bioinformatic analyses failed to reveal

strong candidates. It should be noted that free *trans*-(4-Me)Pro has been previously observed in Nature and therefore could be supplied by the complex fermentation medium (Hulme and Arthington 1954).

In addition to HRM A_7, six new, HRM analogues (HRM A_{1-6}) were discovered through overexpression of *hrmB* in the WT strain (**Figure 3.21**), of which HRM A_6 is likely an artifact. With the exception of HRM A_1 and HRM A_6, all of the analogues had one or more residues replaced with L-leucine or L-valine. Recently, the specificities of all adenylation domains (A domains) responsible for the activation and selection of amino acids in the HRM NRPS were probed using a $\gamma[^{18}O_4]$–ATP mass exchange assay (Crüsemann et al., 2013; Phelan et al., 2009). In disagreement with the leucine substitutions observed in HRM A_{3-5}, the A domains corresponding to the substituted positions did not show high substrate tolerance for leucine. Moreover, the A domain responsible for isoleucine incorporation in HRM revealed *in vitro* selectivity for valine in these studies, correlating with *in silico* predictions and the structure of the minor metabolite HRM A_2. Thus, unknown downstream constraints for residues incorporated into HRM might be present in this system. Our data therefore highlight the potential benefits of *in vivo* manipulation of regulatory genes over *in vitro* or *in silico* predictions towards the production of accepted and bioactive NRPS-derived natural product congeners.

Analogues HRM A_{1-6} also uncovered a previously unseen natural plasticity in HRM biosynthesis and provided useful SAR data that can aid in the design of non-natural active analogues. Replacement of L-isoleucine with L-valine had a modest 10-fold reduction in bactericidal activity against *A. crystallopoietes* ATCC15481 (**Table 3.5**). Previous feedings of various (3-Ncp)Ala analogues revealed flexible substrate tolerances for these substitutions in HRM biosynthesis, while often retaining partial antibiotic activity (Kozhushkov et al., 2005; Zlatopolskiy et al., 2006). From these experiments, it was hypothesized that terminal electron-withdrawing groups like NO_2 and CO_2Me were necessary at these positions for incorporation into HRM. However, acceptance of L-leucine in place of (3-Ncp)Ala in HRM

$A_{3\text{-}5}$ expands and refines the SARs and profiles of accepted amino acids in HRM determined in those studies. Of note, HRM A_3 retained full antimicrobial activity compared to HRM, therefore revealing the D-configured (3-Ncp)Ala unit flanked by (β-Me)Phe as an especially promising candidate for future derivatization. Furthermore, the epimerase domain of this module was able to tolerate L-leucine and invert its configuration. Lastly, as seen with HRM A_6, previous experiments identified the *N*-hydroxy group of Chpca as essential for HRM activity; however, the effect of the chloro functionality remained unclear (Zlatopolskiy et al., 2006). Our data show that the dechlorinated analogue HRM A_1 retains potent, yet slightly reduced antibacterial activity compared to HRM. With these insights, HRM residues that show flexibility for incorporation with retention of activity can subsequently be modified through mutasynthesis to act as 'molecular handles' to pull-down and identify HRM's currently unknown cellular target. Together with the significant increase in stable HRM titers, research concerning HRM biosynthesis will be more tractable and tolerant to further manipulation and discovery.

3.3 Molecular analysis of genes involved in biosynthesis of the unusual building blocks in HRM

HRM is a nonribosomal peptide containing several nonproteinogenic amino acids, such as Chpca, (β-Me)Phe, (4-Pe)Pro, and in particular, (3-Ncp)Ala, which occurs in two diasteromeric forms. Previous feeding studies established the biosynthetic origin of all amino acids (Brandl et al., 2005). Chpca and (β-Me)Phe are derived from Pro and Phe, respectively. 4-Pe-Pro is biosynthesized from L-Tyr involving extensive skeletal reorganization, while L-Lys and 4-hydroxy-L-Lys are precursors of (3-Ncp)Ala (Höfer et al., 2011). However, the precise steps during these transformations are so far unknown.

With the optimized manipulation system of *S. griseoflavus* W-384 available and two cosmids containing the *hrm* gene cluster, pHR6G10 (*hrmA* to part of *hrmO*), and pHR1F4 (part of *hrmO* to *hrmW*), knock-out experiments would be a powerful and general strategy to allocate genes to

building block sub-pathways. The genes *hrmQ* (Chpca), *hrmD* [(4-Pe)Pro], as well as *hrmI* and *hrmJ* [(3-Ncp)Ala] were disrupted via homologous recombination. The culture extracts from resulting mutants were analyzed by LC-MS to detect the production of intermediates. The corresponding complements for these mutants were also prepared for restoring HRM production. These results along with bioassay tests and chemical feeding experiments, provided the deeper insights into the biosynthesis of HRM.

3.3.1 Chpca biosynthesis

The biosynthesis of pyrrole carboxylic acid derivatives is well understood and typically involves attachment of Pro to a free-standing PCP, followed by four-electron reduction by a dehydrogenase to produce the aromatic ring (Walsh et al., 2006). In certain cases, chlorine atoms are attached to the ring by FAD-dependent halogenases (Dorrestein et al., 2005; Zhang and Parry 2007). The homologs to all these enzymes are HrmK, HrmL, HrmM and HrmN encoded in the *hrm* cluster. *In vitro* studies of HrmK suggested that it acts as a free-standing A domain activating Pro that is subsequently attached to PCP encoded by *hrmL* (**Figure 3.35**) (Crüsemann 2012). HrmM is predicted to be a dehydrogenase catalyzing the four-electron oxidation of prolyl-PCP to form 2-pyrroloyl-PCP (Garneau-Tsodikova et al., 2006; Garneau et al., 2005) (**Figure 3.35**). Location of *hrmN* in the gene cluster suggests a role of HrmN in Chpca formation, and HrmN was suspected to be an oxygenase that introduces the hydroxy group to Chcpa. HrmQ has been identified to be a chlorinase involved in chlorination of Chpca by combinatorial expression of *hrmQ* integrated into the clorobiocin biosynthetic gene cluster (Heide et al., 2008). In this study, the genes *hrmN* and *hrmQ* were analyzed to check their roles in Chcpa formation by gene knock-outs and complementations.

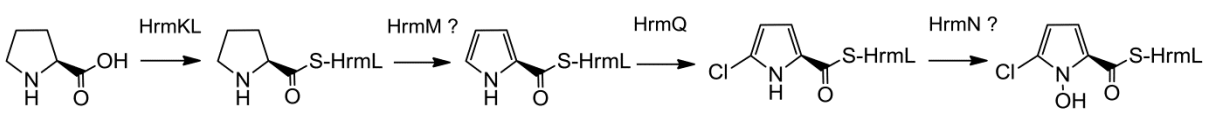

Figure 3.35: Proposed biosynthesis of Chpca.

A PCR-targeted gene replacement strategy was initiated by transforming two cosmids

(pHR6G10 containing *hrmA-hrmO*, and pHR1F4 containing *hrmO-hrmW*) into *E. coli* BW25113/pIJ790, respectively. Two extended apramycin resistance cassettes were individually generated by PCR using long primer pairs XF16F/16R for *hrmN* gene replacement and XF17F/17R for *hrmQ* disruption (**Figure 3.36**), and then separately introduced into *E. coli* BW25113/pIJ790 containing cosmid pHR6G10 and *E. coli* BW25113/pIJ790 harboring cosmid pHR1F4 via electroporation.

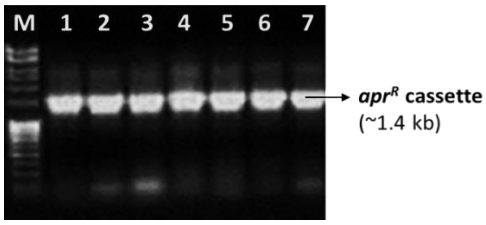

Figure 3.36: Agarose gel analysis of the PCR products of the apramycin resistance gene cassette. Lane M, 100 bp DNA ladder; lanes 1-7, 1.4 kb apr^R cassettes for knocking out of *hrmC*, *hrmD*, *hrmI*, *hrmJ*, *hrmH*, *hrmN*, and *hrmQ*, respectively.

Homologous recombinations occurred, and the resulting apramycin resistants were screened by PCR analysis using the test primer pairs in **Table 4.6**. The results showed that all mutant cosmids contained the apr^R gene (**Figure 3.37A**) and lost the genes that were expected to be replaced.

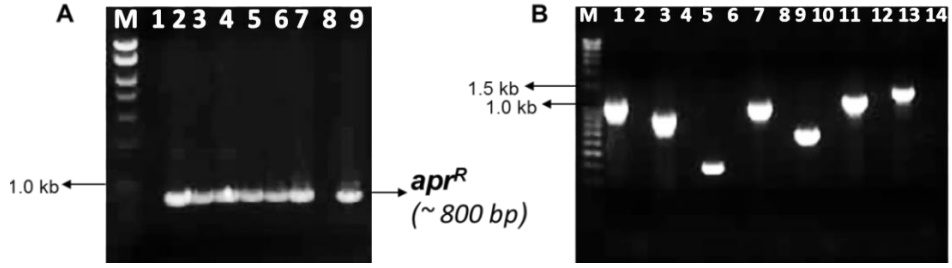

Figure 3.37: Agarose gel analysis of the PCR products from the mutant cosmids (I). **A,** Lane M, 1 kb DNA ladder; lane 1, no PCR product from pHR6G10 using the primer pair XF1F/XF1R (as a negative control); lanes 2-7 and 9, the apramycin resistance gene products amplified from the *hrmC*, *hrmD*, *hrmI*, *hrmJ*, *hrmH* and *hrmQ* mutant cosmids using the same primer pair; 8, no PCR product from pHR1F4 (as a negative control of *hrmQ* mutant cosmid). **B,** Lane M, 1 kb DNA ladder; lanes 1, 3, 5, 7, 9, and 11 are PCR products of *hrmC*, *hrmD*, *hrmI*, *hrmJ*, and *hrmN* amplified from the cosmid pHR6G10 using the corresponding primer pairs; lanes 2, 4, 6, 8, 10,12, no PCR product from the mutant cosmids of *hrmC*, *hrmD*, *hrmI*, *hrmJ*, and *hrmN*; lane 13, PCR products of *hrmQ* amplified from pHR1F4; lane 14, no PCR product from the *hrmQ* mutant cosmid.

To identify whether homologous recombination occurred in the correct position, primer pairs of XF32F/32R and XF33F/33R were individually designed from ~200 bp upstream and downstream of the apramycin resistance cassette in the *hrmN* mutant gene cluster and *hrmQ* mutant gene cluster. For further confirmation of mutant cosmids, a sub-primer pair XF26F/26R was generated from the middle part of the apramycin resistance gene. The DNA sizes amplified from the *hrmN* and *hrmQ* mutant cosmids were both ~1.85 kb using the primer pairs XF32F/32R and XF33F/33R, respectively (**Figure 3.38**, Lanes 12 and 14). The cosmids of pHR6G10 and pHR1F4 were also used for amplification as negative controls, and the PCR products showed the expected sizes (**Figure 3.38**, Lanes 11 and 13).

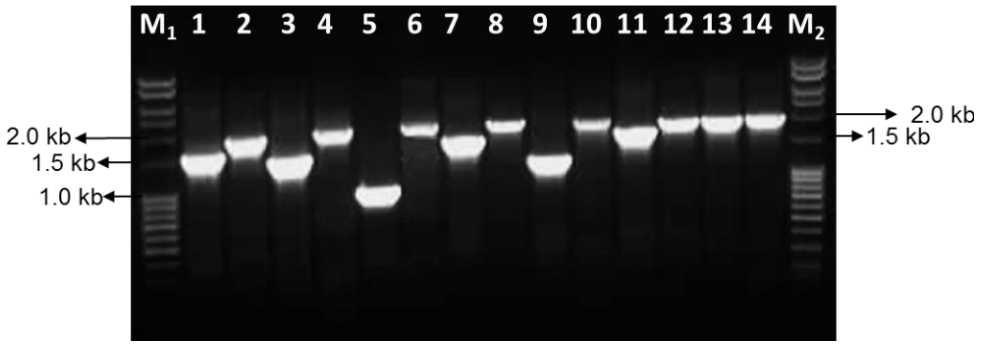

Figure 3.38: Agarose gel analysis of the PCR products from the mutant cosmids (II). Lanes M_1 and M_2, 1 kb DNA ladders; lanes 1, 3, 5, 7, 9 and 11, PCR products from pHR6G10 using the primer pairs XF27F/27R, XF28F/28R, XF29F/29R, XF30F/30R, XF31F/31R, XF32F/32R, respectively; lanes 2, 4, 6, 8, 10 and 12, PCR products from the *hrmC*, *hrmD*, *hrmH*, *hrmI*, *hrmJ*, *hrmN* mutant cosmids using the same primer pairs; lane 13, PCR products amplified from pHR1F4 using the primer pair XF33F/33R; lane 14, PCR products from the *hrmQ* mutant cosmid using the same primers with lane 13.

Since the DNA sizes amplified from the both mutant cosmids and original cosmids were nearly same using the primer pairs XF32F/32R and XF33F/33R, additional amplifications were conducted using primer pairs XF32F/26R, XF26F/26R and XF33F/26R, XF26F/26R, and the wild type cosmids were also used as negative controls The fragments obtained from mutant cosmids were designed to be ~1.0 kb while no product was expected from the original cosmids when correct replacement occurs (**Figure 3.39**, Lanes 21-28).

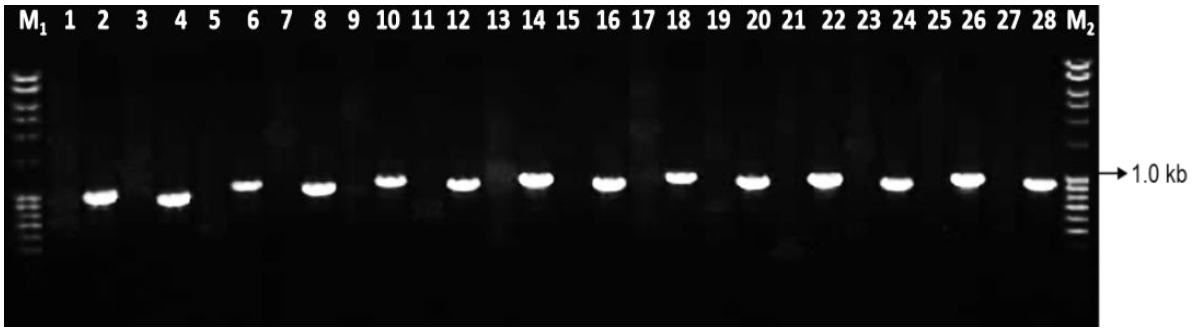

Figure 3.39: Agarose gel analysis of the PCR products from the mutant cosmids (III). Lanes M_1 and M_2, 1 kb DNA ladders. The following primer pairs were used to detect mutant cosmids: lanes 1-4, *hrmC* mutant cosmid with pairs XF26F/27R and XF27F/26R; lanes 5-8, *hrmD* cosmid with pairs XF26F/28R and XF28F/26R; lanes 9-12, *hrmH* mutant cosmid with pairs XF26F/29R and XF29F/26R; lanes 13-16, *hrmI* mutant cosmid with pairs XF26F/30R and XF30F/26R; lanes 17-20, *hrmJ* mutant with pairs XF26F/31R and XF31F/26R,; lanes 21-24, *hrmN* mutant cosmid with pairs XF26F/32R and XF32F/26R; lanes 25-28, *hrmQ* mutant cosmid with pairs XF26F/33R and XF33F/26R; lanes 1, 3, 5, 7, 9, 11, 13, 15, 17, 19, 21, and 23, no DNA product amplified from pHR6G10 (as negative controls); lanes 25 and 27, no DNA product amplified from pHR1F4 (as negative controls).

The mutant cosmids were confirmed based on step-wise PCR analysis and subsequently transformed into methylation-deficient *E. coli* ET12567/pUZ8002 to create demethylated mutant cosmids for further protoplast transformation. The demethylated *hrmN* and *hrmQ* mutant cosmids were individually introduced into *S. griseoflavus W-384* through either protoplast transformation or conjugation. Unfortunately, multiple attempts failed to generate *hrmN* mutant strain. Only one potential *hrmQ* mutant strain was obtained. For further confirmation, the genomic DNA isolated from this strain were analyzed by PCR using the same primer pairs applied in the previous screening of the *hrmQ* mutant cosmid (**Figure 3.40A**, lane 3; **Figure 3.40B**, lanes 9-16).

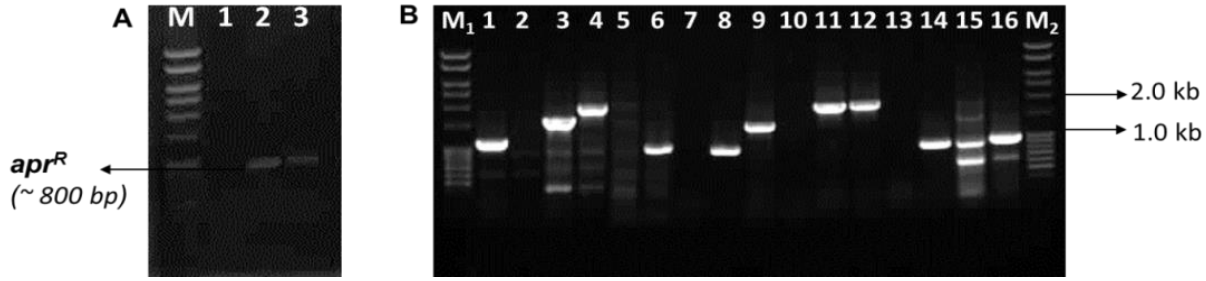

Figure 3.40: Agarose gel analysis of the PCR products from the ΔI and ΔQ. **A,** M, 1 kb DNA ladder; 1, no PCR product from the WT (as a negative control); 2, and 3, the *apr*^{R} from the ΔI and the ΔQ. **B,** Lanes M_1 and M_2, 1 kb DNA ladders; lanes 1-8, PCR analysis of the ΔI; lanes 1 and 2, PCR products from the WT and ΔI using the primer pair XF21F/21R for the *hrmI*; lanes 3 and 4, PCR products from the WT and ΔI using the primer pair XF30F/30R for the DNA fragment containing the *apr*^{R} cassette (~1.85 kb); lanes 5 and 6, PCR products from the WT and ΔI using the primer pair XF26F/30R for the DNA fragment containing one part of *apr*^{R} (~1.0 kb); lanes 7 and 8, PCR products from WT and ΔI using the primer pair XF30F/26R for the DNA fragment containing the other part of *apr*^{R} (~1.0 kb). Lanes 9-16, PCR analysis of the ΔQ, which was similar to that of the ΔI using the different primer paris XF22F/22R, XF33F/33R, XF26F/33R and XF33F/26R. Lanes 9, 10, 11, 13 and 16, PCR products from the WT, as negative controls.

The genotype of the ΔQ generated was verified based on the results of PCR analysis. Subsequent cultivation of the ΔQ and WT strains was carried out for further analyzing the secondary metabolites. After five days of fermentation, the culture supernatants were extracted with EtOAc, evaporated, and redissolved in 500 µL methanol. The extracts from the ΔQ and WT strains were analyzed first by HPLC, but the results did not show an obvious difference between the two cultures at UV of 273 nm. Since the wild type strain only provides a small amount of HRM, a more sensitive detection method (LC-MS) was employed to identify the metabolites and to make sure that the disruption of *hrmQ* was successful. The NRPS can accept and incorporate other metabolites instead of the missing building blocks. Therefore, even if the ΔQ mutant abolished the production of HRM, it is still able to accumulate the HRM A_1 with a loss of chlorine (described in 3.2.2). The exact mass of HRM A_1 is 1095.515 Da $[M+H]^+$, which is present in the WT. LC-MS analysis of the extracts from the WT and ΔQ strains showed that the EIC of 1129.476 Da $[M+H]^+$ (HRM) was not detected in the ΔQ, relative to that of the WT (**Figure 3.41**).

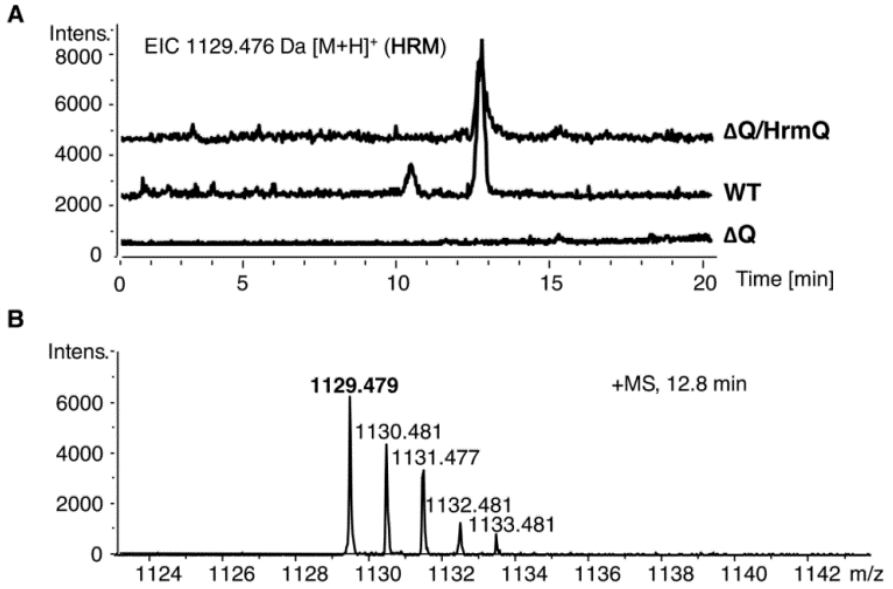

Figure 3.41: LC-MS analysis of the extracts from the WT, ΔQ and ΔQ/HrmQ strains. **A,** Comparison of the EICs of 1129.476 Da $[M+H]^+$ (HRM) from the WT, ΔQ and ΔQ/HrmQ strains. **B,** Observed exact mass of HRM at 12.8 min.

To check if the ΔQ mutant can accumulate HRM A_1, the exact mass of 1095.515 Da $[M+H]^+$ was extracted from the LC-MS data of the both strains. The results showed that the EIC of 1095.515 Da $[M+H]^+$ was observed in the WT and ΔQ strains (**Figure 3.42**).

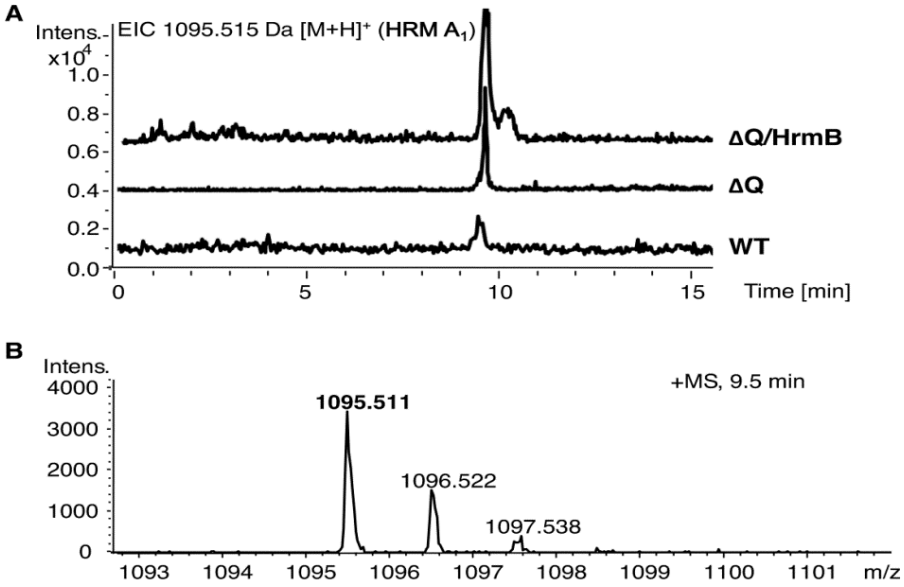

Figure 3.42: LC-MS analysis of the extracts from the WT, ΔQ and ΔQ/HrmB strains. **A,** Comparison of EICs of 1095.515 Da $[M+H]^+$ (HRM A_1) from the WT, ΔQ, and ΔQ/HrmB strains. **B,** Observed exact mass of HRM A_1 at 9.5 min.

To further identify the essential role of HrmQ in the biosynthesis of HRM, the complement of ΔQ, ΔQ/HrmQ, was generated by introducing the *hrmQ* expression plasmid back into ΔQ. To construct this mutant, the *hrmQ* gene was amplified from the genomic DNA of WT using a primer pair of XF22F/22R, then ligated into pBluescript SK(II)+ giving plasmid pXC23 for sequencing. The *hrmQ* fragment was purified from digestion of pXC23 with *Xba*I and *Pst*I, and then inserted into pWHM4* to obtain pXC30 (**Figure 3.43**).

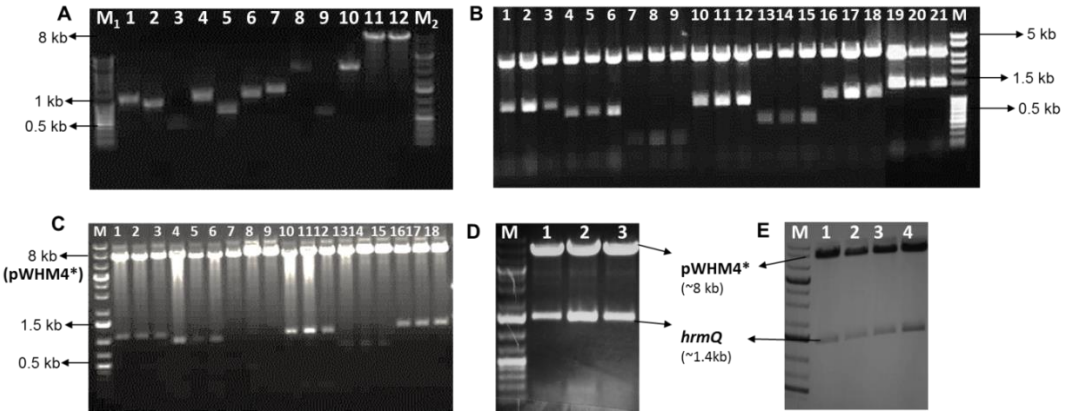

Figure 3.43: Agarose gel analysis of the mutant complements. **A,** Lane M_1, 100 bp DNA ladder; lanes 1-7, purified PCR products of *hrmC*, *hrmD*, *hrmH*, *hrmI*, *hrmJ*, *hrmN* and *hrmQ*, respectively; lane 8, purified pBluescript SK(II)+ after digestion by *Eco*RI and *Xba*I; lane 9, purified PCR product of *hrmB*; lane 10, purified pBluescript SK(II)+ after digestion by *Pst*I and *Xba*I; lane 11, purified pWHM4* after digestion by *Eco*RI and *Xba*I; lane 12, purified pWHM4* after digestion by *Pst*I and *Xba*I; lane M_2, 1 kb DNA ladder. **B,** Lanes 1-3, digestion of pXC17; 4-6, digestion of pXC18; lanes 7-9, digestion of pXC19; lanes 10-12, digestion of pXC20; lanes 13-15, digestion of pXC21; lanes 16-18, digestion of pXC22; lanes 19-21, digestion of pXC23; lane M, 100 bp DNA ladder. **C,** Lane M, 1 kb DNA ladder; lanes 1-3, digestion of pXC24; lanes 4-6, digestion of pXC25; lanes 7-9, digestion of pXC26; lanes 10-12, digestion of pXC27; lanes 13-15, digestion of pXC28; lanes 16-18, digestion of pXC29. **D,** Lane M, 1 kb DNA ladder; lanes 1-3, digestion of pXC30. **F,** Lane M, 1 kb DNA ladder; lanes 1-4, digestion of plasmids isolated from transformants of genomic DNA from ΔQ/HrmQ into *E. coli* DH5α.

pXC30 was introduced into *E. coli*/ET12567 yielding the non-methylated DNA. The resulting demethylated pXC30 was finally transformed into the *hrmQ* mutant to obtain the complement of ΔQ, ΔQ/HrmQ (**Figure 3.43**). LC-MS analysis showed that ΔQ/HrmQ restored HRM production (**Figure 3.41**). Since HRM production was significantly increased in the WT via overexpression of HrmB (described in chapter 4), the *hrmB* overexpression plasmid was also transformed into the ΔQ to give ΔQ/HrmB in order to improve the production of HRM A_1. In

Figure 3.42, it was shown that the ion peak of 1095.515 Da $[M+H]^+$ was increased, but the production of this compound was still very low, which was insufficient for further isolation and structural characterization. The failure in significant increase of expected compound in ΔQ is probably because of the complex regulation system in *Streptomyces* spp..

Based on these results along with previous combinatorial biosynthesis of *hrmQ*, it is further confirmed that HrmQ acts as a chlorinase catalyzing the chloration of HRM.

3.3.2 (3-Ncp)Ala biosynthesis

Previous feeding experiments have revealed that the two units of (3-Ncp)Ala in HRM are derived from lysine (Brandl et al., 2005), which are biosynthesized before assembly of the peptide lactone (Kozhushkov et al., 2005). However, the biosynthetic pathway of ΔQ is still unknown. Only few examples of peptides are known containing nitro groups or cyclopropyl building blocks (Winkler and Hertweck 2007; Kelly et al., 2007; Grogan and Cronan 1997), but no homologs for these building blocks are encoded in the *hrm* cluster. All the *hrm* genes were analyzed to predict their functions during the HRM biosynthesis. However, three *hrm* genes remain unassigned. One is the *hrmT* gene encoding a protein that resembles diaminopimelate epimerases catalyzing the penultimate step in lysine biosynthesis (Scapin and Blanchard 1998). As lysine is a precursor of (3-Ncp)Ala, HrmT presumably serves to provide lysine for the HRM biosynthesis. The additional remaining genes *hrmI* and *hrmJ* have no closer similarity to characterized proteins, but their closest relatives are clustered together with a *hrmT* homolog in *S. avermitilis*, suggesting a role in lysine transformation. It is known that only few examples of proteins are involved in the generation of nitro groups or cyclopropyl units (Gu et al., 2009; Kelly et al., 2007; Vaillancourt et al., 2005). However, none of their homologs were found encoded in HRM biosynthetic gene cluster. In this study, the possible roles of *hrmI* and *hrmJ* were investigated in the (3-Ncp)Ala biosynthesis *in vivo* via gene knock-outs and complements. In addition, HrmI was heterologously expressed for further enzymatic assay *in vitro* to assess its role of biosynthesis of (3-Ncp)Ala.

5.2.2.1 Functional analysis of *hrmI* and *hrmJ in vivo*

The cosmid pHR6G10 containing *hrmI* and *hrmJ*, was used for generation of *hrmI* and *hrmJ* mutants via PCR-targeted gene replacement, in a similar method described for *hrmQ* mutant. The initial amplification of apramycin resistance cassette is shown in **Figure 3.36**. The *hrmI* and *hrmJ* mutant cosmids were confirmed by PCR analysis, shown in **Figure 3.37**-**Figure 3.39**, then transformed into *E. coli* ET12567/pUZ8002 to obtain demethylated DNA. The resulting mutant cosmids were individually introduced into *S. griseoflavus* W-384 through protoplast transformation. Screening of apramycin resistant transformants was performed via identification of their genomic DNA by amplification (**Figure 3.44**).

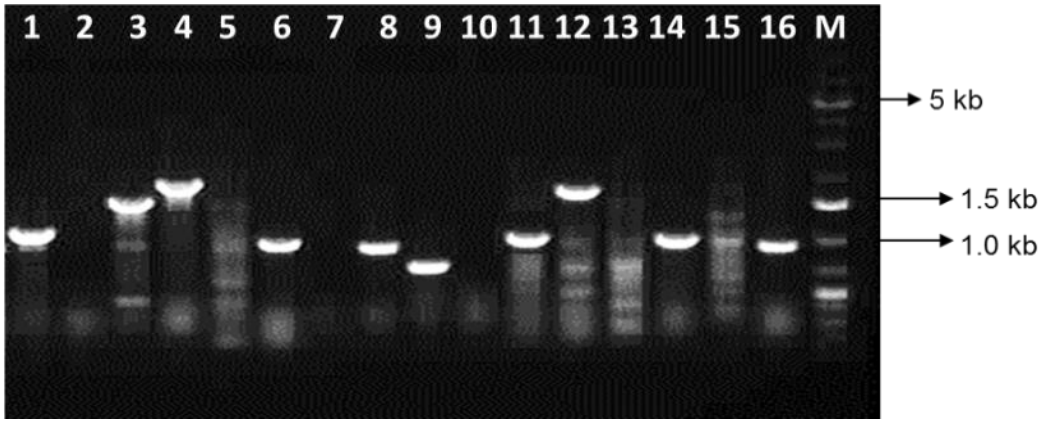

Figure 3.44: Agarose gel analysis of the ΔI and ΔJ strains. Lanes 1-8, Identification of the ΔI. Lanes 2, 4, 6 and 8, PCR products from the ΔI genomic DNA using the primer pairs XF21F/21R (*hrmI* gene), XF30F/30R (DNA fragments containing apr^R cassette), XF26F/30R (DNA fragments containing one part of apr^R cassette) and XF30F/26R (DNA fragments containing the other part of apr^R cassette); lanes 1, 3, 5 and 7, PCR products from the WT genomic DNA, as negative controls. Lanes 9-16, Identification of the ΔJ. Lanes 10, 12, 14, and 16, PCR products from the ΔJ genomic DNA using the primer pairs XF23F/23R (*hrmJ* gene), XF31F/31R (DNA fragments containing apr^R cassette), XF26F/31R (DNA fragments containing one part of apr^R cassette) and XF31F/26R (DNA fragments containing the other part of apr^R cassette); lanes 9, 11, 13 and 15, PCR products from the WT genomic DNA; lane M, 1 kb DNA ladder.

The PCR results showed that *hrmI* and *hrmJ* could not be amplified from ΔI and ΔJ, respectively. The DNA fragments amplified from both mutants were about 1.85 kb that contains the apr^R cassette, while the ones from the WT using the same primer pairs carried *hrmI* and *hrmJ*, with corresponding sizes of ~1.55 kb and 1.15 kb, respectively. Therefore, the DNA

fragments amplified from the mutants were larger than those from the WT. Based on the sizes of DNA fragments amplified shown in **Figure 3.44**, it is proposed that the genotypes of these two mutants were correct, and were used for further experiments.

Similar to ΔQ, it was difficult to recognize the difference between ΔI, ΔJ and WT by HPLC. Therefore, LC-MS was employed to analyze their extracts. The EICs of 1129.476 Da $[M+H]^+$ (HRM) extracted from LC-MS analysis of the ΔI and WT were compared (**Figure 3.45**).

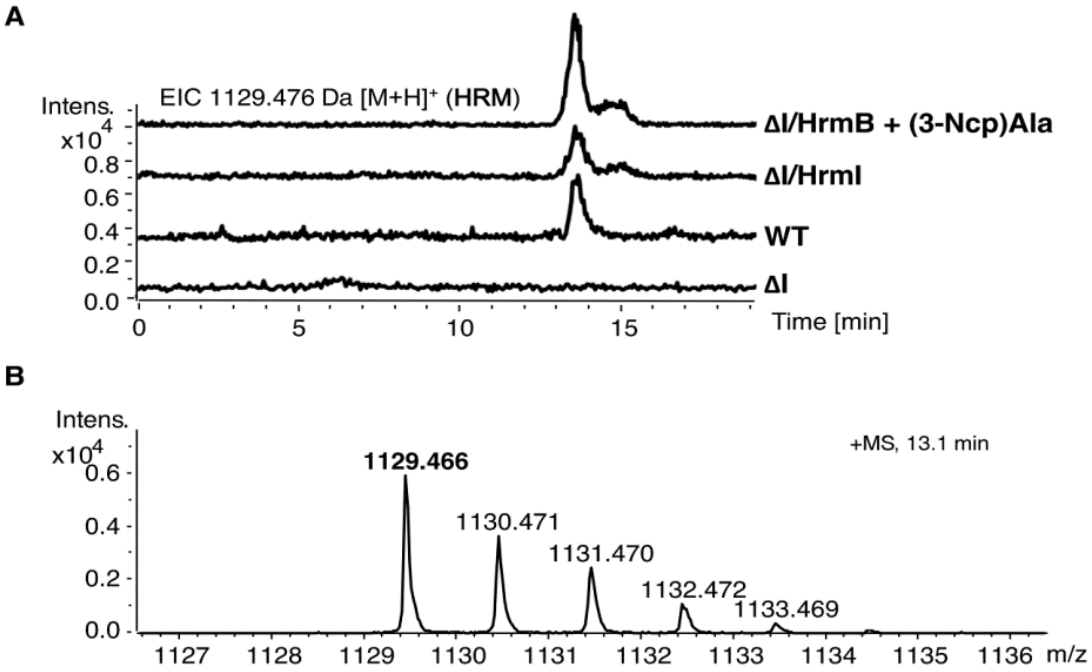

Figure 3.45: LC-MS analysis of the WT, ΔI, ΔI/HrmI and ΔI/HrmB fed with (3-Ncp)Ala. **A,** Comparison of the EICs of 1129.476 Da $[M+H]^+$ from the WT, ΔI, ΔI/HrmI and ΔI/HrmB fed with (3-Ncp)Ala. **B,** Observed exact mass of HRM at 13.1 min.

The results showed that ΔI lost the ability to produce HRM completely, and accumulated compound with the exact mass of 1043.540 Da $[M+H]^+$, observed in the WT (**Figure 3.46**). This exact mass was identical to that of HRM A_5 possessing two units of leucine instead of (3-Ncp)Ala. Therefore, it was postulated that *hrmI* was involved in the biosynthesis of (3-Ncp)Ala.

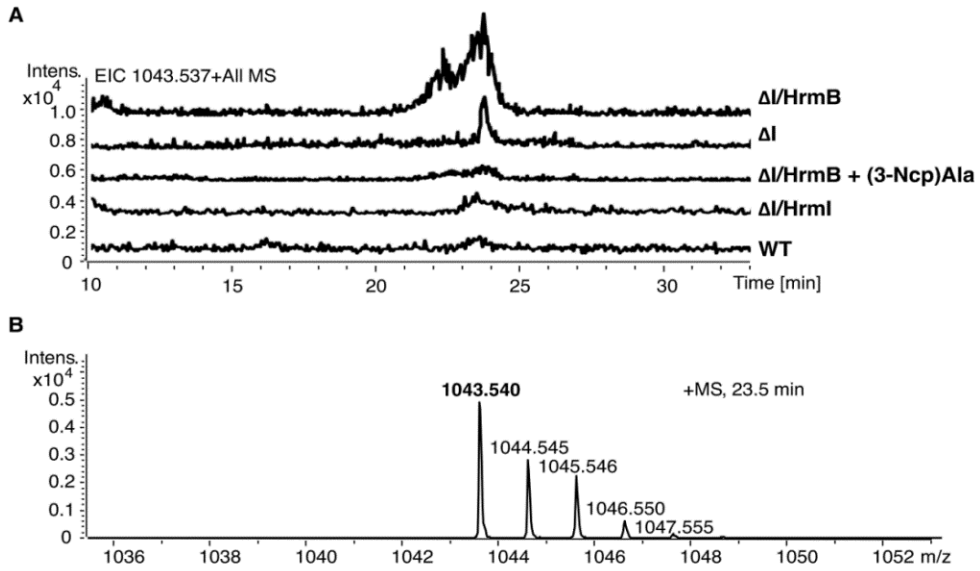

Figure 3.46: LC-MS analysis of the WT, ΔI, ΔI/HrmI, ΔI/HrmB and ΔI/HrmB fed with (3-Ncp)Ala. **A,** Comparison of the EICs of 1045.537 Da $[M+H]^+$ (HRM A_5) from the WT, ΔI, ΔI/HrmI, ΔI/HrmB and ΔI/HrmB fed with (3-Ncp)Ala. **B,** Observed exact mass of HRM A_5 at 23.5 min.

The expression plasmid carrying additional copy of *hrmB* was transformed into ΔI yielding mutant strain ΔI/HrmB, to obtain a sufficient amount of HRM A_5 in ΔI for further analysis. To investigate the essential role of HrmI, the complement of ΔI was constructed by introducing HrmI expression plasmid back to ΔI, assigned as ΔI/HrmI to restore the HRM production. The identification of these constructs was carried out by digestions of plasmids from transformants generated from introducing genomic DNA of corresponding mutants into *E. coli* DH5α (**Figure 3.47**).

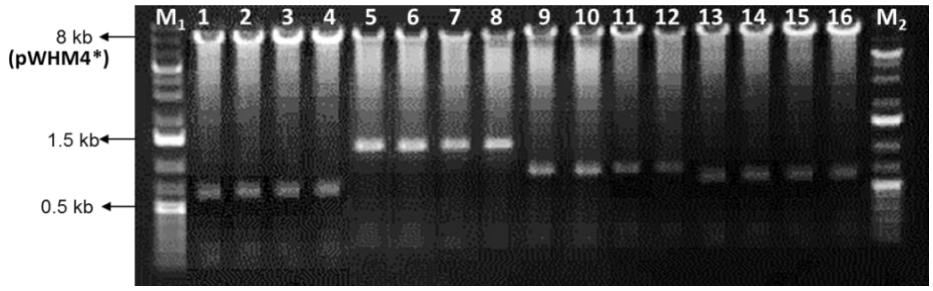

Figure 3.47: Agarose gel analysis of the ΔI/HrmB, ΔI/HrmI, ΔJ/HrmJ and ΔJ/HrmB by digestions. Lanes M_1 and M_2, 1 kb DNA ladders; lanes 1-4, digestions of plasmids from ΔI/HrmB by *Xba*I and *Eco*RI; lanes 5-8, digestions of plasmids from ΔI/HrmI by *Xba*I and *Pst*I; lanes 9-12, digestions of plasmids from ΔJ/HrmJ by *Xba*I and *Eco*RI; lanes 13-16, digestions of plasmids from ΔJ/HrmB by *Xba*I and *Eco*RI.

Subsequently, these resulting mutants were individually cultivated. The extracts from the fermentation cultures were analyzed by LC-MS (**Figure 3.45** and **Figure 3.46**). The EIC of 1129.476 Da $[M+H]^+$ (HRM) from ΔI/HrmI in **Figure 3.45** revealed that HRM production was restored, while the intensity of the ion belonging to HRM A_5, as seen in the EIC of 1043.537 Da $[M+H]^+$, (**Figure 3.46**) was reduced. The increased intensity of ΔI/HrmB in the EIC of 1043.537 Da $[M+H]^+$ suggested that HrmB overexpression upregulated the production. However, yields were still insufficient for MS/MS and NMR analysis. Based on these results, it was proposed that *hrmI* is involved in the biosynthesis of (3-Ncp)Ala. To test whether supplement of (3-Ncp)Ala in the ΔI/HrmB can restore HRM production, ΔI/HrmB was fed with (3-Ncp)Ala gradually during fermentation with final concentration of 0.3 mg/mL. The extracts from the resulting culture was analyzed by LC-MS. LC-MS data showed that HRM production was restored by supplementation of (3-Ncp)Ala (**Figure 3.45**).

A series of experiments similar to those of *hrmI* were also conducted to analyze the function of *hrmJ*. The construction of the *hrmJ* knock-out mutant started with amplification of a 1.4 kb apr^R cassette (**Figure 3.35**). The initial *hrmJ* mutant cosmid was constructed and identified by PCR analysis shown in **Figure 3.37**-**Figure 3.39**. Then the *hrmJ* mutant cosmid was transformed into *E. coli* ET12567/pUZ8002 to obtain the demethylated DNA. The *hrmJ* mutant was grown on R5 plate with apramycin after introducing the demethylated *hrmJ* mutant cosmid into *S. griseoflavus* W-384 by PEG-mediated protoplast transformation. Identification of the resulting *hrmJ* mutant (ΔJ) was carried out by PCR analysis of genomic DNA from the mutant using appropriate primer pairs (**Figure 3.44**, lanes 9-16).

The EIC of 1129.476 Da $[M+H]^+$ from LC-MS analysis of the ΔJ suggested that HRM production was abolished in the ΔJ completely (**Figure 3.48**), while a compound with the exact mass of 1043.537 $[M+H]^+$ was accumulated, which was also detected in the WT (**Figure 3.49**). Since this accumulated compound with the exact mass of 1043.537 in the WT is HRM A_5 with two leucine instead of two (3-Ncp)Ala units, it was proposed that HrmJ, along with HrmI, play an essential role in the biosynthesis of (3-Ncp)Ala.

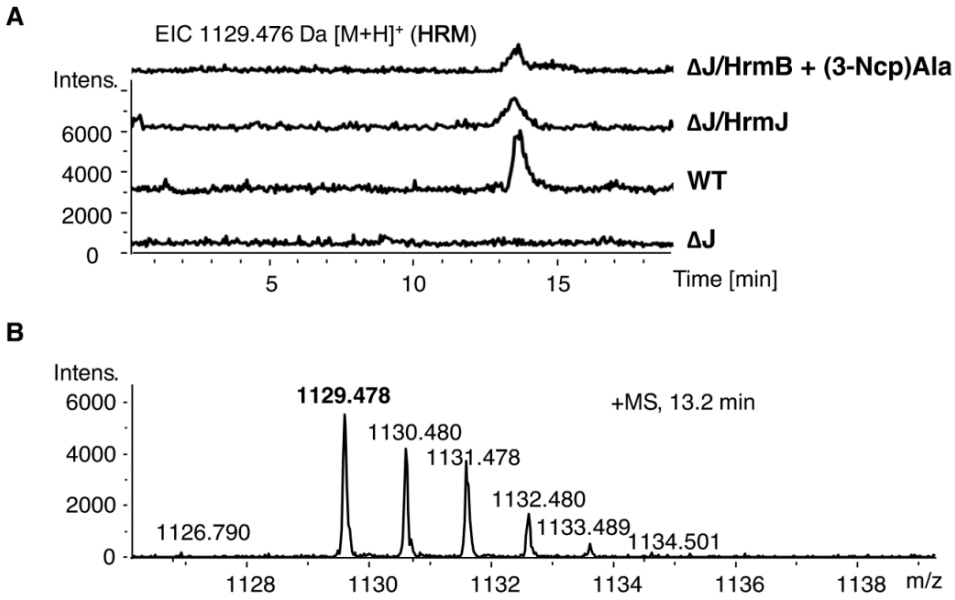

Figure 3.48: LC-MS analysis of the WT, ΔJ, ΔJ/HrmJ and ΔJ/HrmB fed with (3-Ncp)Ala. **A,** Comparison of the EICs of 1129.476 Da $[M+H]^+$ from the WT, ΔJ, ΔJ/HrmJ and ΔJ/HrmB fed with (3-Ncp)Ala. **B,** Observed exact mass of HRM at 13.2 min.

To further determine the essential role of HrmJ, the ΔJ complement (ΔJ/HrmJ) was generated by introducing the *hrmJ* expression plasmid into the ΔJ. The additional copy of *hrmB* was also introduced into ΔJ, yielding the ΔJ/HrmB to increase the production of accumulated compound in the ΔJ. These two resulting mutants were analyzed by enzymatic digestions shown in **Figure 3.47**. Subsequent cultivation of these mutants were carried out, and the extracts from which supernatants were analyzed by LC-MS.

The EIC of 1129.476 Da $[M+H]^+$ from the LC-MS data of ΔJ/HrmJ showed that HRM production was restored by introducing HrmJ back to ΔJ, but the intensity was less than observed for the WT (**Figure 3.48**). The EIC of 1043.537 Da $[M+H]^+$ (HRM A_5) from the LC-MS analysis of ΔJ/HrmB suggested that introduction of HrmB did not significantly upregulate the production of this compound again indicating the presence of a complex regulation system in this strain (**Figure 3.49**).

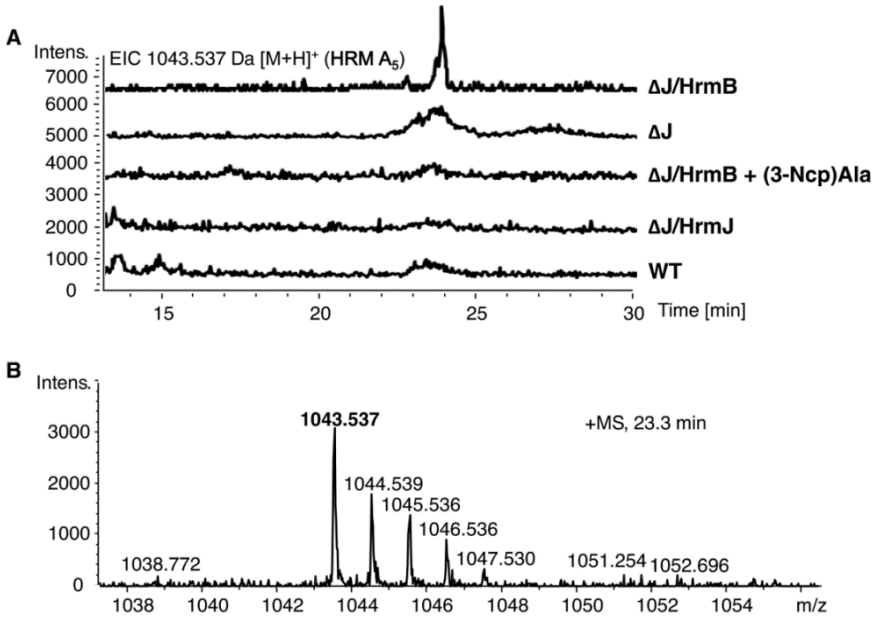

Figure 3.49: LC-MS analysis of the WT, ΔJ, ΔJ/HrmJ, ΔJ/HrmB and ΔJ/HrmB fed with (3-Ncp)Ala. **A,** Comparison of the EICs of 1045.537 Da $[M+H]^+$ from the WT, ΔJ, ΔJ/HrmJ, ΔJ/HrmB and ΔJ/HrmB fed with (3-Ncp)Ala. **B,** Observed exact mass of HRM A_5 at 23.3 min.

To investigate the role of HrmJ in the biosynthesis of (3-Ncp)Ala, chemical feeding of (3-Ncp)Ala into the ΔJ/HrmB mutant was performed (**Figure 3.49**). As expected, HRM production was restored.

Based on all functional studies of *hrmI* and *hrmJ in vivo*, it is suggested that HrmI and HrmJ directly participate in the biosynthesis of (3-Ncp)Ala. Previous characterization of HRM analogues revealed that HRM A_5 exhibits the same exact mass as compounds produced by ΔI and ΔJ. HRM A_5 possesses a structure with both (3-Ncp)Ala residues replaced by leucine. It was suspected that the substance accumulated in ΔI and ΔJ are identical to HRM A_5. Given this hypothesis, leucine was fed into ΔI/HrmB and ΔJ/HrmB during the fermentation, respectively, to increase the production. Afterwards, the supernatants were extracted from their cultures independently, then applied to HPLC to analyze the peptide profiles. The results showed that the substance can only be detected by UV in ΔI/HrmB and ΔI/HrmB fed with leucine. As expected, after feeding leucine, the substance in ΔI/HrmB was increased about three times as compared to that in ΔI/HrmB without feeding (**Figure 3.50**).

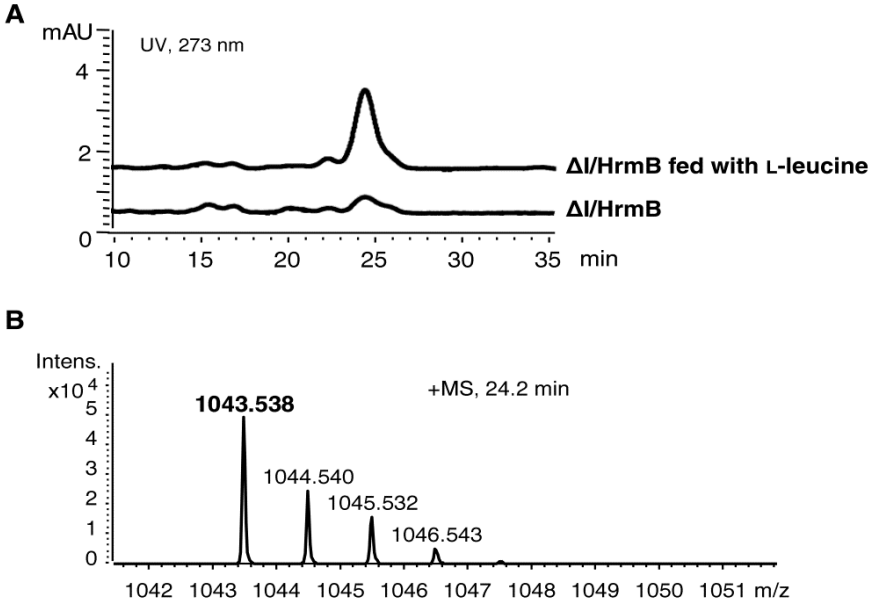

Figure 3.50: LC-MS analysis of the extracts from the ΔI/HrmB and ΔI/HrmB fed with leucine. **A,** Comparison of UV spectra from the ΔI/HrmB and ΔI/HrmB fed with leucine at 24.2 min UV 273 nm. **B,** Observed exact mass of the substance in theΔI/HrmB and ΔI/HrmB fed with leucine at 24.2 min.

However, HPLC analysis of the extracts from ΔJ/HrmB and ΔJ/HrmB fed with leucine showed that the substance in both scenarios was not observed from the UV spectra. Therefore, all of these extracts were further analyzed by LC-MS. The EIC of 1045.537 Da $[M+H]^+$ was detected in the LC-MS data from both ΔJ/HrmB and ΔJ/HrmB fed with leucine (**Figure 3.51**).

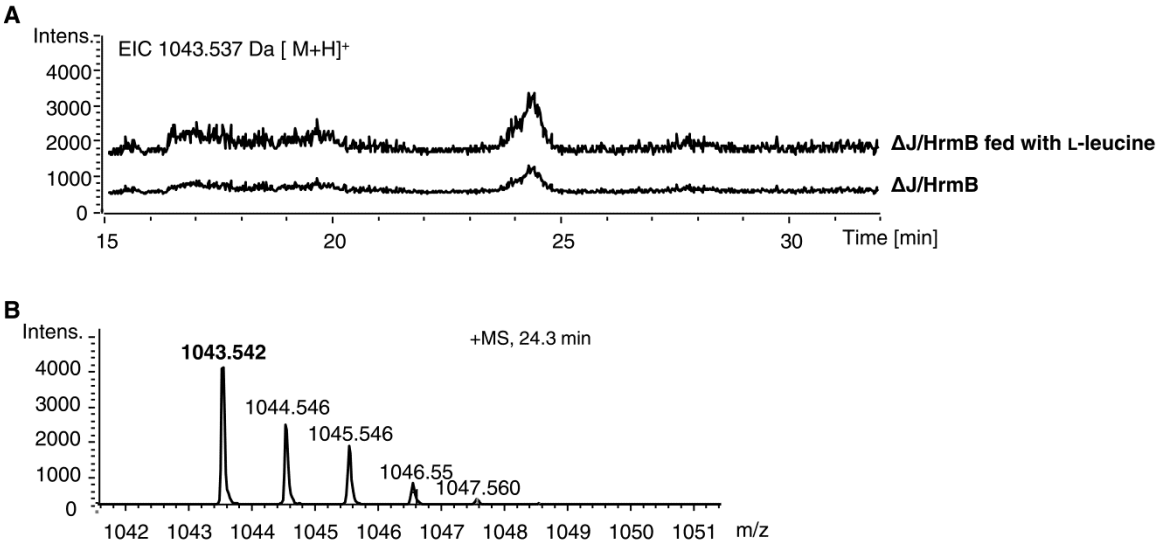

Figure 3.51: LC-MS analysis of the extracts from the ΔJ/HrmB and ΔJ/HrmB fed with leucine. **A,** Comparison of EICs of 1043.537 Da $[M+H]^+$ from the ΔJ/HrmB and ΔJ/HrmB fed with leucine. **B,** Observed exact mass of HRM A_5 at 24.3 min.

Results from the feeding experiments, along with those of previously feeding leucine into the HrmB overproducer, indicated that leucine can be readily incorporated by the *hrm* NRPS, which was also verified by adenylation domain studies *in vitro* (Crüsemann 2012).

5.2.2.2 Heterologous expression of HrmI *in vitro*

From the above experiments of *hrmI* and *hrmJ in vivo*, it was demenstrated that these two genes are involved in the biosynthesis of (3-Ncp)Ala. Previous feeding experiments suggested that (3-Ncp)Ala originating from lysine (Brandl et al., 2005), leading to the proposal of cyclopropanation in (3-Ncp)Ala (**Figure 3.52**). However, it is still unknown how these two proteins function during this process. Previous bioinformatic analysis based on standard BLAST and motif searches revealed that there are no obvious characterized homologs of these two proteins (Höfer et al., 2011). Therefore, PSI-BLAST was employed to search for more distant homologues. The results showed that HrmI shares homology to a distant homologue that is the characterized pyrroloquinoline quinone biosynthesis protein C (PqqC). PqqC is a well-known cofactorless oxidase catalyzing an eight-electron ring-closure oxidation reaction at the final step of PQQ biosynthesis (Magnusson et al., 2004) (**Figure 3.52**). The PSI-BLAST search also revealed that HrmJ is distantly similar to an α-ketoglutarate-dependent L-isoleucine dioxygenase found in *Bacillus thuringiensis*, catalyzing the hydroxylation of L-isoleucine to 4-hydroxyisoleucine (Hibi et al., 2011). Based on the characterized functions of their corresponding homologs and previous feeding experiments (Brandl et al., 2005), the step-wise biosynthetic pathway of (3-Ncp)Ala was postulated, which assigned possible roles of HrmI and HrmJ (**Figure 3.52**).

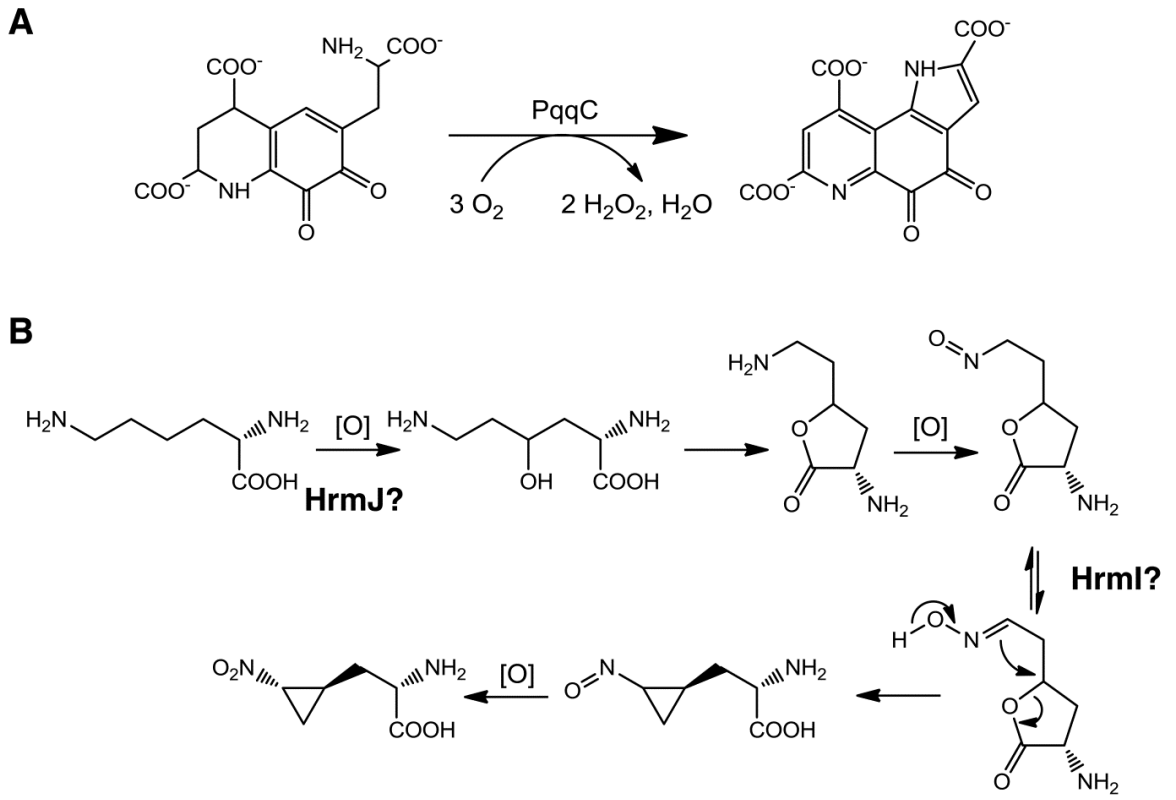

Figure 3.52: A, Final step of PQQ biosynthesis catalyzed by PqqC. **B,** Postulated biosynthetic pathway of (3-Ncp)Ala from feeding studies. HrmI and HrmJ are proposed to be involved in this pathway.

To investigate the precise steps of biosynthesis of (3-Ncp)Ala, these two proteins were heterologously expressed in the Piel group for *in vitro* enzymatic assays. In this study, the focus was heterologous expression of HrmI.

The *hrmI* gene was amplified from genomic DNA of *S. griseoflavus* W-384 using primer pairs of HrmI-F/HrmI-R (for *hrmI* with its stop codon) and HrmI-F/HrmI-chis-R (for *hrmI* without a stop codon), respectively. The resulting PCR products were purified and then independently inserted into p-GEM easy for sequence analysis. The plasmids isolated from their corresponding transformants were identified by enzymatic digestion with *Hin*dIII and *Nde*I (**Figure 3.53A**). DNA sequencing revealed that the plasmids of clone 1-3 carried the correct complete *hrmI* gene. This plasmid was referred to as pXC35A. Clone 11, 12 and 14 all contained the correct *hrmI* gene without a stop codon, the plasmid from which was referred to as pXC35B. The *hrmI* gene fragments were subsequently purified after digestion of pXC35A and pXC35B by *Hin*dIII and *Nde*I, respectively. The expression vectors used here were

pET28b(+) (**Figure 4.4**) carrying both N and C terminal His-tags and pET29b(+) with only a C terminal His-tag. The *hrmI* gene with a stop codon was subcloned into pET28b (+) to obtain pXC36 for expression of HrmI contain N terminal His-tag. As an alternative, the *hrmI* gene without stop codon was ligated into pET29b (+) to get pXC37 for expressing HrmI protein carrying only a C terminal His-tag. After identification of these two expression plasmids (**Figure 3.53B**), they were transformed into *E. coli* BL21(DE) to obtain two heterologous expression strains of HrmI, respectively.

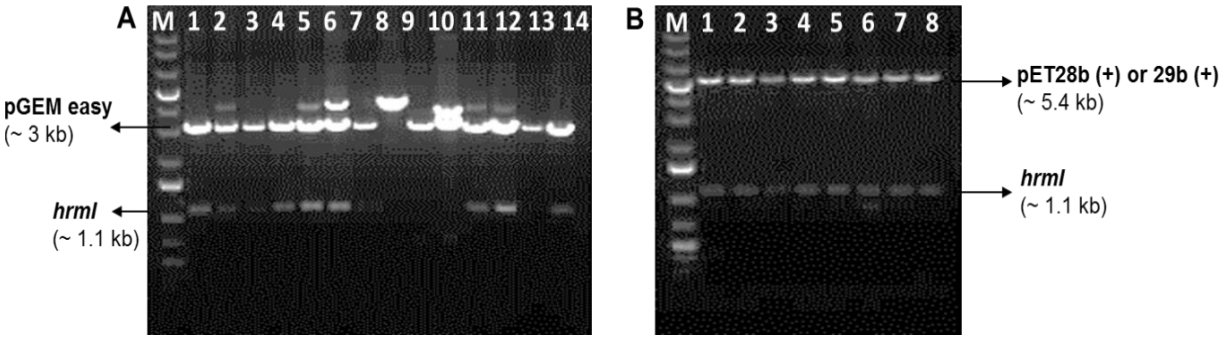

Figure 3.53: Agarose gel analysis of the plasmids, pXC35A, pXC35B, pXC36 and pXC37 by enzymatic digestion. **A,** Lane M, 1 kb DNA ladder; lanes 1-7, screening for pXC35A by digestion with *Nde*I and *Hin*dIII; lanes 8-14, screening for pXC35B by digestion with *Nde*I and *Hin*dIII. **B,** Lane M, 1 kb DNA ladder; lanes 1-4, screening for pXC36 by digestion with *Nde*I and *Hin*dIII; lanes 5-8, Screening for pXC37 by digestion with *Nde*I and *Hin*dIII.

The resulting strains were grown in TB media supplemented with kanamycin at 37 ℃ to an OD600 of 1.5-2.0. Then the cultures were cooled down, and IPTG was added to induce protein expression. The cultures were kept shaking at 16 ℃ overnight. Afterwards, cell pellets were harvested and protein purification was carried out according to the procedure described in Chapter 4. The purified proteins were concentrated via trichloroacetic acid (TCA) precipitation. Roti®-Nanoquant solution was used to determine protein concentration. The identification of proteins was carried out by SDS-PAGE analysis (**Figure 3.54**).

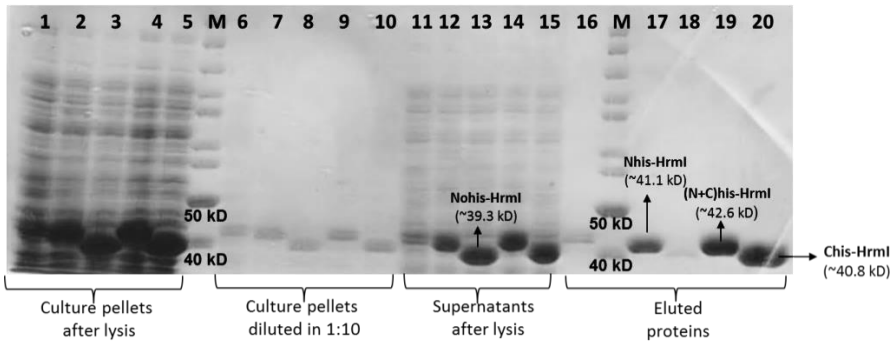

Figure 3.54: SDS-PAGE (9%) of initial protein expression of HrmI. Lanes 1-5, the culture pellets after lysis. Lane 1, culture without induction; lanes 2-5, cultures for expression of, Nhis-HrmI (HrmI with a N terminal His-tag), Nonhis-HrmI (HrmI without any His-tag), (N+C)his-HrmI (HrmI with both C and N terminal His-tags) and Chis-HrmI (HrmI with a C terminal His-tag). Lane M, protein marker; lanes 6-10, culture pellets of samples 1-5 diluted in 1:10; lanes 11-15, supernatants of samples 1-5 after lysis. Lanes 16-20, the proteins from samples 1-5 eluted with 250 mM elution buffer, respectively.

To maintain the activity of HrmI for further storage, the protein stability assay of HrmI with N terminal His-tag (Nhis-HrmI) was conducted by exchanging buffers for this protein into different buffers with a range of pH 6.0-8.0 described in detail in Chapter 4. The SDS-PAGE suggested that the most stable buffer for this protein is 50 mM MES buffer (pH 6.0) (**Figure 3.55**).

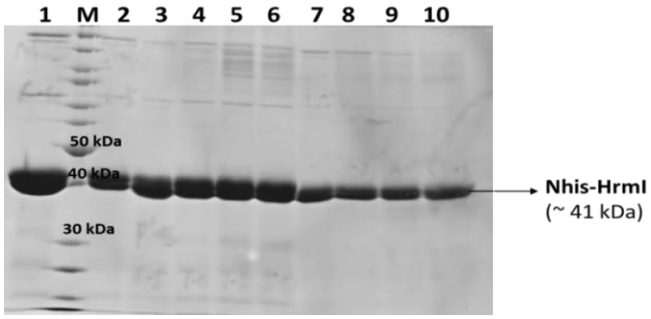

Figure 3.55: SDS-PAGE (12%) of Nhis-HrmI stability assays. Lane 1, HrmI in 50 mM MES, pH 6.0, with 10% (v/v) glycerol; lane M, PageRuler™ Unstained Protein Ladder (molecular weights of pertinent standards labeled on the gel); lane 2, HrmI in 50 mM MES, pH 6.5, with 10% (v/v) glycerol; lane 3, HrmI in 50 mM potassium phosphate buffer at pH 7.0 with 10% (v/v) glycerol; lane 4, HrmI in 50 mM potassium phosphate buffer at pH 7.5 with 10% (v/v) glycerol; lane 5, HrmI in 50 mM potassium phosphate buffer at pH 8.0 with 10% (v/v) glycerol; lane 6, HrmI in 50 mM potassium phosphate buffer at pH 8.5 with 10% (v/v) glycerol; lane 7, HrmI in 50 mM Tris buffer at pH 6.5 with 10% (v/v) glycerol; lane 8, HrmI in 50 mM Tris buffer at pH 7.0 with 10% (v/v) glycerol; lane 9, HrmI in 50 mM Tris buffer at pH 7.5 with 10% (v/v) glycerol; lane 10, HrmI in 50 mM Tris buffer at pH 8.0 with 10% (v/v) glycerol.

The protein samples from stability assay were also tested to determin the protein concentration using Roti®-Nanoquant solution. After incubation of proteins in different buffers at 37 ℃ overnight, the protein concentration in MES buffer (pH 6.0 and 6.5) remained stable as before, while those in the other two buffers were less stable (**Figure 3.56**).

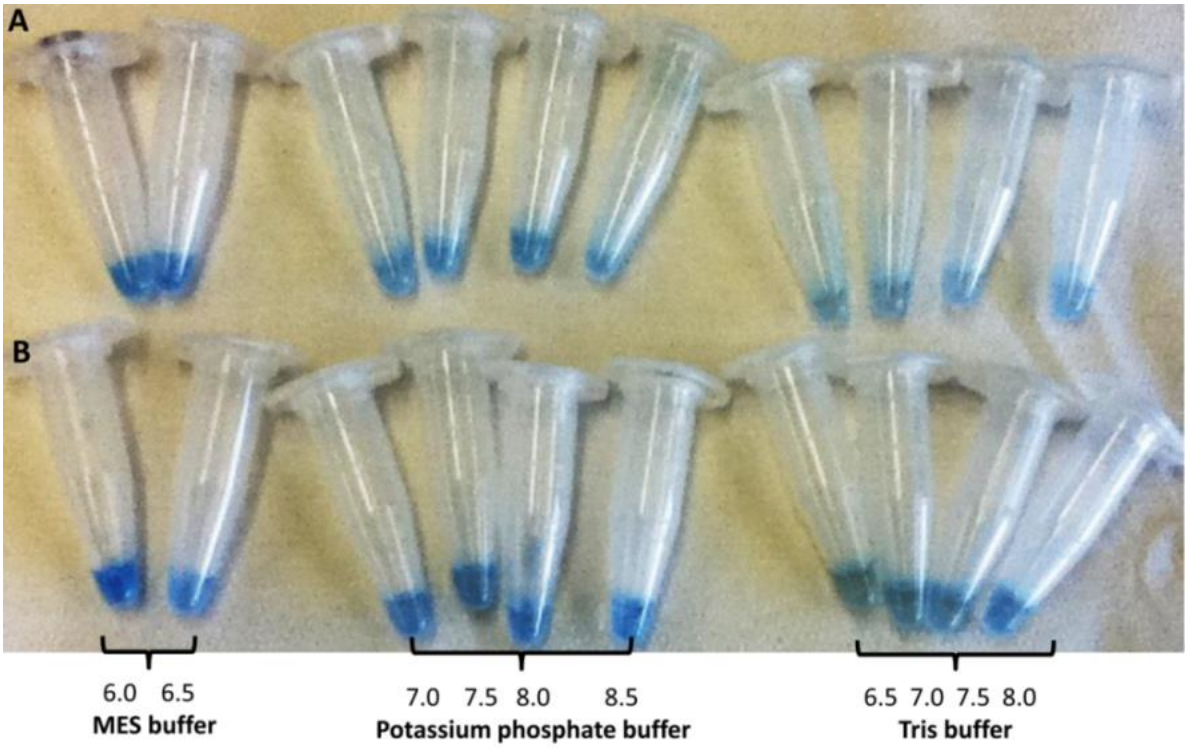

Figure 3.56: Determination of Nhis-HrmI protein concentration and stability by using Roti®-Nanoquant. **A,** Nhis-HrmI in different buffers before incubation. **B**, Nhis-HrmI in different buffers after incubation.

In the present study, functional analysis of *hrmI* and *hrmJ* by gene knock-outs, genetic complementations and chemical feeding studies demonstrated the essential role of these genes in the biosynthesis of (3-Ncp)Ala. The soluble HrmI protein was successfully expressed and the most stable buffer for this protein was established, which is 50 mM MES at pH 6.0, with 10% (v/v) glycerol. Further enzymatic studies will be carried out with the postulated substrate for HrmI or starting with L-Lys for both HrmI and HrmJ.

3.3.3 (4-Pe)Pro biosynthesis

Previous feeding experiments have revealed that (4-Pe)Pro is generated from L-tyrosine via a similar pathway found in lincomycin (Hu et al., 2007) and pyrrolo[1,4]benzodiazepine (anthramycin, tomaymycin and sibiromycin) biosynthesis (Höfer et al., 2011; Hurley 1980; Li et al., 2009a; Li et al., 2009b). Bioinformatic analysis suggested that the *hrm* system contains the clustered genes *hrmCDEFG*, which are homologs found correspondingly in the gene clustes of these compounds (**Figure 3.57**) (Hu et al., 2007; Li et al., 2009a; Li et al., 2009b; Peschke et al., 1995). HrmF, homologous to the characterized LmbB1, has been identified to as a dioxygenase from the linconmycin biosynthetic pathway performing the cleavage of a L-DOPA to the pyrroline intermediate (Colabroy et al., 2008; Höfer et al., 2011). HrmE shows similarity to LmbB2 in lincomycin biosynthesis. Studies on LmbB2 provide indirect evidence that it hydroxylates L-Tyr to give L-DOPA (Neusser et al., 1998). The next steps in (4-Pe)Pro formation likely consist of a methylation catalyzed by HrmC and another carbon-carbon bond cleavage performed by HrmD (**Figure 3.57**). Both enzymes have homologs in the lincomycin pathway, which generates 4-propylproline (Peschke et al., 1995). HrmG encoding a putative γ-glutamyltransferase, is likely involved in biosynthesis of the unusual cytochrome F420-like cofactor (Peschke et al., 1995). Unexpectedly, among the gene cluster generating (4-Pe)Pro-related residues, only the *hrm* system does not encode LmbX-homolog that is proposed to catalyze the cleavage of pyrroline intermediate (Li et al., 2009a; Li et al., 2009b). In this study, Southern hybridization was conducted to search for the gene related to *lmbX* in the genomic DNA of HRM producer. In addition, the roles of *hrmC* and *hrmD* in HRM biosynthesis were analyzed via gene knock-outs and complementations.

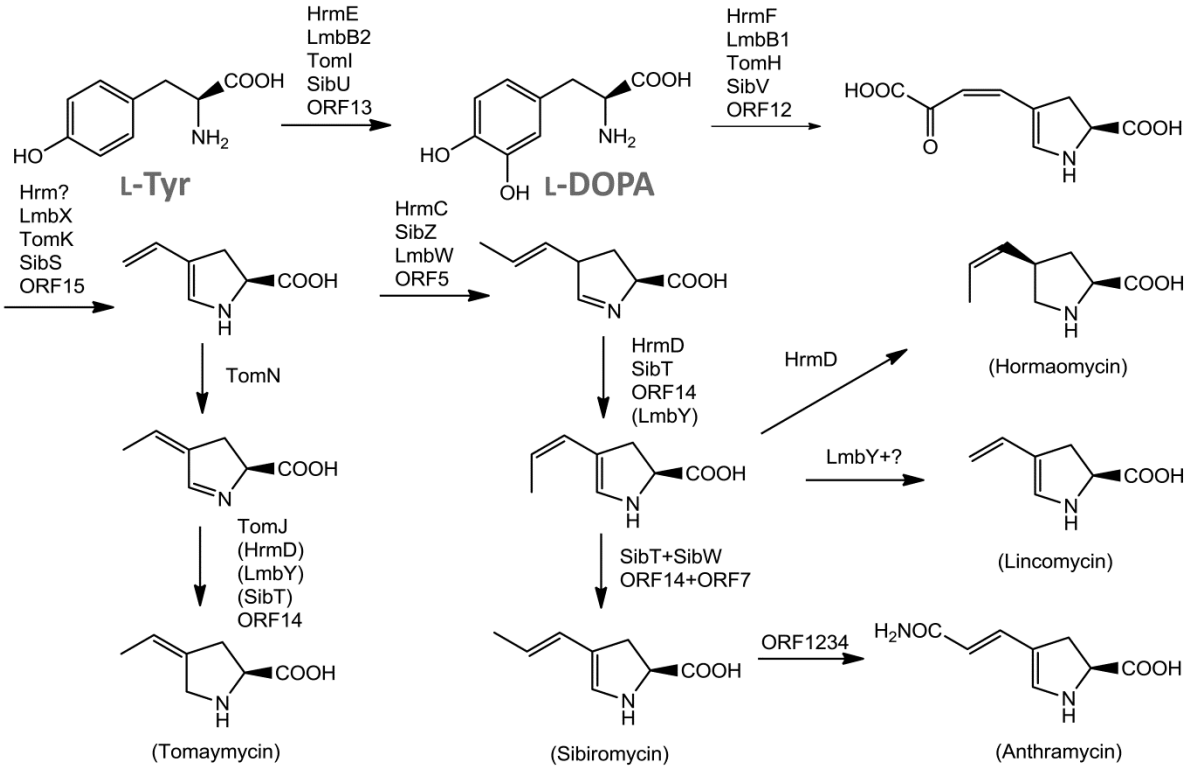

Figure 3.57: Postulated biosynthetic pathway of (4-Pe)Pro. Enzyme homologs from the lincomycin (Lmb), anthramycin (ORFxy), sibiromycin (Sib), tomaymycin (Tom) pathways are also shown. Proteins in parentheses were proposed to convert variants of the substrates shown (Höfer et al., 2011).

3.3.3.1 Screening for an *lmbX* homolog

LmbX has been shown to be essential in the biosynthesis of propylproline moiety in lincomycin (Ulanova et al., 2010).Therefore it was wondered whether an LmbX homolog might be encoded on an unclustered part in the genome of *S. griseoflavus* W-384. To search for this gene, the genomic DNA of HRM producer was initially tested using the degenerated primers derived from an alignment of *lmbX* with all known homologs (*sibS*, *tomK*, and *ORF15* from anthramycin) by amplification. However, no PCR product was observed. To test whether this is a false-negative result generated by non-matching primers, an *lmbX* hybridization probe was generated to further detect its homolog in the genomic DNA by Southern blotting. Likewise, the arrayed library of HRM was screened using the same probe by colony *in situ* hybridization.

The *lmbX* gene fragment was amplified from the genomic DNA of lincomycin producer *Streptomyces lincolnensis* NRRL 2936 using the primer pair of XF6F/6R. The PCR products

were ligated into pBluescript SK(+) to give pXC7 and end sequenced. The *lmbX* gene fragment was digested with *Hin*dIII and *Eco*RI from pXC7and labeled using the DIG-High Prime DNA Labeling Kit, which was used as a probe for hybridization.

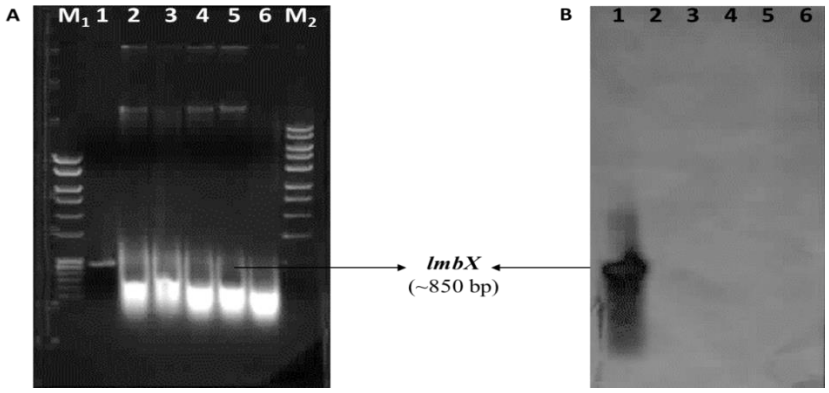

Figure 3.58: Screening for *lmbX*-like gene in the genomic DNA of *S. griseoflavus* W-384 by Southern blotting using *lmbX* as a probe derived from *S. lincolnensis* NRRL 2936. **A,** DNA agarose gel before hybridization. Lane M_1, 100 bp DNA ladder; lane 1, *lmbX* gene; 2, genomic DNA digested by *Bam*HI; lane 3, genomic DNA digested by *Bgl*II; lane 4, genomic DNA digested by *Eco*RI; lane 5, genomic DNA digested by *Hin*dIII; lane 6, genomic DNA digested by *Pst*I; lane M_2, 1 kb DNA ladder. **B,** Lane 1, labeled *lmbX* after hybridization; lanes 2-6, no DNA fragment is labeled from any digestion of genomic DNA after hybridization.

Unfortunately, Southern hybridization using an *lmbX*-derived probe together with either genomic DNA (**Figure 3.58**) or the arrayed library was unsuccessful. During the later course of our studies, a draft genome sequence of *S. griseoflavus* Tü4000, which is identical to the HRM producer, became available (GenBank: NZ_GG657758.1). Investigation of the genome revealed the presence of the *hrm* cluster. In agreement with the PCR and Southern studies, the draft genome lacked an *lmbX* homolog.

3.3.3.2 Functional analysis of *hrmC* and *hrmD in vivo*

To knockout *hrmC* and *hrmD*, the initial apr^R cassettes for *hrmC* and *hrmD* mutations were amplified using the primers XF12F/12R and XF13F/13R, respectively (**Figure 3.36**). The *hrmC* and *hrmD* mutant cosmids were derived from pHR6G10, both of which were identified by PCR analysis before transformation into *E. coli* ET12567 to obtain demethylated DNA (**Figure 3.37**-**Figure 3.39**). The candidates for *hrmD* mutant were successfully grown on an R5

plate containing apramycin after protoplast transformation with demethylated *hrmD* mutant cosmid into *S. griseoflavus* W-384. In contrast, many attempts to introduce the *hrmC* mutant cosmid into *S. griseoflavus* W-384 failed to generate the *hrmC* mutant. The genotype of *hrmD* mutant was verified by PCR analysis of its genomic DNA (**Figure 3.59**).

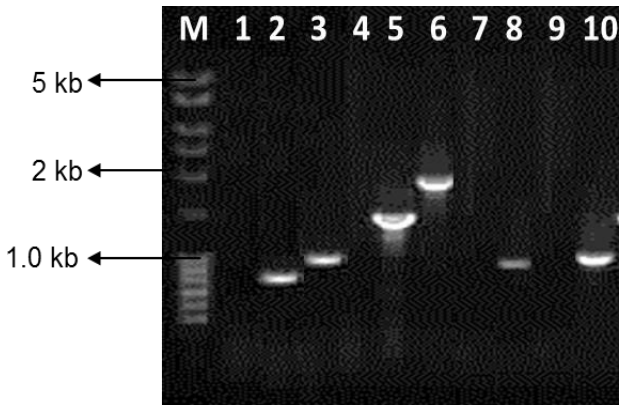

Figure 3.59: Agarose gel analysis of ΔD by PCR. Lane M, 100 bp DNA ladder; lanes 2, 4, 6, 8 and 10, PCR products amplified from the genomic DNA of ΔD using the primer pairs XF1F/1R for apr^R (~800 bp), XF20F/20R for the *hrmD* gene (~900 bp), XF28F/28R for the DNA fragment containing the apr^R cassette (~1.85 kb), XF28F/26R for the DNA fragment containing a half of the apr^R cassette (~1.0 kb) and XF26F/28R for the other half of the apr^R cassette (~1.0 kb), respectively; lanes 1, 3, 5, 7 and 9, PCR products amplified from the genomic DNA of WT using the same primer pairs, respectively (as negative controls).

Similar to previous experiments, the ΔD complement (ΔD/HrmD) was constructed by expression of HrmD in ΔD. In addition, a HrmB overexpression plasmid was introduced into ΔD to obtain ΔD/HrmB for improving the production of substance. Both strains were identified by enzymatic digestions of plasmids from transformants of their genomic DNA into *E .coli* DH5α (**Figure 3.60**). Subsequently, all the strains including the WT, ΔD, ΔD/HrmD and ΔD/HrmB were individually cultivated in the fermentation media for analyzing the secondary metabolites. As shown in **Figure 3.33**, it was identified that HrmD is involved the biosynthesis of (4-Pe)Pro residue in HRM.

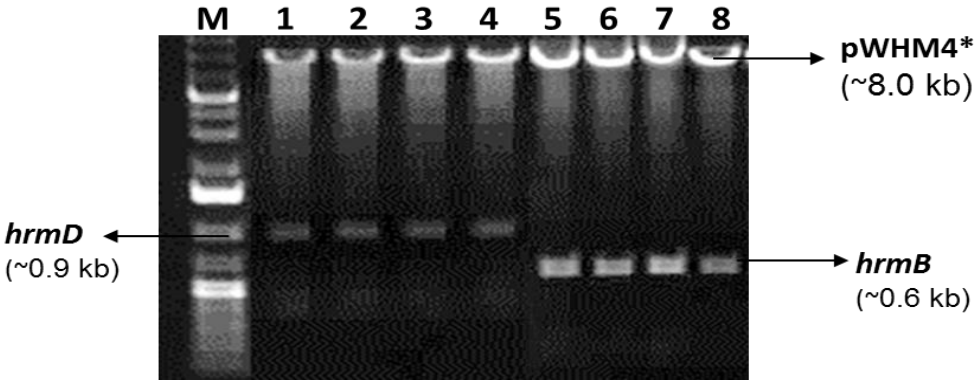

Figure 3.60: Agarose gel analysis of ΔD/HrmD and ΔD/HrmB by enzymatic digestions. Lane M, 1 kb DNA ladder; lanes 1-4, digestions of plasmids by *Xba*I and *Eco*RI isolated from the transformants after introducing genomic DNA of ΔD/HrmD into *E. coli* DH5α; lanes 5-8, digestions of plasmids by *Xba*I and *Eco*RI isolated from the transformants after introducing genomic DNA of ΔD/HrmB into *E. coli* DH5α.

In this section, it was demonstrated that the LmbX-homolog is not needed for the biosynthesis of (4-Pe)Pro by hybridization. Functional analysis of *hrmD* by gene knock-out, complementation and chemical feeding experiments revealed its essential role in (4-Pe)Pro biosynthesis.

3.3.4 Generation of hormaomycin analogues by mutasynthesis

Many HRM analogues have been generated by precursor-directed biosynthesis. Since the supplemented amino acids compete with the natural precursors, the peptide analogs were always obtained in low yields as side products together with authentic HRM, and purification of new compounds has also been a problem (Radzom 2006). These disadvantages can be eliminated by, prior to feeding, genetically inactivating the production of the amino acid that is to be replaced, referred to as mutasynthesis. This strategy was employed to investigate and exploit the *hrm* pathway for analogue production more efficiently.

Click chemistry serves as a practical chemical approach for generating a specific substance quickly and reliably by joining two small units together (Kolb et al., 2001). It has become a powerful tool applied in many areas, such as, drug discovery, combinatorial chemistry, bioconjugation, and radiolabeling. The azide-alkyne cycloaddition catalyzed by copper (I)

(**Figure 3.61A**) is a particularly powerful linking reaction, due to its high quantitative yields, efficiency and specificity (Sekhon 2012). Bioconjugation using the cycloaddition of azides and acetylenes has been successfully applied in tagging living organisms (Deiters et al., 2003; Link and Tirrell 2003), profiling activity-based proteins (Speers et al., 2003) for drug development and labeling DNA for sequencing (Seo et al., 2003).

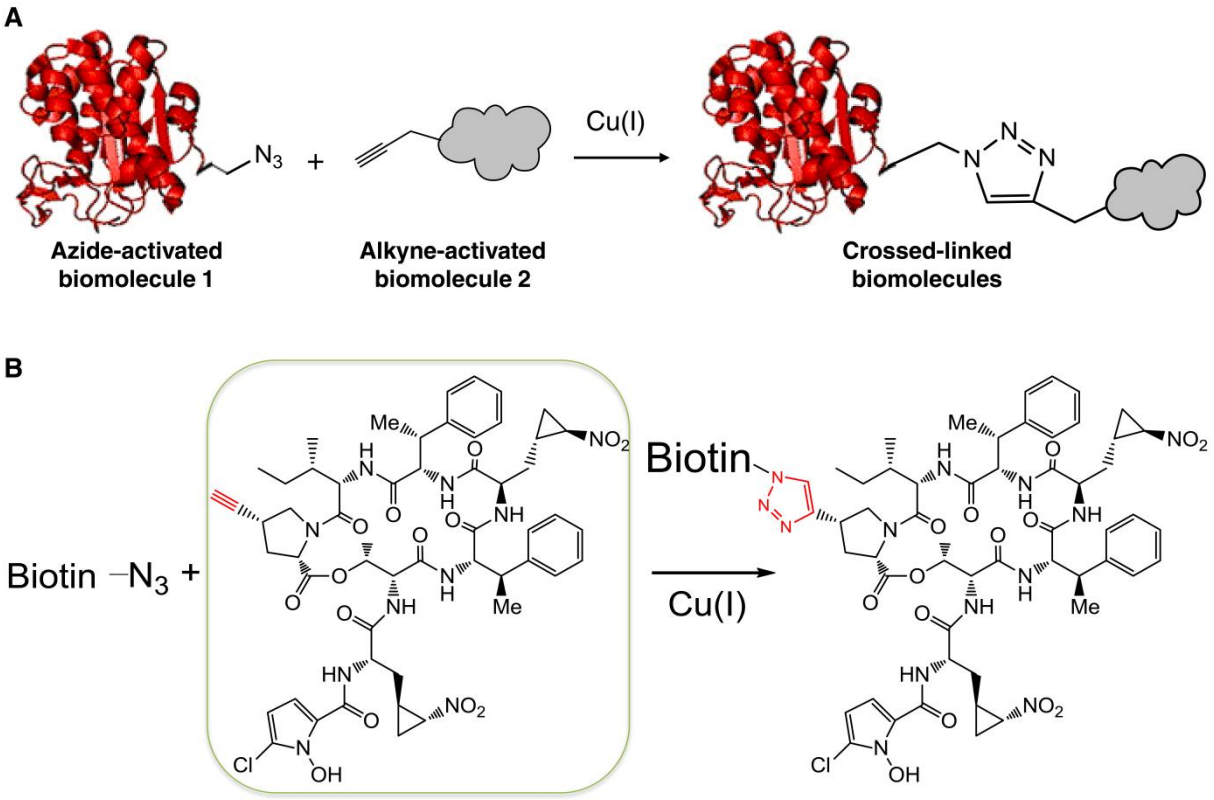

Figure 3.61: Classic click chemistry and its application. **A,** Copper(I)-catalyzed azide–alkyne cycloaddition. **B,** Putative bioconjugation using the cycloaddition of biotin azide and ethinyl-HRM analogue to determine the HRM cellular target.

The cellular targets of HRM hormonal and antibacterial activities were hoped to be investigated (**Figure 3.61B**) via bioconjugation using the cycloaddition of azides and acetylenes and eventually to investigate their corresponding mechanism of action. To employ this reaction, an alkyne-based HRM analogue is required. Since chemical synthesis of this compound is very complex and time-consuming, this compound was expected to be generated via mutagenesis by feeding 4-ethinylproline [(4-Et)Pro] into ΔD.

Approximately 25 mg of (2*S*, 4*S*)-4-ethinylproline [(4-Et)Pro] was synthesized initially by Christoph Kohlhaas. The chemical feeding experiment of ΔD/HrmB with (4-Et)Pro was firstly conducted at a small scale. 50 mL of ΔD/HrmB production media was supplemented with 10 mL (4-Et)Pro (2 mg/mL) every 12 h for 5 times to a final concentration of 0.33 mg/mL. The resulting culture supernatant was extracted and analyzed by LC-MS (**Figure 3.62**). The data revealed a new compound designated as HRM A_8 with a mass of 1113.456 Da $[M+H]^+$ matching to the calculated mass of 1113.445 Da $[M+H]^+$.

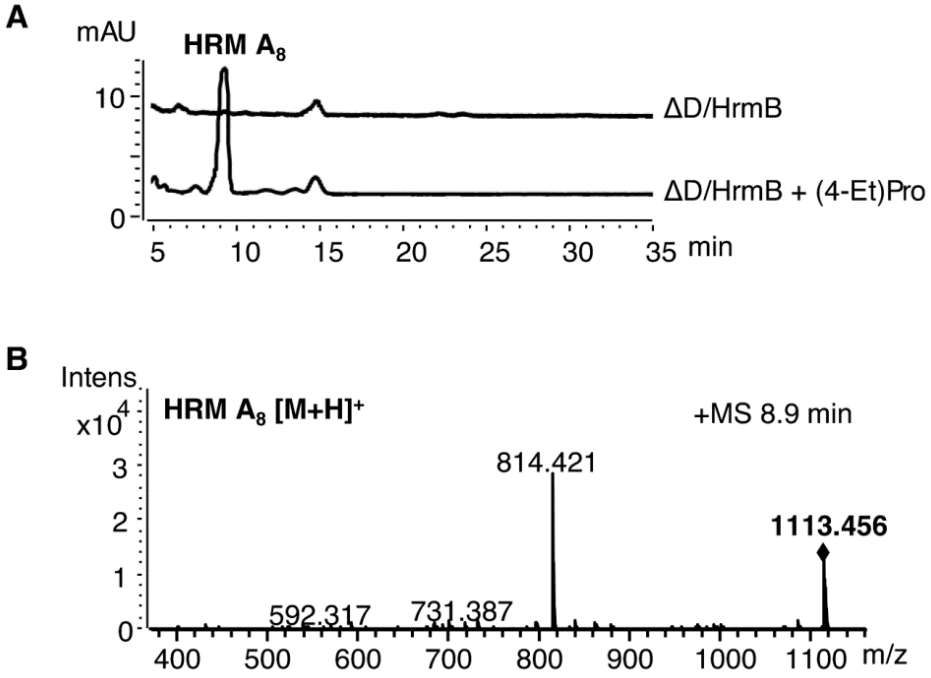

Figure 3.62: LC-MS analysis of the extracts from the ΔD/HrmB and ΔD/HrmB fed with (4-Et)Pro. **A,** Comparison of UV spectra of ΔD/HrmB and ΔD/HrmB fed with (4-Et)Pro at 273 nm. **B,** Observed exact mass of HRM A_8 at 8.9 min.

To test the bioactivity of this new compound for further studies, very small amount of HRM A_8 was isolated by preparative HPLC and applied to bioassay against *A. crystallopoietes* ATCC15481. The inhibition zone suggested HRM A_8 was antibacterially active (**Figure 3.63**), and encouraged us to obtain more of this compound for further structural characterization and bioassay tests.

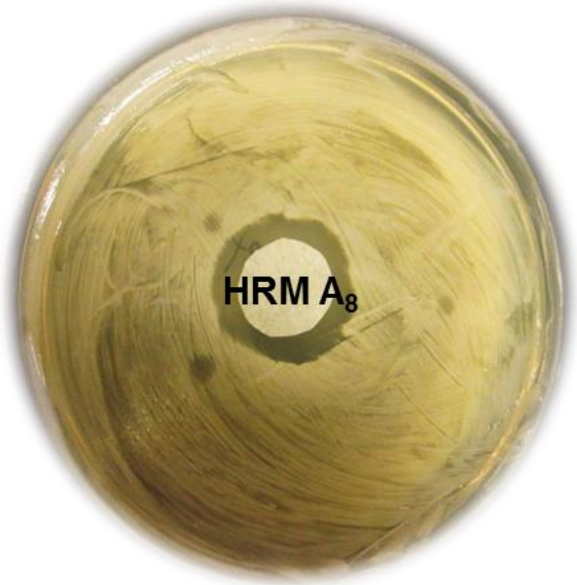

Figure 3.63: Bioassay test of HRM A_8 against *A. crystallopoietes* ATCC15481.

To obtain sufficient amounts of required compound for structural elucidation, 100 mg (4-Et)Pro was synthesized by Pia Schmidt. Subsequent cultivation was carried out at multiple small scales in parallel because *S. griseoflavus* W-384 produces very small amounts of metabolites in large scale fermentation. 100 mg (4-Et)Pro was dissolved in 50 mL sterilized distilled water to a final concentration of 2 mg/mL. 250 mL production medium of ΔD/HrmB was devided into 5 flasks. Each 50 mL production medium was fed with 10 mL of (4-Et)Pro as described above. After feeding, the supernatant from the resulting fermentation culture was combined and extracted with EtOAc. The extracts were applied to preparative HPLC. Unexpectedly, the UV chromatography of the HPLC showed that one more peak adjacent to HRM A_8 was observed. To obtain good separation of these two compounds, the HPLC method was optimized by Andeas Schneider, and eventually obtained 1.8 mg of fraction 1 (Frac. 1) at 11.42 min and 1.9 mg of fraction 2 (Frac. 2) at 12.41 min (**Figure 3.64**). These two fractions were further analyzed using MS/MS and NMR by Dr. Roberta Teta.

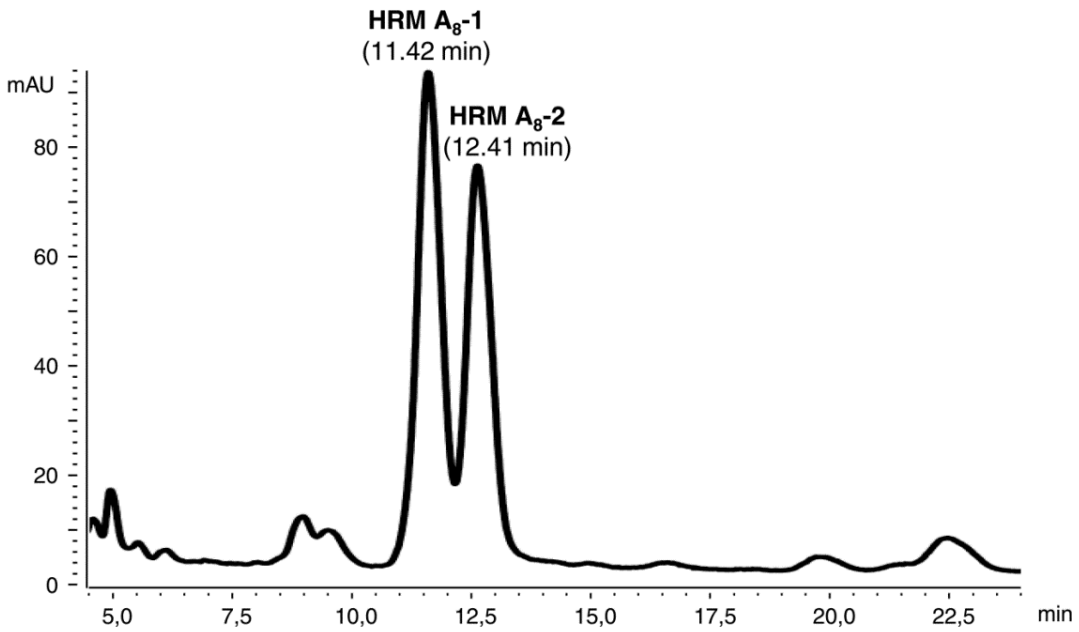

Figure 3.64: Preparative HPLC analysis of extracts from chemical feeding ΔD/HrmB with (4-Et)Pro.

MS/MS spectra of these two compounds were analyzed by Dr. Roberta Teta according to the pattern of tandem MS fragmentation of HRM A_8-1, derived from that of HRM (**Figure 3.65**).

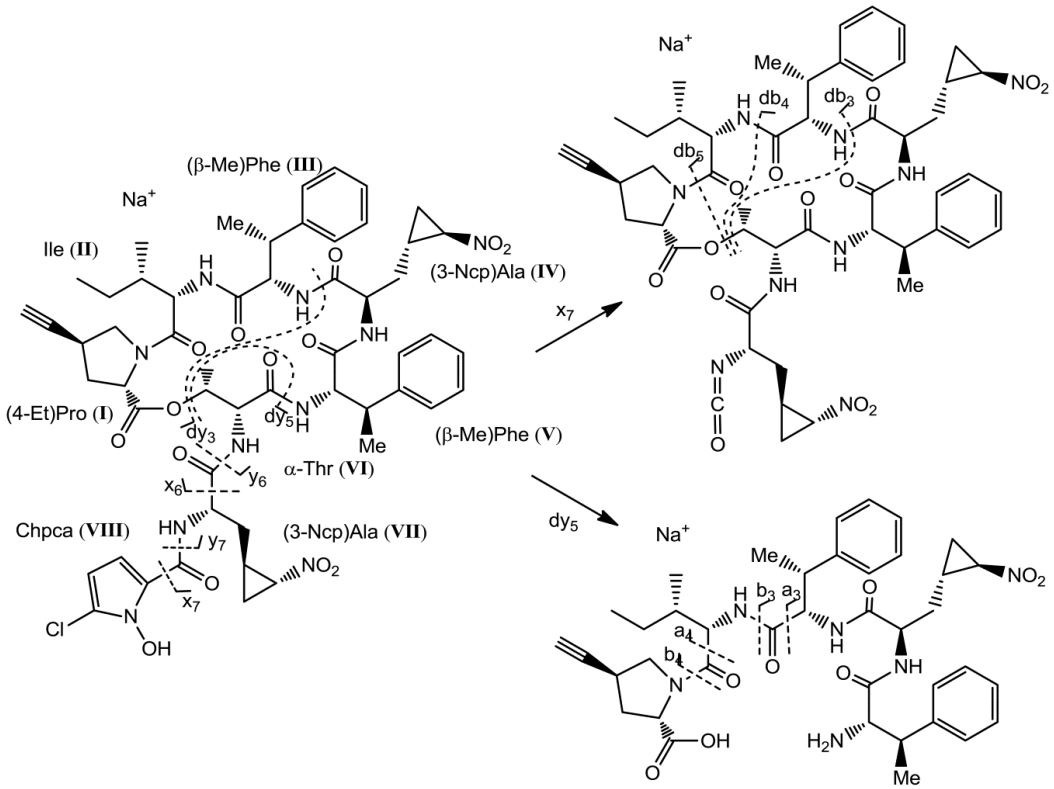

Figure 3.65: Fragmentation of HRM A_8-1 as observed in the ESI MS^2 and MS^3 spectra.

The fragmentations of HRM A_8-1 and HRM A_8-2 were summarized in **Table 3.6**. All the MS/MS and NMR analysis of these two compounds were conducted by Dr. Roberta Teta.

Table 3.6: Most significant fragment ions observed in the ESI-MS^2 and –MS^3 spectra of hormaomycin, HRM A_8-1, and HRM A_8-2.

Fragment	HRM	HRM A_8-1	HRM A_8-2
$[M+Na]^+$	1151.4546	1135.4260	1135.4237
	$C_{55}H_{69}N_{10}O_{14}Na^+$	$C_{54}H_{65}N_{10}O_{14}Na^+$	$C_{54}H_{65}N_{10}O_{14}Na^+$
x_7	1034.4586	1018.4281	1018.4261
	$C_{51}H_{65}N_9O_{13}Na^+$	$C_{50}H_{61}N_9O_{13}Na^+$	$C_{50}H_{61}N_9O_{13}Na^+$
$x_7 \rightarrow db_5$	897.3749	897.3715	897.3732
	$C_{43}H_{54}N_8O_{12}Na^+$	$C_{43}H_{54}N_8O_{12}Na^+$	$C_{43}H_{54}N_8O_{12}Na^+$
$x_7 \rightarrow da_5$	851.3697	851.3662	851.3679
	$C_{42}H_{52}N_8O_{10}Na^+$	$C_{42}H_{52}N_8O_{10}Na^+$	$C_{42}H_{52}N_8O_{10}Na^+$
$x_7 \rightarrow db_4$	784.2915	784.2879	784.2894
	$C_{37}H_{43}N_7O_{11}Na^+$	$C_{37}H_{43}N_7O_{11}Na^+$	$C_{37}H_{43}N_7O_{11}Na^+$
$x_7 \rightarrow da_4$	738.2852	738.2826	738.2849
	$C_{36}H_{41}N_7O_9Na^+$	$C_{36}H_{41}N_7O_9Na^+$	$C_{36}H_{41}N_7O_9Na^+$
$x_7 \rightarrow db_3$	623.2069	623.2044	623.2055
	$C_{27}H_{32}N_6O_{10}Na^+$	$C_{27}H_{32}N_6O_{10}Na^+$	$C_{27}H_{32}N_6O_{10}Na^+$
$x_7 \rightarrow da_3$	577.2011	577.1990	577.2002
	$C_{26}H_{30}N_6O_8Na^+$	$C_{26}H_{30}N_6O_8Na^+$	$C_{26}H_{30}N_6O_8Na^+$
y_7	1008.4798	992.4492	992.4469
	$C_{50}H_{67}N_9O_{12}Na^+$	$C_{49}H_{63}N_9O_{12}Na^+$	$C_{49}H_{63}N_9O_{12}Na^+$
x_6	878.4059	862.3750	862.3729
	$C_{45}H_{57}N_7O_{10}Na^+$	$C_{44}H_{53}N_7O_{10}Na^+$	$C_{44}H_{53}N_7O_{10}Na^+$
y_6	852.4266	836.3957	836.3936
	$C_{44}H_{59}N_7O_9Na^+$	$C_{44}H_{59}N_7O_9Na^+$	$C_{44}H_{59}N_7O_9Na^+$
dy_5	769.3888	753.3585	753.3567
	$C_{40}H_{54}N_6O_8Na^+$	$C_{39}H_{5o}N_6O_8Na^+$	$C_{39}H_{5o}N_6O_8Na^+$
$dy_5 \rightarrow b_4$	632.3046	632.3048	632.3039
	$C_{32}H_{43}N_5O_7Na^+$	$C_{32}H_{43}N_5O_7Na^+$	$C_{32}H_{43}N_5O_7Na^+$
$dy_5 \rightarrow a_4$	586.2992	586.2992	586.2984
	$C_{31}H_{41}N_5O_5Na^+$	$C_{31}H_{41}N_5O_5Na^+$	$C_{31}H_{41}N_5O_5Na^+$
$dy_5 \rightarrow b_3$	519.2206	519.2206	519.2199
	$C_{26}H_{32}N_4O_6Na^+$	$C_{26}H_{32}N_4O_6Na^+$	$C_{26}H_{32}N_4O_6Na^+$
$dy_5 \rightarrow a_3$	473.2153	473.2153	473.2146
	$C_{25}H_{30}N_4O_4Na^+$	$C_{25}H_{30}N_4O_4Na^+$	$C_{25}H_{30}N_4O_4Na^+$

HRM A_8-1. The $[M+Na]^+$ pseudomolecular ion peak of HRM A_8-1 observed at *m/z* 1135.4260 in the high-resolution ESI mass spectrum indicated the molecular formula $C_{54}H_{65}N_{10}O_{16}Cl$ (calcd. *m/z* 1135.4262 for $C_{54}H_{65}N_{10}O_{16}ClNa$), differing from HRM by one less carbon atom and one more degree of unsaturation. This corresponds to the expected formula from replacing the (4-Pe)Pro of HRM with a (4-Et)Pro residue. The MS^2 and MS^3 spectra confirmed that the difference of HRM A_8-1 from HRM is located in the proline residue. Because the fragmentation of HRM has been studied in detail, the assignment of the observed fragments was straightforward. All the fragment ions containing the proline residue (x_7, y_7, x_6, y_7, and dy_7) were less than the respective fragments of HRM by 16 amu, while the remaining fragment ions were identical (**Figure 3.65** and **Table 3.6**).

HRM A_8-2. The $[M+Na]^+$ pseudomolecular ion peak of HRM A_8-2 at *m/z* 1135.4237 suggested the same molecular formula $C_{54}H_{65}N_{10}O_{16}Cl$ as for HRM A_8-1, and the fragments obtained from MS^2 and MS^3 were also identical. Full ^1H and ^{13}C NMR assignment of HRM A_8-2 was achieved through 1D and 2D spectra, which also showed that all the planar structure of the compound is the same as HRM A_8-1. Therefore, the two compounds are stereoisomers. The most remarkable differences in the ^1H NMR signals were the signals of (4-Et)Pro (**Table 3.7**), suggesting a different configuration at (4-Et)Pro-C4, i.e. a different orientation of the ethinyl group. The ROESY spectrum displayed an intense NOE between (4-Et)Pro-H2 and -H4, demonstrating that these two protons are on the same side of the proline five-membered ring. This established the *R* configuration at (4-Et)Pro-C4.

Full NMR characterization of HRM A_8-1 (**Figure 3.66**) was achieved using the usual set of 2D NMR experiments, including COSY, TOCSY, ROESY, HSQC, and HMBC (**Table 3.7** and **Figure 3.67**-**Figure 3.73**). The ^1H NMR spectrum was similar to that of HRM, except for the absence of the signals of the propenyl side chain and the presence of a singlet at δ 2.56 attributable to a terminal alkyne proton. This showed correlation peaks in the HMBC spectrum with (4-Et)Pro-C4 (δ 30.9) and -C1' (δ 83.5). The latter correlation peak was characterized by a very large $^2J_{CH}$ (49.5 Hz), which is peculiar of terminal alkynes. The HMBC spectrum also

displayed the one-bond correlation between (4-Et)Pro-H2' and -C2', which was important for the assignment of (4-Et)Pro-C2' because the relevant correlation peak was not visible in the HSQC spectrum (probably because the $^{1}J_{CH}$ between the two nuclei, 250.0 Hz, was very different from the value for which the experiment was optimized, 155 Hz). The location of the ethinyl group was confirmed by the long range coupling (2.4 Hz) of the alkyne proton (4-Et)Pro-H2' with (4-Et)Pro-H4 evidenced by the COSY spectrum. The stereochemistry at (4-Et)Pro-C4 was determined as *S* on the basis of the weak NOE between (4-Et)Pro-H2' and -H2 observed in the ROESY spectrum, and of the absence of any NOE between (4-Et)Pro-H2 and –H4 (which on the contrary was evident in the stereomeric HRM A_8-2 (**Figure 3.66**), see **Table 3.7** and **Figure 3.74**-**Figure 3.80**.

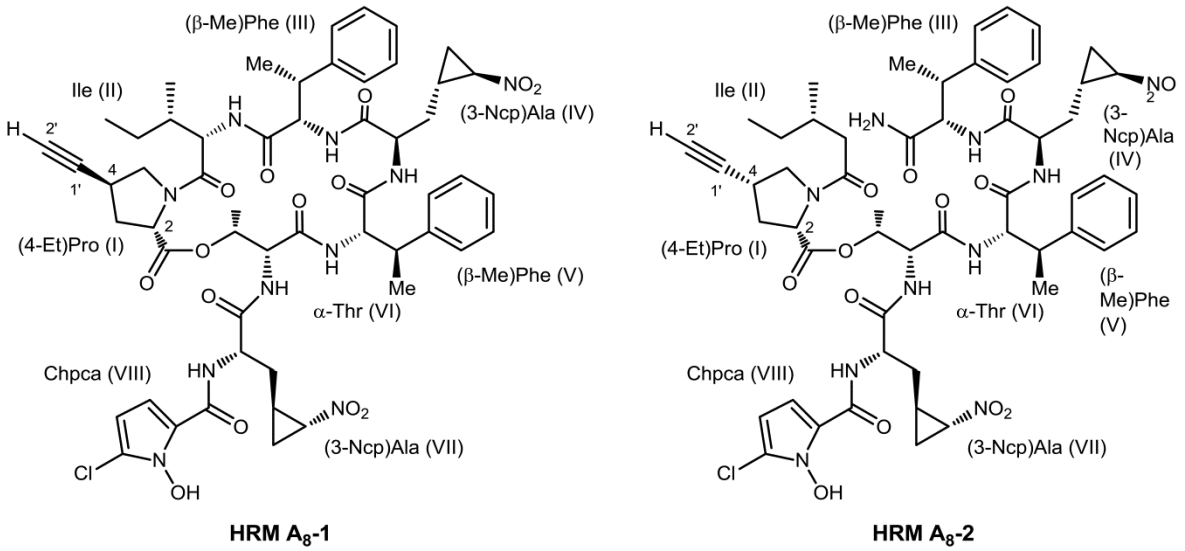

Figure 3.66: The structure of HRM A_8-1 and HRM A_8-2.

Table 3.7: NMR spectroscopic data for compounds HRM A_8-1 and HRM A_8-2 (700 MHz, CD_3OD)

			HRM A_8-1		**HRM A_8-2**	
AA	Pos.		δ_H [mult., *J* (Hz)]	δ_C [mult.]	δ_H [mult., *J* (Hz)]	δ_C [mult.]
(4-Etynyl)Pro (I)	1		-	173.7 I	-	173.5 I
(4-Etynyl)Pro (I)	2		4.14 (t, 7.6)	61.0 (CH)	4.00 (dd, 11.2, 6.2)	61.9 (CH)
(4-Etynyl)Pro (I)	3	a	2.25 (ddd, 12.8, 7.6, 5.4)	36.1 (CH_2)	2.53 (ddd, 12.2, 6.1, 6.1)	36.6 (CH_2)
(4-Etynyl)Pro (I)	3	b	2.19 (ddd, 12.8, 7.6, 6.3)		1.95 (q, 12.0)	
(4-Etynyl)Pro (I)	4		3.30 (m)	30.9 (CH)	3.18 (m)	30.4 (CH)
(4-Etynyl)Pro (I)	5	a	3.96 (dd, 10.1, 6.3)	54.3 (CH_2)	4.41 (m)	53.5 (CH_2)
(4-Etynyl)Pro (I)	5	b	3.92 (t, 10.1, 5.0)		3.49 (t, 10.4)	
(4-Etynyl)Pro (I)	1’		-	83.5 I	-	82.1 I
(4-Etynyl)Pro (I)	2’		2.57 (d, 2.4)	72.4 (CH)	2.61 (d, 2.3)	72.4 (CH)
Ile (II)	1		-	172.0 I	-	172.0 I
Ile (II)	2		4.64 (ovl)	56.2 (CH)	4.57 (dd, 10.5, 1.9)	56.2 (CH)
Ile (II)	3		2.16 (m)	36.4 (CH)	2.18 (m)	36.2 (CH)
Ile (II)	4	a	1.60 (m)	25.5 (CH_2)	1.60 (m)	25.6 (CH_2)
Ile (II)	4	b	1.17 (m)		1.16 (m)	
Ile (II)	5		0.89 (t, 7.5)	10.8 (CH_3)	0.88 (t, 7.4)	10.7 (CH_3)
Ile (II)	1’		0.98 (d, 6.7)	16.4 (CH_3)	0.97 (d, 6.8)	16.4 (CH_3)
(β-Me)Phe (III)	1		-	172.5 I	-	172.6 I
(β-Me)Phe (III)	2		4.52 (dd, 8.6, 4.7)	61.2 (CH)	4.44 (ovl)	61.5 (CH)
(β-Me)Phe (III)	3		3.66 (dq, 4.7, 7.3)	40.5 (CH)	3.62 (dq, 4.8, 7.3)	40.6 (CH)
(β-Me)Phe (III)	4		1.34 (d, 7.3)	14.2 (CH_3)	1.35 (d, 7.3)	14.4 (CH_3)
(β-Me)Phe (III)	1’		-	143.4 I	-	143.3 I
(β-Me)Phe (III)	2’		7.28 (ovl)	128.6 (CH)	7.29 (ovl)	128.6 (CH)
(β-Me)Phe (III)	3’		7.28 (ovl)	129.5 (CH)	7.29 (ovl)	129.6 (CH)
(β-Me)Phe (III)	4’		7.18 (m)	128.0 (CH)	7.19 (m)	128.1 (CH)
(3-Ncp)Ala (IV)	1		-	174.0 I	-	174.4 I
(3-Ncp)Ala (IV)	2		3.89 (ovl)	54.5 (CH)	3.84 (d, 7.9)	54.5 (CH)
(3-Ncp)Ala (IV)	3	a	1.11 (ddd, 14.0, 7.5, 7.5)	33.3 (CH_2)	1.13 (ovl)	33.2 (CH_2)
(3-Ncp)Ala	3	b	0.82 (ddd, 14.0,		0.86 (ovl)	

			HRM A_8-1		HRM A_8-2	
(IV)			7.5, 7.5)			
(3-Ncp)Ala (IV)	1’		1.29 (m)	22.9 (CH)	1.31 (m)	22.8 (CH)
(3-Ncp)Ala (IV)	2’		3.89 (ovl)	60.2 (CH)	3.90 (ddd, 7.1, 3.4, 3.4)	60.2 (CH)
(3-Ncp)Ala (IV)	3’	a	1.51 (ddd, 10.0, 5.6, 3.7)	18.5 (CH_2)	1.50 (ddd, 9.9, 5.7, 3.4)	18.4 (CH_2)
(3-Ncp)Ala (IV)	3’	b	0.66 (m)		0.69 (m)	
(β-Me)Phe (V)	1		-	171.5 I	-	171.5 I
(β-Me)Phe (V)	2		4.64 (d, 8.6)	59.7 (CH)	4.60 (d, 8.8)	59.7 (CH)
(β-Me)Phe (V)	3		3.05 (dq, 8.6, 7.2)	45.2 (CH)	3.05 (dq, 8.6, 7.2)	45.2 (CH)
(β-Me)Phe (V)	4		1.21 (d, 7.2)	18.4 (CH_3)	1.21 (d, 7.2)	18.4 (CH_3)
(β-Me)Phe (V)	1’		-	143.2 I	-	143.2 I
(β-Me)Phe (V)	2’		7.12 (d, 7.5)	129.2 (CH)	7.12 (d, 7.5)	129.1 (CH)
(β-Me)Phe (V)	3’		7.15 (t, 7.5)	129.3 (CH)	7.16 (t, 7.5)	129.3 (CH)
(β-Me)Phe (V)	4’		7.01 (t, 7.5)	127.9 (CH)	7.01 (t, 7.5)	127.9 (CH)
α-Thr (VI)	1		-	169.5 I	-	169.5 I
α-Thr (VI)	2		4.77 (d, 2.2)	59.1 (CH)	4.77 (d, 2.1)	59.2 (CH)
α-Thr (VI)	3		5.43 (dq, 2.2, 6.9)	73.3 (CH)	5.47 (dq, 2.1, 6.8)	73.4 (CH)
α-Thr (VI)	4		1.58 (d, 6.9)	18.6 (CH_3)	1.59 (d, 6.9)	18.6 (CH_3)
(3-Ncp)Ala (VII)	1		-	172.0 I		172.0 I
(3-Ncp)Ala (VII)	2		4.44 (t, 5.5)	54.6 (CH)	4.44 (ovl)	54.7 (CH)
(3-Ncp)Ala (VII)	3	a	2.03 (m)	34.2 (CH_2)	2.04 (m)	34.1 (CH_2)
(3-Ncp)Ala (VII)	3	b	1.73 (m)		1.76 (m)	
(3-Ncp)Ala (VII)	1’		2.01 (m)	22.9 (CH)	2.02 (m)	22.9 (CH)
(3-Ncp)Ala (VII)	2’		4.36 (ddd, 7.0, 3.6, 2.6)	60.4 (CH)	4.37 (ddd, 7.0. 3.6, 2.6)	60.5 (CH)
(3-Ncp)Ala (VII)	3’	a	1.82 (ddd, 10.0, 5.6, 3.6)	18.0 (CH_2)	1.82 (ddd, 9.8, 5.9, 3.6)	17.9 (CH_2)
(3-Ncp)Ala (VII)	3’	b	1.15 (m)		1.17 (m)	
Chpca (VIII)	1		-	161.8 I		161.9 I
Chpca (VIII)	2		-	118.5 I		118.4 I
Chpca (VIII)	3		6.82 (d, 4.8)	110.4 (CH)	6.82 (d, 4.8)	110.4 (CH)
Chpca (VIII)	4		6.07 (d, 4.8)	104.1 (CH)	6.06 (d, 4.8)	104.1 (CH)
Chpca (VIII)	5		-	120.6 I		120.5 I

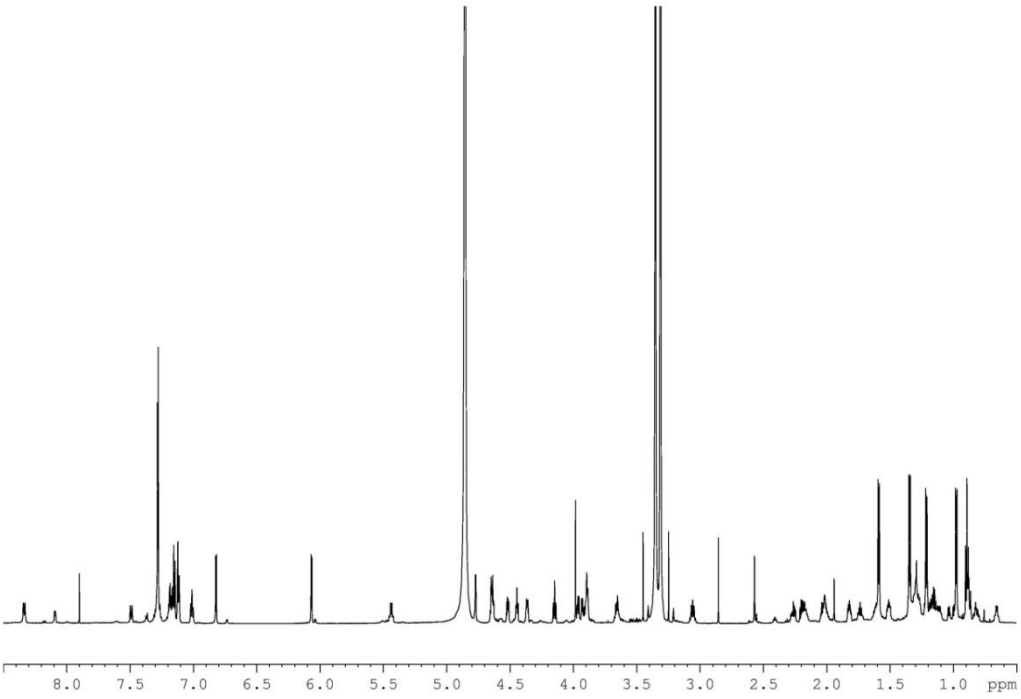

Figure 3.67: ^{1}H NMR spectrum (700MHz, CD_3OD) of HRM A_8-1.

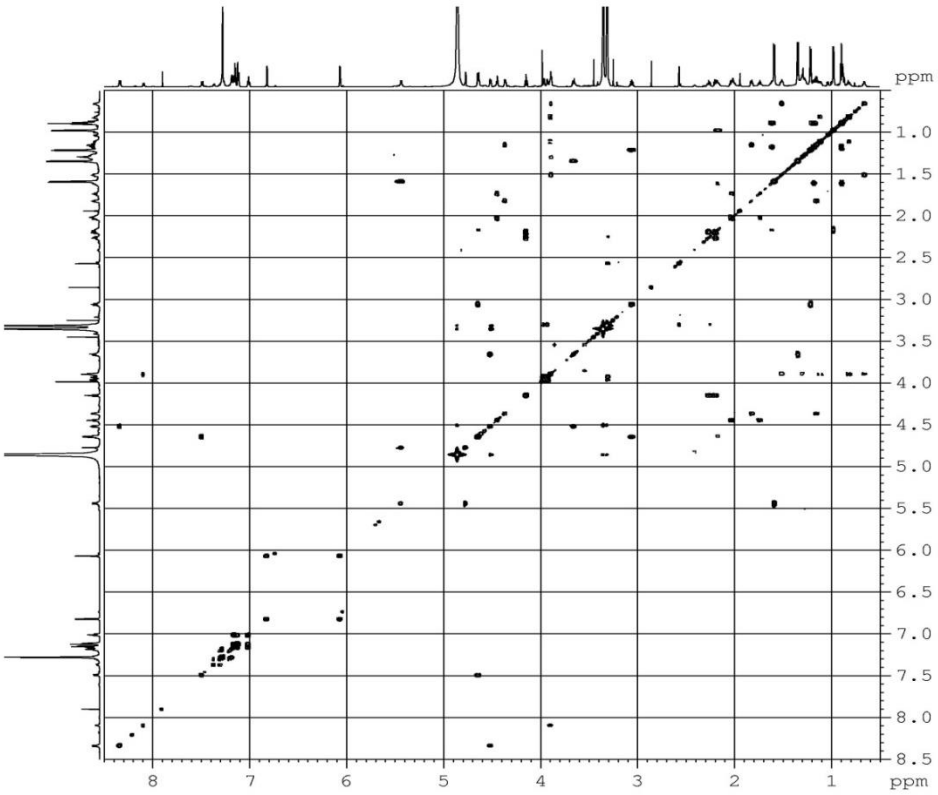

Figure 3.68: COSY spectrum (700MHz, CD_3OD) of HRM A_8-1.

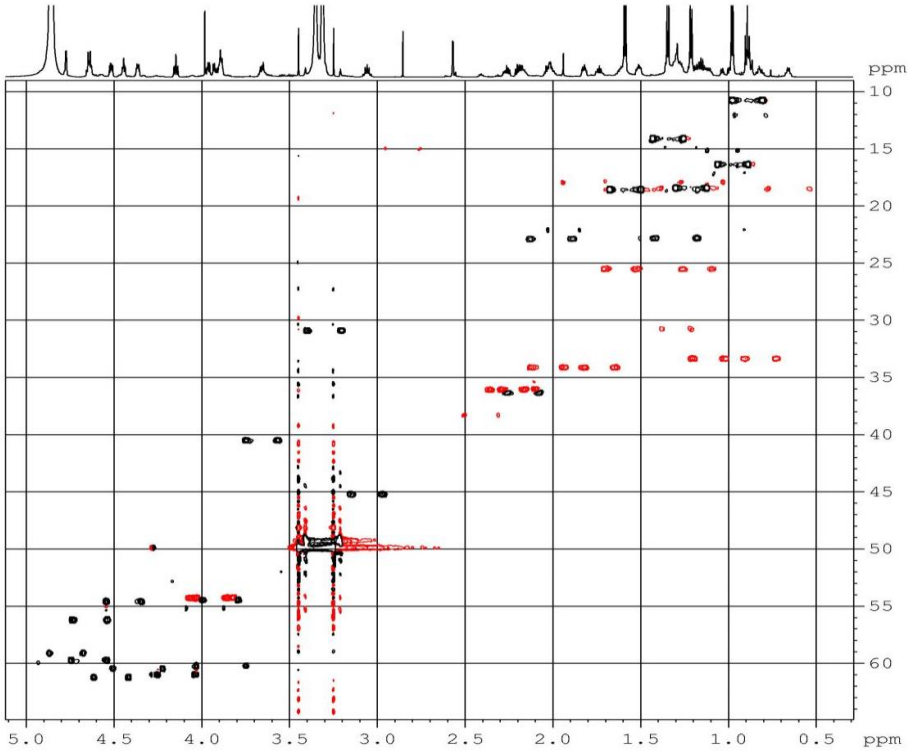

Figure 3.69: HSQC spectrum (700MHz, CD_3OD) of HRM A_8-1 high field expansion.

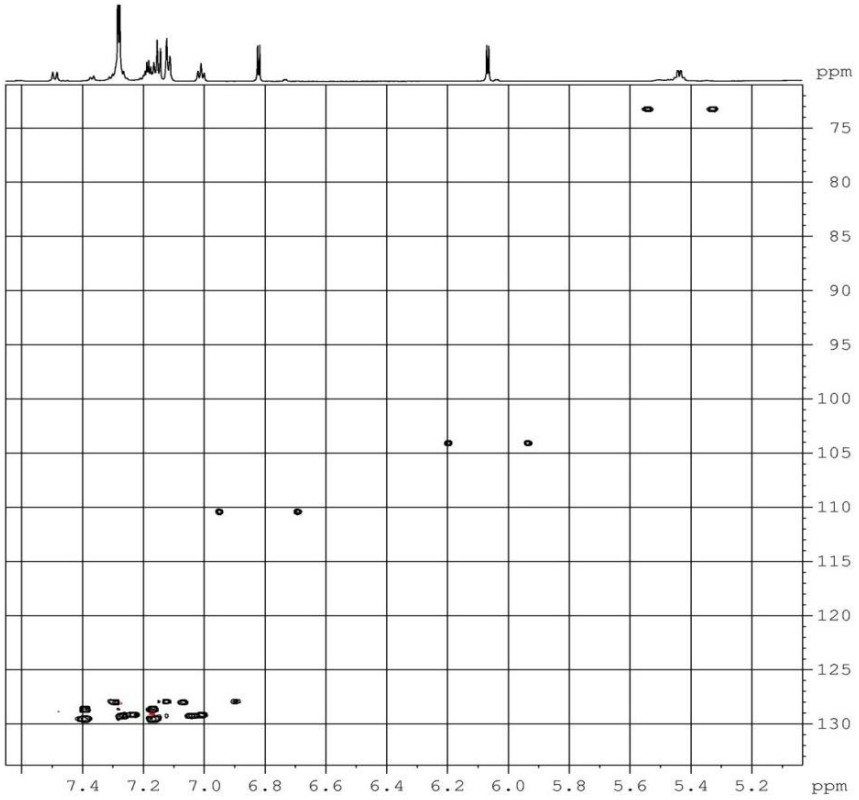

Figure 3.70: HSQC spectrum (700MHz, CD_3OD) of HRM A_8-1 low field expansion.

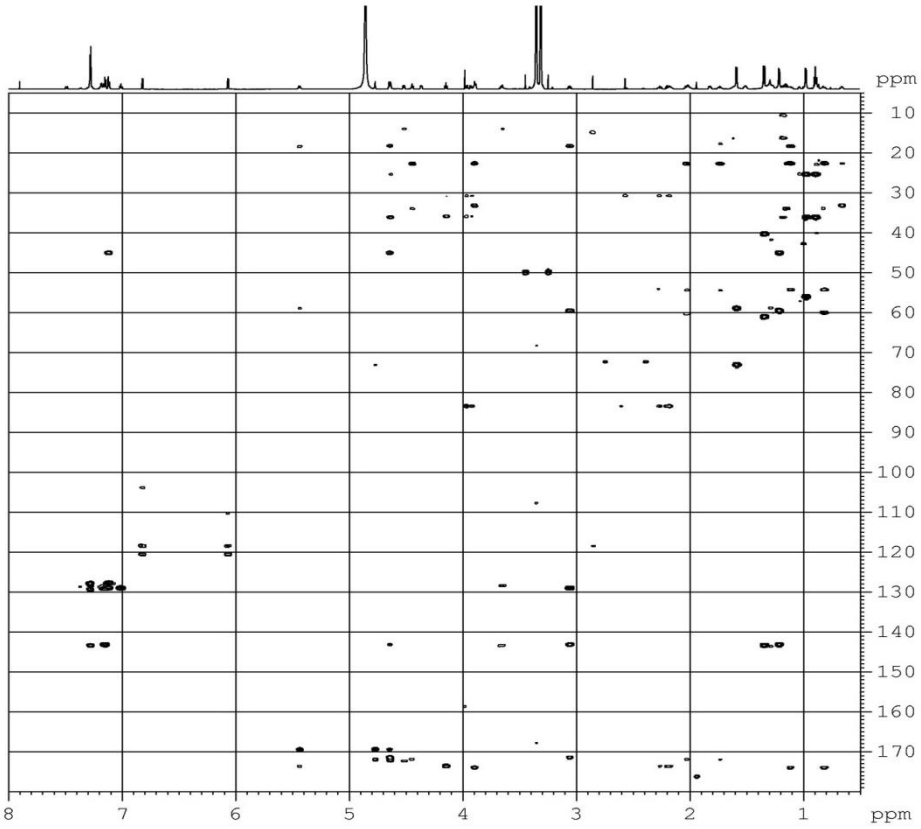

Figure 3.71: HMBC spectrum (700MHz, CD_3OD) of HRM A_8-1.

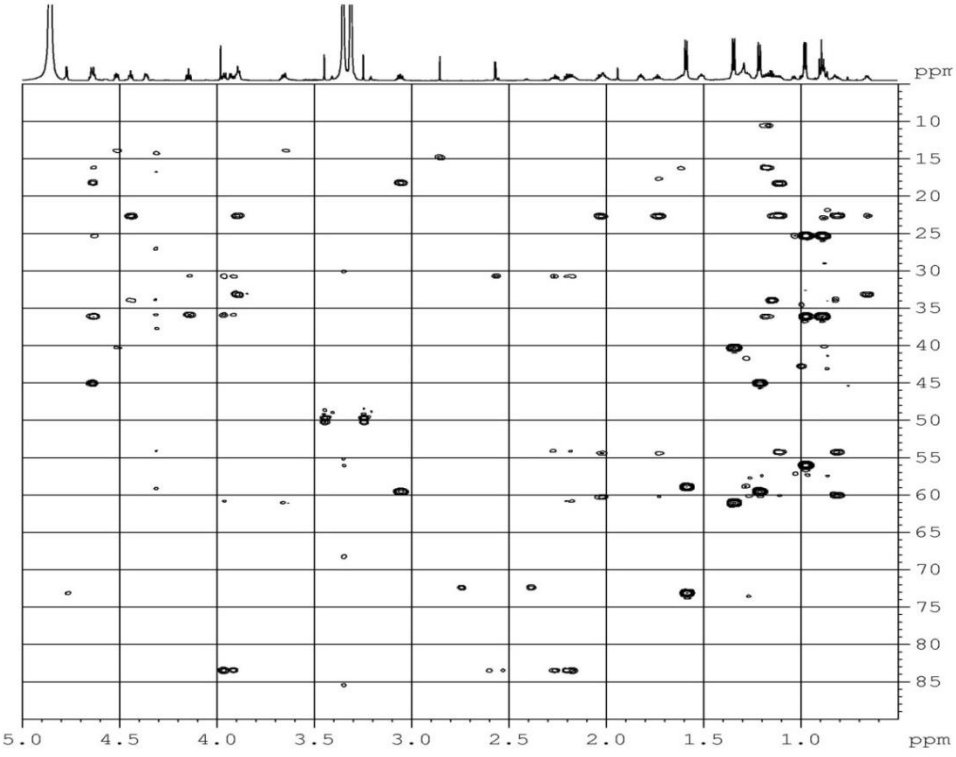

Figure 3.72: HMBC spectrum (700MHz, CD_3OD) of HRM A_8-1 high field expansion.

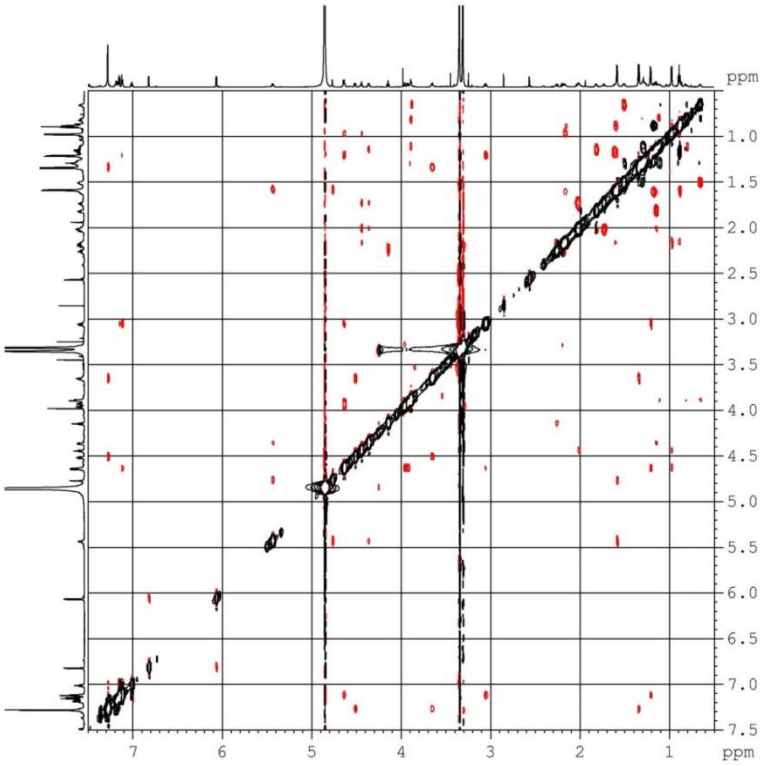

Figure 3.73: ROESY spectrum (700MHz, CD_3OD) of HRM A_8-1.

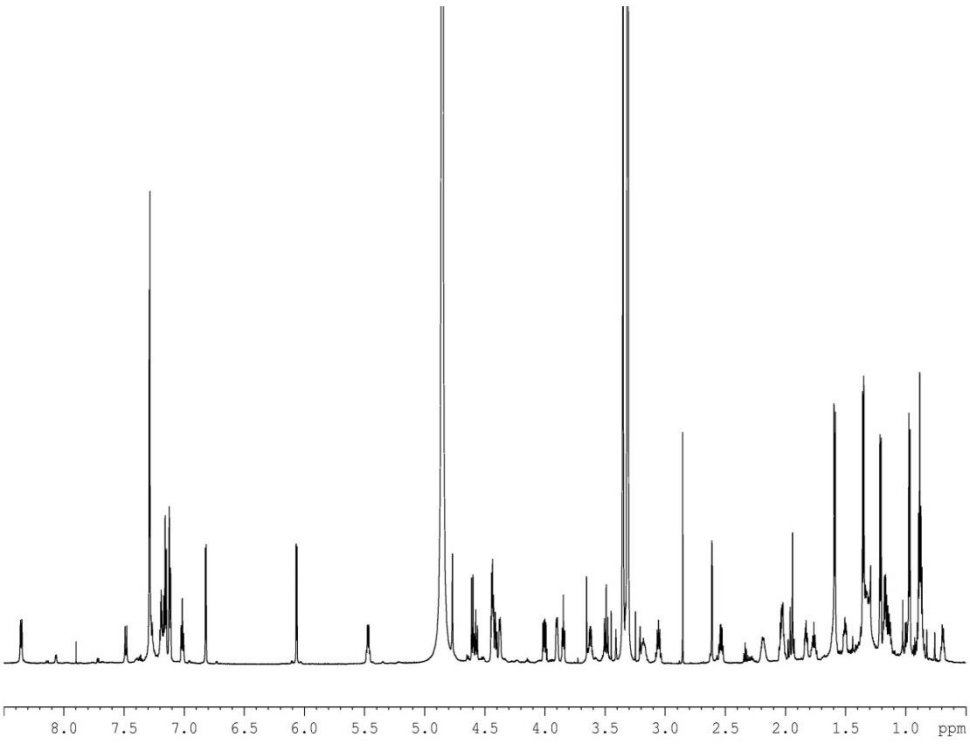

Figure 3.74: ^1H NMR spectrum (700MHz, CD_3OD) of HRM A_8-2.

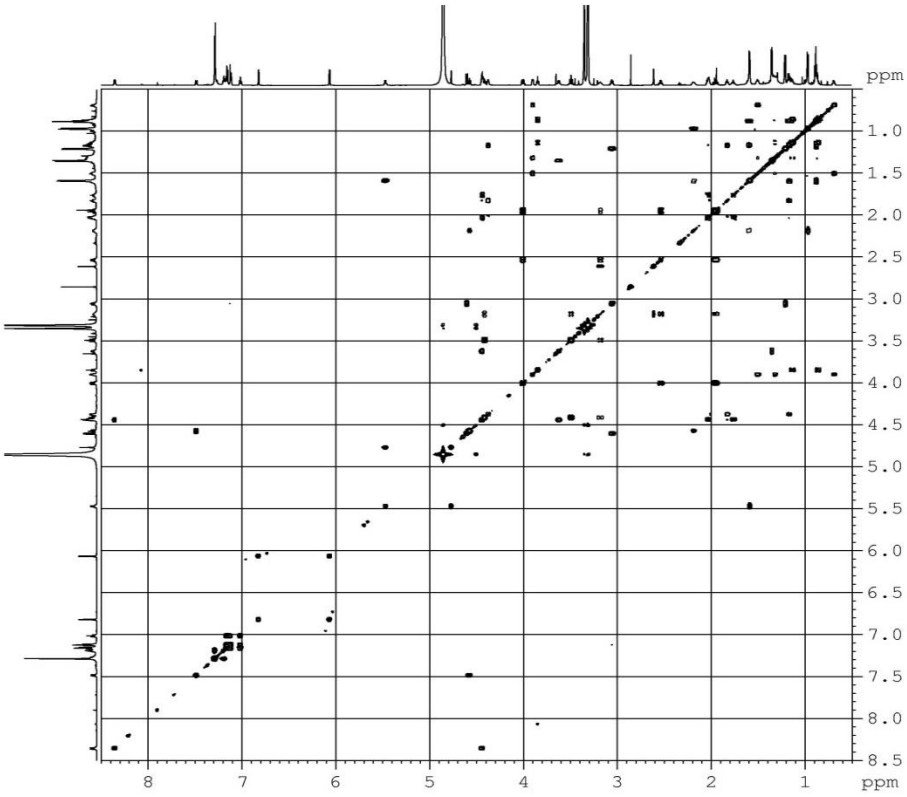

Figure 3.75: COSY spectrum (700MHz, CD_3OD) of HRM A_8-2.

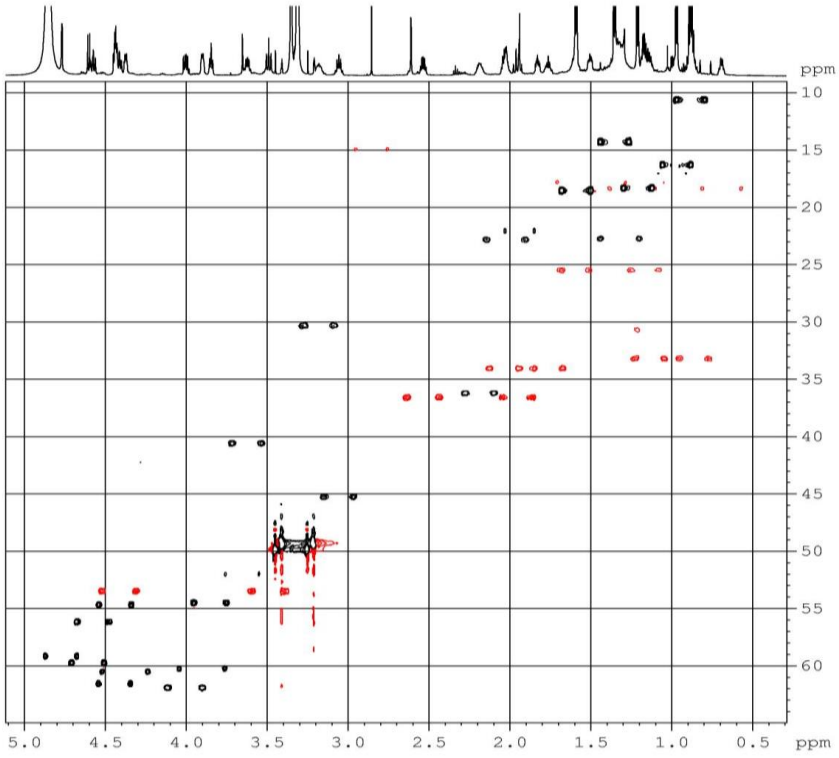

Figure 3.76: HSQC spectrum (700MHz, CD_3OD) of HRM A_8-2 high field expansion.

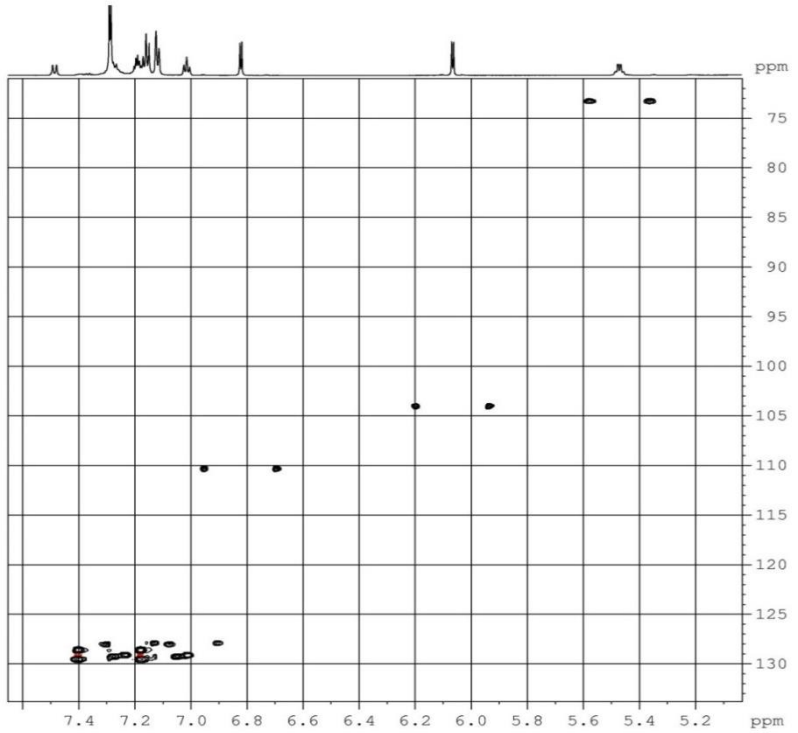

Figure 3.77: HSQC spectrum (700MHz, CD_3OD) of HRM A_8-2 low field expansion.

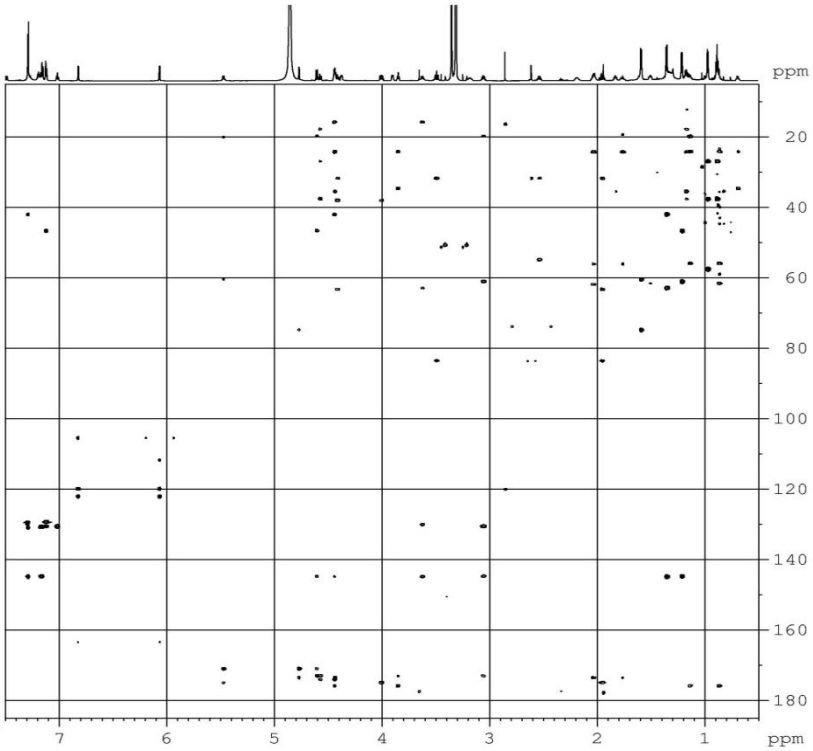

Figure 3.78: HMBC spectrum (700MHz, CD_3OD) of HRM A_8-2.

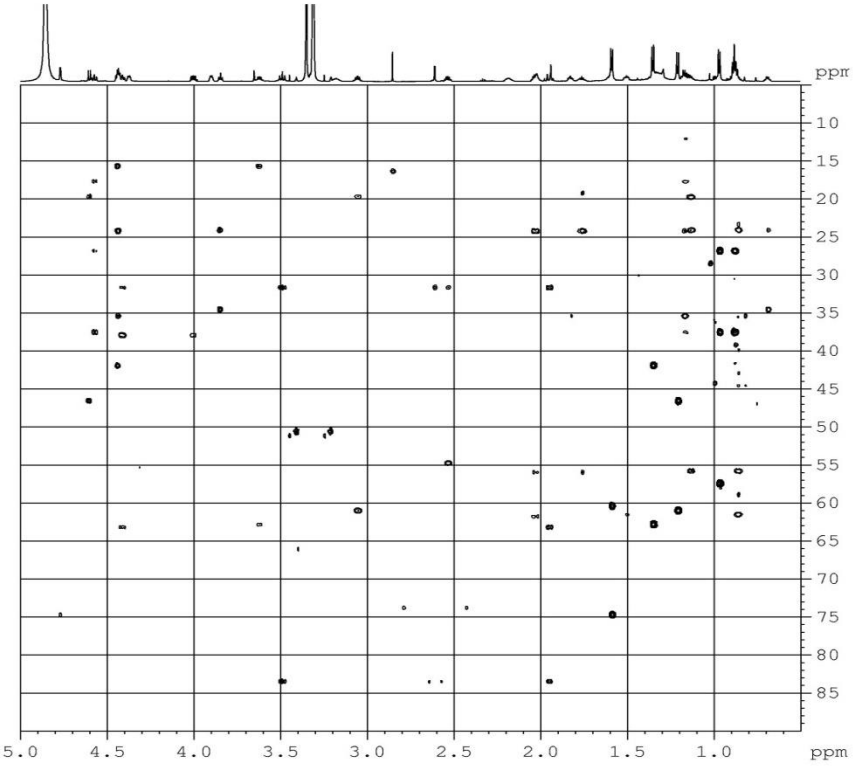

Figure 3.79: HMBC spectrum (700MHz, CD_3OD) of HRM A_8-2 high field expansion.

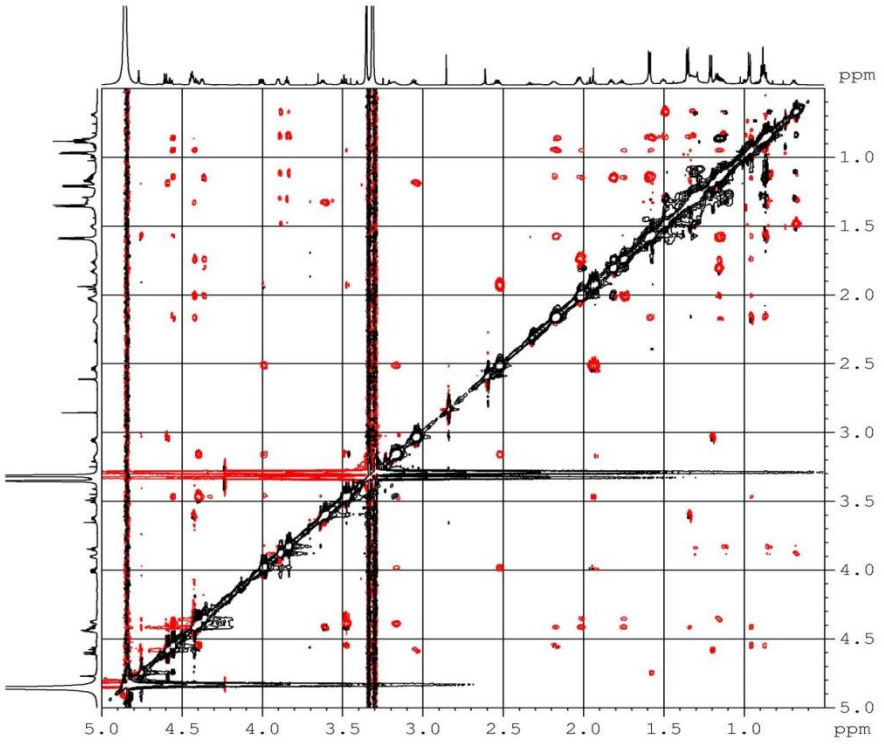

Figure 3.80: ROESY spectrum (700MHz, CD_3OD) of HRM A_8-2 high field expansion.

Finally, HRM A_8-1 and HRMA_8-2 were tested individually against *A. crystallopoietes* ATCC15481, both of which showed potent activities with MICs of 0.01 µg/mL and 0.001

μg/mL, respectively. However, HRM A_8-2 appeared to be more active than HRM A_8-1 (**Figure 3.81**).

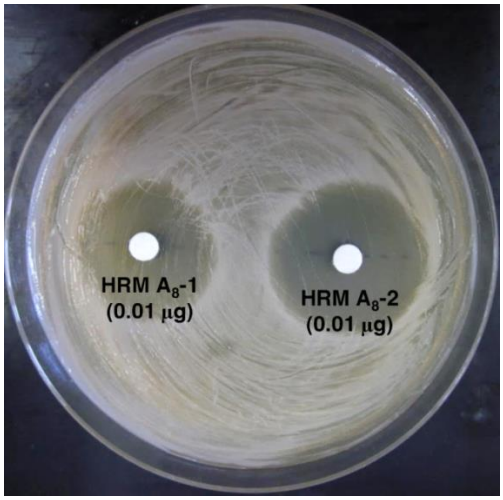

Figure 3.81: Bioassay test of HRM A_8-1 and HRM A_8-2 against *A. crystallopoietes* ATCC15481 with 0.01 μg of two compounds per disc.

In addition, these two compounds were applied to *S. coelicolor* A(3)2 and one of its bald mutant ΔBldK to see whether they could induce the aerial mycelia formation for preliminary test. As shown in **Figure 3.82**, the aerial mycelia formed a circle around the filter paper disk after incubation for 5 ~7 d. The results indicated that these two compounds exhibit hormonal activity similar to HRM. However, HRM A8-2 did not show more obvious effects on aerial mycelia formation than HRM A_8-1, relative to their antibacterial test.

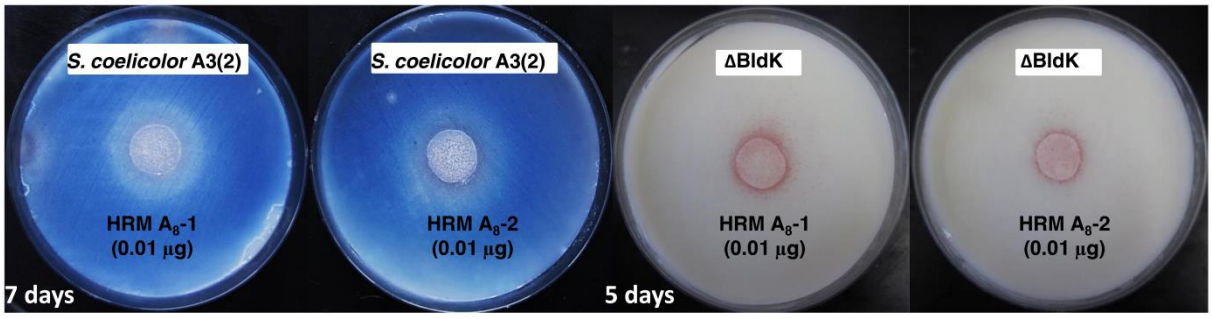

Figure 3.82: Preliminary bioassay test of HRM A_8-1 and HRM A_8-2 on *S. coelicolor* A3(2) and ΔBldK.

In this section, the ethinyl-HRM analogues (HRM A_8-1 and HRM A_8-2) were successfully generated by feeding (4-Et)Pro into the ΔD/HrmB mutant via mutasynthesis, which exhibit

antibacterial and hormonal activities like what HRM possesses. These two compounds will be further applied to bioconjugation using the cycloaddition of azides and acetylenes.

3.3.5 Discussion

HRM acts as a bacterial hormone that induces morphological differentiation and increases antibiotic production in other *Streptomyces* spp. (Andres et al., 1989; Andres et al., 1990). In addition, it is an extremely potent antibiotic against coryneform actinomycetes (Andres et al., 1990). Except for these diverse activities, HRM possesses a remarkable structure (Höfer et al., 2011), which motivated us to exploit and elucidate the biosynthetic machinery of HRM, especially the biosynthesis of unique building blocks existing in HRM, such as Chpca, (3-Ncp)Ala, and (4-Pe)Pro. Previous study has assigned the *hrm* genes suspected to be involved in the biosynthesis of these residues (Höfer et al., 2011), *hrmQ* and *hrmN* for Chpca, *hrmI* and *hrmJ* for (3-Ncp)Ala, as well as *hrmC* and *hrmD* for (4-Pe)Pro. In present study, all these genes were investigated to analyze their roles during HRM biosynthesis by gene knockout, genetic complementation and feeding studies. The results established that *hrmQ* encoding a chlorinase is responsible for catalyzing the chlorination of Chpca, *hrmI* and *hrmJ* are involved in the biosynthesis of (3-Ncp)Ala, and *hrmD* plays an essential role in the biosynthesis of (4-Pe)Pro. HrmI was successfully heterologously expressed, and future enzymatic assays will allow us characterize its function in biosynthesis of (3-Ncp)Ala. In addition, PCR and Southern studies failed to identify a *lmbX* homolog in genomic DNA of HRM producer. The data therefore indicate that this enzyme is not needed for (4-Pe)Pro biosynthesis and that the terminal two-carbon unit of the first pyrroline intermediate is cleaved off by another enzyme.

Overexpression of HrmB led to a significant increase of HRM, suggesting a positive regulatory role of HrmB. Therefore, a HrmB overexpression plasmid was individually introduced into the mutants generated to improve the production of substances as initially applied in *S. griseoflavus* W-384 for increasing HRM production. Unexpectedly, the results showed no obvious change.

The reason for this difference is probably due to the complex regulation system in *Streptomyces* and special physiological properties of HRM. It has been suggested that ~60% *Streptomyces* can produce γ-butyrolactone autoregulators to control their own cellular morphogenesis and secondary metabolism (Yamada 1995). Little is known whether such compounds can act as the signaling bacterial hormone to stimulate the production of antibiotics in other *Streptomyces* spp., such as hormaomycin, goadsporin and avenolide (Andres et al., 1990; Onaka et al., 2001; Kitani et al., 2011). HRM may act as an autoregulator, and bind to its own cellular receptor, and then activate its pathway-specific regulator HrmB to induce the transcription of biosynthetic *hrm* genes and eventually upregulate HRM biosynthesis. Therefore, overexpression of HrmB in *S. griseoflavus* W-384 led to a significant increase of HRM as well as its analogues. However, overexpression of HrmB in the mutants failed to increase the production of substances, which was possibly caused by the complex regulation system in *Streptomyces* spp. and absence of HRM. To examine the role of HRM, additional experiments should be performed by adding HRM to the mutant production culture to see whether HRM can stimulate the production of substances in these mutants. In addition, to investigate the exact regulation role of HrmB, the biosynthetic *hrm* genes should be identified in transcriptional level by RT-PCR analysis in the future.

Mutagenesis is a powerful means to generation of specific substances. In this study, the aim was to obtain one hormaomycin analogue HRM A_8 with (4-Pe)Pro substituted by (4-Et)Pro via feeding of (4-Et)Pro into ΔD. Unexpectedly, two HRM A_8 with different stereochemistry of (4-Et)Pro was generated. These two compounds probably result from feeding a mixture of (4-Et)Pro with different configurations into the ΔD mutant. This mixture might come from changes made in the protocol during the second synthesis of *cis*-(4-Et)Pro, yielding a diastereomeric mixture of the building block. Nevertheless, it was shown that these ethinyl-based HRM analogues possess potent bioactivities against *A. crystallopoietes* ATCC15481 with MIC of 0.01 and 0.001 μg/mL, respectively. SAR studies suggested that change of (4-Pe)Pro residue in HRM has no obvious effect on the antibacterial activity. These two HRM A_8 analogues were individually applied to *S. coelicolor* A3(2) and some of its bald

mutants that previously showed clear aerial mycelia formation by HRM, such as ΔBldC, ΔBldD and ΔBldK for initial test. Although it was observed that HRM A_8-2 was more active than HRM A_8-1 against *A. crystallopoietes* ATCC15481 (**Figure 3.81**), the preliminary hormonal activities induced by these two compounds showed no much difference (**Figure 3.82**). Therefore, they can be further applied to determination of HRM antibacterial and hormonal cellular targets by "Click chemistry".

3.4 Investigation of HRM hormonal activity

Actinomycetes commonly produce low-molecular signals, which act like bacterial hormones called autoregulators by inducing aerial mycelia formation, sporulation and antibiotic production (Beppu 1992; Barabas et al., 1994). These autoregulators are usually active at very low (nM) concentrations and belong to diverse natural product families. The best-characterized autoregulator is butyrolactone A-factor discovered in *S. griseus* in the 1960s (Khokhlov et al., 1967), which triggers sporulation and production of streptomycin, grixazones and polyketides (Horinouchi 2002). But little was known that γ-butyrolactone–type autoregulator can induce the antibiotic production in other species.

Unlike butyrolactone autoregulators, HRM not only induces aerial mycelia formation in various *Streptomyces* species at concentrations as low as 50 ng/mL, but also increases antibiotic production in other *Streptomyces* spp. (Andres et al., 1990). In this study, HRM was applied to a series of bald mutants derived from *S. coelicolor* A3(2) and *S. griseus* IFO 13350 to obtain the first insights into the regulatory mechanism of action and provide the basis for further determination of the as-of-yet unknown molecular target of HRM.

3.4.1 Hormaomycin hormonal assay against *S. coelicolor* A3(2)

Streptomycetes possess a complex life cycle. *S. coelicolor* A3(2) is the genetically best-characterized and first fully sequenced *Streptomyces* strain (Bentley et al., 2002). It has

been revealed that morphological differentiation in *S. coelicolor* involves three major protein families, SapB family, chaplins and rodlins family, and the protein family encoded by *bld* genes. SapB, a surfactant peptide secreted on rich media that coats aerial mycelia to allow the growth of aerial hyphae into the atmosphere. The chaplins and rodlins, are produced around aerial mycelia to form hydrophobic sheaths, facilitating aerial mycelia escape into the air (Flärdh and Buttner 2009). The Bld proteins determine production of SapB and chaplins, which are required for initiation of aerial hyphae formation (Kelemen and Buttner 1998; Claessen et al., 2006). Numerous bald (*bld*) mutants that are defective in aerial mycelia formation have been generated to discover the factors (Chater 2001). Most *bld* genes encode regulatory proteins involved in an extracellular signaling cascade that controls the initiation of morphogenesis. The *bld* mutants are blocked in the earlier stage of development, which are defective in erecting aerial hyphae (Pope et al., 1996). A series of *bld* mutants have been created genetically and characterized, such as *bldA* (Leskiw et al., 1991), *bldB* (Pope et al., 1998), *bldD* (Elliot 1998), *bldH* (Champness 1988), *bldK* (Nodwell et al., 1996), *bldC* (Hunt et al., 2005), and *bldM* (Molle and Buttner 2000). A hierarchy of *bld* genes has been proposed based on extracellular complementation studies, in which each mutant can complement the aerial mycelia formation in mutants to the left (Willey et al., 1991; Willey et al., 1993; Nodwell and Losick 1998; Molle and Buttner 2000; Elliot et al., 2001):

[*bldJ* (formerly *bld261*)] < [*bldK*, *bldL*] < [*bldA*, *bldH*] < [*bldG*]< [*bldC*] < [*bldD*, *bldM*]

However, the *bld* genes do not always conform to this linear cascade. For instance, the *bldB* mutant cannot be complemented by any other mutants or growth on minimal medium supplemented with mannitol (Pope et al., 1996). It has been suggested that this hierarchal signaling cascade involves at least five extracellular signals. Each signal induces the production and release of the next signal, eventually leading to the production of *bldD*-dependent SapB and other morphogens, which result in aerial mycelia formation (Kelemen and Buttner 1998). In this study, the *bldA*, *B*, *C*, *D*, *H*, *K*, and *M* mutants obtained from the John Innes Center were tested to check whether HRM can restore their aerial mycelia

formation to analyze the regulation mechanism of HRM. It was hoped that insights from these studies can help to narrow down the celluar targets of HRM in the aerial mycelia formation.

It has been shown previously that HRM was effective in inducing aerial mycelia formation in five strains of *Streptomyces* (Andres et al., 1990). However, none of them was *S. coelicolor* A3(2). Therefore, *S. coelicolor* A3(2) was exposed to HRM to test whether morphological differentiation can be induced. The strain was assayed by an agar diffusion method at HRM concentrations of 0.01 μg per paper disc on Gauze I solid medium. After three days of incubation at 30 ℃, it was observed that white aerial mycelia were produced around the paper disc along with a blue pigment (**Figure 3.83**). However, after five days of growth, the aerial mycelia formed a lawn and covered the whole plate and started producing gray spores. This result suggested that HRM can accelerate aerial mycelia formation in *S. coelicolor* A3(2). To understand the HRM regulatory hierarchy, HRM was subsequently applied to the *bld* mutants derived from *S. coelicolor* A3(2) in a similar manner.

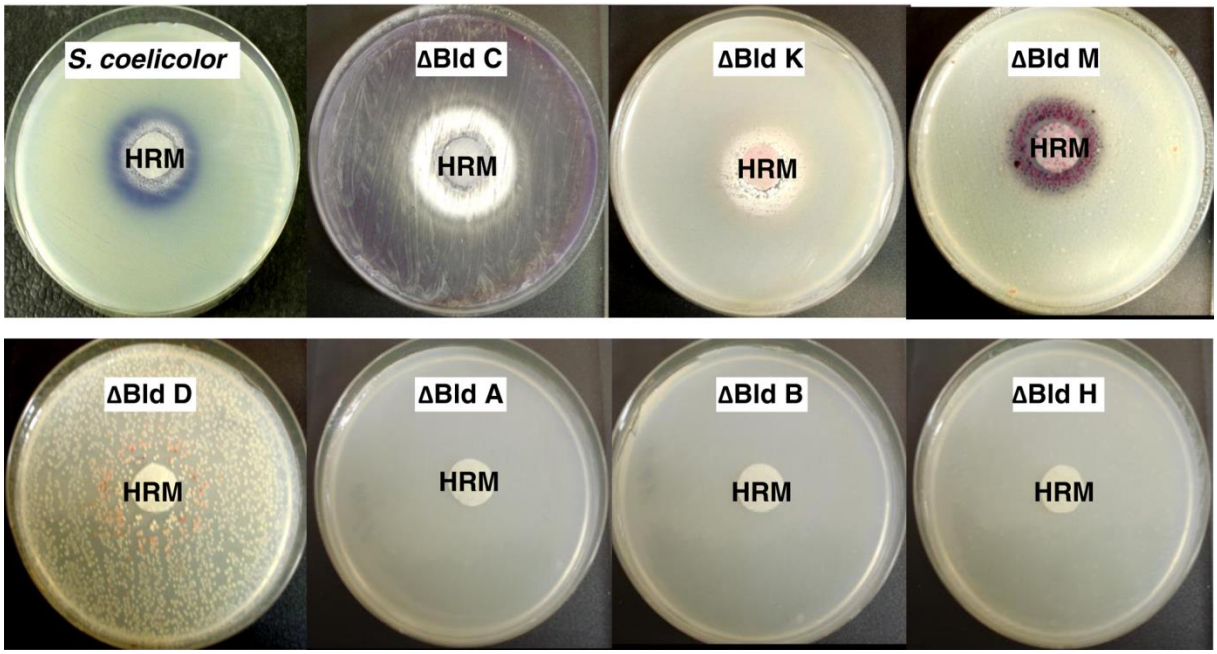

Figure 3.83: HRM hormonal activity assay against *S. coelicolor* A3(2) and its bald mutant derivatives on Gauze I medium plates with 0.01 μg HRM added to each paper disc. J2166 (ΔBldC), NS17 (ΔBldK), *bldM* mutant (ΔBldK), *bldD* mutant (ΔBldD), J1700 (ΔBldA), J669 (ΔBldB), and WC109 (ΔBldH) are the bald mutants derived from *S. coelicolor* A3(2).

Unexpectedly, the results showed that HRM only induced sporulation or pigment formation in J2166 (ΔBldC), NS17 (ΔBldK), and the *bldM* mutant (ΔBldM) and *bldD* mutant (ΔBldD) but not J1700 (ΔbldA), J669 (ΔBldB) and WC109 (ΔBldH) (**Figure 3.83**).

It has been shown previously that goadsporin (GS), a 19-amino-acid polypeptide discovered in *Streptomyces* sp. TP-A0584, could induce sporulation and/or secondary metabolite in 36 *Streptomyces* strains. However, the regulatory mode of action for this compound has not been demonstrated yet. For comparison, GS obtained from Prof. Hiroyasu Onaka at the University of Tokyo was applied to the above mentioned *S. coelicolor* strains in the same way. After incubation for three days, similar results to that of HRM were observed (**Figure 3.84**). The only difference was the speed of aerial mycelia formation, where after three days of growth, the aerial mycelia covered the entire plate, and the surrounding area of the paper disc displayed larger density of aerial mycelia.

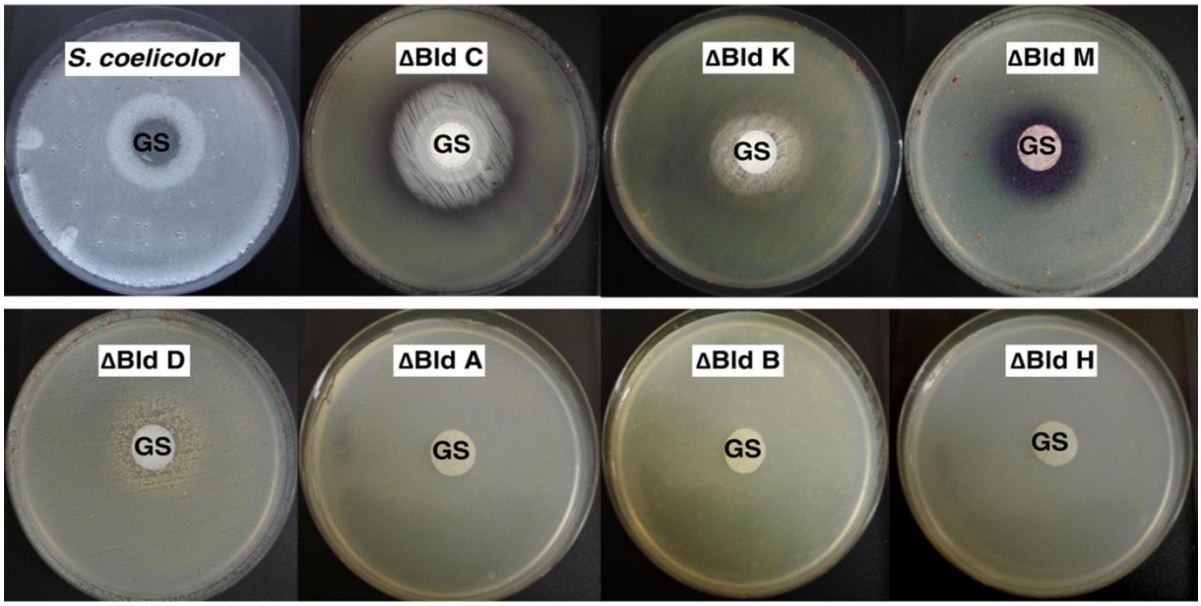

Figure 3.84: GS hormonal activity assay against *S. coelicolor* A3(2) on Gauze I medium plates with 0.01 μg GS added to each paper disc. ΔBldC, K, M, D, A, B, H are bald mutants derived from *S. coelicolor*A3(2).

Aerial mycelium formation in *Streptomyces* spp. commonly relies on the composition of media. Previous studies suggested that *Streptomyces* strains used in the HRM hormonal assay could produce aerial mycelia on poor SY agar abundantly, but nearly failed to form aerial mycelia on

rich SYC agar (Andres et al., 1990). To investigate the HRM hormonal activity, HRM was applied to its own producer, *S. griseoflavus* W-384, grown on SYC agar. It was shown that the aerial mycelia formation of *S. griseoflavus* W-384 was induced by HRM at concentration of 1 μg (**Figure 3.85**). This showed that HRM can induce aerial mycelia formation in not only its producing strain but also the other *Streptomyces* spp., while GS only had such an effect on other *Streptomyces* spp., but not its own producer *S.* sp. TP-A0584 (Onaka et al., 2001).

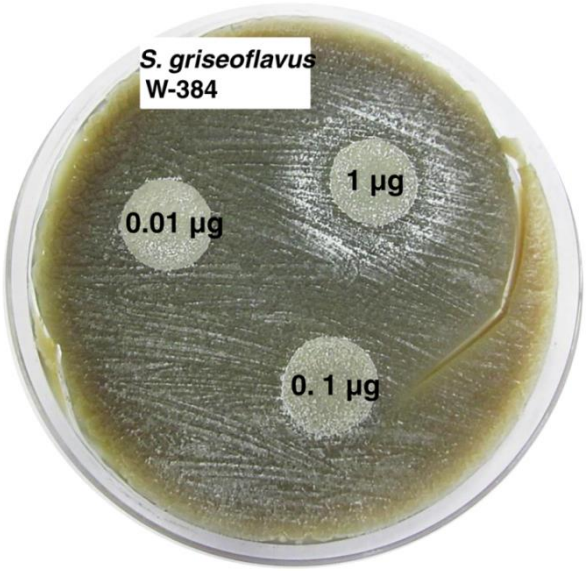

Figure 3.85: Aerial mycelia formation induced by HRM in its own producer, *S. griseoflavus* W-384. The paper discs contained 0.01, 0.1 and 1 μg HRM.

Subsequently, *S. coelicolor* A3(2) along with its mutants were spread on rich SYC plates, and then exposed to HRM and GS with concentrations of 1 μg per disc, respectively. The plates were incubated at 30 ℃ for 7-10 days. It was observed that both HRM and GS could induce aerial mycelia formation and/or secondary metabolites in some of the test strains (**Figure 3.86** and **Figure 3.87**).

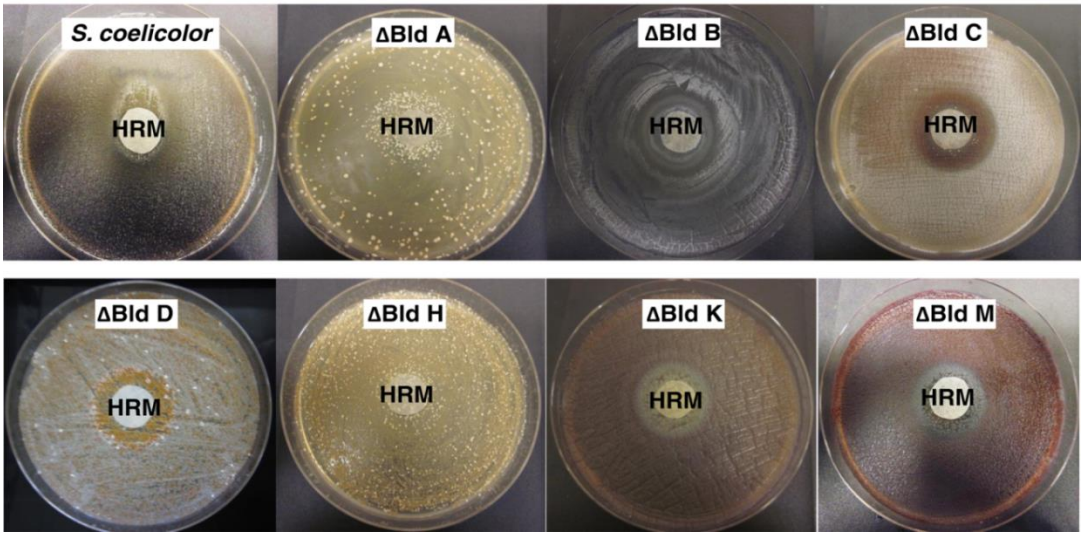

Figure 3.86: Aerial mycelium-inducing activity of HRM in *S. coelicolor* A3(2) and its related mutants on SYC agar plates with 1 μg of HRM added to each paper disc.

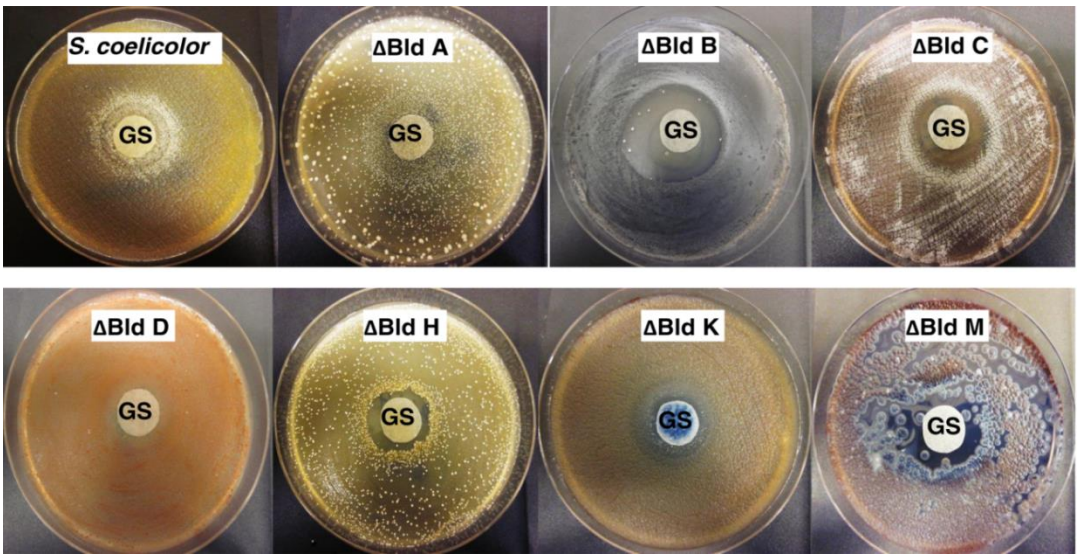

Figure 3.87: Aerial mycelium-inducing activity of GS in *S. coelicolor* A3(2) and its related mutants on SYC agar plates with 1 μg of GS added to each paper disc.

Comparing aerial mycelia-inducing activities of GS and HRM on SYC media with that on Gauze's media, J1700 (ΔbldA), J669 (ΔBldB) and WC109 (ΔBldH) exhibited ring-shaped zones of aerial mycelia surrounding paper discs on SYC plates. However, inhibition zones were shown near the paper discs in several *S. coelicolor* mutant strains with the addition of both GS and HRM, such as J669 (ΔBldB), J2166 (ΔBldC), the *bldD* and *M* null mutants (ΔBldD and M) derived from *S. coelicolor* M600. The results further supported previous observations that formation of aerial mycelia by GS was dose-dependent, effective at less than 1.8 μM (Onaka et

al., 2001). It has been shown that GS inhibited the growth of *S. coelicolor* A3(2) at an MIC of 3.2 μg/mL on Bennett's agar medium (Onaka et al., 2001), while GS induced mycelia formation of *S. coelicolor* A3(2) on an SYC plate at concentration of 1 μg (~60 μM) in the present study. These results indicated that aerial mycelia formation induced by HRM and GS in *Streptomyces* spp. depends on the composition of media as well as the concentrations of HRM and GS.

3.4.2 HRM hormonal assay against *S. griseus* DSM 40236 and *bld* mutants derived from *S. griseus* IFO 13350

Relative to *S. coelicolor*, the signaling pathway involved in aerial mycelia formation in *S. griseus* is well-studied, designated as the A-factor signaling cascade. In this pathway, the hormone-like signaling molecule A-factor binds to its own receptor ArpA, which leads to the activation of AdpA, a global regulator governing the expression of downstream genes responsible for morphological differentiation and secondary metabolism (Horinouchi 2002). Several bald mutants derived from *S. griseus* IFO 13350 were generated in the group of Prof. Horinouchi (Yamazaki 2000; 2003b; 2003a; 2004). In this study, to understand HRM and GS hormonal regulation mechanism, three of these mutants, ΔAdpA, ΔAdsA, and ΔAfsA, obtained from Prof. Horinouchi were assayed along with the wild type strain *S. griseus* DSM 40236. ΔAfsA is unable to synthesize A-factor, which fails to initiate the A-factor signaling cascade for morphogenesis and streptomycin or pigment production. ΔAdpA is a mutant of a global transcriptional activator with an inability to produce aerial mycelia and streptomycin. ΔAdsA is a mutant of AdsA that is required for the formation of aerial mycelia.

Before application of HRM to the mutants derived from *S. griseus* IFO 13350, the concentration of HRM was tested for inducing aerial mycelia formation in *S. griseus* DSM 40236 in a range from 0.1–10 μg per paper disc. After incubation of plates at 30 ℃ for almost 20 days, it was shown that a white aerial mycelia zone was produced around the paper discs at 1 μg and 10 μg (**Figure 3.88**). Compared with the hormonal assay employed with *S. coelicolor*, more HRM was required for inducing aerial mycelia formation in *S. griseus*.

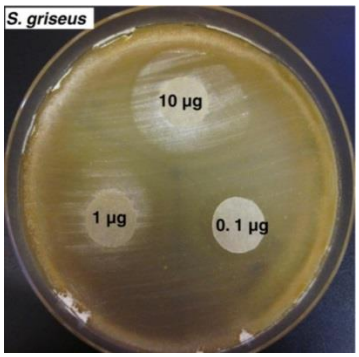

Figure 3.88: Aerial mycelia-inducing activity of HRM in *S. griseus* DSM 40236 on SYC agar medium. The paper discs contained 0.1 μg, 1 μg and 10 μg hormaomycin.

Thus, to obtain distinguishable effects, the mutants related to *S. griseus* IFO 13350 were assayed by application of HRM and GS at concentrations of 10 μg per disc, respectively. After growth of these strains at 30 ℃ for 20 days, it was observed that both HRM and GS could stimulate the ring-shaped aerial mycelia formation in the wild type strain (**Figure 3.89**). During incubation, aerial mycelia zone firstly showed up in *S. griseus* induced by HRM, the density of which was the largest. It seems that HRM is more active than GS in this strain. Moreover, HRM only had effect on one mutant, ΔAdsA, while GS had no influence on any of the mutants.

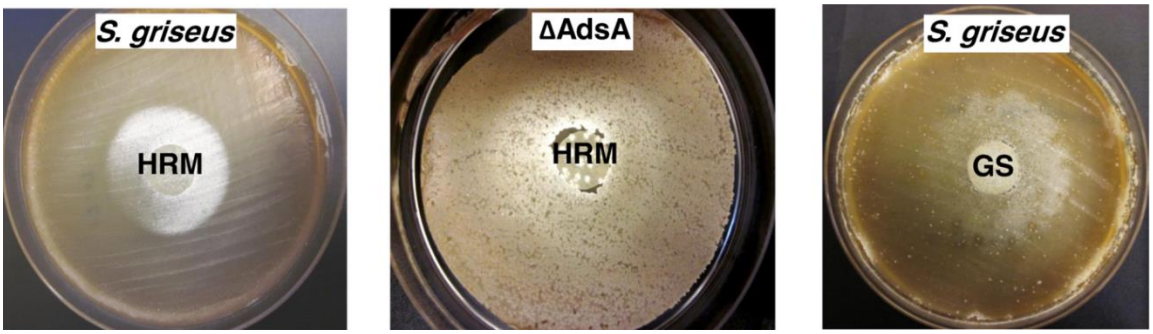

Figure 3.89: Aerial mycelium-inducing activity of HRM and GS in *S. griseus* DSM 40236 and ΔadsA derived from *S. griseus* IFO 13350 with 10 μg of HRM or GS added to each paper disc.

3.4.3 Discussion

The formation of aerial mycelia in *S. coelicolor* is controlled by a regulatory cascade involving products of the *bld* genes (*bldJKLAHGCDM*), which ultimately result in transcription of the *ram* cluster encoding the biosynthesis of SapB. SapB is a biosurfactant lantipeptide that facilitates the emergence of aerial hyphae into the atmosphere from the vegetative mycelium on

rich media. In addition, the hydrophobic chaplins and rodlins secreted around the aerial hyphae play a crucial role in helping aerial hyphae escape into the air (Flärdh and Buttner 2009).

In this study, the regulation mechanism of HRM was investigated to understand the effects of this signal on the morphological differentiation in *Streptomyces* via an aerial mycelium-inducing assay. For the assay applied to *S. coelicolor* A3(2) and its *bld* mutants, HRM was able to induce the aerial mycelia formation in *S. coelicolor* A3(2) and some of its mutants, J2166, K, D, and M on Gauze I medium plates, but failed to stimulate mycelia formation in J1700 (ΔBldA), J669 (ΔBldB) and WC109 (ΔBldH). According to the published hierarchy, if HRM can complement the mycelia formation of ΔBldD or M, the production of aerial mycelia should have been restored in all the other mutants except for ΔBldB. However, HRM showed no effect on formation of aerial hyphae in ΔBldA/H. It has been suggested that ΔBldB results in a global defect in the regulation of carbon utilization, which fails to erect aerial mycelia formation (Pope et al., 1996). This is in partial agreement with the result that HRM cannot induce morphogenesis in ΔBldB. Previous studies illustrated that GS possesses hormone-like activity by promoting aerial mycelia formation in various *Streptomyces*. GS was applied to *S. coelicolor* and its mutants to test whether GS had the same effect as HRM. After cultivation, the assay showed similar results to that of HRM, which indicated that HRM and GS played a similar role in the regulation of aerial mycelia formation although they possess different chemical structures. Nevertheless, how they function in this pathway is still unclear. Since the nutritional status often affects differentiation in *Streptomyces*, rich SYC agar medium was employed to perform the same assay with HRM or GS for inducing aerial mycelium formation. The results showed again that HRM and GS had similar effects on *S. coelicolor* as well as its mutants on SYC agar plates. However, compared to the assay performed on Gauze I media, it was shown that both HRM and GS could induce the aerial mycelia formation or pigment production in all the test strains. The difference between these two media is that SYC contains a rich nitrogen source, like yeast extract and casamino acids. Interestingly, under sufficient nutrition conditions, the synthesis of (p)ppGpp (an intracellular metabolic signal) is induced in the wild type strain that would directly activate the expression

of genes involved in morphological differentiation and antibiotic production. (Hesketh et al., 2007; Hesketh et al., 2001). Therefore, SYC media might have provided sufficient nutrition of nitrogen, amino acids and carbon sources to induce the accumulation of (p)ppGpp and lead to aerial mycelia formation and/or pigment production in all the mutants on some level. When HRM or GS was applied to these mutants at an earlier stage of growth, they promoted rapid growth of aerial mycelia around the paper disc to form an observable zone. Additionally, GS and HRM inhibited the growth of ΔBldB, H, D and M at 1 μg per disc, which suggested that GS and HRM act as a bacterial hormone to promote morphological differentiation and secondary metabolism at very low doses. Previous extracellular complementation studies on the *S. colicolor* mutants were carried out on R2YE. To obtain comparable results and to continue to analyze the regulation mechanisms of HRM and GS in this signaling cascade, the same assay should be performed on R2YE plates in the future.

The morphological differentiation and secondary metabolism in *Streptomyces* spp. is regulated by a complex network involving multiple environmental, intracellular and extracellular factors taking place at different levels. Sometimes, cross-talk occurs between different signaling systems (Galperin 2004; Huang et al., 2005). The present studies provide a basis for further studying HRM's hormonal activity. To deeply understand and elucidate HRM's hormonal mechanism of action, "Click chemistry" will be employed via cycloaddition of azides and acetylenes catalyzed by copper(I). This method has been successfully applied to probe targeted biomolecules of drugs in living organisms (Willand et al., 2010; Deiters et al., 2003; Hong et al., 2010; Anderson et al., 2012). This could allow us to determine the cellular target of HRM using the mutasynthesized alkyne-labeled HRM, HRM A_8, generated in this study. This could be achieved by incubating HRM A_8 with protein extracts from *S. coelicolor* A3(2) or *S. griseus* (hormonal activity), both of which have been completely sequenced (Bentley et al., 2002; Ohnishi et al., 2008). After labeling, HRM-binding proteins can be enriched by conjugating the alkyne moiety to a biotinylated probe, followed by binding to streptavidin beads.

3.5 Investigation for a *trans*-AT PKS-derived polyketide in *S. griseoflavus* W-384

With the growing number of microbial genome sequences available in the public databases, genome mining has been considered as a promising and efficient tool for unraveling the new bioactive metabolites that are encoded by orphan gene clusters or overlooked under standard detection conditions (Winter et al., 2011). This approach has been successfully employed to discover the bioactive natural products in many different organisms, such as, terrequinone A in fungi (Bok et al., 2006), orfamides in pseudomonads (Gross et al., 2007), avermitilol in streptomycetes (Chou et al., 2010), thailandamides in *Burkholderia thailandensis* (Nguyen et al., 2008), and onnamides in yet unculturable bacteria from the complex metagenome of the marine sponge (Piel et al., 2004) (**Figure 1.13**).

The draft genome sequence of *S. griseoflavus* Tü 4000, which is identical to the HRM producer *S. griseoflavus* W-384, was performed by the Broad Institute of MIT and Harvard and is accessible in GenBank (NZ_GG657758.1). In the present study, this genome sequence was further analyzed to search for the product of a newly discovered *trans*-AT PKS gene cluster with unknown function in order to identify the corresponding polyketide via gene inactivation.

3.5.1 Completing the gene sequence of the *trans*-AT PKS gene cluster

An automated antibiotic and Secondary Metabolite Analysis SHell (antiSMASH) search was employed to analyze the secondary metabolite biosynthesis gene clusters (Medema et al., 2011). The results revealed 23 gene clusters, one of which is a putative *trans*-AT PKS gene cluster with 10 sequence gaps (**Figure 3.91**).

Primers were designed starting 50-200 bp away from both sides of these gaps to amplify DNA fragments covering gaps. The PCR products were purified and sequenced (**Figure 3.90**).

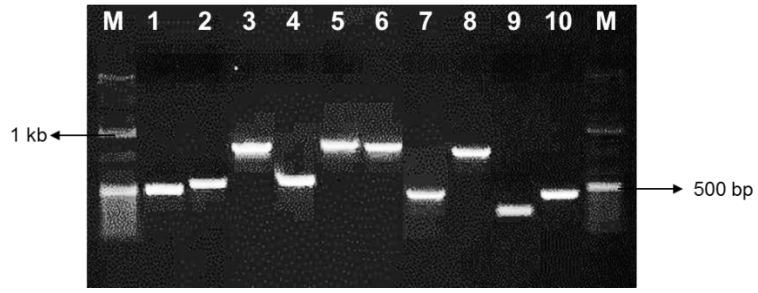

Figure 3.90: Agarose gel analysis of PCR products of ten gaps in *trans*-AT PKS gene cluster for sequencing. Lane M, 100 bp DNA ladder, lanes 1-10, PCR products of gaps 1-10, respectively.

Finally, the complete DNA sequence of this *trans*-AT PKS gene cluster was obtained (**Figure 3.91**), measuring 111.165 kb in length. The entire gene cluster contains 50 open reading frames (ORFs) that were designated as *orf1-orf50*.

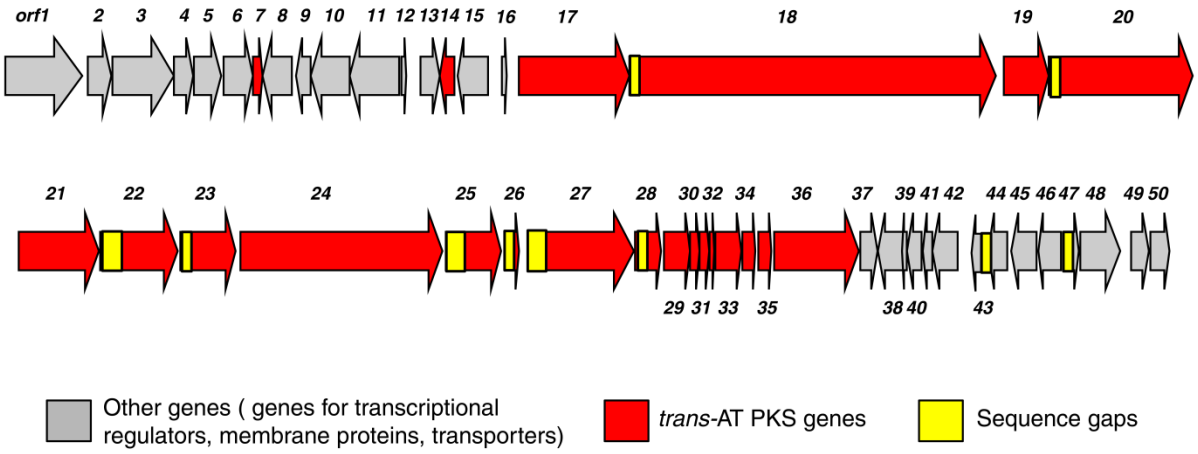

Figure 3.91: The complete genetic map of *trans*-AT PKS gene cluster (~111 kb) from *S. griseoflavus* Tü4000. The gene cluster contains 50 ORFs from *orf1-orf50*.

All the domains in this *trans*-AT PKS were initially analyzed manually and the biosynthetic pathway of the putative polyketide was predicted by Prof. Piel. The data revealed 16 KS domains, 9 KR domains, 14 ACP domains, 2 MT domains, 5 DH domains and one ER domain (**Figure 3.92**). Neither of the PKS modules harbors integral AT domains. The *orf28 gene* was predicted to encode discrete AT domain. The complete gene cluster was analyzed again after covering ten sequence gaps, which resulted in an additional gene that possibly encode a KR domain in Orf21 (**Figure 3.92**).

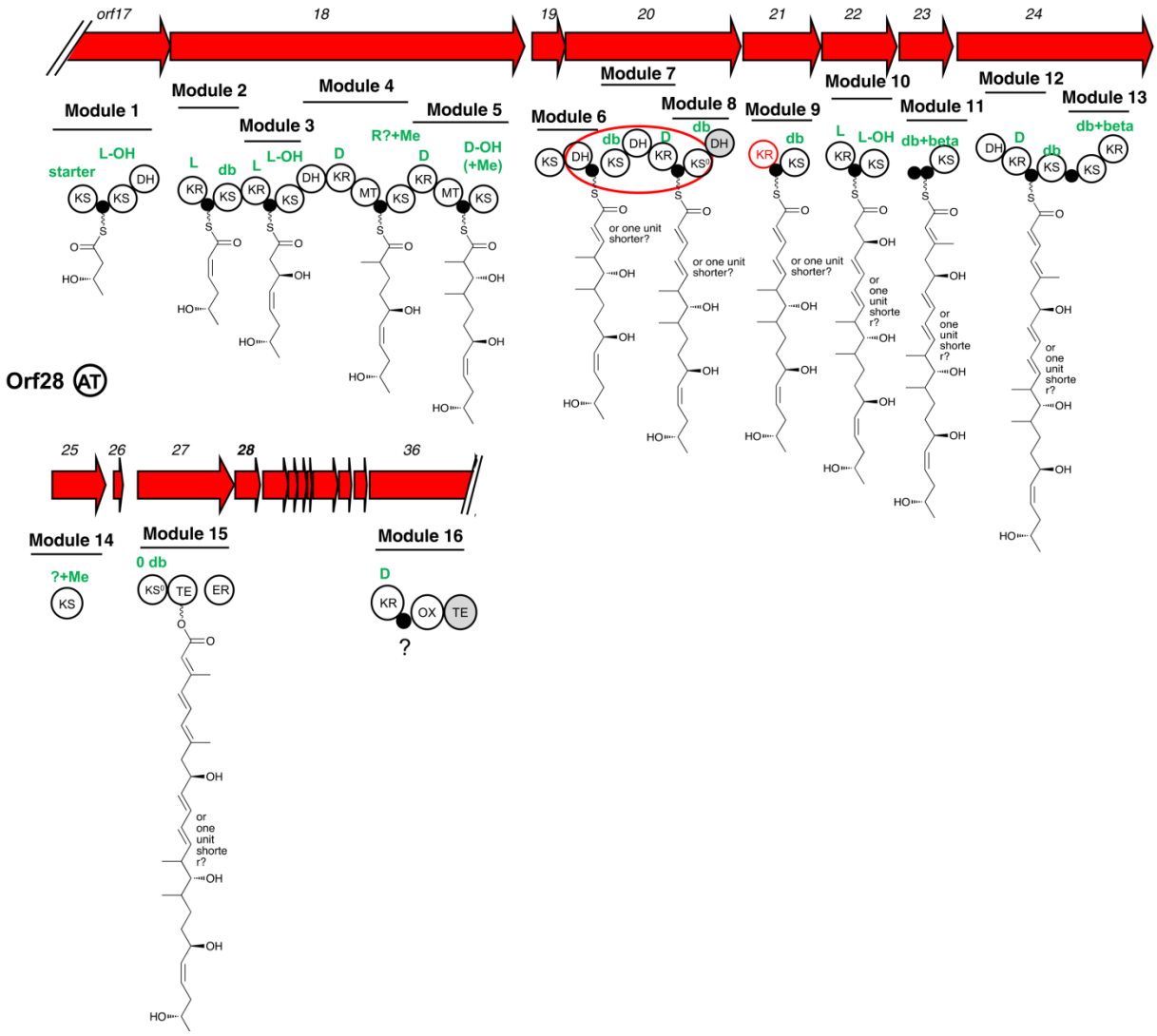

Figure 3.92: The module architecture of the *trans*-AT PKS proteins with their domains and substrate specificity and configuration predicted manually based on phylogenetic analysis by Prof. Piel. The shown intermediates are hypothetical structures based on the predicted substrate specificity of KS domains. **L-OH,** L-configuration of β-OH functionally installed on modules 1, 3 and 10; **D-OH**, D-configuration of β-OH functionally installed on module 5; **D,** KRs contain D configuration motifs. **MT,** responsible for α-methyl branch at the substrate attached to modules 4 and 5; **KS^0,** a KS that is unable to elongate the polyketide chain; **db,** double bond formation; **db + beta,** double bond + beta-branch.

3.5.2 Generation of a *trans*-AT PKS mutant to isolate the potential polyketide

In order to identify the potential *trans*-AT PKS product and assign the functions of genes involved in its biosynthesis, the genes encoding KS domains were chosen to be targets for generation of gene-disruption mutants by a single cross-over strategy.

To increase the efficiency of a single cross-over for attaining potential mutants, the *orf20* gene encoding two PKS modules were targeted to be disrupted. The *orf20* gene was amplified from the genomic DNA of *S. griseoflavus* W-384 using the corresponding primer pair of MFF1-RE/MFR1-RE listed in **Table 4.6**. The resulting DNA fragment was ~8.4 kb, encoding two DH, two ACP and two KS and one KR domains. The PCR fragments were digested with *Hin*dIII and subsequently inserted into pBluescript SK II(+) treated with the same restriction enzyme and end-sequenced. The resulting plasmid was named pXC15. The PKS gene was purified from digestion of pXC15 and ligated into pHZ199 (Hu et al., 1994) to yield pXC16 (**Figure 3.93**).

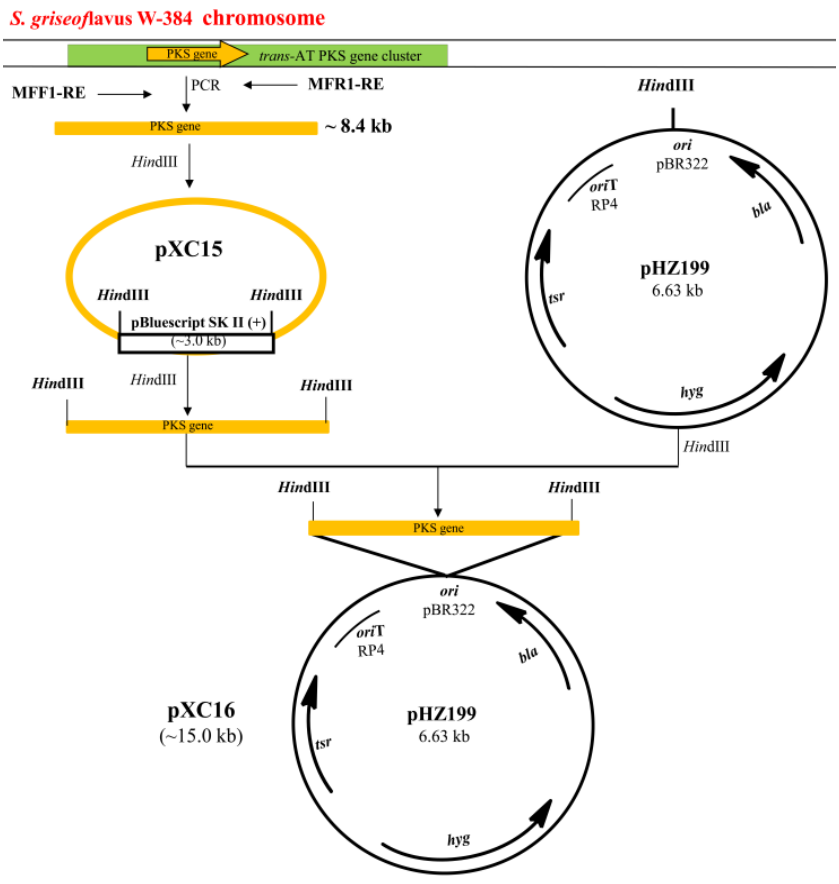

Figure 3.93: The strategy for construction of pXC15 and pXC16 for generation of a *trans*-AT PKS knock-out mutant of *S. griseoflavus* W-384. The ~8.4 kb PCR product was cloned into pBluescript SK II(+) vector to yield pXC15. After verification by sequencing, the PKS gene was purified following digestion of pXC15 with *Hin*dIII and inserted into pHZ199 treated with the same enzyme to obtain pXC16.

The plasmids pXC15 and pXC16 were confirmed by enzymatic digestion before conjugation (**Figure 3.94**).

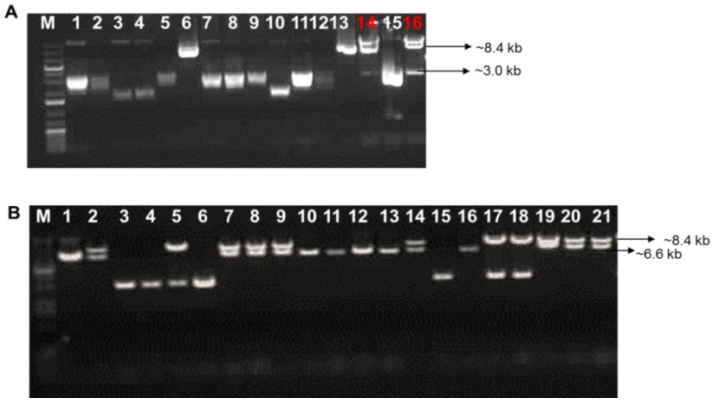

Figure 3.94: Agarose gel analysis of pXC15 and pXC16 by digestion with *Hin*dIII. **A,** screening of *E. coli* DH5α transformants with pXC15; lane M, 1 kb Plus DNA ladder; Clones **14** and **16** were identified with the desired inserts. PKS gene was ~8.4 kb, vector pBluescript SK II(+) was ~3.0 kb. **B,** screening of *E. coli* DH5α transformants of pXC16. Lane M, 1 kb Plus DNA ladder, Clones 7, 8, 9, 14, 19, 20 and 21 were transformants with the expected inserts. pHZ199 is the suicide vector, ~6.6 kb.

The suicide plasmid pXC16 was introduced into *E. coli* ET12567/pUZ8002 for further conjugation into *S. griseoflavus* W-384. Once single cross-over occurs, the suicide plasmid will be integrated into the genome, so that the conjugants will show thiostrepton resistance (**Figure 3.95**). After multiple attempts, a single conjugant was obtained and grown on MS agar plate supplemented with 12.5 μg/mL thiostrepton.

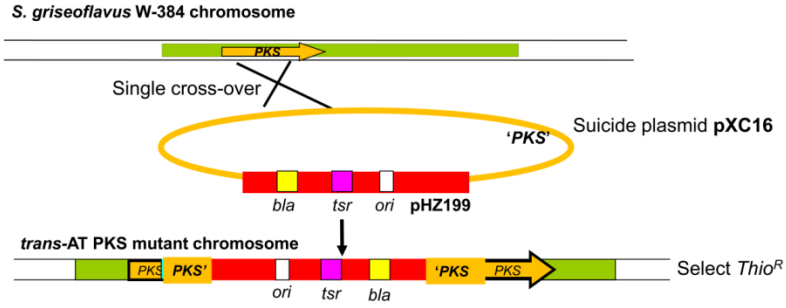

Figure 3.95: The single cross-over strategy. 'PKS' indicates the PKS gene inserted into suicide plasmid pXC16. Once single cross over occurs, the suicide plasmid will integrate into the chromosome of wild type to interrupt the expression of PKS gene and generate two copies of PKS gene. The resulting mutant will exhibit thiostrepton resistance.

The genomic DNA was isolated from the culture of this conjugant and identified by PCR

using the primer pairs XF38F/38R and XF39F/39R for the hygromycin resistance gene (*Hyg*^{R}) and thiostrepton resistance gene (*Thio*^{R}), respectively (**Figure 3.96**). Based on the PCR results, it was suspected that the conjugant obtained was the *trans*-AT PKS mutant.

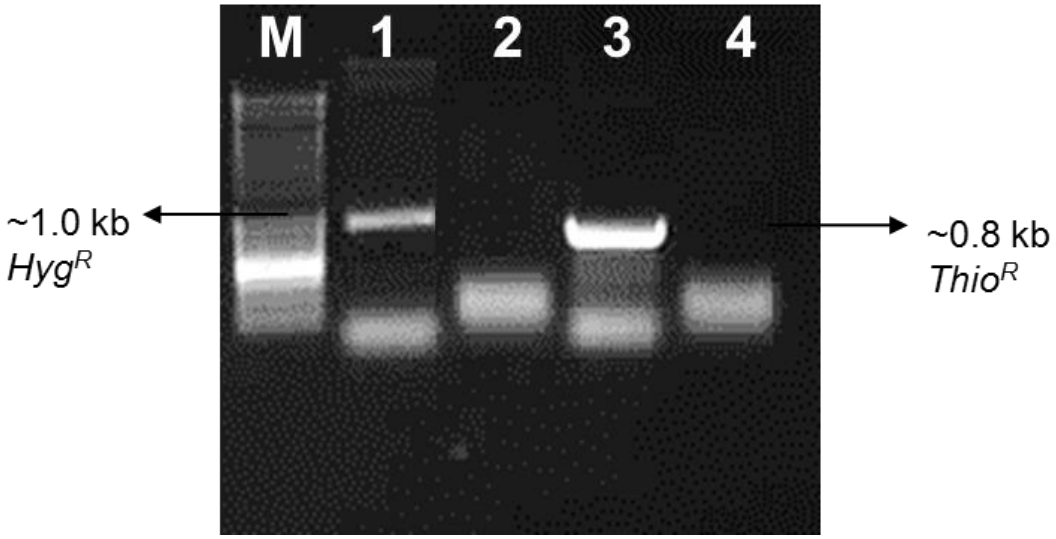

Figure 3.96: Identification of the Δ*trans*-AT PKS candidate by PCR amplification. Lane M, 1 kb DNA ladder; lane 1, *Hyg*^{R} (~1.0 kb)amplified from genomic DNA of the Δ*trans*-AT PKS candidate using the primer pair XF38F/38R; lane 3, *Thio*^{R} (~0.8 kb) amplified from genomic DNA of the Δ*trans*-AT PKS candidate using the primer pair XF39F/39R; lanes 2 and 4, absence of the PCR product amplified from genomic DNA of the WT using the same primer pairs (as negative controls).

The putative *trans*-AT mutant (Δ*trans*-AT PKS) and WT strains were cultivated according to the general fermentation procedure used for *S. griseoflavus* W-384 described in Chapter 4. The culture supernatants from both strains were extracted and analyzed by HPLC. In principle, if the targeted PKS is inactivated, the potential polyketide will be absent in the mutant strain compared to the WT strain. Comparison of HPLC traces from the extracts of Δ*trans*-AT PKS and WT strains showed that one peak (**a**) in the WT strain disappeared (**Figure 3.97**).

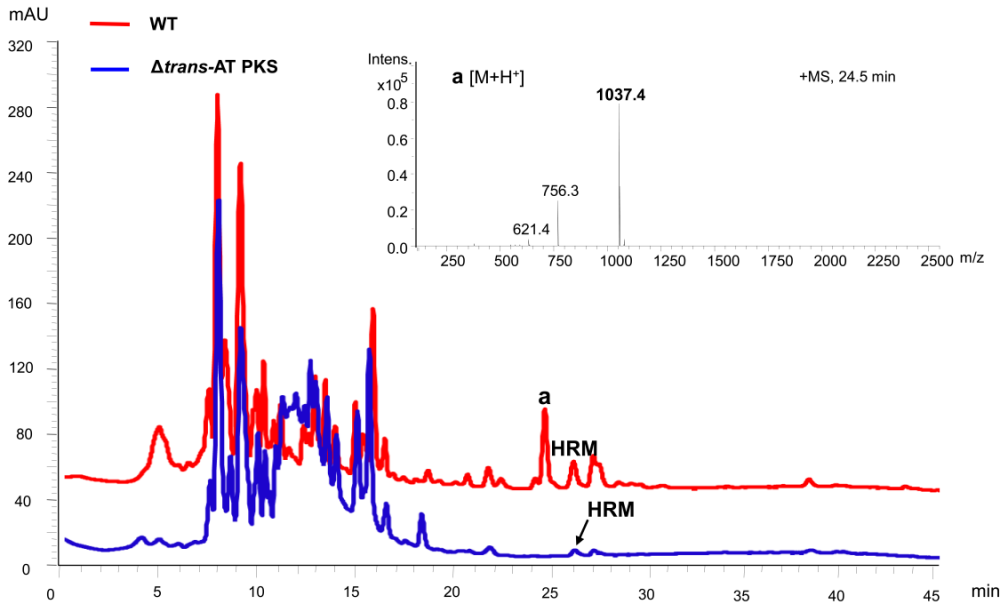

Figure 3.97: Comparison of HPLC traces from extracts of the Δ*trans*-AT PKS and WT. Compound **a,** was present in the the WT strain and absent in the Δ*trans*-AT PKS; **HRM,** produced in both the Δ*trans*-AT PKS and WT. The mass of **a** is 1037.4 Da $[M+H]^+$.

The extracts from the WT and Δ*trans*-AT PKS were also subjected to LC/MS analysis. The result showed compound **a** with a mass of 1037.4 Da $[M+H]^+$. To characterize the structure of compound **a**, 0.5 mg of compound **a** was purified from 1 L fermentation culture of WT by Reiko Ueoka and further structurally elucidated by Dr. Roberta Teta in University of Napoli. The NMR analysis revealed a known cyclic depsipeptide, termed WS9326A, which was also previously isolated from *Streptomyces violaceusniger* No. 9326. WS9326A is a potent tachykinin antagonist and exhibits weak antimicrobial activity (Hashimoto et al., 1992). Its chemical structure is similar to skyllamycin (Pohle et al., 2011) (**Figure 3.98**). The isolation of a peptide based on a presumed PKS knock-out was surprising. It was suspected that the putative Δ*trans*-AT PKS mutant obtained might have been a false positive resulting from the coincidental high sequence similarity with the suicide plasmid. Therefore, the genomic DNA of this putative Δ*trans*-AT PKS was investigated by PCR analysis using the specific primers and Southern blotting. However, neither of these studies showed the expected results. Since the sequence of suicide vector pHZ199 is not available, the position of the integrated region could not be detected in the genomic DNA by sequencing.

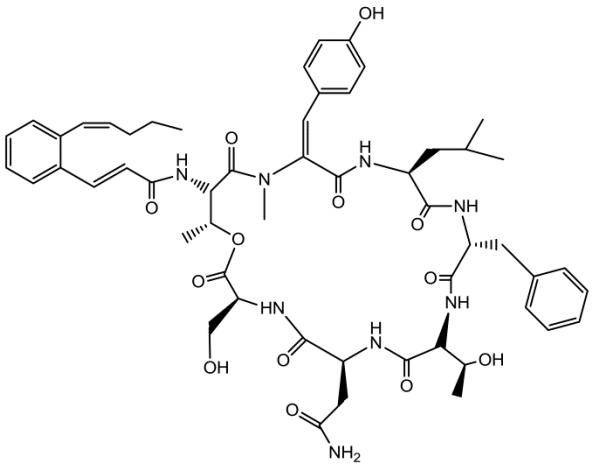

WS9326A
Streptomyces violaceusniger No. 9326

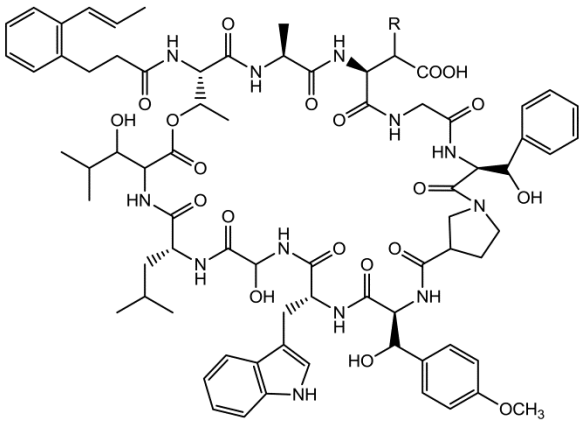

Skyllamycin A R=CH_3
Skyllamycin B R=H
Streptomyces sp. Acta 2897

Figure 3.98: The structure of WS9326 and skyllamycins.

As described above, the PKS gene (*orf20*) targeted in this study encodes two KS, two DH and one KR domains (**Figure 3.92**). To inactive the function of this PKS, four gene fragments were targeted instead of the entire PKS gene. The gene fragments consisted of the DH, ACP in module 6 and KS in module 7 domain-coding regions (~2.1 kb), one (~4.1 kb) encoding the DH, ACP in module 6, and the KS and DH in module 7, one (~1.9 kb) encoding the KR in module 7, and ACP and KS^0 in module 8, the last one (~4.1 kb) encoding the DH and KR in module 7, and the ACP and KS^0 in module 8. These four gene fragments were amplified, referred to as KS_1, KS_1', KS_2 and KS_2', and purified and digested with *Hin*dIII. Then, all of these fragments were individually ligated into pBluescript SK II(+) to obtain pXC32, pXC38, pXC39, pXC40 and end-sequenced independently. Since thiostrepton is not as sensitive as apramycin during screening of *Streptomyces* mutants, the $Thio^R$ of pHZ199 was replaced by the apr^R. The resulting suicide vector was assigned as pXC41 (**Figure 3.99**).

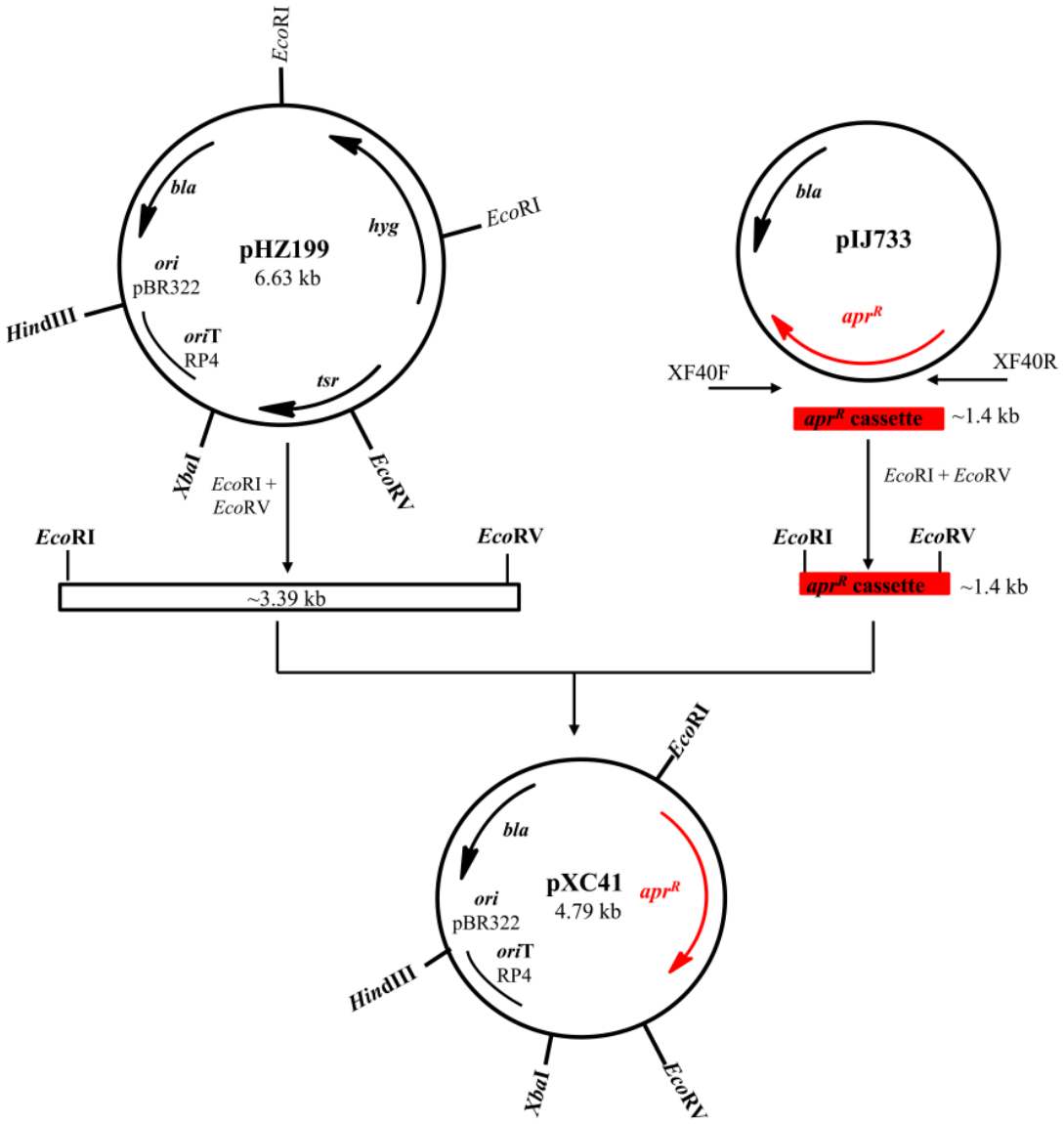

Figure 3.99: The strategy for construction of the new suicide vector pXC41. The plasmid pHZ199 (Hu et al., 1994) was digested with *Eco*RI and *Eco*RV, then the resulting ~3.39 kb DNA fragment was harvested as a new vector backbone with essential functional elements, *bla*, *ori*T, and *ori*. The apramycin resistance cassette (~1.4 kb) was amplified from pIJ733 (Gust et al., 2003), digested by *Eco*RI and *Eco*RV and subsequently inserted into the 3.39 kb vector backbone to give the new suicide vector pXC41 with apr^R instead of $Thio^R$.

The four gene fragments from the corresponding plasmids with correct sequences were purified (**Figure 3.100A**) and inserted into pXC41 to give pXC42, pXC43, pXC44 and pXC45, respectively. These newly obtained suicide plasmids were confirmed by enzymatic digestion with *Eco*RI and *Xba*I. The results showed the expected sizes (**Figure 3.100B** and **C**), suggesting the plasmids were ready for further conjugation.

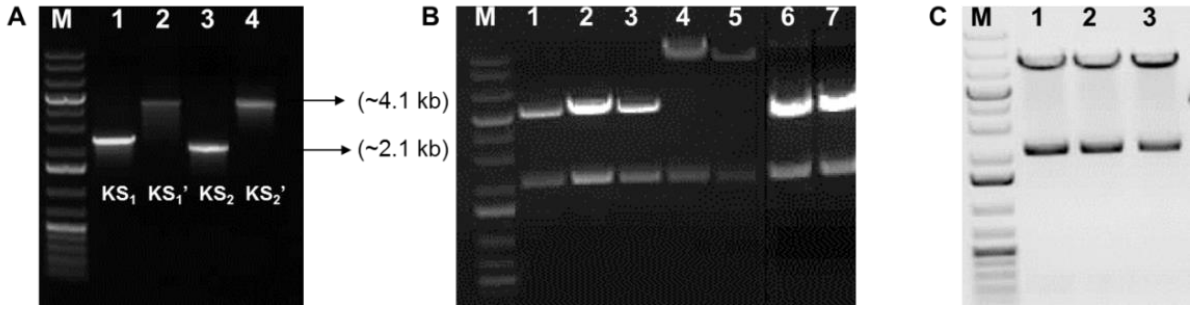

Figure 3.100: Agarose gel analysis of the suicide plasmids by enzymatic digestion. **A,** Lane M, 1 kb Plus DNA ladder; lanes 1-4, The DNA fragments of KS_1, KS_1', KS_2, and KS_2' purified from pXC32, pXC38, pXC39, and pXC40, respectively. **B,** Identification of suicide plasmids by enzymatic digestion with *Eco*RI and *Xba*I. Lane M, 1 kb Plus DNA ladder; lanes 1-3, digestion of pXC42; lanes 4-5, digestion of pXC43; lanes 6-7, digestion of pXC44. **C,** Lane M, 1 kb Plus DNA ladder; lanes 1-3, digestion of pXC45 by *Eco*RI and *Xba*I. After digestion, all the suicide plasmids share the same DNA fragment of ~2.13 kb.

The four suicide plasmids from *E. coli* DH5α were individually transformed into *E. coli* ET12567/pUZ8002. The resulting strains were used for conjugation with *S. griseoflavus* W-384. The conjugation was performed according to the standard procedure. After several days of incubation, a few transformants from pXC42, pXC43 and pXC45 were observed on a MS agar plate supplemented with apramycin and nalidixic acid. A few apramycin resistant transformants were independently inoculated into MS liquid medium with appropriate antibiotics and grown for two days. Their genomic DNA was extracted and analyzed by PCR using specific primers, and that of the WT as a negative control. The specific primers were designed based on the model of expected mutant genome after single cross-over occurring (**Figure 3.101**). For example, one primer pair of KSF2/XCKSR2, the forward primer KSF2 started from upstream of the target KS gene in the WT genomic DNA and the reverse primer XCKSR2 started from the plasmid pXC41; for the other pair, forward primer XCKSF1 started from the plasmid pXC41 and reverse primer XCKSR1 started from downstream of the target KS gene in the WT genomic DNA.

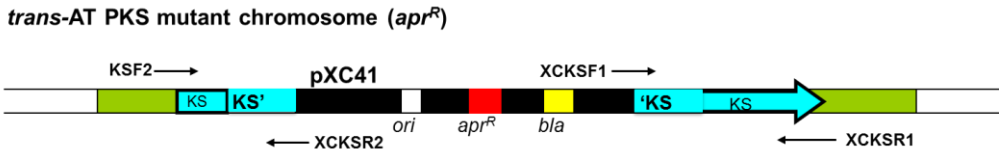

Figure 3.101: The putative *trans*-AT PKS mutant genome derived from pXC45 generated after single cross-over. The plasmid carrying the 'KS' gene which was identical with the target KS gene in the WT genome was integrated into the genome of the WT after single cross-over recombination. The *trans*-AT PKS gene cluster is in green. The pXC41 integrated into the genome is in black with the essential functional elements. The target KS gene in the WT genome was disrupted by pXC45 to bring an additional copy of KS gene.

Unfortunately, there was no expected PCR product amplified from the transformants derived from pXC42, pXC43, except for the apramycin resistance gene. However, there was one transformant generated from pXC45, named W-384/pXC45, which was promising. The PCR products suggested the expected genotype (**Figure 3.102**). To confirm this mutant, the PCR products amplified using the primer pair of XCKSF1/R1 were sequenced. Comparison of the resulting DNA sequence and *trans*-AT gene cluster sequence, revealed that the recombination occurred in the beginning position of the gene for the DH in module 7.

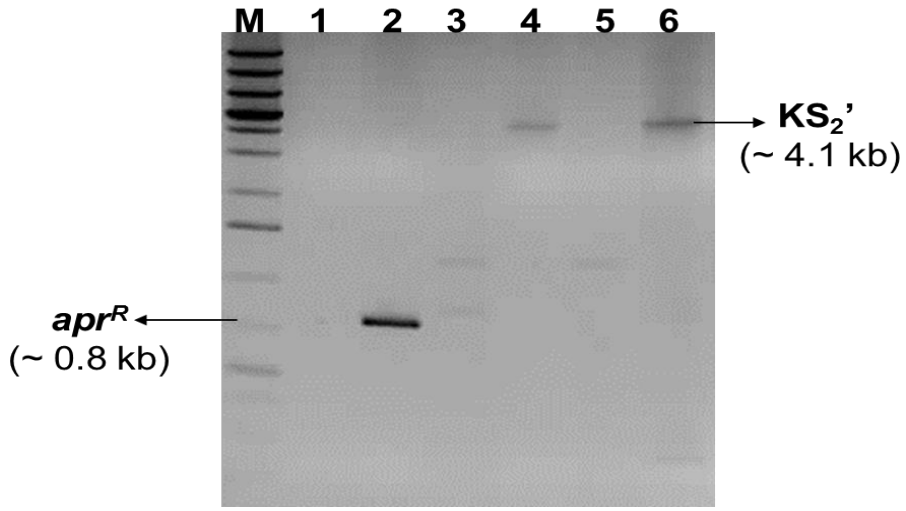

Figure 3.102: Agarose gel analysis of the W-384/pXC45 by PCR amplification. Lane M, 1 kb Plus DNA ladder; lanes 1 and 2, PCR products amplified from the genomic DNA of the WT and W-384/pXC45 using the primer pair XF1F/1R (for the *apr*^{R}); lanes 3 and 4, PCR products amplified from the genomic DNA of the WT and W-384/pXC45 using the primer pair KSF2/XCKSR2 for the KS_2' gene fragment (~4.1 kb); lanes 5 and 6, PCR products amplified from the genomic DNA of the WT and W-384/pXC45 using the primer pair XCKSF1/R1 for the KS_2' gene fragment (~4.1 kb).

The W-384/pXC45 mutant was cultivated along with the WT strain in the MMS media. After

five days of fermentation, the supernatants from their cultures were extracted and analyzed by LC-MS.

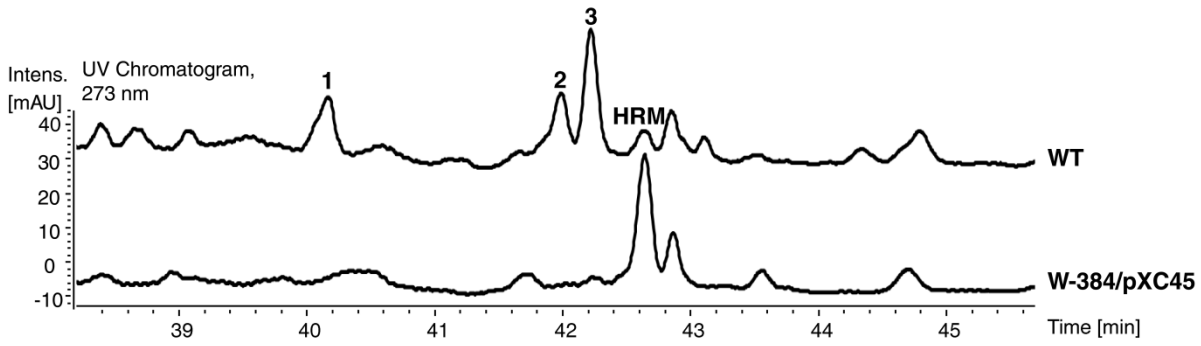

Figure 3.103: Comparison of HPLC traces of the WT and W-384/pXC45 at UV of 273 nm. Compounds **1**, **2** and **3**, were present in the WT at 40.2 min, 42 min and 42.2 min, but absent in W-384/pXC45; **HRM,** was present in the both strains at 42.6 min.

Comparison of the HPLC profiles from LC-MS analysis of the WT and W-384/pXC45 mutant showed that compounds **1, 2** and **3** were absent in W-384/pXC45, which were suspected as putative *trans*-AT PKS-derived polyketides (**Figure 3.103**). The corresponding exact masses of the three compounds were detected. Based on previous structural prediction of this compound by Prof. Piel, the calculated mass of one structural proposal (**Figure 3.92**) or the potential polyketide is ~477.321 Da $[M+H]^+$. Comparison of the exact masses for these three compounds between the WT and W-384/pXC45 showed that the exact masses of 409.210 Da $[M+H]^+$ for compound **2** and 414.273 Da $[M+H]^+$ for compound **3** were obviously observed only in the WT (**Figure 3.104**). Since the exact mass of 414.273 Da $[M+H]^+$ was closer to the mass of the predicted polyketide, compound **3** might be the potential *trans*-AT PKS-derived polyketide. However, these results are still based on preliminary analysis. Further studies need to be carried out to identify the structures.

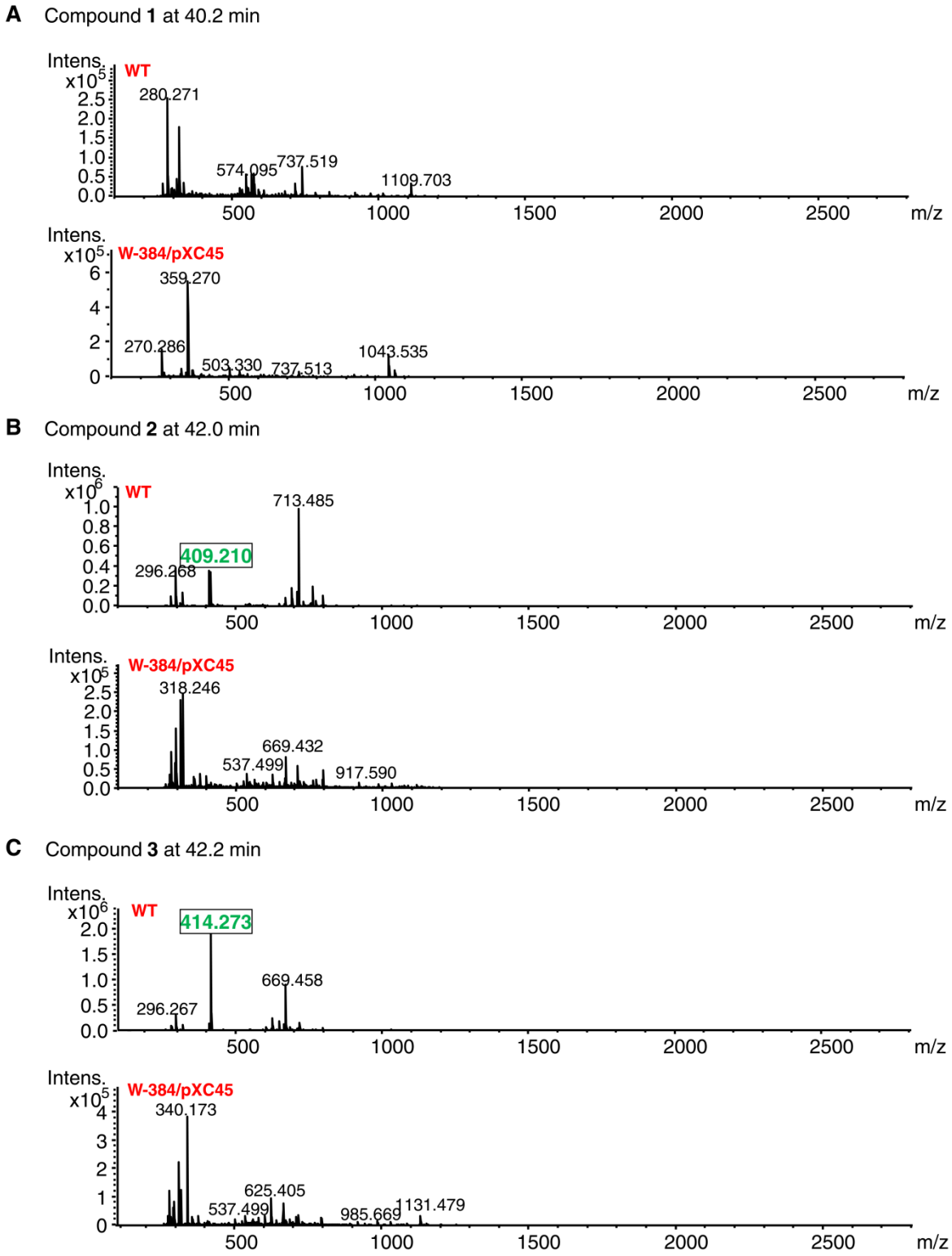

Figure 3.104: Comparison of the exact masses of compounds **1**, **2** and **3** from the LC-MS data of the WT and W-384/pXC45 extracts. A, comparison of the exact mass of the compound **1** at 40.2 min in the WT and W-384/pXC45; B, comparison of the exact mass of the compound **2** at 42.0 min in the WT and W-384/pXC45; C, comparison of the exact mass of the compound **3** at 42.2 min in the WT and W-384/pXC45.

3.5.3 Discussion

Bioinformatic analysis revealed a *trans*-AT PKS gene cluster in the genome of the HRM producer *S. griseoflavus* W-384. In this study, the aim was to identify its corresponding polyketide via a combination of gene knockouts with comparative metabolic profiling. Firstly, ten sequence gaps were closed in the putative *trans*-AT PKS gene cluster in NCBI database by PCR amplification and sequencing. The modular architecture and the substrate specificity and configuration were predicted previously by Prof. Piel via manual basic local alignment search tool (BLAST) search. After completing the entire gene cluster, the PKS genes were further analyzed using the automated antiSMASH to predict the essential functional domains. Compared to previous modular construction predicted by Prof. Piel (**Figure 3.92**), one missing KR domain encoded by *orf21* was found in the module 9.

To isolate the putative polyketide, a PKS gene, *orf20* encoding two KS, two DH, two ACP and one KR was targeted to create *trans*-AT PKS mutant. The results showed that the expected *trans*-AT PKS-derived polyketide was not discovered and a skyllamycin-like cyclic depsipeptide was observed. To further confirm if this mutant possessed the correct genotype, the genomic DNA of this initial *trans*-AT PKS mutant was analyzed by Southern blotting and PCR amplification using the specific primers. Although this mutant exhibits thiostrepton resistance, the single cross-over may have occurred somewhere else in the chromosome of wild type strain, perhaps due to coincidental high sequence similarity with the suicide plasmid.

Many successful examples for construction of gene disrupted mutants via single cross-over were published with less than 1 kb of the internal region of target gene (Sioud et al., 2007; Xiang and Moore 2003), which can make screening work much easier. Therefore, the target PKS gene coding region was reduced from 8.4 kb to 4 kb and 2 kb, respectively. Moreover, given that thiostrepton was not as sensitive as apramycin in previous studies during screening of *S. griseoflavus W-384* mutants, the suicide vector pHZ199 was modified by replacing the $Thio^R$ with an apr^R to generate the new suicide vector pXC41. Similar conjugations were carried out with the newly constructed suicide plasmids, which led to the generation of one

potential *trans*-AT PKS mutant W-384/pXC45. The genotype of this mutant was confirmed by PCR analysis. The metabolic profile of this mutant was compared to that of wild type strain by HPLC, resulting in the detection of three potential candidate compounds. Comparison of the exact masses of the compounds **1**, **2**, and **3** from LC-MS analysis of the WT and W-384/pXC45 extracts indicated that the compound **3** with the exact mass of 414.273 Da $[M+H]^+$, which was only detected in the WT, might be the potential *trans*-AT PKS-derived polyketide due to its mass relatively close to the predicted mass. Since these results were observed in the positive mode for the first LC-ESI MS analysis, to confirm these results, these three compounds need to be isolated and detected by ESI-MS in both positive and negative modes. In addition, the current UV chromatogram was detected at UV of 273 nm which is the optimal wave-length for HRM detection. Therefore, these extracts should be also scanned in a full wave-length range to optimize the UV conditions for better separation of the putative polyketides and to obtain first insights into their chromophore. To further identify and characterize these three candidates, large scale of fermentation of the WT needs to be carried out to obtain sufficient amounts of these three peaks for structural elucidation directly via NMR analysis. Once the polyketide is structurally characterized, not only its biosynthetic pathway can be predicted based on the structure, but also its corresponding biosynthetic gene cluster can be annotated more precisely. Moreover, its bioactivity will be tested further for drug discovery.

3.6 Summary and outlook

HRM is a depsipeptide produced by *S. griseoflavus* W-384. It possesses a remarkable structure bearing chlorine, nitro or cyclopropyl moieties (Andres et al., 1989). HRM exhibits a variety of bioactivities including anticorynebacterial (Andres et al., 1990) and antimalarial (Otoguro et al., 2003). Additionally, it acts as a signaling metabolite that can induce morphological differentiation and increase antibiotic production in other *Streptomyces* spp. (Andres et al., 1990). However, the biosynthetic pathway of HRM and its antibacterial and hormonal mechanism were still largely unknown and were the major interest of this project.

The *hrm* gene cluster was isolated in previous studies (Höfer et al., 2011), allowing us to bioinformatically analyze genes involved in the HRM biosynthesis. However, studies of HRM biosynthesis have been hampered by genetically inefficient manipulation of its producing strain *S. griseoflavus* W-384. In addition, the inconsistent and low production of HRM in the wild type strain has prevented us from investigation of its antibacterial and hormonal mechanism of action.

To solve the problems mentioned above, the first achievement of this project was the establishment of an optimal genetic manipulation system of *S. griseoflavus* W-384 for further molecular analysis of *hrm* genes. With the optimized system in hand, three putative regulatory genes, *hrmA*, *hrmB* and *hrmH* were genetically manipulated, which resulted in the generation of two HRM overproducers. HRM production was increased as much as 135-fold for HrmB overexpression strain. Additionally, six more HRM analogues were obtained from the HrmB overproducer. However, manipulation of *hrmH* by gene knockout, a putative negative regulatory gene, did not increase and abolish HRM production, but led to the isolation of an additional HRM analogue containing a (4-Me)Pro residue instead of (4-Pe)Pro. Overexpression of *hrmH* in *S. griseoflavus* W-384 also did not have an influence on HRM production. It was postulated that HrmH may act as an unusual regulator governing the biosynthesis of (4-Pe)Pro. Investigation of the origin of (4-Me)Pro suggested that (4-Me)Pro was not an intermediate in (4-Pe)Pro biosynthesis and there was no convincing gene candidate from the genome sequence for this building block. Thus, (4-Me)Pro would rather originate from the fermentation medium. Defining the precise mechanism for HrmH as transcriptional, translational, or small-molecule-mediated regulation in HRM biosynthesis will be the focus of future studies.

HRM consists of eight building blocks, some of which are unusual, such as Chpca, (3-Ncp)Ala and (4-Pe)Pro. In this work, to elucidate the HRM biosynthesis, the aim was to identify and analyze the biosynthetic genes involved in these unusual building blocks by gene knock-outs as well as genetic and chemical complementations. The gene knock-out and

genetic complementation of *hrmQ* further proved that HrmQ is a halogenase catalyzing the chlorination of Chpca. The results also showed that *hrmI* and *hrmJ* are essential for the biosynthesis of (3-Ncp)Ala. To further investigate the roles of HrmI and HrmJ *in vitro* during the biosynthesis from L-Lys to (3-Ncp)Ala, soluble HrmI was successfully expressed in *E. coli*, and intitial buffer stability tests were performed in this work. Enzymatic assays of HrmI will be pursued via combination of HrmJ expressed by Dr. Crüsemann in 2012. Manipulation of *hrmD* revealed its indispensable role in the biosynthesis of (4-Pe)Pro. Additionally, an eighth HRM analogue (HRM A_8) was generated by feeding (4-Et)Pro into *hrmD* mutant. HRM A_8 will be further employed to determine the molecular target of antibacterial and hormonal activities by "Click chemistry".

In this work, the new analogues HRM $A_{1\text{-}7}$ document a previously unseen natural plasticity in HRM biosynthesis. All the analogues including HRM A_8 generated by mutasynthesis provided useful SAR data that can aid in the design of non-natural active analogues. In addition, the HRM overproducer will be used for providing sufficient amount of HRM to screen the potential drug candidate and also can be applied to increasing the antibiotic production in other *Streptomyces* spp..

HRM, as a bacterial hormone, can induce the aerial mycelia formation in other *Streptomyces* spp.. To test its hormonal activity and understand the mechanism, in this study, HRM was applied to seven *bld* mutants derived from well-known *S. coelicolor* A3(2) and three "bald" mutants generated from *S. griseus*. The results showed that HRM did induce the mycelia formation of some of the "bald" mutants and all the wild type strains including its producing strain *S. griseoflavus* W-384. However, some *bld* mutants that were expected to form aerial hyphae failed to produce the aerial mycelia after exposure to HRM. Since the HRM hormonal mechanism is still unknown, "Click chemistry" is currently being employed to determine the cellular targets of HRM for its antibacterial and hormonal activities, which eventually will help us to understand how HRM induce the aerial mycelia formation and the antibacterial mode of action.

Bioinformatic analysis revealed a *trans*-AT PKS gene cluster in the genome of *S. griseoflavus* W-384. As a side project of this work, I aimed to identify a *trans*-AT PKS-derived polyketide from *S. griseoflavus* W-384 via genome mining. In this study, the sequence of the *trans*-AT PKS gene cluster was completed. A putative *trans*-AT PKS mutant was generated via single cross-over. The initial comparative metabolic profiling by HPLC between the WT and this mutant showed that three obvious metabolites were absent in the mutant. Due to the structural difference between the polyketide and HRM, the UV wavelength used for detection of these two different compounds is supposed to be different. To further analyze the extracts from these two strains, the detection conditions will be further optimized. The fermentation in a large scale will be carried out to isolate the potential *trans-AT* PKS-derived polyketide and elucidate its structure. Furthermore, the *trans-AT* PKS gene cluster will be annotated according to the structure of this polyketide. With this polyketide and its gene cluster in hand, the bioactivity of this *trans-AT* PKS-derived polyketide will be tested for potential drug candidate and novel natural products could be generated by genetically engineering its biosynthetic pathway.

Chapter 4 Materials and Methods

4.1 Chemicals and materials

Table 4.1: Chemicals and materials used in this study.

Chemicals and materials	source
Agarose	Roth, Karlsruhe
Chemicals for different solution and buffers	Fluka, Seelze
	Merck, Darmstadt
	Roth, Karlsruhe
	Sigma-Aldrich, Seelze
	KMF, Lohmar
DNA and protein ladders	Roth, Karlsruhe
	Fermentas
	Invitrogent, Karlsruhe
dNTPs	Invitrogen, Karlsruhe
Ingredients for all kinds of media	Difco, Detroit, USA
	Merck, Darmstadt
	Oxoid, Wesel
	Roth, Karlsruhe
	Fluka, Seelze
Ni-NTA-Agarose	MACHENREY-NAGEL, Düren
Solvents	Fisher scientific, Schwerte
	Merck, Darmstadt
Hybond N^+ nylonmembranes	Amersham Bioscience, Freiburg
Membrane filters BA 85 (0.2 µm and 0.45 µm)	Schleicher & Schuell, Dassel
3MM Whatman filter paper	Whatman, Maidstone, GB
X-ray film Hyperfilm-MP	Amersham Bioscience, Freiburg

4.2 Enzymes

Table 4.2: Enzymes used in this study.

Enzymes	source
Antarctic phosphatase	NEB, Frankfurt/Main
Expand High Fidelity^{PLUS} PCR System	Roche
Lysozyme	Roth, Karlsruhe
Restriction enzymes	NEB, Frankfurt/Main, Jena Bioscience, Jena
RNase A	Roth, Karlsruhe
T4 DNA ligase	Jena Bioscience, Jena
Taq DNA polymerase	NEB, Frankfurt/Main

4.3 Antibiotics

Table 4.3: Antibiotics used in this study.

Antibiotic	Stock solution (mg/mL)	Solvent	Final conc. (µg/mL)		Source
			Streptomyces spp.	***E. coli***	
Ampicillin	100	Water	-	100	Roth
Apramycin	50	Water	25	50	Sigma
Chloramphenicol	25	Ethonal	-	25	Fluka
Erythromycin	50	Water	25	25	Sigma
Kanamycin	50	Water	25	50	Roth
Nalidixic acid	25	0.3 M NaOH	20	25	Roth
Spectinomycin	50	Water	50	50	Sigma
Streptomycin	25	Water	25	25	Sigma
Thiostrepton	50	DMSO	25	-	AppliChem

4.4 Media

4.4.1 Cultivation media for *Escherichia coli* strains

LB (Luria Broth) (per Liter)

Tryptone	10 g
Yeast extract	5 g
NaCl	10 g
(Agar)	15 g

SOB (per Liter)

Tryptone	20 g
Yeast extract	5 g
NaCl	0.58 g
KCl	0.19 g
After autoclaving, add:	
$MgCl_2.6H_2O$ (1M)	10 mL

$MgSO_4.7H_2O$ (1M)	10 mL

SOC (per Liter)

D-glucose	3.60 g	in **SOB**

TB :

A)

Tryptone	12 g
Yeast extract	24 g
Glycerol	4 mL

Distilled water to **900 mL**, autoclave.

B)

Salt solution (per Liter)

KH_2PO_4 (170 mM)	23.14 g
$K_2HPO_4.3H_2O$ (720 mM)	164.5 g

Autoclaving,

Before using for cultivation, mix **900 mL** of **A** and **100 mL** of **B**

4.4.2 Cultivation media for *Streptomyces* strains

GYM (per Liter)

Glucose	4 g
Yeast extract	4 g
Malt extract	4 g
$CaCO_3$	2 g
Agar	20 g
pH	7.0-7.2

GSY (per Liter)

Soluble starch	2 g

Yeast extract	5 g
NaCl	0.5 g
KNO_3	1 g
K_2HPO_4	0.5 g
$MgSO_4.7H_2O$	0.5 g
$FeSO_4.7H_2O$	0.1 g
Agar	20 g
pH	7.0

YD (per Liter)

Yeast extract	4 g
Maltose	10 g
Glucose	4 g
$MgCl_2$	2 g
$CaCl_2$	1.5 g
Agar	15 g
pH	7.2

Gauze I (per Liter)

Soluble starch	20 g
Yeast extract	5 g
K_2HPO_4	0.5 g
$MgSO_4.7H_2O$	0.5 g
KNO_3	0.5 g
$FeSO_4.7H_2O$	0.01 g
NaCl	0.5 g
Agar	20 g
pH	7.0

R5 (per Liter)

Sucrose	103 g
D-glucose	10 g
$MgCl_2.6\ H_2O$	10.12 g
K_2SO_4	0.25 g
Difco casamino acids	0.1 g
Yeast extract	5 g
Trace element solution	2 mL
TES	5.73 g
Distilled water to	1 L

Divide the solution into 5 × 250 mL flasks, 100ml per each with 2.2 g Difico Bacto Agar. Then close the flasks and autoclave.

After autoclaving , add to each flask in the order list:

KH_2PO_4 (0.5%)	10 mL
$CaCl_2.2H_2O$ (5M)	0.4 mL
L-proline (20%)	1.5 mL
NaOH (1 M) adjust	pH to 7.3

Trace elements solution (per Liter) (used for **R5** medium preparation)

$ZnCl_2$	40 g
$FeCl_2.6H_2O$	200 g
$CuCl_2.2H_2O$	10 g
$MnCl_2$	10 g
$Na_2B_4O_7.10H_2O$	10 g
$(NH_4)_6Mo_7O_4.4H_2O$	10 g

MS (per Liter)

Mannitol	20 g
Soypeptone	20 g

(Agar)	20 g
Tap water	1L

SY (per Liter)

Soluble starch	20 g
Yeast extract	4 g
Agar	20 g
pH	7.0

SYC (per Liter)

Casamino acids 10 g into **SY**

MM (per Liter) (Kieser 2000)

$(NH_4)_2SO_4$	1 g
K_2HPO_4	0.5 g
$MgSO_4.7H_2O$	0.2 g
$FeSO_4.7H_2O$	0.01 g
D-glucose	10 g
Agar	20 g
pH	7.0

YEME (per Liter) (Kieser 2000)

Yeast extract	3 g
Peptone	5 g
Malt extract	3 g
D-glucose	10 g
Sucrose	340 g
After autoclaving, add:	
$MgCl_2.6H_2O$ (2.5 M)	2 mL
Glycine (20%)	25 mL

pH	7.0

MMS (per Liter)

D-mannitol	10 g
Meat extract	20 g
Soypeptone	20 g
NaCl	0.2 g
$ZnSO_4.7H_2O$	0.5 g
Tap water	1 L
pH	7.0

TSB (per Liter)

Oxoid Tryptone Soya Broth powder	30 g

2 × YT (per Liter)

Tryptone	16 g
Yeast extract	10 g
NaCl	5 g

TSBY (per Liter)

Tryptone	30 g
Yeast extract	5 g
Sucrose	10.3 g
pH	7.2

Super YEME (per Liter)

Sucrose	103 g
Difco yeast extract	3 g
Difco Bacto-peptone	5 g

Amino acid mixture	10 mL
Glucose	10 g
$MgCl_2.6H_2O$	1.1 g
Glycine	5 g
Cystine	0.075 g
pH	7.2

Amino acid mixture (per Liter) (used for **Super YEME** medium preparation)

Proline	0.75 g
Arginine	0.75 g
Histidine	1 g
Uracil	0.15 g

SGGP (per Liter)

Peptone	4 g
Yeast extract	4 g
Casamino acid	4 g
Glycine	2 g
$MgSO_4 \cdot 7H_2O$	0.5 g
H_2O	960 mL
pH	7.2
After autoclaving, add:	
Glucose (50%)	20 mL
KH_2PO_4 (0.5 M)	20 mL

4.5 Buffers

4.5.1 Buffers for plasmid isolation

Buffer I

Tris-HCl (pH 8.0)	50 mM
EDTA	10 mM
RNase A	100 μg/mL

Buffer II

NaOH	200 mM
SDS	1%

Buffer III

Potassium acetate	3 M (pH 5.5)

4.5.2 Buffers for protoplast transformation

P buffer

Sucrose	103 g
K_2SO_4	0.25 g
$MgCl_2.6H_2O$	2.02 g
Trace element solution	2 mL
Distilled water to	800 mL

Dispense in 80 mL aliquots and autoclave. Before using, add to each flask in order:

KH_2PO_4 (0.5%)	1 mL
$CaCl_2.2H_2O$ (3.68%)	10 mL
TES buffer (5.73%, adjusted to pH7.2)	10 mL

4.5.3 Buffers for protein purification

Lysis buffer (per Liter)

$NaH_2PO_4.2H_2O$	50 mM
NaCl	300 mM
Imidazole	10 mM
Glycerol	100 mL
pH	8.0

Washing buffer I (per Liter)

$NaH_2PO_4.2H_2O$	50 mM
NaCl	300 mM
Imidazole	20 mM
Glycerol	100 mL
pH	8.0

Washing buffer II (per Liter)

$NaH_2PO_4.2H_2O$	50 mM
NaCl	300 mM
Imidazole	40 mM
Glycerol	100 mL
pH	8.0

Elution buffer (per Liter)

$NaH_2PO_4.2H_2O$	50 mM
NaCl	300 mM
Imidazole	250 mM
Glycerol	100 mL
pH	8.0

10 × Running buffer (per Liter)

Tris-base	30.28 g
Glycine	187.7 g
SDS	10 g

Destaining solution (per Liter)

Methanol	250 mL
Acetic acid	100 mL

Protein gel loading dye (2 ×)

Tris-HCl (pH 6.8)	0.09 M
Glycerol	20%
SDS	2%
Bromophenol blue	0.1 M
DDT	0.02%

4.5.4 Buffers for preparation of genomic DNA from *Streptomyces* strains

STE buffer

NaCl	75 mM
EDTA	25 mM
Tris	20 mM
pH	7.5

TE buffer (Sambrook 2001)

Tris	10 mM
EDTA	1 mM
pH	8.0

4.5.5 Buffers for agarose gel electrophoresis of DNA fragments (Sambrook 2001)

DNA loading buffer (10 × per Liter)

Sucrose	500 g
EDTA (pH 8.0)	160 mM
Bromophenol Blue	0.5 g
Xylene cyanol	0.5 g

TAE buffer (50 × per Liter)

Tris	242 g
Glacial acetic acid	57.1 mL
EDTA (pH 8.0)	100 mL

4.5.6 Buffers for DNA-DNA hybridization

-Southern Blotting:

Depurination buffer

HCl	2.5 N
Autoclave	

Denaturing buffer

NaOH	0.5 N
NaCl	1.5 M
Autoclave	

Neutralization buffer

Tris-HCl (pH 8.0)	1 M
NaCl	1.5 M
Autoclave	

Transfer buffer (20 × SSC per Liter)

NaCl	175.3 g
Na_3Citrate	88.2 g
pH	7.0
Autoclave	

-Colony *in situ* hybridization:

Lysis buffer (per Liter)

SDS	100 g

-Washing buffer:

Wash solution I (2 × per Liter)

SSC (20 ×)	200 mL
SDS (10%)	10 mL

Wash solution II (0.5 × per Liter)

SSC (20 ×)	25 mL
SDS (10%)	10 mL

Maleic Acid buffer (per Liter)

Maleic Acid	11.607 g
NaOH	7.88 g
NaCl	8.77 g
pH	7.5
Autoclave	

Washing buffer (per Liter)

Maleic acid buffer (pH 7.5)	997 mL

Tween-20	3 mL
Autoclave	

Detection buffer (5 ×)

Tris-HCl	0.5 M
NaCl	0.5 M
pH	9.5
Autoclave	

4.6 Strains, plasmids and primers

4.6.1 Strains

Table 4.4: Strains used in this study.

Strain	Relevant Genotype	Reference/Strain No.
Escherichia coli		
DH5α	*recA endA supE44 hsdR17*	(Hanahan 1983)
ET12567/pUZ8002	*recF dam*$^{-}$ *dcm*$^{-}$ *Cml*^{R} *Str*^{R} *Tet*^{R} *Km*^{R}	(Gust et al., 2003)
BW25113	K12 derivative: *⊿araBAD, ⊿rhaBAD*	(Gust et al., 2003)
XL1-Blue	*endA1 gyrA96*(*nalR*) *thi-1 recA1 relA1 lac hsdR17*	Stratagene, Heidelberg
BL21(DE)	F-, *ompT*, *hsd*S (rBB-mB-), *gal*, *dcm* (DE3)	(Studier et al., 1990)
Arthrobacter crystallopoietes ATCC15481	G^{+}, coryneform bacteria hormaomycin bioassay test	(Andres et al., 1990)
Streptomyces coelicolor		
A(3)2	wild type	(Hopwood 1967)
J1700	*bldA* null mutant (ΔBldA)	John Innes Center
J669	*bld*B43 *aga*A1 *cys*D18 *mth*B2 (ΔBldB)	John Innes Center
J2166	M600 *bldC* null mutant in frame	John Innes Center
ΔBldD	M600 *bldD* null mutant in frame	John Innes Center
WC109	*bldH* null mutant (ΔBldH)	John Innes Center
NS17	*bldK* null mutant (ΔBldK)	John Innes Center
ΔBldM	M600 *bldM* in frame apramycin resistant	John Innes Center

Strain	Relevant Genotype	Reference/Strain No.
Streptomyces griseus		
subsp. *griseus*	streptomycin wild producer	DSM 40236
ΔAfsA (IFO 13350)	no aerial mycelia formation and loss of A-factor productivity	Prof. Horinouchi
ΔAdpA (IFO 13350)	no aerial mycelia formation and streptomycin production	Prof. Horinouchi
ΔAdsA (IFO 13350)	no aerial mycelia but with streptomycin production or pigment production	Prof. Horinouchi
Streptomyces lincolnensis NRRL2936	lincomycin wild producer	(Mason et al., 1963)
Streptomyces griseoflavus		
W-384	hormaomycin wild producer	Prof. Zeeck
ΔC	*hrmC* knockout, apr^R	This study
ΔD	*hrmD* knockout, apr^R	This study
ΔH	*hrmH* knockout, apr^R	This study
ΔI	*hrmI* knockout, apr^R	This study
ΔJ	*hrmJ* knockout, apr^R	This study
ΔN	*hrmN* knockout, apr^R	This study
ΔQ	*hrmQ* knockout, apr^R	This study
ΔC/HrmB	HrmB overexpression in ΔC, apr^R, tsr^R	This study
ΔD/HrmB	HrmB overexpression in ΔD, apr^R, tsr^R	This study
ΔH/HrmB	HrmB overexpression in ΔH, apr^R, tsr^R	This study
ΔI/HrmB	HrmB overexpression in ΔI, apr^R, tsr^R	This study
ΔJ/HrmB	HrmB overexpression in ΔJ, apr^R, tsr^R	This study
ΔN/HrmB	HrmB overexpression in ΔN, apr^R, tsr^R	This study
ΔQ/HrmB	HrmB overexpression in ΔQ, apr^R, tsr^R	This study
XC1	HrmA overexpression in *S. griseoflavus* W-384, apr^R	This study
XC2	HrmB overexpression in *S. griseoflavus* W-384, apr^R	This study
ΔQ/HrmB	HrmB overexpression in ΔQ, apr^R, tsr^R	This study
XC3	HrmA and HrmB overexpression in wild producer, apr^R, tsr^R	This study
ΔD/HrmD	HrmD expression in ΔD, apr^R, tsr^R	This study
ΔH/HrmH	HrmH expression in ΔH, apr^R, tsr^R	This study
ΔI/HrmI	HrmI expression in ΔI, apr^R, tsr^R	This study
ΔJ/HrmJ	HrmJ expression in ΔJ, apr^R, tsr^R	This study
ΔQ/HrmQ	HrmQ expression in ΔQ, apr^R, tsr^R	This study

Strain	Relevant Genotype	Reference/Strain No.
DSM: Deutsche Sammlung von Mikroorganismen und Zellkulturen, NRRL: Northern Regional Research Laboratories.		

4.6.2 Plasmids

Table 4.5: Plasmids used in this study.

Cosmid/Plasmid	Description	References
pHR6G10	pWEB based cosmid with part of *hrm* gene cluster (*hrmA-hrmO*)	(Höfer et al., 2011)
pHR1F4	pWEB based cosmid with part of *hrm* gene cluster (*hrmO-hrmW*)	(Höfer et al., 2011)
pSET152	5.5 kb, *aac(3)IV*, *oriT*, *int*, *attp* pUC18	(Bierman 1992)
pHZ199	6.6 kb, *tsr, bla, hyg, oriT*, pUC18	(Hu et al., 1994)
pIJ773	4.3 kb, *aac(3)IV, bla, oriT* RK2, FRT	(Gust et al., 2003)
pWHM4*	7.9 kb, *permE*, lacZa, tsr, bla*	(Matseliukh 2001)
pHZ1358	11 kb, *bla, neo, SV40 ori,cosE1 oriT*	(Kieser 2000)
pGEM easy	3.0 kb, *bla*, *f1 ori*, *lacZ*	Promega
pET28b	5.4 kb, km^R, *f1 ori*,pBR322 *ori*, C and N terminal His− tag	Novagen
pET29b	5.4 kb, km^R , *f1 ori* , T7 Promoter, MCS, *lacI*, C Terminal His−Tag, N Terminal S−Tag	Novagen
pXC1	3.8 kb, *aac(3)IV*, pBluescript SK II(+)	This study
pXC2	5.0 kb, 2.1 kb of *hrmH* left arm ligated to pBluescript SK II(+)	This study
pXC3	5.0 kb, 2.1 kb of *hrmH* right arm ligated to pBluescript SK II(+)	This study
pXC4	7.3 kb, left arm plus right arm of *hrmH* ligated to pBluescript SK II(+)	This study
pXC5	8.2 kb, left arm plus right arm of *hrmH* with apr^R in between ligated to pBluescript SK II(+)	This study
pXC6	10 kb, *hrmH* suicide plasmid, pDH5	This study
pXC7	3.85 kb, *lmbX* (0.85 kb) ligated to pBluescript SK II(+)	This study
pXC8	16.8 kb, *hrmH* suicide plasmid, pHZ1358	This study
pXC9	12.5 kb, *hrmH* suicide plasmid, pHZ199	This study
pXC10	8.9 kb, tsr^R replaceb by apr^R, in pWHM4*	This study
pXC11	3.5 kb, *hrmB* (0.6 kb) ligated to pBluescript SK II(+)	This study
pXC12	4.0 kb, *hrmA* (1.0 kb) ligated to pBluescript SK II(+)	This study
pXC13	9.5 kb, *hrmB* (0.6 kb) ligated to pXC10	This study
pXC14	10 kb, *hrmA* (1.0 kb) ligated to pXC10	This study
pXC15	11.3 kb, *orf20* (8.4 kb) from *trans*-AT PKS gene cluster of *S. griseoflavus* W-384 genome ligated to pBluescript SK II(+)	This study

Cosmid/Plasmid	Description	References
pXC16	15.5 kb, *orf20* (8.4 kb) from *trans*-AT PKS gene cluster of *S. griseoflavus* W-384 genome ligated to pHZ199	This study
pXC17	3.9 kb, *hrmC* (1.08 kb) ligated to pBluescript SK II (+)	This study
pXC18	3.8 kb, *hrmD* (0.9 kb) ligated to pBluescript SK II (+)	This study
pXC19	3.4 kb, *hrmH* (0.4 kb) ligated to pBluescript SK II (+)	This study
pXC20	4.0 kb, *hrmI* (1.053 kb) ligated to pBluescript SK II (+)	This study
pXC21	3.7 kb, *hrmJ* (0.7 kb) ligated to pBluescript SK II (+)	This study
pXC22	4.1 kb, *hrmN* (1.17 kb) ligated to pBluescript SK I I(+)	This study
pXC23	4.4 kb, *hrmQ* (1.4 kb) ligated to pBluescript SK II (+)	This study
pXC24	9.0 kb, *hrmC* (1.08 kb) ligated to pWHM4*	This study
pXC25	8.8 kb, *hrmD* (0.9 kb) ligated to pWHM4*	This study
pXC26	8.3 kb, *hrmH* (0.4 kb) ligated to pWHM4*	This study
pXC27	8.9 kb, *hrmI* (1.053 kb) ligated to pWHM4*	This study
pXC28	8.6 kb, *hrmJ* (0.7 kb) ligated to pWHM4*	This study
pXC29	9.1 kb, *hrmN* (1.17 kb) ligated to pWHM4*	This study
pXC30	9.4 kb, *hrmQ* (1.4 kb) ligated to pWHM4*	This study
pXC31	8.5 kb, *hrmB* (0.6 kb) ligated to pWHM4*	This study
pXC32	5.1 kb, ~2.1 kb DNA containing the first KS domain coding gene in *orf20* (8.4 kb) in *trans*-AT PKS gene cluster of *S. griseoflavus* W-384 genome ligated to pBluescript SK II(+)	This study
pXC35A	4.05 kb, *hrmI* with stop codon ligated to pGEM easy	This study
pXC35B	4.05 kb, *hrmI* with stop codon ligated to pGEM easy	This study
pXC36	6.4 kb, *hrmI* with stop codon ligated to pET28b(+)	This study
pXC37	6.4 kb, *hrmI* without stop codon ligated to pET29b(+)	This study
pXC38	9.1 kb, ~4.1 kb DNA containing the first KS domain coding gene in *orf20* (8.4 kb) in *trans*-AT PKS gene cluster of *S. griseoflavus* W-384 genome ligated to pBluescript SK II(+)	This study
pXC39	4.9 kb, ~1.9 kb DNA containing the second KS domain coding gene in *orf20* in *trans*-AT PKS gene cluster of *S. griseoflavus* W-384 genome ligated to pBluescript SK II(+)	This study
pXC40	9.1 kb, ~4.1 kb DNA containing the second KS domain coding gene in *orf20* (8.4 kb) in *trans*-AT PKS gene cluster of *S. griseoflavus* W-384 genome ligated to pBluescript SK II(+)	This study
pXC41	4.8 kb,$Thio^R$ replaced by apr^R, in pHZ199	This study
pXC42	6.9 kb, ~2.1 kb DNA containing the first KS domain coding gene in *orf20* in *trans*-AT PKS gene cluster of *S. griseoflavus* W-384 genome ligated to pXC41	This study

Cosmid/Plasmid	Description	References
pXC43	8.9 kb, ~4.1 kb DNA containing the first KS domain coding gene in *orf20* in *trans*-AT PKS gene cluster of *S. griseoflavus* W-384 genome ligated to pXC41	This study
pXC44	6.7 kb, ~1.9 kb DNA containing the second KS domain coding gene in *orf20* in *trans*-AT PKS gene cluster of *S. griseoflavus* W-384 genome ligated to pXC41	This study
pXC45	11.5 kb, ~4.1 kb DNA containing the second KS domain coding gene in *orf20* in *trans*-AT PKS gene cluster of *S. griseoflavus* W-384 genome ligated to pXC41	This study

4.6.3 Primers

Table 4.6: Primers used in this study.

Primer Name	Target Gene	Sequence
XF1F	*apr*^{R} (~0.8 kb)	5' –GCTCTAGAGTGCAATACGAATGGCGAAAAGCCG– 3'
XF1R		5' –TCCCCGCGGGCTCTAGATCAGCCAATCGACTGGCG– 3'
XF2F	left arm of *hrmH*	5' –CCCAAGCTTGGGCGAGAGAATGATCGGTTC– 3'
XF2R		5' –GCTCTAGACCTGTCCTCCCCA ACA AGTGAC– 3'
XF3F	right arm of *hrmH*	5'-GCTCTAGATACCGGATCCGTTGCAGGAAAAACCTCC TGAGAATC– 3'
XF3R		5' –ATAAGAATGCGGCCGCCCCAAGCTTGGGGTTCCCCG GCGTCGAGC– 3'
XF6F	*lmbX*	5' –GGAATTCATGATCGTGGTCCCGTTC– 3'
XF6R		5' –CCCAAGCTTCTACACGGAAGCGACCGC– 3'
XF9F	*apr*^{R} cassette (~1.4 kb)	5' –CCATCGATCTGACGCCGTTGGATACACCAG– 3'
XF9R		5' –CCGGATATCTTAGCCAATCGACTGGCGAGCG– 3'
XF10F	*hrmA*	5' – GCTCTAGAGGGGACTCATGAACCGGGCCC– 3'
XF10R		5' – GGAATTCTCAGGCCGACGGGGTAGGGC– 3'
XF11F	*hrmB*	5' –CAAGCTTTTAATTAAGGAGGAGGAACACCATGACC ACCTAC– 3'
XF11R		5' –GGAATTCTCAAACCGCTCTGTCGAGAAC– 3'
XF12F	*apr*^{R} cassette for *hrmC* replacement	5' –TTGCTGACGTCAACCATCGGAAGAGGTTGTAACGC TGTGA TTCCGGGGATCCGTCGACC– 3'
XF12R		5' –GCCGTTCCGGCAGGATCACCACTCCGACGCGCA CGCTCAT GTAGGCTGGAGCTGCTTC– 3'
XF13F	*apr*^{R} cassette for *hrmD* replacement	5' –CTTCTACGACCTCGCACCGGCCGCGGAGGAC TGAGCGTGATTCCGGGGATCCGTCGACC– 3'
XF13R		5' –GGCCGCGGCCTCCGGCGTCGGTTCGCCCGGTC CGGATCA TGTAGGCTGGAGCTGCTTC– 3'

Primer Name	Target Gene	Sequence
XF14F	apr^R cassette for *hrmI* replacement	5' –CCGTTGCAGGAAAAACCTCCTGAGAATCTTGG ACGCGTGATTCCGGGGATCCGTCGACC– 3'
XF14R		5' –TAACCACGGTCGTTGAGCGGCATGCGCGTGACC TCCTCATG TAGGCTGGAGCTGCTTC– 3'
XF15F	apr^R cassette for *hrmJ* replacement	5' –ACTCCGCCGCACACACGTCCTGAGGAGGTCAC GCGCATGA TTCCGGGGATCCGTCGACC– 3'
XF15R		5' –CCCGGTTCCGGGGGTGCTGCTCATGACCGCCG CTCCTCAT GTAGGCTGGAGCTGCTTC– 3'
XF16F	apr^R cassette for *hrmN* replacement	5' –GTCGAGAACTGACGCCGACACACCGAGGGGGA ACGCATG ATTCCGGGGATCCGTCGACC– 3'
XF16R		5' –GGCAGGCGCCGAGTCGGGGACGACGGGGGCGGG CCGTCA TGTAGGCTGGAGCTGCTTC– 3'
XF17F	apr^R cassette for *hrmQ* replacement	5' –CCTGCGGGAAATGAATCCGACGAGTGAGGGAGA AAAATG ATTCCGGGGATCCGTCGACC– 3'
XF17R		5' –CTCGATCTCGTCGGAAACGAGCAGGGGTGGGCG AGCTCA TGTAGGCTGGAGCTGCTTC– 3'
XF18F	apr^R cassette for *hrmH* replacement	5' –GCTGCGACGCCAATGTCACTTGTTGGGGAGGAC AGGGTG ATTCCGGGGATCCGTCGACC– 3'
XF18R		5' –GATTCTCAGGAGGTTTTTCCTGCAACGGATCCG GTATCATGTAGGCTGGAGCTGCTTC– 3'
XF19F	*hrmC*	5' –AACTGCAGGAGGGCTGTGGCGGACTAC– 3'
XF19R		5' –GCTCTAGATCAGTCCTCCGCGGCCGG– 3'
XF20F	*hrmD*	5' –AACTGCAGGAGGAGCGTGCGCGTCGGAG– 3'
XF20R		5' –GCTCTAGATCAGAGTGCGCGCACCG– 3'
XF21F	*hrmI*	5' –AACTGCAGGAGAAGCGTGATGATTCCTG– 3'
XF21R		5' –GCTCTAGATCAGGACGTGTGTGCGGC– 3'
XF22F	*hrmQ*	5' –AACTGCAGGAGGGAAATGAGCGACTTC– 3'
XF22R		5' –GCTCTAGATCAGAAGAGCGGAGCCGC– 3'
XF23F	*hrmJ*	5' –GCTCTAGAGGAGGGCATGCCGCTCAAC– 3'
XF23R		5' –GGAATTCTCAGCCCTCGGCCAGGGC– 3'
XF24F	*hrmH*	5' –GCTCTAGAGGAGGGGGTGACCACTTCTTC– 3'
XF24R		5' –GGAATTCTCACTCGTTCACCAGCGCGTC– 3'
XF25F	*hrmN*	5' –GCTCTAGAGGGGAACATGGAACACCGGAC– 3'
XF25R		5' –GGAATTCTCACCAGTCGAAGTTGCGCAC– 3'
XF26F	Identification of	5' –ATCGAGGCCCTGCGTGCTGC– 3'
XF26R	mutants	5' –AGGGCCTCGATCAGTCCAAG– 3'
XF27F	ΔC mutant	5' –CGCAAGCAGGTCCGGGCGAG– 3'
XF27R		5' –GGGTGGCGGAAGTTCGGCGA– 3'
XF28F	ΔD mutant	5' –CTCCGGCCGGAAGATGCTCC– 3'
XF28R		5' –ACACGCTGCGCCCGGCGGTC– 3'

Primer Name	Target Gene	Sequence
XF29F	ΔH mutant	5' –GCGCGGGGCGGCCGTTCAAG– 3'
XF29R		5' –CCAGTACGTCGTGCAGCTCC– 3'
XF30F	ΔI mutant	5' –CGCCTCCCTCCAGGACGTGA– 3'
XF30R		5' –CGGATTCCGCCGGCCACGGG– 3'
XF31F	ΔJ mutant	5' –TCGGACTTCCGCGCGAGGGC– 3'
XF31R		5' –CACGATGGCCTGGTGGCCGC– 3'
XF32F	ΔN mutant	5' –GCGGCACTCACCAAGATCTC– 3'
XF32R		5' –CCGTGGATCTCGACGCACTG– 3'
XF33F	ΔQ mutant	5' –CTGCGCGTGAACTACAGTCC– 3'
XF33R		5' –CTCGTGGGTCGCATGTCCGT– 3'
MFF1-RE	*orf 20* (~8.4 kb) in	5' –GCGAAGCTTGTGAGGAGGACGTCGAGGA
	trans-AT PKS gene	CCTGTA– 3'
MFR1-RE	cluster	5' –GCGAAGCTTGAGCACGGTCTCCTCGGCTC– 3'
XF38F	hygromycin resistance	5' –ATGGGTAAAAAGCCTGAAC– 3'
XF38R	gene	5' –TTATTCCTTTGCCCTCGGAC– 3'
XF39F	thiostrepton resistance	5' –ATGACTGAGTTGGACACCATC– 3'
XF39R	gene	5' – TTATCGGTTGGCCGCGAGATTC– 3'
Gap1-F	*trans*-AT PKS gene	5' –GCAGGAAGTCCGGTATCTGTT– 3'
Gap1-R	cluster Gap1	5' –CACAGGCGAGGTAGAGGACTT– 3'
Gap2-F	*trans*-AT PKS gene	5' –CGGCTCGCTGAGAGCAACA– 3'
Gap2-R	cluster Gap2	5' –CCCGGTGCTCCTTGACGTT– 3'
Gap3-F	*trans*-AT PKS gene	5' –GCCATCGGCTCGCTGAGAGCAA– 3'
Gap3-R	cluster Gap3	5' –CGTCCTCCTCACCGGCGACGAA– 3'
Gap4-F	*trans*-AT PKS gene	5' –CGTGACCGCCATGCCGGAACT– 3'
Gap4-R	cluster Gap4	5' –CGGGTTGCGGTGGTCGGCTT– 3'
Gap5-F	*trans*-AT PKS gene	5' –GTCGTCGCCGCGCCGGAGTA– 3'
Gap5-R	cluster Gap5	5' –CCGTCGAGGAGGCCGAAGGTCA– 3'
Gap6-F	*trans*-AT PKS gene	5' –CTACGTGGCGGGATCGGTGTT– 3'
Gap6-R	cluster Gap6	5' –GAGCAGGACACCGTGCCGTTT– 3'
Gap7-F	*trans*-AT PKS gene	5' –CCGAACGAGGCACCGGAACA- 3'
Gap7-R	cluster Gap7	5' –GGCCGGGTGGTGGTCTGAGA– 3'
Gap8-F	*trans*-AT PKS gene	5' –GCGCTACCGCACGCGGTTCA– 3'
Gap8-R	cluster Gap8	5' –GGTGGAGGCCAGCGGAAGCA– 3'
Gap9-F	*trans*-AT PKS gene	5' –GTCGGCCTCCACGACGACAA– 3'
Gap9-R	cluster Gap9	5' –CGCGACCAGGTTCTCCCAGAA– 3'
Gap10-F	*trans*-AT PKS gene	5' –GCGCTCTGGTCCATGAAGAT– 3'
Gap10-R	cluster Gap10	5' –GCCGCTGCTGCATGAGAT– 3'
XCKS-F1	identification of	5' –CGCCGTTGGATACACCAAGGAAA– 3'
XCKS-R1	Δ*trans*-AT PKS	5'-CAGCACGAGACCGTCCTCCGT– 3'

Primer Name	Target Gene	Sequence
XCKS-F2	identification of Δ*trans*-AT PKS	5’ –CTGATCGTTCTCTCCGCGAAGGA– 3’
XCKS-R2:		5’ –TCGGGTTTCGCCACCTCTGACT– 3’
XCF2’-RE	ACP+KS_2 (~2.0 kb) from *orf20* in *trans*-AT PKS gene cluster	5’ –GCGAAGCTTGGGCAAGGACCGTACCGGGAA– 3’
MFFR1-RE		5’ –GCGAAGCTTGAGCACGGTCTCCTCGGCTC– 3’
XCF2-RE	DH+KR+ACP+KS_2 (~4.0 kb) from *orf20* in *trans*-AT PKS gene cluster	5’ –GCGAAGCTTCGTGTGCGACGACGACGGAA– 3’
MFFR1-RE		5’ –GCGAAGCTTGAGCACGGTCTCCTCGGCTC– 3’
XF40F	apr^R cassette (~1.4 kb)	5’ –GGAATTCCTGACGCCGTTGGATACACCAAG– 3’
XF40R		5’ –CCGGATATCTCAGCCAATCGACTGGCGAGCG– 3’

4.7 General methods

4.7.1 Cultivation and maintenance of *E. coli*

E. coli strains were routinely cultivated at 37 ℃ on LB agar plates or in LB liquid medium. The strains containing plasmids were grown on plates or in liquid media with the appropriate antibiotics. *E. coli* strains were stored at -80 ℃ in 30% glycerol.

4.7.2 Cultivation and maintenance of *Streptomyces* spp.

Streptomyces strains were grown on GYM or MS plates for sporulation and R5 or Gauze I plates for regeneration of protoplast transformation. The liquid cultures were generally grown at 27-30 ℃ for 2-5 d in TSB, MS or another various fermentation media. Strains harboring plasmids were inoculated on plates or in liquid media containing the appropriate antibiotics. Spore suspensions were prepared by adding 500 μL sterilized water on the surface of a well sporulated plate, gently scraping the spores off with a sterilized cotton bud, pipetting to mix the spores and water, filtering the spores suspension into a Falcon tube via replacing the plunger of syringe into the syringe with one piece of cotton on the bottom, then harvesting spores pellet through centrifugation and resuspending the spores pellet into certain volume (depending on

the pellet size) of sterilized 20% (v/v) glycerol. The spore suspensions were stored at -70 ℃.

4.7.3 Isolation of DNA from bacteria and manipulation of bacteria and DNA

4.7.3.1 Isolation DNA plasmid from *E. coli*

3 mL overnight culture was harvested by centrifugation at 12000 rpm for one min twice. 200 μL Buffer I was added into the cell pellets after decanting the supernatants and mixed with cells by vortexing. 300 μL Buffer II was immediately add into the mixture above and mixed by inverting the tubes several times. Then the tube with cells mixture was inverted again to mix after adding 300 μL Buffer III Immediately. The cell debris was spun down at 14000 rpm for 5 min. Most of the supernatant was transferred into a new 1.5 mL tube and mixed with 400 μL phenol/chloroform by vortexing two seconds and then spun at 14000 rpm for 5 min. Around 600 μL upper layer was transferred into a new tube and the same volume of isopropanol was added to precipitate DNA by vortexing two seconds and leaving on ice for 5 min, then spinning down at 14000 rpm for 5 min to precipitate DNA. DNA pellet was washed with 500 μL 70% ethanol by spinning for 2 min at 14000 rpm. The DNA white pellet was dried under the clean bench for 30 min after discarding the ethanol completely, dissolved in 50 μL TE buffer and stored at -20 ℃.

4.7.3.2 Isolation of genomic DNA from *Streptomyces* spp.

Streptomyces spore suspension was inoculated in 20 mL MS or TSB media with appropriate antibiotics and grown at 30 ℃, 250 rpm for 2 d. The mycelia of 2 mL culture were harvested by centrifugation at 12000 rpm for 2 min, washed with 1 mL TE buffer by spinning at 12000 rpm for 1 min, resuspended the mycelia in 500 μL STE buffer with 5 mg/mL (final concentration) lysozyme after removing TE buffer then incubated at 37 ℃, 250 rpm for 3 h in a shaker. Afterwards, 500 μL 10% SDS and 100 μL 3M NaAC (pH 5.3) were added to the mycelia, the suspension was mixed by vortexing and incubated at 37 ℃, 250 rpm , at least 30 min. 250 μL phenol/chloroform/isopropanol was added and mixed by vortexing 30 sec. Around 800 μL upper layer was transferred into new tube after centrifugation for 5 min at 14000 rpm and mixed

with 250 μL phenol/chloroform/isopropanol by vortexing 30 sec. Around 750 μL of the upper layer was transferred into a new tube, mixed with 750 μL isopropanol to precipitate DNA by spinning at 10000 rpm for 5 min after centrifugation again for 5 min at 1400 rpm. The resulting white pellet was washed with 500 μL 70% ice-cold ethanol, dried under the clean bench after removing the ethanol completely and dissolved in 50 μL TE buffer.

4.7.4 Preparation of *E. coli* competent cells and DNA transformation

4.7.4.1 Chemical competent cells preparation and DNA transformation

4.7.4.1.1 Chemical competent cells preparation

One single colony from activated *E. coli* agar plate was inoculated into 3-5 mL fresh LB liquid media, incubated in a shaker at 37 ℃, 250 rpm overnight. 100 μL overnight culture was transferred into 10 mL fresh LB and kept shaking at 37 ℃ for 2-2.5 h till the OD600 was up to 0.4-0.6, then the culture was dispensed into 1.5 mL tubes and left on ice for 20 min. The cell pellet was harvested by centrifugation at 4 ℃, 4000 rpm for 10 min and washed with 1 mL 0.1 M freezing $CaCl_2$ after discarding the supernatant and resuspended gently, lefts on ice for another 20 min. Then the cell pellet was collected by centrifugation at 4 ℃, 4000 rpm for 10 min and washed with $CaCl_2$ again. Then, the cell pellet was resuspended in 100 μL freezing 0.1 M $CaCl_2$ containing 15% glycerol after removing the supernatant completely and stored at -70 ℃.

4.7.4.1.2 DNA transformation

1 μL (100 ng/μL) DNA was mixed with 50 μL competent cells in a 1.5 mL tube gently and left on ice for 30 min. The cells were heat-shocked at 42 ℃ for 90 sec in a water bath and placed on ice immediately for 2-4 min. Then 800 μL fresh LB was added into the cells and mixed. The mixture was incubated in a shaker at 37 ℃ for 45-60min. The cell pellets were sedimented at 5000 rpm for 5 min after incubation, resuspended the cells with the remaining LB after discarding the supernatant and spread on LB agar plates containing suitable antibiotics.

4.7.4.2 Electronic competent cells preparation and DNA transformation

One single colony from activated *E. coli* agar plate was inoculated into 3-5 mL fresh LB liquid media with suitable antibiotics at 37 ℃, shaken at 200 rpm overnight. 500 uL overnight culture was added into 50 mL fresh LB, then shaken at 37 ℃ for 2-3 h till the OD600 is up to 0.4-0.6. Then the culture was dispensed into 50 mL Falcon tubes on ice. The cells pellet was collected by centrifugation at 4000 rpm for 5 min at 4 ℃, and resuspended by gently mixing in 40 mL ice-cold 10% glycerol and washed again with ice-cold the same volume of 10% glycerol. The cell pellet was resuspended into the remaining glycerol after discarding most of the supernatant and dispensed into 10 tubes, 100 μL per each, stored at -70 ℃.

4.7.4.2.1 Electroporation transformation

Around 100 ng (1-2 μL) of DNA was mixed with 50 μL cell suspension. Then the electroporation was carried out in a 0.2 cm ice-cold electroporation cuvette using a BIO-RAD Gene Pulser Immediately 1 mL ice-cold SOC or LB media was added to shocked cells and the mixture was shaken at 37 ℃ for 1 h. The culture was spun at 5000 rpm for 5 min. The cell pellet was mixed with remaining media after decanting 800 mL supernatant. The mixture was spread onto LB agar plate containing appropriate antibiotics.

4.7.5 Protoplast preparation and DNA transformation

4.7.5.1 Protoplast preparation

One single colony or 50 μL spores suspension was inoculated into 40 mL MS media (or with suitable antibiotics) and shaken at 30 ℃ for two days. The mycelium was harvested by centrifugation at 3000 rpm for 10 min. The supernatant was decanted gently, the mycelia were washed by adding 40 mL 10.3% sucrose and centrifugation at 3000 rpm for 10 min twice. After decanting the supernatant, the mycelia were resuspended in 15 mL P buffer, mixed with lysozyme to final concentration 1.5 mg/mL, incubated at 30 ℃ for 1.5 h, the tube with mycelia was gently inverted every 10-15 min until a creamy suspension formed, then another 5 mL P buffer was added to the mix and incubated for further 10 min to release the protoplasts. The

protoplasts were filtered through cotton wool, transferred to a new Falcon tube and spun down by centrifugation at 3000 rpm for 7 min. The protoplasts pellet was resuspended in 1 mL P buffer after decanting the supernatant and dispensed into 1.5 mL tubes and stored at -70 ℃.

4.7.5.2 DNA transformation

50 μL protoplasts were dispensed in 1.5 mL tube, 5 μL DNA solution was added to the inside of the tube wall.and mixed with the protoplasts by tapping tube. Then, 200 μL 25% PEG1000 was added into the protoplasts and mixed by pipetting up and down 4 times. The protoplasts suspension was plated on dried R5 plate. Then the plate was incubated at 30 ℃, after 14-20 h, and overlaid with appropriate antibiotics for selection and kept incubation at 30 ℃ for 5-7 days.

4.7.6 Conjugation from *E. coli* to *Streptomyces*

To prepare competent cells of *E. coli* ET12567/pUZ8002, the bacteria were grown in the presence of kanamycin (25 μg/mL) and chloramphenicol (25 μg/mL) to maintain selection for pUZ8002 and the *dam* mutation, respectively. The *oriT*-containing vector was transformed into competent cells for screening of the incoming plasmid only. A single colony from the transformants was inoculated into 10 mL LB containing chloramphenicol, kanamycin and the antibiotic used to select for the *oriT*-containing plasmid and grown overnight. The overnight culture was diluted at 1:100 in fresh LB plus antibiotic selection and grown at 37 ℃ to OD600 of 0.4-0.6. The cells was harvested by centrifugation and washed twice with an equal volume of LB (to remove antibiotics that might inhibit *Streptomyces*) and resuspended in 0.1 volume of LB. While washing the *E. coli* cells, for each conjugation approximately 1×10^8 *Streptomyces* spores were added to 500 μL 2 × YT broth and heat-shocked at 50 ℃ for 10 min, then cooled down. 500 μL of *E. coli* cells were added to 0.5 mL heat-shocked spores, mixed and spun down briefly. Most of the supernatant was decanted, the cell pellet was then resuspended in the residual liquid and plated on MS agar with 10 mM $MgCl_2$ and incubated at 30 ℃ for 16-20 h. The plate was overlaid with 1.5 mL sterilized water containing 0.5 mg nalidixic acid and appropriate antibiotics for plasmid selection. The antibiotic solution was spread evenly and

kept incubation at 30 ℃ for 3-7 d. The potential conjugants were picked off to selective media containing antibiotics and nalidixic acid (25 μg/mL).

4.7.7 DNA agrose gel electrophoresis

DNA Agarose gel electrophoresis was carried out according to the protocol of described by Samhook. DNA fragments were separated on 0.8%, 1.0% and 1.5% (depending on DNA sizes) agarose gel containing 0.1 μg/mL ethidium bromide. A volume DNA solution mixed with 1/10 volume DNA loading dye was loaded into the well of the gel. Electrophoresis was performed at 60-125 V for 1-10 h (for different purposes) in 1 x TAE buffer. The DNA gel was visualized by illumination with UV light.

4.7.8 DNA fragment purification from agarose gel (QIA quick Gel Extraction Kit Protocol)

The DNA fragment was excised from the agarose gel with a clean, sharp scalpel. The gel slices were weighed in a colorless tube. 3 volumes of Buffer QG was added to 1 volume of gel (100 mg) and incubated at 50 ℃ for 10 min until the gel slices have completely been dissolved. One gel volume of isopropanol was added to the sample and mixed. The QIA quick spin column was placed in a 2 mL provided collection tube. To bind DNA, the sample was applied to the QIA quick column, and spun for one min at 13000 rpm. The flow-through was discarded and the QIA quick column was placed back in the same collection tube. 500 μL of Buffer QG was added to the column and spun for one min at 13000 rpm. 750 μL of Buffer PE was added to the column and spun for one min at 13000 rpm. The flow-through was discarded and the column was spun for an additional 1 min at 13000 rpm. The column was placed into a clean 1.5 mL tube. Finally, 30-50 μL of Buffer EB was applied to the center membrane of column and spun for one min.

4.7.9 DNA digestion with restriction enzymes

The digestion of DNA was carried out with 2 units of restriction enzyme per 1 μg DNA in a reaction containing appropriate 1 × reaction buffer recommended by manufacturer and water filled up to desired volume, then incubated at 37 ℃ for 1-3 h, then inactivated by heating at 65 ℃ for 10 min. In this study, basically, two different volumes of DNA digestion volume were set up, 10 μL volume for testing the DNA size and 100 μL volume for isolating DNA fragment , which described as follows:

Table 4.7: The composition of digestion.

Composition	**10 μL**		**100 μL**	
	Single digestion	**Double digestion**	**Single digestion**	**Double digestion**
DNA	1 μL	1 μL	30 μL	30 μL
Enzyme I	0.5 μL	0.5 μL	5 μL	5 μL
Enzyme II	-	0.5 μL	-	5 μL
10 × Buffer	1 μL	1 μL	10 μL	10 μL
10 × BSA	1 μL	1 μL	10 μL	10 μL
dd H_2O	6.5 μL	6 μL	45 μL	40 μL

4.7.10 DNA precipitation

DNA precipitation was applied to concentrating DNA or desalting the buffers after digestion, dephosphorylation and ligation of DNA in case of inhibition to further studies. 1/10 volume of 3 M sodium acetate (pH 5.2) plus 2-3 volumes of cold 100% ethanol were added to the solution containing DNA. One volume was the volume of the solution containing the DNA. The solution was then placed at -20 ℃ for 2 h and finally was centrifuged at 14000 rpm for 15 min at 4 ^{o}C. The ethanol was removed and the pellet was rinsed once with 70% ethanol by centrifugation for 5 min at 14000 rpm at 4 ^{o}C. The ethanol was discarded and the pellet was allowed to dry in vacuum and then resuspended in clean aqueous for use.

4.7.11 Dephosphorylation of linearized plasmid vector

To avoid self-religation of the linearized vector after digestion, dephosphorylation of the vector was carried out by adding 1/10 volume of 10 × Antarctic Phosphatase Reaction Buffer to 1 μg of DNA digested with a restriction enzyme, then mixed with 1 μL of Antarctic Phosphatase (5 units) and incubated for 1 h at 37 ^{o}C. Afterwards, the reaction was inactivated by heating at 65 ^{o}C for 15 min. Then the plasmid vector after dephosphorylation was desalted by going through gel extraction column or precipitation for proceeding with ligation.

4.7.12 Ligation of DNA fragments

DNA fragments for ligation were basically purified using Qiagen or Fermentas gel extraction kit and mixed with a ratio of insert: linearized vector = 3:1. The DNA concentration was quantified by loading 1 μL of each fragment on the gel as well as DNA marker of known concentration. Ligation reactions were performed in a 10 μL final volume at 16 ℃ overnight using ligation kit of Jena Bioscience.

4.7.13 DNA sequencing

DNA sequencing was performed by GATC Biotech.

4.7.14 PCR methods

4.7.14.1 General PCR methods

All the PCRs were carried out in 50 μL reaction volume using Expand High Fidelity^{PLUS} PCR System (Roche) for cloning or PCR-targeting strategy and using normal *Taq* DNA polymerase (NEB) for analysis of all the constructs and mutants. The components and amplification conditions were summarized in tables:

Table 4.8: The components of PCR reaction.

Components	Volume		Final conc.
Primer 1 (100 pmoles/µL)	0.5 µL	0.5 µL	20 pmoles
Primer 2 (100 pmoles/µL)	1 µL	0.5 µL	20 pmoles
Template DNA		1 µL	5-500 ng (genomic DNA)
	10 µL		100 pg-10 ng (plasmid DNA)
5 x Reaction buffer (Roche)	-	-	1 ×
10 x Reaction buffer(NEB)	1 µL	5 µL	1 ×
dNTPs (10 mM)		1 µL	50 µM (per each)
DMSO	2.5 µL	2.5 µL	5%
DNA polymerase (Roche)	0.5 µL	-	2.5 Units
DNA polymerase (NEB)	-	0.25 µL	2.5 Units
Milli-Q H_2O	34 µL	39.25 µL	

4.7.14.2 Standard PCR amplification conditions

The PCR amplification protocol in this study mostly was designed for analysis of constructs, mutants and specific gene DNA fragments as follows:

Table 4.9: PCR reaction cycles.

Steps	Temperature	Time	Cycles
Initial denaturation	94 or 95 ℃	2 min	1 ×
Denaturation	94 or 95 ℃	10 – 30 sec	(25 – 35) ×
Annealing	55 ℃ – 68 ℃	30 – 45 sec	
Elongation	68 or 72 ℃	30 sec – 5 min	
Final elongation	68 or 72 ℃	7 or 10 min	1 ×

The denaturation temperature was chosen according to the protocols of two different DNA *Taq* polymerases from Roche (94 ℃) and NEB (95 ℃). Optional annealing temperature between 55-68 ℃ was used depending on the melting temperature of primers. For the elongation temperature, normal *Taq* DNA polymerase from NEB usually was set up to 72 ℃ and Expand High Fidelity^{plus} was set up to 68 ℃ for the target fragment which were longer than 3 kb or 72 ℃ for the regular fragments between 100 bp-3 kb. The elongation time was changed based on the length of PCR products.

4.7.14.3 PCR amplification of the extended resistance cassette

All the PCR amplifications were performed according to the instructions of the Expand high fidelity PCR system (Roche). The reaction condition was set up as above in **Table 4.8**.

To amplify the extended apramycin resistance cassette, a PCR was carried out by taking the apramycin resistance gene cassette purified after digestion of pIJ773 (Gust et al., 2003) as a template and using the suitable long primers under the following cycle conditions in **Table 4.10**.

Table 4.10: PCR program for amplification of the extended resistance cassette.

Steps	Temperature	Time	Cycles
Initial denaturation	94 ℃	2 min	1 ×
Denaturation	94 ℃	45 sec	
Annealing	50 ℃	45 sec	10 ×
Extension	72 ℃	45 sec	
Denaturation	94 ℃	45 sec	
Annealing	55 ℃	45 sec	15 ×
Extension	72 ℃	45 sec	
Final extension	72 ℃	5 min	

4.7.15 DNA-DNA hybridization

4.7.15.1 Southern blotting

After agarose gel electrophoresis, the gel and membrane were processed for DNA transfer, the area of the gel without any DNA was removed and a small part from the lower right corner of the gel was cut off for further direction identification. The gel was incubated into depurination buffer for 15 min and rinsed gently in Milli-Q water, then the DNA was denatured by incubating the gel in denaturation solution for 30 min and the gel was rinsed in Milli-Q water again. For neutralization, the gel was incubated in neutralization solution for 30 min. Then blotting stack was assembled. Meanwhile, a piece of Immobilon-Ny^{+} membrane to the size of the gel was prepared and wetted by carefully laying it on top of Milli-Q water in a shallow tray. The tray was gently agitated once the membrane was wet to completely immerse the membrane. Then,

the membrane was transferred into a second tray containing transfer buffer (20 × SSC). Three sheets of Whatman 3MM filter paper, the size of the membrane in 20 × SSC were wetted, then the blot stack (**Figure 4.1**) was set up by placing the gel on the bottom, the membrane in the middle and the three sheets of filter paper on the top. The bubbles between these three layers were rolled out with pipette. Then, the 10 cm high stack of paper towels was placed on top of the filter paper and a glass plate was placed on top of the stack. Finally, the 250 g weight was placed on top of the plate to let the DNA transfer from gel to the membrane for 16 h.

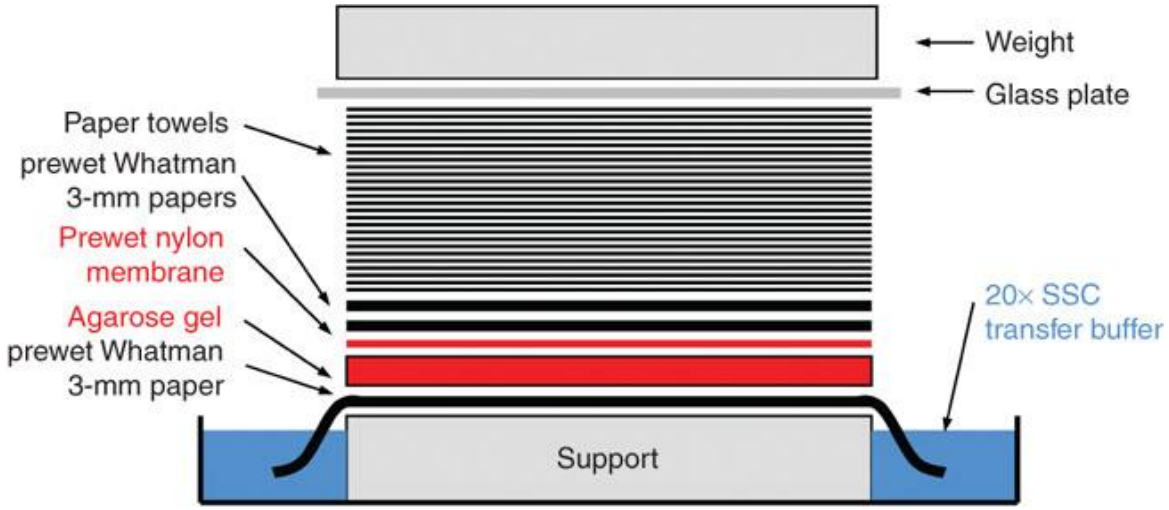

Figure 4.1: Capillary blotting stack (Southern blotting) (Amersham Bioscience).

After this time, the paper towels and filter paper were removed. The blot membrane was lifted carefully with a pair of forceps and rinsed in 6 × SSC to remove any free particles of agarose. The blot membrane was put on a piece of filter paper to dry for 15 min at 80 ℃. Then DNA fixation was performed by UV cross-linking (254 nm, 5000 μJ/cm^2) for 5 min or placing it between two sheets of clean filter paper in a vacuum oven at 80 ℃ for 1-2 h.

4.7.15.2 Colony *in situ* hybridization

The membrane was placed on the LB agar plate containing appropriate antibiotics. The bacterial single colony from the library was transferred to the membrane with a 96-well inoculator, The membrane with plate was incubated at 37 ℃, overnight, then lifted off the plates and placed onto the filter paper soaked into lysis buffer for 3 min (DNA lysis), the

membrane was transferred onto the filter paper soaked into denaturation buffer for 5 min (DNA denaturation), transferred onto the filter paper soaked into neutralization buffer for 5 min, then placed on one sheet of clean filter paper to dry at room temperature for 30 min. The DNA fixation was performed by incubating the membrane at 80 ℃ in a vacuum oven for 2 h. Afterwards, the blot membrane was rinsed in a shallow tray with washing buffer to gently remove the cell debris. Then the membrane was placed between two pieces of clean filter paper to dry.

4.7.16 PCR targeted gene replacement in *S. griseoflavus* W-384

To identify the function of genes involved in hormaomycin biosynthesis, several mutants of hormaomycin producer were generated by using the following approach called REDIRECT© Technology: PCR targeting system which is much more efficient than the traditional gene replacement strategy in *Streptomyces* spp..

4.7.16 .1 PCR primer design

Two long PCR primers (58 bp and 59 bp) were designed for each gene disruption. The procedure was described in chapter. All the long primers used in this study were displayed in **Table 4.6**.

4.7.16 .2 Purification of the PCR template

Around 10 μg plasmid DNA of pIJ773 (**Figure 4.2**) (Gust et al., 2003) was digested with 50 units of *Eco*RI and 50 units of *Hin*dIII in 1 × Buffer B in a 100 μL reaction volume at 37 ℃ for 5 h. About 1382 bp apramycin resistance gene cassette was extracted from gel and purified using Qiagen gel kit. The resulting DNA fragment was eluted in Milli-Q water (pH 8.0) at a concentration of 100 ng/μL.

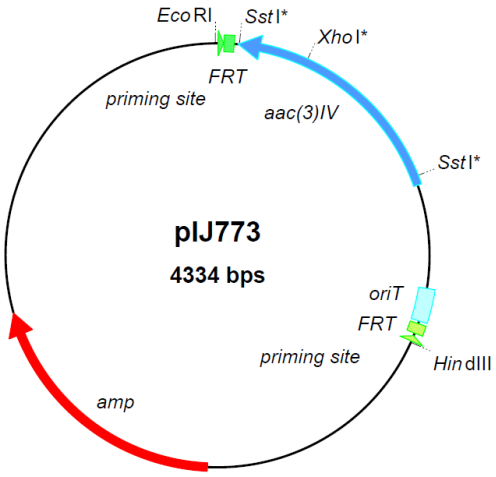

Figure 4.2: The physical map of plasmid pIJ773 (Gust et al., 2003). *aac(3)IV*, apramycin resistance gene; *amp*, ampicillin resistance gene; *oriT* of plasmid RP4, transferring DNA; FRT, FLP recognition targets.

4.7.16.3 PCR amplification of the extended resistance cassette

All the conditions were described in **Table 4.8**. The specific PCR fragment with the length of 1.46 kb was amplified, purified from gel and finally eluted in in Milli-Q water (pH 8.0) at a concentration of 200 ng/μL.

4.7.16.4 Introduction of cosmids into *E. coli* BW25113/pIJ790 by electroporation

E. coli BW25113 carrying a plasmid pIJ790 (**Figure 4.3**) (Gust et al., 2003) containing chloramphenicol resistance gene *cat* and a temperature sensitive origin of replication requiring 30 ℃ for replication was grown overnight at 30 ℃ in LB medium with 25 μg/mL chloramphenicol. 100 μL overnight culture of *E. coli* BW25113/pIJ790 was inoculated into 10 mL SOB containing 20 mM $MgSO_4$ and 25 μg/mL chloramphenicol to prepare the electro-competent cells. 2 μL of cosmid DNA was mixed with 50 μL competent cells suspension. Then electroporation was performed according to the procedure described above. After incubation at 30 ℃ for 1 h.The cells were spread on LB plates containing 50 μg/mL kanamycin, 25 μg/mL chloramphenicol and 100 μg/mL ampicillin.

4.7.16.5 PCR targeting of cosmids

One transformant of *E. coli* BW25113/pIJ790 containing a *Streptomyces* cosmid was inoculated in 5 mL of LB medium and grown overnight at 30 ℃. 100 µL of overnight culture was inoculated in 10 mL SOB-$MgSO_4$ medium containing 100 µg/mL ampicillin, 50 µg/mL kanamycin and 25 µg/mL chloramphenicol with 10 mM L-arabinose inducing the *red* gene and shaken at 30 ℃, 220 rpm to OD_{600} of ~0.4, and followed by preparation of electro-competent cells. Then, the PCR product of extended the resistance cassette was transformed into *E. coli* BW25113/pIJ790 containing a *Streptomyces* cosmid by electroporation. The cell culture was spread on LB plate containing 100 µg/mL ampicillin, 50 µg/mL kanamycin and 50 µg/mL apramycin and incubated overnight at 37 ℃. (The higher temperature could promote the loss of pIJ790).

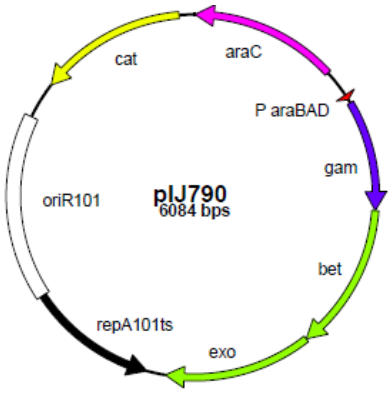

Figure 4.3: The physical map of plasmid pIJ790 for λ-RED recombination (Gust et al., 2003). (*araC*, encodes arabinose activator; *bet*, encodes single strand DNA binding protein; *cat*, chloramphenicol resistance gene; *exo*, exonuclease gene, promotes recombination together with *bet*; *gam*, gene product inhibits the host exonuclease V; *ori*R101, origin of replication; ParaBAD, L-arabinose inducible promoter; *rep*A101ts, temperature-sensitive replicon.

Homologous recombination occurred and many colonies were observed in the next day. The bigger colonies from resulting transformants were inoculated into 5 mL of LB containing 100 µg/mL ampicillin, 50 µg/mL kanamycin and 50 µg/mL apramycin, respectively and shaken overnight at 37 ℃, 200 rpm. All potential mutant cosmids were isolated and analyzed by PCR. PCR analysis with a primer pair (test primers) annealing just ~100 bp outside the region affected by homologous recombination will generate the expected fragment after gene

disruption. The target mutant cosmid was isolated and transformed into *E. coli* ET12567/pUZ8002 by electroporation to get the unmethylated DNA for transformation into *Streptomyces* spp..

4.7.16.6 Transformation of mutant cosmids to *S. griseoflavus* W-384

A mutant cosmid was introduced into *S. griseoflavus* W-384 by protoplast transformation described above. After incubation 16-18 h, the R5 plate was overlayed with 1.5 mL sterilized water containing 25 μL apramycin (50 mg/mL). And the plate was kept incubation at 30 ℃ for 5-7 d. Homologous recombination occurred and the transformants with apramycin resistance grew on the plate. The transformants from R5 plates were replica-plated on a GYM plate containing 25 μg/mL apramycin with or without 25 μg/mL kanamycin. Double cross-over exconjugants should be kanamycin sensitive and apramycin resistant. Each potential double cross-over exconjugants or transformants was inoculated into 10 mL MS media containing 25 μg/mL apramycin and shaken at 30 ℃, 220 rpm for 2 d. The genomic DNA of each transformant was isolated and the expected gene replacement in the genome was confirmed by PCR with different pairs of test primers (**Table 4.6**).

4.7.17 DIG-DNA probe labeling

(DIG-DNA labeling was carried out according to the procedure of Roche DIG High Prime DNA Labeling and Detection Starter Kit I)

Around 1 μg template DNA (linear or supercoiled) was added into autoclaved double distilled water to a final volume of 16 μL to a reaction vial. The DNA was denatured by heating in a boiling water bath for 10 min and quickly chilling in an ice/water bath. Around 4 μL DIG-High Prime (vial 1) was mixed thoroughly and added into the denatured DNA, the mixture was spun down briefly and incubated for 16-20 h at 37 ℃. The reaction was stopped by adding 2 μL 0.2 M EDTA (pH 8.0) or by heating to 65 ℃ for 10 min.

4.7.17.1 Southern hybridization

The appropriate volume of DIG Easy Hyb buffer (10 mL/100 cm^2 filter paper) was pre-heated to hybridization temperature 42 ℃. The blot membrane was placed into the hybridization bag with preheated hybridization solution and incubated at 42 ℃ for 30 min with gentle agitation. The DIG-labeled DNA probe (about 25 ng/mL DIG Easy Hyb buffer) was denatured by boiling for 5 min and rapidly cooling in ice/water. The denatured DIG-labeled DNA probe was added to the pre-heated DIG Easy Hyb buffer (3.5 mL/100 cm^2 membrane) and mixed well gently to avoid foaming. The mixture with hybridization solution and the denatured probe was added to the membrane in the hybridization bag and incubated for 4-20 h at 42 ℃ with gentle agitation.

4.7.17.2 Stringency washes

The membrane was washed in 2 ×SSC, 0.1% SDS for 5 min twice at 15-25 ℃ under constant agitation. Then, it was rinsed in 0.5 ×SSC, 0.1% SDS (pre-warmed to wash temperature) for 15 min twice at 68 ℃ under constant agitation. Meanwhile, the 1 ×working solution was prepared by diluting 10 ×Blocking solution (vial 6) 1:10 with Maleic acid buffer. Anti-Digoxigenin-AP (vial 4) was spun down for 5 min at 10000 rpm in the original vial prior to each use, and 5 μL of it was carefully taken from the surface and diluted into 25 mL 1 ×Blocking buffer. (can be stored at 4 ℃ for 12 h). 200 μL of NBT/BCIP stock solution (vial 5) was added to 10 mL of Detection buffer for color development.

4.7.17.3 Washing membrane and detection of signals

After hybridization and stringency washes, the membrane was rinsed briefly for 5 min in washing buffer and incubated for 30 min in 100 mL blocking solution. Then the membrane was placed in 20 mL Antibody solution and incubated for 30 min. The membrane was washed in 100 mL washing buffer for 15 min twice and transferred in 20 mL Detection buffer to equilibration for 2-5 min. Finally, the membrane was incubated in 10 mL freshly prepared color substrate solution in an appropriate container in the dark without shaking during color development. The reaction was stopped, when desired spot or band intensities are achieved, by

washing the membrane for 5 min with 50 mL of sterile double distilled water or with TE-buffer.

4.7.18 Protein expression and purification

4.7.18.1 Protein expression in *E. coli*

The target gene was cloned into expression vector pET28b (+) (**Figure 4.4**) an N-terminal His-Tag in addition to an optional C-terminal His-Tag sequence or pET29b carrying an N-terminal S-Tag plus an optional C-terminal His-Tag sequence under the control of T7 promoter, then transformed into *E. coli* BL21(DE). A single colony of the resulting transformants was inoculated into 5 mL of TB or LB media supplemented with 100 μg/mL of kanamycin and grown at 37 ℃, 250 rpm overnight. 1mL of overnight culture was transferred into 100 mL of fresh TB or LB media containing 100 μg/mL of kanamycin and grown at 37 ℃ for 3-5 h until OD600 up to 1.5-2.0, then the flask with bacteria was immediately placed on ice for cooling down. 100 μL of 1 M IPTG (stock solution) was added into the bacteria culture to a final concentration of 1 mM IPTG for induction, and cultivated at 16 ℃, 250 rpm, overnight.

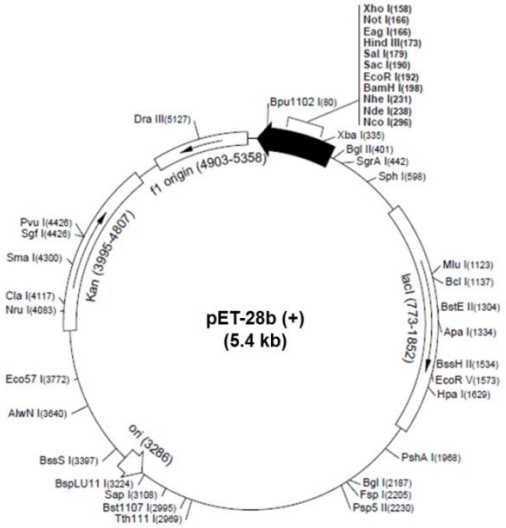

Figure 4.4: Plasmid map of pET-28b (+) (Novagen). The pET-28b(+) vector carries an N-terminal His-Tag/thrombin/T7-Tag configuration in addition to an optional C-terminal His-Tag sequence. Unique sites are shown on the circle map. The T7 expression region is reversed on the circular map due to the sequence numbering from the pBR322 convention. The f1 origin is oriented so that infection with helper phage will produce virions containing single-stranded DNA that corresponds to the coding strand. Therefore, the T7 terminator primer should be used when performing single stranded sequencing.

4.7.18.2 Protein purification

A 50 mL Falcon tube was pre-weighed, then the cell pellets of *E. coli* BL21(DE) containing the expression plasmid of the target gene were harvested by centrifugation at 7000 rpm for 5 min, the supernatant was decanted completely. The Falcon tube with cell pellets was weighed again to calculate the net weight of the cell pellets. 4 mL lysis buffer per gram cell pellets was added into the tube, the cell pellets were resuspended gently with tips at 4 ℃. Sonication was processed on the cell suspension 5 times, 10 sec, 70-90W in an ice/water bath. Afterwards, the lysis supernatant was collected by centrifugation of the cell lysis aliquot at 11000 rpm for 30 min. The lysis supernatant was transferred into a new Falcon tube, mixed with 400 µL Ni-Resin agarose and incubated on ice with gently constant shaking for 1 h. The mixture above was centrifugated at 850 rcf for 10 min at 4 ℃. The supernatant was decanted immediately to get the pellets. The pellets with Resin and protein were added into the column, then rinsed with 2 mL of 20 mM washing buffer twice. Then, the column was rinsed by 2 mL of 40 mM washing buffer again. Finally, the protein was eluted off the column by 250 mM elution buffer.

4.7.18.3 TCA protein precipitation

To prepare 100% (w/v) TCA, 25 g TCA was dissolved into 17.5 mL dH_2O, store at RT. 1 volume of TCA stock was mixed with 4 volumes of protein sample by vortexing and spinning down at 14000 rpm at 4 ℃ for 15 min, the supernatant was removed from white pellet completely. The white pellet was resuspended with 1 × SDS loading dye and heated up at 95 ℃ for 10 min before loading sample onto SDS gel.

4.7.18.4 Protein color development

To test the protein concentration before loading sample on SDS gel, 40 µL of protein sample was mixed with 160 µL Roti-Nanoquant, the color would be changed into blue from brown.

4.7.18.5 Desalting and buffer exchange

Desalting refers to the removal of salts from a sample, while buffer exchange refers to the replacement of one set of buffer salts with another set. Both goals are easily accomplished by size exclusion chromatography. Desalting is accomplished by first equilibrating the chromatography column with water. Buffer exchange, however, is performed by first equilibrating with the column resin with a buffer the sample should end up in. In both cases, the buffer constituents carrying the sample into the column will be replaced by the solution with which the column is pre-equilibrated.

Eluted protein fractions (3.0 mL of 250 mM imidazole) were desalted into 50 mM Tris (pH 7.0, 7.5, 8.0, 8.5) with 10% (v/v) glycerol, 50 mM MES (pH 6.0, 6.5) with 10% (v/v) glycerol, 50 mM potassium phosphate buffer (pH 6.5, 7.0, 7.5, 8.0) with 10% (v/v) glycerol using PD-10 disposable desalting columns as described by the manufacturer.

4.7.18.6 Protein stability assay

Reactions (200 μL) containing ~100 μg of protein in 50 mM buffer were incubated overnight at 37 ℃. Buffers MES (pH 6.0, 6.5), potassium phosphate (pH 6.5, 7.0, 7.5, 8.0), and Tris (pH 7.0, 7.5, 8.0, 8.5) were used in this experiment. The supernatants from reactions were harvested by spinning down at 14000 rpm for 30 min, and then precipitated by TCA. The supernatants were discarded and the pellets were resuspended in 20 μL of 1 × SDS loading dye in ~1.0 M Tris, pH 8.5, to neutralize the acid. The resulting aliquots were analyzed by SDS-PAGE. The most stable protein in corresponding buffer showed the highest density on the SDS-PAGE gel.

4.7.18.7 SDS-Polyacrylamide Gel Electrophoresis (SDS-PAGE)

SDS-PAGE was widely used to separate proteins based on their size. The proteins were denatured by a powerful detergent SDS and loaded to a discontinuous polyacrylamide gel composed of a resolving gel on the bottom with higher acrylamide concentration to let the proteins go through the gel slowly for separating the proteins and a stacking gel with very low

acrylamide concentration and used to form the wells into which the protein is loaded. Ammonium persulfate and TEMED were added to final concentrations of 1% and 0.1%, respectively, to initiate polymerization. In this study, the resolving gel and stacking gel were prepared as following recipes (**Table 4.11**):

Table 4.11: The components of SDS-polyacrylamide gel.

Composition	12% Resolving gel (15 mL)	4% Stacking gel (5 mL)
dd H_2O	6.75 mL	3.25 mL
Resolving gel buffer (1M Tris-HCl, pH 8.8, 10% SDS)	3.75 mL	-
Stacking gel buffer (1M Tris-HCl, pH 6.8, 10% SDS)	-	1.25 mL
40% acrylamide	4.5 mL	500 μL
10% APS	150 μL	50 μL
TEMED	15 μL	5 μL

The purified protein sample was mixed with the equivalent volume of 1 × SDS loading dye and denatured by heating at 95 ℃ for 10 min. The denatured protein sample was centrifuged at 14000 rpm for 1 min, and 10 μL of the supernatants was loaded into stacking gel well. Then electrophoresis was performed at 110 V for 1 h until the loading dye line almost arrived at the bottom of gel. Afterwards, the protein gel was carefully lifted up, gently transferred into a shallow tray with staining buffer and incubated for 30 min with constant shaking. Then, the gel was rinsed with water several times and incubated in 10% acetic acid to destain by heating up in microwave oven for 90 sec, then rinsed several times and showed the protein band. To get clearer protein gel, the gel was incubated in 10% acetic acid with constant shaking overnight at room temperature.

4.7.19 Fermentation of *S. griseoflavus* W-384 strains

50 μL of *Streptomyces* spores suspension was inoculated into 20 mL MMS (for seed culture) in 50 mL Falcon tube and grown at 27 ℃, 250 rpm for 2 d. 5 mL of seed culture was transferred into 45 mL fresh MMS media (for production culture) in 250 mL baffled flask and kept growing at 27 ℃, 250 rpm for 3 d. For the preparative isolation of compounds, the cells were cultured as

described above by using 10 × 250 mL flasks in parallel for cultivation 3 times with 1.5 L of cultures in total.

4.7.20 Chemical complementation of mutants

The mutant strains derived from *S. griseoflavus* W-384 were individually fed with different amino acids. After two-day seed culture cultivation, production cultures were inoculated and immediately fed the above individual amino acids. During three days of growth in production medium, the amino acids were added every 12 hours for a total of five times with a final concentration of 0.3 mg/mL. Extraction and analysis of hormaomycin and its derivatives followed as described below.

4.7.21 HPLC and LC-MS analysis of secondary metabolites from *S. griseoflavus* W-384 strains

After fermentation, the culture was sedimented by spinning down at 14000 rpm for 10 min. The supernatant was transferred into a new falcon tube and extracted three times with EtOAc. After evaporation, the residue was resuspended in appropriate amount of methanol for further HPLC and LC-MS analysis and bioassay.

The secondary metabolites from *S. griseoflavus* W-384 was analyzed by Jasco HPLC system with a reverse-phase column (KNAUER Eurospher II 100-5 RP C-18, 5um, 4.0 mm x 250mm) and LC-MS (Bruker Daltonics) at a flow rate 1.0 mL/min, for 50 min using acetonitrile (75%) and water supplemented with 0.1% TFA (v/v) (25%). The detection wavelength was 273nm. The retention times of HRM and HRM derivatives (HRM A_1-A_8) are: 7.2 min (HRM A_7), 8.9 min (HRM A_8), 10.2 min (HRM A_1, HRM A_2), 13.4 min (HRM), 20.3 min (HRM A_3, HRM A_4), 23.4 min (HRM A_5) and 38.5 min (HRM A_6). For the *trans*-AT PKS gene cluster mutants, the reversed-phase HPLC analysis was performed under the following conditions: column temperature, 40 °C; gradient elution, solvent A (CH_3CN) and solvent B (0·5% TFA in H_2O), gradient profile (0-5 min, 5% A; 5-35 min, 100% A; 35-40 min, 100% A; 40-45 min, 5% A;

flow rate, 1.0 mL/min; 250-280 nm.

4.7.22 MS and NMR analysis of HRM analogues

High-resolution ESI-MS spectra were performed on a Thermo LTQ Orbitrap XL mass spectrometer, running Xcalibur 2.1.0 software. The spectra were recorded by infusion into the ESI source using methanol as the solvent. The instrument was first autotuned on the *m/z* value of the ion to be fragmented. Then, the $[M+H]^+$ ion of each compound was isolated in the linear ion trap and fragmented by CID. Sets of consecutive, high-resolution, full MS/MS scans were acquired in centroid or profile mode and analyzed using the QualBrowser software (Thermo). NMR spectra were acquired on Varian Unity Inova spectrometers at 700 MHz; chemical shifts were referenced to the residual solvent signal (CD_3OD: δ_H 3.31). For an accurate measurement of the coupling constants, the one-dimensional ^1H NMR spectra were transformed at 64 K points (digital resolution: 0.09 Hz).

4.7.23 Antibacterial and hormonal assays

The detection of HRM and its derivatives was prepared by applying 20 μL of culture supernatant to paper discs on LB plated covered with *A. crystallopoietes* as the test strain. The inhibition zones on plates were observed after incubation at 30 ℃ overnight. To determine the MICs of hormaomyin and its analogues, five different dilutions of these compounds were added to *A. crystallopoietes* cells in a final 5 mL of LB medium and cultivated at 37 ℃, 250 rpm, overnight. The lowest concentration with no visible bacterial growth was designated as MIC.

10 μL (1×10^8 spores/μL) spores suspension of *S. coelicolor*, *S. griseus* and 100 μL mycelia pellets stock of their corresponding *bld* mutants were spread on Gauze I media plates, hormaomycin or goadsporin in methanol were absorbed in paper discs, and the discs dried, placed on the plates and incubated at 30 ℃. Pigment production and cell differentiation around the paper disc were observed every 24 hours.

4.7.24 Methanolysis of HRM and HRM A_7

Less than 0.1 mg of HRM or HRM A_7, dissolved in 100 μL of methanol, was dried and redissolved in 15 μL MeOH before addition of 10 μL of sodium methoxide and incubation at room temperature overnight. The mixture was then partitioned between H_2O (750 μL) and EtOAc (750 μL × 3), the ethyl acetate fractions were dried, and the resulting peptide fragments were analyzed by ESI-MS/MS (Nakao et al., 2004).

Abbreviations

(3-Ncp)Ala	3-(*trans*-2’-nitrocyclopropyl)alanine
(4-Et)Pro	4-ethinylproline
(4-Me)Pro	4-methylproline
(4-Pe)Pro	4-(*Z*)-propenylproline
6-dEB	6-deoxyerythronolide B
(β-Me)Phe	(2*S*,3*R*)-3-methylphenylalanine
aac(3)IV, apr^{R}	apramycin resistance gene
ACT	actinorhodin
ACP	acyl carrier protein
A domain	adenylation domain
A factor	2-isocapryloyl-3*R*-hydroxymethyl-γ-butyrolactones
AHBA	3-amino-5-hydroxybenzoic acid
amp	ampicillin resistance gene
AMP	adenosine monophosphate
APS	ammonium persulfate
ARO	aromatase domain
Arp	A-factor-specific receptor
AT domain	acyl transferase domain
ATP	adenosine triphosphate
*att*B phage	attachment site on bacterial chromosome
*att*P	attachment site on phage
bla	β-lactamase gene
BLAST	basic local alignment search tool
bp	base pair
C	cytosine
calcd.	calculated
cat	gene encoding chloramphenicol acetyltransferase

C domain	condensation domain
CDA	calcium-dependent antibiotics
Chpca	5-chloro-1-hydroxypyrrole-2-carboxylic acid
CHSs	naringenin-chalcone synthases
CID	collision-induced dissociation
cis- AT PKs	*cis*-AT polyketides
CLF	chain length factor domain
CoA	coenzyme A
Conc.	concentration
cos	cohesive site
COSY	correlation spectroscopy
Crp	cyclic AMP receptor protein
CYC	cyclase/cyclization domain
d	day/days
dATP	deoxyadenosine triphosphate
DEBS	6-deoxyerythronolide B synthase
DH	dehydratase domain
DMSO	dimethyl sulfoxide
ECF	extracytoplasmic function
E domain	epimerase/epimerization domain
EDTA	ethylenediamine tetracetic acid
e.g.	exempli gratia (Latin) means “for example”
EIC	extracted ion chromatogram
ER	enoyl reductase domain
ESI-MS	electrospray ionization mass spectrometry
EtOAc	ethylacetate
FAD	flavin adenine dinucleotide
F domain	Formylation domain
G	guanine

GlcNAc	N-acetylglucosamine
GS	goadsporin
h	hour/hours
HBM	4-hydroxy-2-2'-bipyrrole-5-methanol
HMBC	heteronuclear multiple-bond correlation spectroscopy
HPLC	high performance liquid chromatography
HRM	hormaomycin
HSQC	heteronuclear single-quantum correlation spectroscopy
i.e.	id est (Latin) means "that is"
int	gene encoding integrase of phage
IPTG	isopropyl β- D-1-thiogalactopyranoside
kb	kilobase
KR	ketoreductase domain
KS	ketosynthase domain
LAL	large ATP-binding regulators of the LuxR
LB	Luria-Bertani medium
LC-MS	liquid chromatography-mass spectrometry
L-DOPA	L-3,4-dihydroxyphenylalanine
MCS	multiple cloning site
MES	2-(*N*-morpholino)ethanesulfonic acid
MIC	minimum inhibition concentration
min	minute/minutes
MS	mass spectroscopy
MT domain	methyltransferase domain
m/z	mass- to- charge ratios
NaAC	sodium acetate
NADH	nicotinamide adenine dinucleotide
NBT	nitro-blue tetrazolium
NMT domain	N-methylation domain

NMR	nuclear magnetic resonance
NOESY	nuclear overhauser effect spectroscopy
NRPs	nonribosomal peptides
NRPS	nonribosomal peptide synthetases
nt	nucleotide
OD	optical density
ORF	open reading frame
ori	origin of replication
oriT	origin of transfer
Ox domain	oxidation domain
PCP	peptidyl carrier peptide
PCR	polymerase chain reaction
PDB	Precursor-directed biosynthesis
PEG	polyethylene glycol
PKs	polyketides
PKS	polyketide synthase
PKSs	polyketide synthases
PKs-NRPs	hybrids of polyketides and nonribosomal peptides
PLP	pyridoxal phosphate
(p)ppGpp	guanosine pentaphosphate
PPTase	phosphopantethienyl transferase
r	resistance
RBS	ribosomal binding site
rcf	relative centrifugal force
RED	undecylprodigiosin
Red domain	Reduction domain
RNA	ribonucleic acid
ROESY	rotating frame nuclear overhauser effect spectroscopy
rpm	revolutions per minute

RT	room temperature
RT-PCR	reverse transcription polymerase chain reaction
S.	*Streptomyces*
s	sensitive
SAM	s-adenosylmethionine
SAR	structure activity relationship
SARP	*Streptomyces* antibiotic regulatory protein
SDS	sodium dodecyl sulphate
SDS-PAGE	sodium dodecyl sulfate polyacrylamide gel electrophoresis
sec	second/seconds
SSC	solution of sodium citrate
STSs	stilbene synthases
TAE buffer	tris-acetic acid EDTA buffer
TCA	trichloroacetic acid
T domain	thiolation domain
TE domain	termination domain
TE buffer	Tris-EDTA buffer
TEMED	tetramethylethylenediamine
TOCSY	total correlation spectroscopy
trans-AT PKs	*trans*-AT polyketides
tsr/Thio^{R}	thiostrepton resistance gene
Tra	transfer protein
UV	ultra-violet
whi	gene involved in *Streptomyces* differentiation
X-gal	5-bromo-4-chloro-3-indolyl beta-D-galactopyranoside

References

Anderson, C.T., Wallace, I.S., and Somerville, C.R. (2012). Metabolic click-labeling with a fucose analog reveals pectin delivery, architecture, and dynamics in *Arabidopsis* cell walls. Proc. Natl. Acad. Sci. USA *109*, 1329-1334.

Andres, N., Wolf, H., and Zahner, H. (1990). Hormaomycin, a new peptide lactone antibiotic effective in inducing cytodifferentiation and antibiotic biosynthesis in some *Streptomyces* species. Z. Naturforsch. (C) *45*, 850-855.

Andres, N., Wolf, H., Zahner, H., Rossner, E., Zeeck, A., Konig, W.A., and Sinnwell, V. (1989). Hormaomycin, a novel peptide lactone with morphogenetic activity on *Streptomyces*. Helv. Chim. Acta. *72*, 426-437.

Angert, E.R. (2005). Alternatives to binary fission in bacteria. Nat. Rev. Microbiol. *3*, 214-224.

Ankenbauer, R.G., Staley, A.L., Rinehart, K.L., and Cox, C.D. (1991). Mutasynthesis of siderophore analogues by *Pseudomonas aeruginosa*. Proc. Natl. Acad. Sci. USA *88*, 1878-1882.

Arias, P., Fernandez-Moreno, M.A., and Malpartida, F. (1999). Characterization of the pathway-specific positive transcriptional regulator for actinorhodin biosynthesis in *Streptomyces coelicolor* A3(2) as a DNA-binding protein. J. Bacteriol. *181*, 6958-6968.

Atta, M., Mulliez, E., Arragain, S., Forouhar, F., Hunt, J.F., and Fontecave, M. (2010). *S*-adenosylmethionine-dependent radical-based modification of biological macromolecules. Curr. Opin. Struc. Biol *20*, 684-692.

Austin, M.B., and Noel, A.J.P. (2003). The chalcone synthase superfamily of type III polyketide synthases. Nat. Prod. Rep. *20*, 79-110.

Baltz, R.H., and Matsushima, P. (1981). Protoplast fusion in *Streptomyces*: conditions for efficient genetic recombination and cell regeneration. J. Gen. Microbiol. *127*, 137-146.

Banskota, A.H., McAlpine, J.B., Sorensen, D., Ibrahim, A., Aouidate, M., Piraee, M., Alarco, A.M., Farnet, C.M., and Zazopoulos, E. (2006). Genomic analyses lead to novel secondary metabolites. J. Antibiot. *59*, 533-542.

Barabas, G., Penyige, A., and Hirano, T. (1994). Hormone-like factors influencing differentiation of *Streptomyces* cultures. FEMS Microbiol. Rev. *14*, 75-82.

Bentley, S.D., Chater, K.F., Cerdeno-Tarraga, A.M., Challis, G.L., Thomson, N.R., James, K.D., Harris, D.E., Quail, M.A., Kieser, H., Harper, D., et al. (2002). Complete genome sequence of the model actinomycete *Streptomyces coelicolor* A3(2). Nature *417*, 141-147.

Beppu, T. (1992). Secondary metabolites as chemical signals for cellular differentiation. Gene *115*, 159-165.

Bergmann, S., Schumann, J., Scherlach, K., Lange, C., Brakhage, A.A., and Hertweck, C. (2007). Genomics-driven discovery of PKS-NRPS hybrid metabolites from *Aspergillus nidulans*. Nat. Chem. Biol. *3*, 213-217.

Bertrand, S., Schumpp, O., Bohni, N., Monod, M., Gindro, K., and Wolfender, J.-L. (2013). *De novo* production of metabolites by fungal co-culture of *Trichophyton rubrum* and *Bionectria ochroleuca*. J. Nat. Prod. 10.1021/np400258f.

Bibb, M.J. (2005). Regulation of secondary metabolism in streptomycetes. Curr. Opin. Microbiol. *8*, 208-215.

Bibb, M.J., Janssen, G.R., and Ward, J.M. (1985). Cloning and analysis of the promoter region of the erythromycin resistance gene (*ermE*) of *Streptomyces erythraeus*. Gene *38*, 215-226.

Bibb, M.J., Molle, V., and Buttner, M.J. (2000). σ^{BldN}, an extracytoplasmic function RNA polymerase sigma factor required for aerial mycelium formation in *Streptomyces coelicolor* A3(2). J. Bacteriol. *182*, 4606-4616.

Bibb, M.J., Ward, J.M., and Hopwood, D.A. (1978). Transformation of plasmid DNA into *Streptomyces* at high-frequency. Nature *274*, 398-400.

Bierman, M., Logan, R., O'Brien, K., Seno, E.T., Rao, R.N., and Schoner, B.E. . (1992). Plasmid cloning vectors for the conjugal transfer of DNA from *Escherichia coli* to *Streptomyces* spp. Gene *116*, 43-49.

Bignell, D.R., Warawa, J.L., Strap, J.L., Chater, K.F., and Leskiw, B.K. . (2000). Study of the *bldG* locus suggests that an anti-anti-σ factor and an anti-σ factor may be involved in *Streptomyces coelicolor* antibiotic production and sporulation. Microbiology *146*, 2161-2173.

Birch, A.J. (1963). The biosynthesis of antibiotics. Pure and Appl. Chem., 527-538.

Bok, J.W., Hoffmeister, D., Maggio-Hall, L.A., Murillo, R., Glasner, J.D., and Keller, N.P. (2006). Genomic mining for *Aspergillus* natural products. Chem. Biol. *13*, 31-37.

Bormann, C., Lauer, B., Kalmanczhelyi, A., Sussmuth, R., and Jung, G. (1999). Novel nikkomycins Lx and Lz produced by genetically engineered *Streptomyces tendae* Tü901. J. Antibiot. *52*, 582-585.

Brandl, M., Kozhushkov, S.I., Zlatopolskiy, B.D., Alvermann, P., Geers, B., Zeeck, A., and de Meijere, A. (2005). The biosynthesis of 3-(*trans*-2-nitrocyclopropyl)alanine, a constituent of the signal metabolite hormaomycin. Eur. J. Org. Chem. *1*, 123-135.

Brautaset, T., Sekurova, O.N., Sletta, H., Ellingsen, T.E., Strom, A.R., Valla, S., and Zotchev, S.B. (2000). Biosynthesis of the polyene antifungal antibiotic nystatin in *Streptomyces noursei*

ATCC 11455: analysis of the gene cluster and deduction of the biosynthetic pathway. Chem. Biol. *7*, 395-403.

Cacho, R.A., Jiang, W., Chooi, Y.H., Walsh, C.T., and Tang, Y. (2012). Identification and characterization of the echinocandin B biosynthetic gene cluster from *Emericella rugulosa* NRRL 11440. J. Am. Chem. Soc. *134*, 16781-16790.

Capstick, D.S., Willey, J.M., Buttner, M.J., and Elliot, M.A. (2007). SapB and the chaplins: connections between morphogenetic proteins in *Streptomyces coelicolor*. Mol. Microbiol. *64*, 602-613.

Chakraburtty, R., and Bibb, M. (1997). The ppGpp synthetase gene (*relA*) of *Streptomyces coelicolor* A3(2) plays a conditional role in antibiotic production and morphological differentiation. J. Bacteriol. *179*, 5854-5861.

Challis, G.L. (2008a). Genome mining for novel natural product discovery. J. Med. Chem. *51*, 2618-2628.

Challis, G.L. (2008b). Mining microbial genomes for new natural products and biosynthetic pathways. Microbiology *154*, 1555-1569.

Challis, G.L., and Ravel, J. (2000). Coelichelin, a new peptide siderophore encoded by the *Streptomyces coelicolor* genome: structure prediction from the sequence of its non-ribosomal peptide synthetase. FEMS Microbiol. Lett. *187*, 111-114.

Challis, G.L., Ravel, J., and Townsend, C.A. (2000). Predictive, structure-based model of amino acid recognition by nonribosomal peptide synthetase adenylation domains. Chem. Biol. *7*, 211-224.

Champness, W.C. (1988). New loci required for *Streptomyces coelicolor* morphological and physiological differentiation J. Bacteriol. *170*, 1168-1174.

Chater, K. (1999). David Hopwood and the emergence of *Streptomyces* genetics. Int. Microbiol. *2*, 61-68.

Chater, K.F. (2001). Regulation of sporulation in *Streptomyces coelicolor* A3(2): a checkpoint multiplex? Curr. Opin. Microbiol. *4*, 667-673.

Chater, K.F., and Chandra, G. (2008). The use of the rare UUA codon to define "expression space" for genes involved in secondary metabolism, development and environmental adaptation in *Streptomyces*. J. Microbiol. *46*, 1-11.

Chen, C.H., Lang, G., Mitova, M.I., Murphy, A.C., Cole, A.L.J., Din, L.B., Blunt, J.W., and Munro, M.H.G. (2006). Pteratides I-IV, new cytotoxic cyclodepsipeptides from the Malaysian *Basidiomycete Pterula* sp. J. Org. Chem. *71*, 7947-7951.

Chen, X.H., Koumoutsi, A., Scholz, R., Eisenreich, A., Schneider, K., Heinemeyer, I.,

Morgenstern, B., Voss, B., Hess, W.R., Reva, O., et al. (2007). Comparative analysis of the complete genome sequence of the plant growth-promoting bacterium *Bacillus amyloliquefaciens* FZB42. Nat. Biotechnol. *25*, 1007-1014.

Chen, Y.H., Yin, M., Horsman, G.P., and Shen, B. (2011). Improvement of the enediyne antitumor antibiotic C-1027 production by manipulating its biosynthetic pathway regulation in *Streptomyces globisporus*. J. Nat. Prod. *74*, 420-424.

Cheng, Y.Q., Tang, G.L., and Shen, B. (2003). Type I polyketide synthase requiring a discrete acyltransferase for polyketide biosynthesis. Proc. Natl. Acad. Sci. USA *100*, 3149-3154.

Chou, W.K.W., Fanizza, I., Uchiyama, T., Komatsu, M., Ikeda, H., and Cane, D.E. (2010). Genome mining in *Streptomyces avermitilis*: cloning and characterization of SAV-76, the synthase for a new sesquiterpene, avermitilol. J. Am. Chem. Soc. *132*, 8850-8851.

Claessen, D., de Jong, W., Dijkhuizen, L., and Wosten, H.A.B. (2006). Regulation of *Streptomyces* development: reach for the sky! Trends Microbiol. *14*, 313-319.

Colabroy, K.L., Hackett, W.T., Markham, A.J., Rosenberg, J., Cohen, D.E., and Jacobson, A. (2008). Biochemical characterization of L-DOPA 2,3-dioxygenase, a single-domain type I extradiol dioxygenase from lincomycin biosynthesis. Arch. Biochem. Biophys. *479*, 131-138.

Condurso, H.L., and Bruner, S.D. (2012). Structure and noncanonical chemistry of nonribosomal peptide biosynthetic machinery. Nat. Prod. Rep. *29*, 1099-1110.

Cortes, J., Haydock, S.F., Roberts, G.A., Bevitt, D.J., and Leadlay, P.F. (1990). An unusually large multifunctional polypeptide in the erythromycin-producing polyketide synthase of *Saccharopolyspora erythraea*. Nature *348*, 176-178.

Crone, W.J.K., Leeper, F.J., and Truman, A.W. (2012). Identification and characterisation of the gene cluster for the anti-MRSA antibiotic bottromycin: expanding the biosynthetic diversity of ribosomal peptides. Chem. Sci. *3*, 3516-3521.

Crüsemann, M. (2012). Studien zur Biosynthese des Hormaomycins., Universität Bonn.

Crüsemann, M., Kohlhaas, C., and Piel, J. (2013). Evolution-guided engineering of nonribosomal peptide synthetase adenylation domains. Chem. Sci. *4*, 1041-1045.

D'Alia, D., Eggle, D., Nieselt, K., Hu, W.S., Breitling, R., and Takano, E. (2011). Deletion of the signalling molecule synthase ScbA has pleiotropic effects on secondary metabolite biosynthesis, morphological differentiation and primary metabolism in *Streptomyces coelicolor* A3(2). Microb. Biotechno. *4*, 239-251.

Dangel, V., Eustaquio, A.S., Gust, B., and Heide, L. (2008). *novE* and *novG* act as positive regulators of novobiocin biosynthesis. Arch. Microbiol. *190*, 509-519.

Datsenko, K.A., and Wanner, B.L. (2000). One-step inactivation of chromosomal genes in

Escherichia coli K-12 using PCR products. Proc. Natl. Acad. Sci. USA *97*, 6640-6645.

de la Fuente, A., Lorenzana, L.M., Martin, J.F., and Liras, P. (2002). Mutants of *Streptomyces clavuligerus* with disruptions in different genes for clavulanic acid biosynthesis produce large amounts of holomycin: possible cross-regulation of two unrelated secondary metabolic pathways. J. Bacteriol. *184*, 6559-6565.

Deiters, A., Cropp, T.A., Mukherji, M., Chin, J.W., Anderson, J.C., and Schultz, P.G. (2003). Adding amino acids with novel reactivity to the genetic code of *Saccharomyces cerevisiae*. J. Am. Chem. Soc. *125*, 11782-11783.

Delzer, J., Fiedler, H.P., Muller, H., Zahner, H., Rathmann, R., Ernst, K., and Konig, W.A. (1984). New nikkomycins by mutasynthesis and directed fermentation. J. Antibiot. *37*, 80-82.

Demain, A.L., and Elander, R.P. (1999). The β-lactam antibiotics: past, present, and future. Ant. v. Leeuwenhoek *75*, 5-19.

Derouaux, A., Dehareng, D., Lecocq, E., Halici, S., Nothaft, H., Giannotta, F., Moutzourelis, G., Dusart, J., Devreese, B., Titgemeyer, F., et al. (2004a). wsCrp of *Streptomyces coelicolor* is the third transcription factor of the large CRP-FNR superfamily able to bind cAMP. Biochem. Bioph. Res. Co *325*, 983-990.

Derouaux, A., Halici, S., Nothaft, H., Neutelings, T., Moutzourelis, G., Dusart, J., Titgemeyer, F., and Rigali, S. (2004b). Deletion of a cyclic AMP receptor protein homologue diminishes germination and affects morphological development of *Streptomyces coelicolor*. J. Bacteriol. *186*, 1893-1897.

Donadio, S., and Katz, L. (1992). Organization of the enzymatic domains in the multifunctional polyketide synthase involved in erythromycin formation in *Saccharopolyspora erythraea*. Gene *111*, 51-60.

Dorrestein, P.C., Yeh, E., Garneau-Tsodikova, S., Kelleher, N.L., and Walsh, C.T. (2005). Dichlorination of a pyrrolyl-S-carrier protein by $FADH_2$-dependent halogenase PltA during pyoluteorin biosynthesis. Proc. Natl. Acad. Sci. USA *102*, 13843-13848.

Elliot, M., Damji, F., Passantino, R., Chater, K., and Leskiw, B. . (1998). The *bldD* gene of *Streptomyces coelicolor* A3(2): a regulatory gene involved in morphogenesis and antibioticproduction. J. Bacteriol. *180*, 1549-1555.

Elliot, M.A., Bibb, M.J., Buttner, M.J., and Leskiw, B.K. (2001). BldD is a direct regulator of key developmental genes in *Streptomyces coelicolor* A3(2). Mol. Microbiol. *40*, 257-269.

Eppelmann, K., Stachelhaus, T., and Marahiel, M.A. (2002). Exploitation of the selectivity-conferring code of nonribosomal peptide synthetases for the rational design of novel peptide antibiotics. Biochemistry *41*, 9718-9726.

Eustaquio, A.S., Gust, B., Li, S.M., Pelzer, S., Wohlleben, W., Chater, K.F., and Heide, L.

(2004). Production of 8'-halogenated and 8'-unsubstituted novobiocin derivatives in genetically engineered *Streptomyces coelicolor* strains. Chem. Biol. *11*, 1561-1572.

Felnagle, E.A., Barkei, J.J., Park, H., Podevels, A.M., McMahon, M.D., Drott, D.W., and Thomas, M.G. (2010). MbtH-like proteins as integral components of bacterial nonribosomal peptide synthetases. Biochemistry *49*, 8815-8817.

Felnagle, E.A., Jackson, E.E., Chan, Y.A., Podevels, A.M., Berti, A.D., McMahon, M.D., and Thomas, M.G. (2008). Nonribosomal peptide synthetases involved in the production of medically relevant natural products. Mol. Pharm. *5*, 191-211.

Fenical, W., and Jensen, P.R. (2006). Developing a new resource for drug discovery: marine actinomycete bacteria. Nat. Chem. Biol. *2*, 666-673.

Finking, R., and Marahiel, M.A. (2004). Biosynthesis of nonribosomal peptides1. Annual Review Of Microbiology *58*, 453-488.

Fischbach, M.A., and Walsh, C.T. (2006). Assembly-line enzymology for polyketide and nonribosomal peptide antibiotics: logic, machinery, and mechanisms. Chem. Rev. *106*, 3468-3496.

Flärdh, K., and Buttner, M.J. (2009). *Streptomyces* morphogenetics: dissecting differentiation in a filamentous bacterium. Nat. Rev. Microbiol. *7*, 36-49.

Flett, F., Mersinias, V., and Smith, C.P. (1997). High efficiency intergeneric conjugal transfer of plasmid DNA from *Escherichia coli* to methyl DNA-restricting streptomycetes. FEMS Microbiol. Lett. *155*, 223-229.

Floss, H.G. (2006). Combinatorial biosynthesis-potential and problems. J. Biotechnol. *124*, 242-257.

Freeman, M.F., Gurgui, C., Helf, M.J., Morinaka, B.I., Uria, A.R., Oldham, N.J., Sahl, H.G., Matsunaga, S., and Piel, J. (2012). Metagenome mining reveals polytheonamides as posttranslationally modified ribosomal peptides. Science *338*, 387-390.

Frey, P.A., Hegeman, A.D., and Ruzicka, F.J. (2008). The radical SAM superfamily. Crit. Rev. Biochem. *43*, 63-88.

Funa, N., Awakawa, T., and Horinouchi, S. (2007). Pentaketide resorcylic acid synthesis by type III polyketide synthase from *Neurospora crassa*. J. Biol. Chem. *282*, 14476-14481.

Funa, N., Ohnishi, Y., Fujii, I., Shibuya, M., Ebizuka, Y., and Horinouchi, S. (1999). A new pathway for polyketide synthesis in microorganisms. Nature *400*, 897-899.

Galm, U., Heller, S., Shapiro, S., Page, M., Li, S.M., and Heide, L. (2004). Antimicrobial and DNA gyrase-inhibitory activities of novel clorobiocin derivatives produced by mutasynthesis. Antimicrob. Agents Chemother. *48*, 1307-1312.

Galperin, M.Y. (2004). Bacterial signal transduction network in a genomic perspective. . Environ. Microbiol. *6*, 552-567.

Gao, C., Hindra, Mulder, D., Yin, C., and Elliot, M.A. (2012). Crp is a global regulator of antibiotic production in *Streptomyces*. mBio *3*.

Garneau-Tsodikova, S., Dorrestein, P.C., Kelleher, N.L., and Walsh, C.T. (2006). Protein assembly line components in prodigiosin biosynthesis: characterization of PigA,G,H,I,J. J. Am. Chem. Soc. *128*, 12600-12601.

Garneau, S., Dorrestein, P.C., Kelleher, N.L., and Walsh, C.T. (2005). Characterization of the formation of the pyrrole moiety during clorobiocin and coumermycin A1 biosynthesis. Biochemistry *44*, 2770-2780.

Gottelt, M., Kol, S., Gomez-Escribano, J.P., Bibb, M., and Takano, E. (2010). Deletion of a regulatory gene within the *cpk* gene cluster reveals novel antibacterial activity in *Streptomyces coelicolor* A3(2). Microbiology *156*, 2343-2353.

Gramajo, H.C., Takano, E., and Bibb, M.J. (1993). Stationary-phase production of the antibiotic actinorhodin in *Streptomyces coelicolor* A3(2) is transcriptionally regulated. Mol. Microbiol. *7*, 837-845.

Grogan, D.W., and Cronan, J.E. (1997). Cyclopropane ring formation in membrane lipids of bacteria. Microbiol. Mol. Biol. R *61*, 429-441.

Gross, H., Stockwell, V.O., Henkels, M.D., Nowak-Thompson, B., Loper, J.E., and Gerwick, W.H. (2007). The genomisotopic approach: a systematic method to isolate products of orphan biosynthetic gene clusters. Chem. Biol. *14*, 53-63.

Gu, L.C., Wang, B., Kulkarni, A., Geders, T.W., Grindberg, R.V., Gerwick, L., Hakansson, K., Wipf, P., Smith, J.L., Gerwick, W.H., et al. (2009). Metamorphic enzyme assembly in polyketide diversification. Nature *459*, 731-735.

Gust, B., Challis, G.L., Fowler, K., Kieser, T., and Chater, K.F. (2003). PCR-targeted *Streptomyces* gene replacement identifies a protein domain needed for biosynthesis of the sesquiterpene soil odor geosmin. Proc. Natl. Acad. Sci. USA *100*, 1541-1546.

Hahn, D.R., Solenberg, P.J., McHenney, M.A., and Baltz, R.H. (1991). Transposition and transduction of plasmid DNA in *Streptomyces* spp. J. Ind. Microbiol. *7*, 229-234.

Hanahan, D. (1983). Studies on transformation of *Escherichia coli* with plasmids. J. Mol. Biol. *166*, 557-580.

Harvey, C.J., Puglisi, J.D., Pande, V.S., Cane, D.E., and Khosla, C. (2012). Precursor directed biosynthesis of an orthogonally functional erythromycin analogue: selectivity in the ribosome macrolide binding pocket. J. Am. Chem. Soc. *134*, 12259-12265.

Hashimoto, M., Hayashi, K., Murai, M., Fujii, T., Nishikawa, M., Kiyoto, S., Okuhara, M., Kohsaka, M., and Imanaka, H. (1992). WS9326A, a novel tachykinin antagonist isolated from *Streptomyces violaceusniger* No. 9326. II. Biological and pharmacological properties of WS9326A and tetrahydro-WS9326A (FK224). J. Antibiot. *45*, 1064-1070.

Hassall, C.H., Morton, R.B., Ogihara, Y., and Phillips, D.A.S. (1971). Amino-acids and peptides. Part XII. The molecular structures of the monamycins, cyclodepsipeptide antibiotics. J. Chem. Soc. *0*, 526-532.

Haydock, S.F., Aparicio, J.F., Molnar, I., Schwecke, T., Khaw, L.E., Konig, A., Marsden, A.F., Galloway, I.S., Staunton, J., and Leadlay, P.F. (1995). Divergent sequence motifs correlated with the substrate specificity of (methyl)malonyl-CoA:acyl carrier protein transacylase domains in modular polyketide synthases. FEBS. Lett. *374*, 246-248.

He, M. (2006). Pipecolic acid in microbes: biosynthetic routes and enzymes. J. Ind. Microbiol. Biotechnol. *33*, 401-407.

Heide, L., Westrich, L., Anderle, C., Gust, B., Kammerer, B., and Piel, J. (2008). Use of a halogenase of hormaomycin biosynthesis for formation of new clorobiocin analogues with 5-chloropyrrole moieties. Chembiochem *9*, 1992-1999.

Henikoff, S., Wallace, J.C., and Brown, J.P. (1990). Finding protein similarities with nucleotide sequence databases. Methods Enzymol. *183*, 111-132.

Hertweck, C. (2009). The biosynthetic logic of polyketide diversity. Angew Chem. Int. Ed. *48*, 4688-4716.

Hesketh, A., Chen, W.Q., Ryding, J., Chang, S., and Bibb, M. (2007). The global role of ppGpp synthesis in morphological differentiation and antibiotic production in *Streptomyces coelicolor* A3(2). Genome Biol. *8*.

Hesketh, A., Sun, J., and Bibb, M. (2001). Induction of ppGpp synthesis in *Streptomyces coelicolor* A3(2) grown under conditions of nutritional sufficiency elicits *act*II-ORF4 transcription and actinorhodin biosynthesis. Mol. Microbiol. *39*, 136-144.

Hibi, M., Kawashima, T., Kodera, T., Smirnov, S.V., Sokolov, P.M., Sugiyama, M., Shimizu, S., Yokozeki, K., and Ogawa, J. (2011). Characterization of *Bacillus thuringiensis* L-Isoleucine dioxygenase for production of useful amino acids. Appl. Environ. Microb. *77*, 6926-6930.

Höfer, I., Crüsemann, M., Radzom, M., Geers, B., Flachshaar, D., Cai, X.F., Zeeck, A., and Piel, J. (2011). Insights into the biosynthesis of hormaomycin, an exceptionally complex bacterial signaling metabolite. Chem. Biol. *18*, 381-391.

Hong, V., Steinmetz, N.F., Manchester, M., and Finn, M.G. (2010). Labeling live cells by copper-catalyzed alkyne-azide click chemistry. Bioconjugate. Chem. *21*, 1912-1916.

Hopwood, D.A. (1999). Forty years of genetics with *Streptomyces*: from *in vivo* through *in vitro*

to *in silico*. Microbiology *145*, 20.

Hopwood, D.A. (1967). Genetic analysis and genome structure in *Streptomyces coelicolor*. Bacteriol. Rev. *31*, 373-403.

Hopwood, D.A. (2006). Soil to genomics: the *Streptomyces* chromosome. Annu. Rev. Genet. *40*, 1-23.

Hopwood, D.A. (2007). *Streptomyces* in nature and medicine: the antibiotic makers. (Oxford University Press: Oxford.

Hopwood, D.A., Malpartida, F., Kieser, H.M., Ikeda, H., Duncan, J., Fujii, I., Rudd, B.A.M., Floss, H.G., and Omura, S. (1985). Production of 'hybrid' antibiotics by genetic engineering. Nature *314*, 642-644.

Hopwood, D.A., Wright, H.M., and Bibb, M.J. (1977). Genetic recombination through protoplast fusion in *Streptomyces*. Nature *268*, 171-174.

Horinouchi, S. (2002). A microbial hormone, A-factor, as a master switch for morphological differentiation and secondary metabolism in *Streptomyces griseus*. Front. Biosci. *7*, D2045-D2057.

Horinouchi, S. (2007). Mining and polishing of the treasure trove in the bacterial genus *Streptomyces*. Biosci. Biotech. Bioch *71*, 283-299.

Horinouchi, S. (1996). *Streptomyces* genes involved in aerial mycelium formation. FEMS Microbiol. Lett. *141*, 1-9.

Horinouchi, S., and Beppu, T. (1992). Autoregulatory factors and communication in actinomycetes. Annu. Rev. Microbiol. *46*, 377-398.

Hu, Y., Phelan, V., Ntai, I., Farnet, C.M., Zazopoulos, E., and Bachmann, B.O. (2007). Benzodiazepine biosynthesis in *Streptomyces refuineus*. Chem. Biol. *14*, 691-701.

Hu, Z., Bao, K., Zhou, X., Zhou, Q., Hopwood, D.A., Kieser, T., and Deng, Z. (1994). Repeated polyketide synthase modules involved in the biosynthesis of a heptaene macrolide by *Streptomyces* sp. FR-008. Mol. Microbiol. *14*, 163-172.

Huang, J., Shi, J., Molle, V., Sohlberg, B., Weaver, D., Bibb, M.J., Karoonuthaisiri, N., Lih, C.J., Kao, C.M., Buttner, M.J., et al. (2005). Cross-regulation among disparate antibiotic biosynthetic pathways of *Streptomyces coelicolor*. Mol. Microbiol. *58*, 1276-1287.

Hulme, A.C., and Arthington, W. (1954). Methyl proline in young apple fruits. Nature *173*, 588-589.

Hunt, A.C., Servin-Gonzalez, L., Kelemen, G.H., and Buttner, M.J. (2005). The *bldC* developmental locus of *Streptomyces coelicolor* encodes a member of a family of small

DNA-binding proteins related to the DNA-binding domains of the MerR family. J. Bacteriol. *187*, 716-728.

Huo, L.J., Rachid, S., Stadler, M., Wenzel, S.C., and Muller, R. (2012). Synthetic biotechnology to study and engineer ribosomal bottromycin biosynthesis. Chem. Biol. *19*, 1278-1287.

Hurley, L.H. (1980). Elucidation and formulation of novel biosynthetic pathways leading to the pyrrolo[1,4]benzodiazepine antibiotics anthramycin, tomaymycin, and sibiromycin. Acc. Chem. Res. *13*, 263-269.

Hwang, Y.S., Kim, E.S., Biro, S., and Choi, C.Y. (2003). Cloning and analysis of a DNA fragment stimulating avermectin production in various *Streptomyces avermitilis* strains. Appl. Environ. Microb. *69*, 1263-1269.

Igarashi, Y., Kan, Y., Fujii, K., Fujita, T., Harada, K., Naoki, H., Tabata, H., Onaka, H., and Furumai, T. (2001). Goadsporin, a chemical substance which promotes secondary metabolism and morphogenesis in streptomycetes II. Structure determination. J. Antibiot. *54*, 1045-1053.

Ikeda, H., Ishikawa, J., Hanamoto, A., Shinose, M., Kikuchi, H., Shiba, T., Sakaki, Y., Hattori, M., and Omura, S. (2003). Complete genome sequence and comparative analysis of the industrial microorganism *Streptomyces avermitilis*. Nat. Biotechnol. *21*, 526-531.

Ikeda, H., and Omura, S. (1995). Control of avermectin biosynthesis in *Streptomyces avermitilis* for the selective production of a useful component. J. Antibiot. *48*, 549-562.

Jenke-Kodama, H., Borner, T., and Dittmann, E. (2006). Natural biocombinatorics in the polyketide synthase genes of the actinobacterium *Streptomyces avermitilis*. PLoS Comput. Biol. *2*, 1210-1218.

Johnson, R.S., Martin, S.A., Biemann, K., Stults, J.T., and Watson, J.T. (1987). Novel fragmentation process of peptides by collision-induced decomposition in a tandem mass spectrometer: differentiation of leucine and isoleucine. Anal. Chem. *59*, 2621-2625.

Joshi, M.V., Bignell, D.R.D., Johnson, E.G., Sparks, J.P., Gibson, D.M., and Loria, R. (2007). The AraC/XylS regulator TxtR modulates thaxtomin biosynthesis and virulence in Streptomyces scabies. Mol. Microbiol. *66*, 633-642.

Katz, E., Williams, W.K., Mason, K.T., and Mauger, A.B. (1977). Novel actinomycins formed by biosynthetic incorporation of *cis*- and *trans*-4-methylproline. Antimicrob. Agents Chemother. *11*, 1056-1063.

Kelemen, G.H., and Buttner, M.J. (1998). Initiation of aerial mycelium formation in *Streptomyces*. Curr. Opin. Microbiol. *1*, 656-662.

Kelly, W.L., Boyne, M.T., 2nd, Yeh, E., Vosburg, D.A., Galonic, D.P., Kelleher, N.L., and Walsh, C.T. (2007). Characterization of the aminocarboxycyclopropane-forming enzyme

CmaC. Biochemistry *46*, 359-368.

Kennedy, J. (2008). Mutasynthesis, chemobiosynthesis, and back to semi-synthesis: combining synthetic chemistry and biosynthetic engineering for diversifying natural products. Nat. Prod. Rep. *25*, 25-34.

Kennedy, J., Auclair, K., Kendrew, S.G., Park, C., Vederas, J.C., and Hutchinson, C.R. (1999). Modulation of polyketide synthase activity by accessory proteins during lovastatin biosynthesis. Science *284*, 1368-1372.

Kenneth, L., and Rinehart, Jr. (1977). Mutasynthesis of new antibiotics. Pure and Appl. Chem. *49*, 1361-1384.

Khokhlov, A.S., Tovarova, II, Borisova, L.N., Pliner, S.A., Shevchenko, L.N., Kornitskaia, E., Ivkina, N.S., and Rapoport, I.A. (1967). The A-factor, responsible for streptomycin biosynthesis by mutant strains of *Actinomyces streptomycini*. Dokl. Akad. Nauk SSSR *177*, 232-235.

Kieser, H.M., Kieser, T., and Hopwood, D.A. (1992). A combined genetic and physical map of the *Streptomyces coelicolor* A3(2) chromosome. J. Bacteriol. *174*, 5496-5507.

Kieser, T., Bibb, M.J., Buttner, M.J., Chater, K.F., and Hopwood, D.A. (2000). Practical *Steptomyces* genetics. (The John Innes Foundation, Norwich.

Kitani, S., Miyamoto, K.T., Takamatsu, S., Herawati, E., Iguchi, H., Nishitomi, K., Uchida, M., Nagamitsu, T., Omura, S., Ikeda, H., et al. (2011). Avenolide, a *Streptomyces* hormone controlling antibiotic production in *Streptomyces avermitilis*. Proc. Natl. Acad. Sci. USA *108*, 16410-16415.

Knobloch, T., Harmrolfs, K., Taft, F., Thomaszewski, B., Sasse, F., and Kirschning, A. (2011). Mutational biosynthesis of ansamitocin antibiotics: a diversity-oriented approach to exploit biosynthetic flexibility. Chembiochem *12*, 540-547.

Kodani, S., Hudson, M.E., Durrant, M.C., Buttner, M.J., Nodwell, J.R., and Willey, J.M. (2004). The SapB morphogen is a lantibiotic-like peptide derived from the product of the developmental gene *ramS* in *Streptomyces coelicolor*. Proc. Natl. Acad. Sci. USA *101*, 11448-11453.

Kolb, H.C., Finn, M.G., and Sharpless, K.B. (2001). Click Chemistry: diverse chemical function from a few good reactions. Angew Chem. Int. Ed. Engl. *40*, 2004-2021.

Komatsu, M., Tsuda, M., Omura, S., Oikawa, H., and Ikeda, H. (2008). Identification and functional analysis of genes controlling biosynthesis of 2-methylisoborneol. Proc. Natl. Acad. Sci. USA *105*, 7422-7427.

Kondo, S., Yasui, K., Natsume, M., Katayama, M., and Marumo, S. (1988). Isolation, physico-chemical properties and biological activity of pamamycin-607, an aerial

mycelium-inducing substance from *Streptomyces alboniger*. J. Antibiot. *41*, 1196-1204.

König, C.C., Scherlach, K., Schroeckh, V., Horn, F., Nietzsche, S., Brakhage, A.A., and Hertweck, C. (2013). Bacterium induces cryptic meroterpenoid pathway in the pathogenic fungus *Aspergillus fumigatus*. Chembiochem *14*, 938-942.

Korner, H., Sofia, H.J., and Zumft, W.G. (2003). Phylogeny of the bacterial superfamily of Crp-Fnr transcription regulators: exploiting the metabolic spectrum by controlling alternative gene programs. FEMS Microbiol. Rev. *27*, 559-592.

Kozhushkov, S.I., Zlatopolskiy, B.D., Brandl, M., Alvermann, P., Radzom, M., Geers, B., de Meijere, A., and Zeeck, A. (2005). Hormaomycin analogues by precursor-directed biosynthesis-synthesis of and feeding experiments with amino acids related to the unique 3-(*trans*-2 '-nitrocyclopropyl)alanine constituent. Eur. J. Org. Chem. 10.1002/ejoc.200400608, 854-863.

Lambrecht, J.A., Browne, B.A., and Downs, D.M. (2010). Members of the YjgF/YER057c/UK114 family of proteins inhibit phosphoribosylamine synthesis *in vitro*. J. Biol. Chem. *285*, 34401-34407.

Lautru, S., Deeth, R.J., Bailey, L.M., and Challis, G.L. (2005). Discovery of a new peptide natural product by *Streptomyces coelicolor* genome mining. Nat. Chem. Biol. *1*, 265-269.

Lawlor, E.J., Baylis, H.A., and Chater, K.F. (1987). Pleiotropic morphological and antibiotic deficiencies result from mutations in a gene encoding a tRNA-like product in *Streptomyces coelicolor* A3(2). Genes Dev. *1*, 1305-1310.

Leadlay, P.F., Staunton, J., Oliynyk, M., Bisang, C., Cortes, J., Frost, E., Hughes-Thomas, Z.A., Jones, M.A., Kendrew, S.G., Lester, J.B., et al. (2001). Engineering of complex polyketide biosynthesis-insights from sequencing of the monensin biosynthetic gene cluster. J. Ind. Microbiol. Biot *27*, 360-367.

Leskiw, B.K., Lawlor, E.J., Fernandezabalos, J.M., and Chater, K.F. (1991). TTA codons in some genes prevent their expression in a class of developmental, antibiotic-negative, *Streptomyces* mutants. Proc. Natl. Acad. Sci. USA *88*, 2461-2465.

Li, L., Deng, W., Song, J., Ding, W., Zhao, Q.F., Peng, C., Song, W.W., Tang, G.L., and Liu, W. (2008). Characterization of the saframycin a gene cluster from *Streptomyces lavendulae* NRRL 11002 revealing a nonribosomal peptide synthetase system for assembling the unusual tetrapeptidyl skeleton in an iterative manner. J. Bacteriol. *190*, 251-263.

Li, W., Chou, S.C., Khullar, A., and Gerratana, B. (2009a). Cloning and characterization of the biosynthetic gene cluster for tomaymycin, an SJG-136 monomeric analog. Appl. Environ. Microb. *75*, 2958-2963.

Li, W., Khullar, A., Chou, S., Sacramo, A., and Gerratana, B. (2009b). Biosynthesis of

sibiromycin, a potent antitumor antibiotic. Appl. Environ. Microb. *75*, 2869-2878.

Lin, X., Hopson, R., and Cane, D.E. (2006). Genome mining in *Streptomyces coelicolor*: molecular cloning and characterization of a new sesquiterpene synthase. J. Am. Chem. Soc. *128*, 6022-6023.

Link, A.J., and Tirrell, D.A. (2003). Cell surface labeling of *Escherichia coli* via copper(I)-catalyzed 3+2 cycloaddition. J. Am. Chem. Soc. *125*, 11164-11165.

Loria, R., Kers, J., and Joshi, M. (2006). Evolution of plant pathogenicity in *Streptomyces*. Annu. Rev. Phytopathol *44*, 469-487.

Luesch, H., Hoffmann, D., Hevel, J.M., Becker, J.E., Golakoti, T., and Moore, R.E. (2003). Biosynthesis of 4-methylproline in cyanobacteria: cloning of *nosE* and *nosF* genes and biochemical characterization of the encoded dehydrogenase and reductase activities. J. Org. Chem. *68*, 83-91.

Luzhetskyy, A., Pelzer, S., and Bechthold, A. (2007). The future of natural products as a source of new antibiotics. Curr. Opin. Investig. Drugs *8*, 608-613.

Madduri, K., Kennedy, J., Rivola, G., Inventi-Solari, A., Filippini, S., Zanuso, G., Colombo, A.L., Gewain, K.M., Occi, J.L., MacNeil, D.J., et al. (1998). Production of the antitumor drug epirubicin (4'-epidoxorubicin) and its precursor by a genetically engineered strain of Streptomyces peucetius. Nat. Biotechnol. *16*, 69-74.

Magnusson, O.T., Toyama, H., Saeki, M., Rojas, A., Reed, J.C., Liddington, R.C., Klinman, J.P., and Schwarzenbacher, R. (2004). Quinone biogenesis: structure and mechanism of PqqC, the final catalyst in the production of pyrroloquinoline quinone. Proc. Natl. Acad. Sci. USA *101*, 7913-7918.

Mangoni, A. (2012). Strategies for structural assignment of marine matural products through advanced NMR-based techniques. In *Handbook of Marine Natural Products* (E. Fattorusso, ed.). (Spinger: Heidelberg, Germany). pp. 519-546.

Martin, R.G., and Rosner, J.L. (2001). The AraC transcriptional activators. Curr. Opin. Microbiol. *4*, 132-137.

Mason, D.J., Dietz, A., and Deboer, C. (1963). Lincomycin, a new antibiotic. I. Discovery and biological properties. J. C. Sylvester, Editor. Antimicrobial Agents and Chemotherapy[long dash]1962. Proceedings Second Interscience Conference on Antimicrobioal Agents and Chemotherapy, <Go to ISI>://BCI:BCI19634400011571, 554-559.

Matseliukh, A.B. (2001). Genetic transformation of *Streptomyces globisporus* strain 1912: restriction barrier and plasmid compatibility. Mikrobiol. Z. (Ukraine). *63*, 15-22.

Matsuno, K., Yamada, Y., Lee, C.K., and Nihira, T. (2004). Identification by gene deletion analysis of *barB* as a negative regulator controlling an early process of virginiamycin

biosynthesis in *Streptomyces virginiae*. Arch. Microbiol. *181*, 52-59.

Matsushima, P., and Baltz, R.H. (1985). Efficient plasmid transformation of *Streptomyces ambofaciens* and *Streptomyces fradiae* protoplasts. J. Bacteriol. *163*, 180-185.

Mazodier, P., Petter, R., and Thompson, C. (1989). Intergeneric conjugation between *Escherichia coli* and *Streptomyces* species. J. Bacteriol. *171*, 3583-3585.

McAlpine, J.B., Bachmann, B.O., Piraee, M., Tremblay, S., Alarco, A.M., Zazopoulos, E., and Farnet, C.M. (2005). Microbial genomics as a guide to drug discovery and structural elucidation: ECO-02301, a novel antifungal agent, as an example. J. Nat. Prod. *68*, 493-496.

McArthur, H.A.I. (1998). The novel avermectin, doramectin-a successful application of mutasynthesis. In *Development in Industrial Microbiology* (C.R. Hutchinson, and McAlpine, J., ed.). (Society for Industrial Microbiology: Fairfax, Virginia). pp. 43-48.

McCormick, J.R., and Flardh, K. (2012). Signals and regulators that govern *Streptomyces* development. FEMS Microbiol. Rev. *36*, 206-231.

McDaniel, R., Thamchaipenet, A., Gustafsson, C. Fu, H., Betlach, M., and Ashley, G. (1999). Multiple genetic modifications of the erythromycin gene cluster to produce a library of novel 'unnatural' natural products. Proc. Natl. Acad. Sci. USA *96*, 1846-1851.

Medema, M.H., Blin, K., Cimermancic, P., de Jager, V., Zakrzewski, P., Fischbach, M.A., Weber, T., Takano, E., and Breitling, R. (2011). antiSMASH: rapid identification, annotation and analysis of secondary metabolite biosynthesis gene clusters in bacterial and fungal genome sequences. Nucleic Acids Res. *39*, 339-346.

Menzella, H.G., and Reeves, C.D. (2007). Combinatorial biosynthesis for drug development. Curr. Opin. Microbiol. *10*, 238-245.

Merrick, M.J. (1976). A morphological and genetic mapping study of bald colony mutants of *Streptomyces coelicolor*. J. Gen. Microbiol. *96*, 299-315.

Moldenhauer, J., Goetz, D.C.G., Albert, C.R., Bischof, S.K., Schneider, K., Suessmuth, R.D., Engeser, M., Gross, H., Bringmann, G., and Piel, J. (2010). The final steps of bacillaene biosynthesis in *Bacillus amyloliquefaciens* FZB42: direct evidence for β, γ dehydration by a *trans*-acyltransferase polyketide synthase. Angew. Chem. Int. Ed. Engl. *49*, 1465-1467.

Molle, V., and Buttner, M.J. (2000). Different alleles of the response regulator gene *bldM* arrest *Streptomyces coelicolor* development at distinct stages. Mol. Microbiol. *36*, 1265-1278.

Morishita, R., Kawagoshi, A., Sawasaki, T., Madin, K., Ogasawara, T., Oka, T., and Endo, Y. (1999). Ribonuclease activity of rat liver perchloric acid-soluble protein, a potent inhibitor of protein synthesis. J. Biol. Chem. *274*, 20688-20692.

Moss, S.J., Carletti, I., Olano, C., Sheridan, R.M., Ward, M., Math, V., Nur-E-Alam, M., Brana,

A.F., Zhang, M.Q., Leadlay, P.F., et al. (2006). Biosynthesis of the angiogenesis inhibitor borrelidin: directed biosynthesis of novel analogues. Chem. Commun. 10.1039/b602931k, 2341-2343.

Nakao, Y., Yoshida, W.Y., Takada, Y., Kimura, J., Yang, L., Mooberry, S.L., and Scheuer, P.J. (2004). Kulokekahilide-2, a cytotoxic depsipeptide from a cephalaspidean mollusk *Philinopsis speciosa*. J. Nat. Prod. *67*, 1332-1340.

Neusser, D., Schmidt, H., Spizek, J., Novotna, J., Peschke, U., Kaschabeck, S., Tichy, P., and Piepersberg, W. (1998). The genes *lmbB1* and *lmbB2* of *Streptomyces lincolnensis* encode enzymes involved in the conversion of L-tyrosine to propylproline during the biosynthesis of the antibiotic lincomycin A. Arch. Microbiol. *169*, 322-332.

Newman, D.J. (2008). Natural products as leads to potential drugs: an old process or the new hope for drug discovery? J. Med. Chem. *51*, 2589-2599.

Nguyen, T., Ishida, K., Jenke-Kodama, H., Dittmann, E., Gurgui, C., Hochmuth, T., Taudien, S., Platzer, M., Hertweck, C., and Piel, J. (2008). Exploiting the mosaic structure of *trans*-acyltransferase polyketide synthases for natural product discovery and pathway dissection. Nat. Biotechnol. *26*, 225-233.

Nodwell, J.R., and Losick, R. (1998). Purification of an extracellular signaling molecule involved in production of aerial mycelium by *Streptomyces coelicolor*. J. Bacteriol. *180*, 1334-1337.

Nodwell, J.R., McGovern, K., and Losick, R. (1996). An oligopeptide permease responsible for the import of an extracellular signal governing aerial mycelium formation in *Streptomyces coelicolor*. Mol. Microbiol. *22*, 881-893.

Nybo, S.E., Shepherd, M.D., Bosserman, M.A., and Rohr, J. (2010). Genetic manipulation of *Streptomyces* species. Curr. Protoc. Microbiol. *6*, 76-83.

Ohnishi, Y., Ishikawa, J., Hara, H., Suzuki, H., Ikenoya, M., Ikeda, H., Yamashita, A., Hattori, M., and Horinouchi, S. (2008). Genome sequence of the streptomycin-producing microorganism *Streptomyces griseus* IFO 13350. J. Bacteriol. *190*, 4050-4060.

Ohnishi, Y., Kameyama, S., Onaka, H., and Horinouchi, S. (1999). The A-factor regulatory cascade leading to streptomycin biosynthesis in *Streptomyces griseus*: identification of a target gene of the A-factor receptor. Mol. Microbiol. *34*, 102-111.

Ohnishi, Y., Yamazaki, H., Kato, J.Y., Tomono, A., and Horinouchi, S. (2005). AdpA, a central transcriptional regulator in the A-factor regulatory cascade that leads to morphological development and secondary metabolism in *Streptomyces griseus*. Biosci. Biotech. Bioch *69*, 431-439.

Oka, T., Tsuji, H., Noda, C., Sakai, K., Hong, Y.M., Suzuki, I., Munoz, S., and Natori, Y. (1995).

Isolation and characterization of a novel perchloric acid soluble protein inhibiting cell free protein. J. Biol. Chem. *270*, 30060-30067.

Omura, S., Mamada, H., Wang, N.J., Imamura, N., Oiwa, R., Iwai, Y., and Muto, N. (1984). Takaokamycin, a new peptide antibiotic produced by *Streptomyces* sp. J. Antibiot. *37*, 700-705.

Onaka, H., Tabata, H., Igarashi, Y., Sato, Y., and Furumai, T. (2001). Goadsporin, a chemical substance which promotes secondary metabolism and morphogenesis in streptomycetes - I. Purification and characterization. J. Antibiot. *54*, 1036-1044.

Otoguro, K., Ui, H., Ishiyama, A., Arai, N., Kobayashi, M., Takahashi, Y., Masuma, R., Shiomi, K., Yamada, H., and Omura, S. (2003). *In vitro* antimalarial activities of the microbial metabolites. J. Antibiot. *56*, 322-324.

Pan, E., Oswald, N.W., Legako, A.G., Life, J.M., Posner, B.A., and MacMillan, J.B. (2013). Precursor-directed generation of amidine containing ammosamide analogs: ammosamides E-P. Chem. Sci. *4*, 482-488.

Peirú, S., Gramajo, H.C., and Menzella, H.G. (2010). Recombinant approaches to large polyketide molecules as potential drugs. Drug Discov. Today *7*, 105-113.

Peschke, U., Schmidt, H., Zhang, H.Z., and Piepersberg, W. (1995). Molecular characterization of the lincomycin-production gene cluster of *Streptomyces lincolnensis* 78-11. Mol. Microbiol. *16*, 1137-1156.

Pfeifer, B., Hu, Z.H., Licari, P., and Khosla, C. (2002). Process and metabolic strategies for improved production of *Escherichia coli*-derived 6-deoxyetythronolide B. Appl. Environ. Microb. *68*, 3287-3292.

Phelan, V.V., Du, Y., McLean, J.A., and Bachmann, B.O. (2009). Adenylation enzyme characterization using γ-($^{18}O_4$)-ATP pyrophosphate exchange. Chem. Biol. *16*, 473-478.

Piel, J. (2010). Biosynthesis of polyketides by *trans*-AT polyketide synthases. Nat. Prod. Rep. *27*, 996-1047.

Piel, J. (2002). A polyketide synthase-peptide synthetase gene cluster from an uncultured bacterial symbiont of *Paederus beetles*. Proc. Natl. Acad. Sci. USA *99*, 14002-14007.

Piel, J., Hui, D., Wen, G., Butzke, D., Platzer, M., Fusetani, N., and Matsunaga, S. (2004). Antitumor polyketide biosynthesis by an uncultivated bacterial symbiont of the marine sponge *Theonella swinhoei*. Proc. Natl. Acad. Sci. USA *101*, 16222-16227.

Pohle, S., Appelt, C., Roux, M., Fiedler, H.-P., and Suessmuth, R.D. (2011). Biosynthetic gene cluster of the non-ribosomally synthesized cyclodepsipeptide skyllamycin: deciphering unprecedented ways of unusual hydroxylation reactions. J. Am. Chem. Soc. *133*, 6194-6205.

Pope, M.K., Green, B., and Westpheling, J. (1998). The *bldB* gene encodes a small protein

required for morphogenesis, antibiotic production, and catabolite control in *Streptomyces coelicolor*. J. Bacteriol. *180*, 1556-1562.

Pope, M.K., Green, B.D., and Westpheling, J. (1996). The bld mutants of *Streptomyces coelicolor* are defective in the regulation of carbon utilization, morphogenesis and cell-cell signalling. Mol. Microbiol. *19*, 747-756.

Radzom, M. (2006). Beiträge zur Biosynthese der antiparasitären Naturstoffe Hormaomycin und Borrelidin sowie Strukturaufklärung von Sekundärmetaboliten aus Actinomyceten., University of Göttingen.

Rascher, A., Hu, Z.H., Buchanan, G.O., Reid, R., and Hutchinson, C.R. (2005). Insights into the biosynthesis of the benzoquinone ansamycins geldanamycin and herbimycin, obtained by gene sequencing and disruption. Appl. Environ. Microb. *71*, 4862-4871.

Recio, E., Colinas, A., Rumbero, A., Aparicio, J.F., and Martin, J.F. (2004). PI factor, a novel type quorum-sensing inducer elicits pimaricin production in *Streptomyces natalensis*. J. Biol. Chem. *279*, 41586-41593.

Reeves, C.D., Murli, S., Ashley, G.W., Piagentini, M., Hutchinson, C.R., and McDaniel, R. (2001). Alteration of the substrate specificity of a modular polyketide synthase acyltransferase domain through site-specific mutations. Biochemistry *40*, 15464-15470.

Rigali, S., Titgemeyer, F., Barends, S., Mulder, S., Thomae, A.W., Hopwood, D.A., and van Wezel, G.P. (2008). Feast or famine: the global regulator DasR links nutrient stress to antibiotic production by *Streptomyces*. EMBO Rep. *9*, 670-675.

Rinehart, K.L. (1977). Mutasynthesis of new antibiotics. Pure Appl. Chem. *49*, 1361-1384.

Ritacco, F.V., Graziani, E.I., Summers, M.Y., Zabriskie, T.M., Yu, K., Bernan, V.S., Carter, G.T., and Greenstein, M. (2005). Production of novel rapamycin analogs by precursor-directed biosynthesis. Appl. Environ. Microb. *71*, 1971-1976.

Roepstorff, P., and Fohlman, J. (1984). Proposal for a common nomenclature for sequence ions in mass spectra of peptides. Biomed. Mass Spectrom. *11*, 601-601.

Rössner, E., Zeeck, A., and Konig, W.A. (1990). Elucidation of the structure of hormaomycin. Angew. Chem. Int. Edit. Engl. *29*, 64-65.

Rubin-Pitel, S.B., Zhang, H., Vu, T., Brunzelle, J.S., Zhao, H., and Nair, S.K. (2008). Distinct structural elements dictate the specificity of the type III pentaketide synthase from *Neurospora crassa*. Chem. Biol. *15*, 1079-1090.

Sakaguchi, K. (1990). Invertrons, a class of structurally and functionally related genetic elements that includes linear DNA plasmids, transposable elements, and genomes of adeno-type viruses. Microbiol. Rev. *54*, 66-74.

Sambrook, J., and Russel, D.W. (2001). Molecular cloning-a laboratory manual. (Cold Spring Harbor Laboratory Press: Cold Spring Harbor.

Samel, S.A., Marahiel, M.A., and Essen, L.-O. (2008). How to tailor non-ribosomal peptide products - new clues about the structures and mechanisms of modifying enzymes. Mol. Biosyst. *4*, 387-393.

Scapin, G., and Blanchard, J.S. (1998). Enzymology of bacterial lysine biosynthesis. Adv. Enzymol. Relat. Areas Mol. Biol. *72*, 279-324.

Sekhon, B.S. (2012). Click chemistry: current developments and applications in drug discovery. J. Pharm. Educ. Res. *3*, 77-85.

Seo, T.S., Li, Z.M., Ruparel, H., and Ju, J.Y. (2003). Click chemistry to construct fluorescent oligonucleotides for DNA sequencing. J. Org. Chem. *68*, 609-612.

Shen, B. (2003). Polyketide biosynthesis beyond the type I, II and III polyketide synthase paradigms. Curr. Opin. Chem. Biol. *7*, 285-295.

Shen, B., Du, L.C., Sanchez, C., Edwards, D.J., Chen, M., and Murrell, J.M. (2002). Cloning and characterization of the bleomycin biosynthetic gene cluster from *Streptomyces verticillus* ATCC15003. J. Nat. Prod. *65*, 422-431.

Shier, W.T., Rinehart, K.L., and Gottlieb, D. (1969). Preparation of four new antibiotics from a mutant of *Streptomyces fradiae*. Proc. Natl. Acad. Sci. USA *63*, 198-204.

Sioud, S., Karray-Rebai, I., Aouissaoui, H., Aigle, B., Bejar, S., and Mellouli, L. (2007). Targeted gene disruption of the cyclo (L-Phe, L-Pro) biosynthetic pathway in *Streptomyces* sp. US24 strain. J. Biomed. Biotechnol. *6*, 91409.

Speers, A.E., Adam, G.C., and Cravatt, B.F. (2003). Activity-based protein profiling in vivo using a copper(I)-catalyzed azide-alkyne [3 + 2] cycloaddition. J. Am. Chem. Soc. *125*, 4686-4687.

Stachelhaus, T., Mootz, H.D., and Marahiel, M.A. (1999). The specificity-conferring code of adenylation domains in nonribosomal peptide synthetases. Chem. Biol. *6*, 493-505.

Staunton, J. (1998). Combinatorial biosynthesis of erythromycin and complex polyketides. Curr. Opin. Chem. Biol. *2*, 339-345.

Staunton, J., and Weissman, K.J. (2001). Polyketide biosynthesis: a millennium review. Nat. Prod. Rep. *18*, 380-416.

Staunton, J., and Wilkinson, B. (1997). Biosynthesis of erythromycin and rapamycin. Chem. Rev. *97*, 2611-2630.

Stratigopoulos, G., Gandecha, A.R., and Cundliffe, E. (2002). Regulation of tylosin production

and morphological differentiation in *Streptomyces fradiae* by TylP, a deduced gamma-butyrolactone receptor. Mol. Microbiol. *45*, 735-744.

Studier, F.W., Rosenberg, A.H., Dunn, J.J., and Dubendorff, J.W. (1990). Use of T7 RNA polymerase to direct expression of cloned genes. Methods Enzymol. *185*, 60-89.

Takano, E., Gramajo, H.C., Strauch, E., Andres, N., White, J., and Bibb, M.J. (1992). Transcriptional regulation of the *redD* transcriptional activator gene accounts for growth-phase-dependent production of the antibiotic undecylprodigiosin in *Streptomyces coelicolor* A3(2). Mol. Microbiol. *6*, 2797-2804.

Ulanova, D., Novotna, J., Smutna, Y., Kamenik, Z., Gazak, R., Sulc, M., Sedmera, P., Kadlcik, S., Plhackova, K., and Janata, J. (2010). Mutasynthesis of lincomycin derivatives with activity against drug-resistant staphylococci. Antimicrob. Agents Chemother. *54*, 927-930.

Vaillancourt, F.H., Yeh, E., Vosburg, D.A., O'Connor, S.E., and Walsh, C.T. (2005). Cryptic chlorination by a non-haem iron enzyme during cyclopropyl amino acid biosynthesis. Nature *436*, 1191-1194.

Volff, J.N., and Altenbuchner, J. (1998). Genetic instability of the *Streptomyces* chromosome. Mol. Microbiol. *27*, 239-246.

Volokhan, O., Sletta, H., Sekurova, O.N., Ellingsen, T.E., and Zotchev, S.B. (2005). An unexpected role for the putative 4'-phosphopantetheinyl transferase-encoding gene *nysF* in the regulation of nystatin blosynthesis in *Streptomyces noursei* ATCC 11455. FEMS Microbiol. Lett. *249*, 57-64.

Waldron, C., Matsushima, P., Rosteck, P.R., Broughton, M.C., Turner, J., Madduri, K., Crawford, K.P., Merlo, D.J., and Baltz, R.H. (2001). Cloning and analysis of the spinosad biosynthetic gene cluster of *Saccharopolyspora spinosa*. Chem. Biol. *8*, 487-499.

Walsh, C.T., Garneau-Tsodikova, S., and Howard-Jones, A.R. (2006). Biological formation of pyrroles: nature's logic and enzymatic machinery. Nat. Prod. Rep. *23*, 517-531.

Walsh, C.T., O'Connor, S.E., and Schneider, T.L. (2003). Polyketide-nonribosomal peptide epothilone antitumor agents: the EpoA, B, C subunits. J. Ind. Microbiol. Biot *30*, 448-455.

Wang, J., Wang, W., Wang, L., Zhang, G., Fan, K., Tan, H., and Yang, K. (2011). A novel role of 'pseudo' γ-butyrolactone receptors in controlling γ-butyrolactone biosynthesis in *Streptomyces*. Mol. Microbiol. *82*, 236-250.

Watve, M.G., Tickoo, R., Jog, M.M., and Bhole, B.D. (2001). How many antibiotics are produced by the genus *Streptomyces*? Arch. Microbiol. *176*, 386-390.

Weber, G., Schorgendorfer, K., Schneiderscherzer, E., and Leitner, E. (1994). The peptide synthetase catalyzing cyclosporine production in *Tolypocladium niveum* is encoded by a giant 45.8-kilobase open reading frame. Curr. Genet. *26*, 120-125.

Wenzel, S.C., Kunze, B., Hofle, G., Silakowski, B., Scharfe, M., Blocker, H., and Müller, R. (2005). Structure and biosynthesis of myxochromides S1-3 in *Stigmatella aurantiaca*: evidence for an iterative bacterial type I polyketide synthase and for module skipping in nonribosomal peptide biosynthesis. Chembiochem *6*, 375-385.

Wilkinson, B., and Micklefield, J. (2007). Mining and engineering natural-product biosynthetic pathways. Nat. Chem. Biol. *3*, 379-386.

Willand, N., Desroses, M., Toto, P., Dirie, B., Lens, Z., Villeret, V., Rucktooa, P., Locht, C., Baulard, A., and Deprez, B. (2010). Exploring drug target flexibility using *in situ* click chemistry: application to a mycobacterial transcriptional regulator. ACS Chem. Biol. *5*, 1007-1013.

Willey, J., Santamaria, R., Guijarro, J., Geistlich, M., and Losick, R. (1991). Extracellular complementation of a developmental mutation implicates a small sporulation protein in aerial mycelium formation by *Streptomyces coelicolor*. Cell *65*, 641-650.

Willey, J., Schwedock, J., and Losick, R. (1993). Multiple extracellular signals govern the production of a morphogenetic protein involved in aerial mycelium formation by *Streptomyces coelicolor*. Genes Dev. *7*, 895-903.

Wilson, D.J., Xue, Y.Q., Reynolds, K.A., and Sherman, D.H. (2001). Characterization and analysis of the PikD regulatory factor in the pikromycin biosynthetic pathway of *Streptomyces venezuelae*. J. Bacteriol. *183*, 3468-3475.

Wilson, Z.E., and Brimble, M.A. (2009). Molecules derived from the extremes of life. Nat. Prod. Rep. *26*, 44-71.

Winkler, R., and Hertweck, C. (2007). Biosynthesis of nitro compounds. Chembiochem *8*, 973-977.

Winter, J.M., Behnken, S., and Hertweck, C. (2011). Genomics-inspired discovery of natural products. Curr. Opin. Chem. Biol. *15*, 22-31.

Xiang, L., and Moore, B.S. (2003). Characterization of benzoyl coenzyme A biosynthesis genes in the enterocin-producing bacterium "*Streptomyces maritimus*". J. Bacteriol. *185*, 399-404.

Yamada, Y. (1995). Butyrolactone autoregulataors, inducers of secondary metabolites, in *Streptomyces*. 日本放線菌学会誌 *9*, 57-65.

Yamazaki, H., Ohnishi, Y., and Horinouchi, S. (2003a). Transcriptional switch on of *ssgA* by A-factor, which is essential for spore septum formation in *Streptomyces griseus*. J. Bacteriol. *185*, 1273-1283.

Yamazaki, H., Ohnishi, Y., and Horinouchi, S. (2000). An A-factor-dependent extracytoplasmic function sigma factor (σ^{AdsA}) that is essential for morphological development in *Streptomyces griseus*. J. Bacteriol. *182*, 4596-4605.

Yamazaki, H., Takano, Y., Ohnishi, Y., and Horinouchi, S. (2003b). *amfR*, an essential gene for aerial mycelium formation, is a member of the AdpA regulon in the A-factor regulatory cascade in *Streptomyces griseus*. Mol. Microbiol. *50*, 1173-1187.

Yamazaki, H., Tomono, A., Ohnishi, Y., and Horinouchi, S. (2004). DNA-binding specificity of AdpA, a transcriptional activator in the A-factor regulatory cascade in *Streptomyces griseus*. Mol. Microbiol. *53*, 555-572.

Yu, T., and Floss, H.G. (2005). Ansamitocins (Maytansinoids). In *Antitumor Agents from Natural Products* (G.M. Cragg, Newman, D.J., and Kingston, D.G.I., ed.). (CRC press Taylor and Francis: Boca Raton, Florida.). pp. 321-337.

Zhang, X., and Parry, R.J. (2007). Cloning and characterization of the pyrrolomycin biosynthetic gene clusters from *Actinosporangium vitaminophilum* ATCC 31673 and *Streptomyces* sp. strain UC 11065. Antimicrob. Agents Chemother. *51*, 946-957.

Zhou, X., Wei, Y., Zhu, H., Wang, Z., Lin, J., Liu, L., and Tang, K. (2008). Protoplast formation, regeneration and transformation from the taxol-producing fungus *Ozonium* sp. Afr. J. Biotechnol. *7*, 2017-2024.

Ziemert, N., Ishida, K., Weiz, A., Hertweck, C., and Dittmann, E. (2010). Exploiting the natural diversity of microviridin gene clusters for the discovery of novel tricyclic depsipeptides. Appl. Environ. Microbiol. *76*, 3568-3574.

Zlatopolskiy, B.D., and de Meijere, A. (2004). First total synthesis of hormaomycin, a naturally occurring depsipeptide with interesting biological activities. Chem. Eur. J. *10*, 4718-4727.

Zlatopolskiy, B.D., Radzom, M., Zeeck, A., and de Meijere, A. (2006). Synthesis and precursor-directed biosynthesis of new hormaomycin analogues. Eur. J. Org. Chem. 10.1002/ejoc.200500856, 1525-1534.

Selbstständigkeitserklärung

Hiermit erkläre ich, die eingereichte Arbeit selbstständig verfasst und keine anderen Hilfsmittel und Quellen als die angegebenen benutzt zu haben.

Diese Arbeit ist weder identisch noch teilidentisch mit einer Arbeit, die an der Rheinischen Friedrich-Wilhelms-Universität Bonn oder einer anderen Hochschule zur Erlangung eines akademischen Grades oder als Prüfungsleistung vorgelegt worden ist.

Die Promotionsordnung der Mathematisch-Naturwissenschaftlichen Fakultät der Rheinischen Friedrich-Wilhelms-Universität Bonn ist mir bekannt.

Xiaofeng Cai

Bonn, den 16. 07. 2013